The Role of T Lymphocytes in Myocardial Ischaemia/Reperfusion Injury

Stephen Edward Boag

Institute of Genetic Medicine

Faculty of Medical Sciences

This thesis is submitted for the degree of

Doctor of Philosophy

March 2016

Abstract

Myocardial infarction is the greatest cause of mortality worldwide, and a source of considerable morbidity. Treatment of ST-elevation MI (STEMI) has improved enormously with the advent of primary percutaneous coronary intervention (PPCI), but ischaemia/reperfusion (I/R) injury remains an important complication. Evidence from animal studies points to a role for lymphocytes, and in particular T cells, in myocardial I/R injury, but this has not yet been studied in humans. The goal of my PhD was to investigate this phenomenon in human patients treated with PPCI, with particular emphasis on T cell kinetics, their relationship to I/R injury, and the potential mechanisms involved.

I retrospectively analysed a large database of MI patients treated with PPCI. I demonstrated that lymphopaenia during admission was an independent predictor of increased long-term mortality, confirming the prognostic relevance of lymphocytes in this setting for the first time. I then studied a prospectively recruited cohort of STEMI patients, determining lymphocyte subset kinetics with detailed flow-cytometric analysis. T cells were acutely depleted from the circulation within minutes of reperfusion, with highly differentiated effector cells showing the greatest changes. Trans-coronary gradients suggested some cells were sequestered into the reperfused myocardium. Cardiac MRI analysis revealed a significant relationship between post-reperfusion effector T cell kinetics and microvascular obstruction (MVO), a component of I/R injury, raising the possibility of a mechanistic link. This discovery was driven primarily by positive findings in cytomegalovirus seropositive patients, who had higher percentages of highly differentiated T cells. Analysis of chemokine receptors subsequently identified CX3CR1, with its ligand fractalkine, as the prime candidate for a key role in effector T cell kinetics post-reperfusion, potentially influencing MVO. These findings identify a possible therapeutic target in I/R injury post-PPCI, opening up a new avenue for further research and future treatment development.

Declaration

This thesis is submitted for the degree of Doctor of Philosophy at Newcastle University. The research described herein was conducted at the Institute of Genetic Medicine, Newcastle University, and the Freeman Hospital, Newcastle upon Tyne Hospitals NHS Trust, between August 2012 and July 2015 under the supervision of Professor Ioakim Spyridopoulos. All of the work described here is my own, except where otherwise clearly stated in the text. Throughout this research I was funded by a British Heart Foundation Clinical Research Training Fellowship grant.

I certify that none of the material offered has been previously submitted by me for a degree or other qualification at this or any other university.

Stephen Boag
November 2015

Acknowledgements

I would like to express my great thanks to the many individuals and organisations who have helped to make this work possible.

I would like to thank the British Heart Foundation for funding me to conduct this research through a Clinical Research Training Fellowship Grant.

My sincere thanks are also due to my principal supervisor, Professor Ioakim Spyridopoulos. His involvement was critical in the conception and realisation of this work, and his relentless positivity proved a necessary foil to my own pessimism in the more challenging moments. I would also like to thank my additional supervisors, Dr Rajiv Das and Mr W Andrew Owens for their support and guidance throughout.

I have been fortunate to work with many dedicated clinical and laboratory professionals who have assisted me in numerous ways. The support of the interventional cardiologists at the Freeman Hospital, Newcastle upon Tyne, has been indispensible, enabling me to recruit patients to my study at all hours. Of particular note, the skills of Dr Mohaned Egred were crucial in obtaining many of the coronary sinus blood samples, while Dr Alan Bagnall's critical feedback on prospective manuscript submissions has been invaluable. The support of Professor Azfar Zaman has also been greatly appreciated, including his provision of the cardiac MRI analysis software used in the study. I would also like to express my gratitude to the many nursing staff on the Coronary Care Unit, who have made great efforts to call me day or night whenever a potential patient may be en-route.

A number of my laboratory colleagues and collaborators have also been of considerable help during my project. The most notable of these are Dr Evgeniya Shmeleva, who conducted the ELISA assay to quantify fractalkine in my patients' serum samples, and Dr Karim Bennaceur, who performed the RT-PCR assay on the peripheral blood mononuclear cells that I had isolated. I would also like to thank

Mr Nicholas Howard, who put in considerable work collating blood results and developing the initial database on which the analysis in chapter 4 was performed.

Lastly, and most importantly, I would like to thank my family, without whose support I could never have completed this project. My own parents, David and Joan Boag, as well as my parents-in-law, Peter and Frances Cranfield have all supported me in a number of ways throughout. I would also like to thank Alfie and Poppy, who have helped to keep me relatively sane during the more taxing periods. My greatest thanks, however, are due to my wife, Katie, to whom I dedicate this thesis. Her love, tolerance, encouragement and support have been truly essential. She has been woken as many times as I have with phone calls in the middle of the night, and my work has impacted her life as much as my own. My gratitude towards her is immeasurable.

Publications

To date, the following manuscripts have been published wholly, or in part, from the work described in this thesis:

Boag, SE, Das, R, Shmeleva, EV, Bagnall, A, Egred, M, Howard, N, Bennaceur, K, Zaman, A, Keavney, B, Spyridopoulos, I. T lymphocytes and fractalkine contribute to myocardial ischemia/reperfusion injury in patients. *J Clin Invest*. 2015; 125(8): 3063-76.

Hoffmann, J[*], Shmeleva, EV[*], Boag, SE[*], Fiser, K, Bagnall, A, Murali, S, Dimmick, I, Pircher, H, Martin-Ruiz, C, Egred, M, Keavney, B, von Zglinicki, T, Das, R, Todryk, S, Spyridopoulos, I. Myocardial ischemia and reperfusion leads to transient CD8 immune deficiency and accelerated immunosenescence in CMV-seropositive patients. *Circ Res*. 2015;116(1):87–98.

[*] Equally contributing co-first authors

Shmeleva, EV, Boag, SE, Murali, S, Bennaceur, K, Das, R, Egred, M, Purcell, I, Edwards, R, Todryk, S, Spyridopoulos, I. Differences in immune responses between CMV-seronegative and -seropositive patients with myocardial ischemia and reperfusion. *Immun Inflamm Dis*. 2015;3(2):56–70.

Contents

List of Figures

List of Tables

List of Abbreviations

AAR	Area at risk
ACE	Angiotensin converting enzyme
ACS	Acute coronary syndrome
ANOVA	Analysis of variance
APC	Antigen presenting cell
ARB	Angiotensin receptor blocker
ATP	Adenosine triphosphate
BCR	B cell receptor
BD	Becton Dickinson
BMI	Body mass index
CABG	Coronary artery bypass grafting
CAD	Coronary artery disease
CD	Cluster of differentiation
cDNA	Complementary DNA
CI	Confidence interval
CMP	Common myeloid precursor
CMR	Cardiac magnetic resonance imaging
CMV	Cytomegalovirus
CS	Coronary sinus
CT	Cycle threshold
CTLs	Cytotoxic T lymphocytes
CV	Coefficient of variation
DAMP	Danger associated molecular pattern
DAPT	Dual antiplatelet therapy
DC	Dendritic cell
DMSO	Dimethyl sulfoxide
DNA	Deoxyribonucleic acid
ECG	Electrocardiogram
EDTA	Ethylenediaminetetraacetic acid

EDV	End diastolic volume
ELISA	Enzyme-linked immunosorbent assay
ELR	Glutamic acid-leucine-arginine
ERK	Extracellular-signal-regulated kinase
ESV	End systolic volume
FACS	Fluorescence activated cell sorting
FBC	Full blood count
FITC	Fluorescein isothiocyanate
FMO	Fluorescence minus one
FSC	Forward scatter
g	Grams
GLP	Glucagon-like-peptide
GP	Glycoprotein
GRO	Growth regulated oncogene
H_2O	Water
H_2O_2	Hydrogen peroxide
HASTE	Half-Fourier acquisition single shot turbo spin echo
HCMV	Human cytomegalovirus
HEV	High endothelial venules
hr	Hours
HR	Hazard ratio
IFN	Interferon
IL	Interleukin
iNKT	Invariant NKT cell
IP-10	Interferon-γ induced protein-10
IQR	Interquartile range
I/R	Ischaemia/reperfusion
kg	Kilograms
KO	Knockout
LAD	Left anterior descending artery
LBBB	Left bundle branch block

LGE	Late gadolinium enhancement
LPS	Lipopolysaccharide
LV	Left ventricular/ventricular
LVEF	Left ventricular ejection fraction
MACE	Major adverse cardiovascular events
MBG	Myocardial blush grade
MCP	Monocyte chemotactic protein
MFI	Mean fluorescence intensity
MHC	Major histocompatibility complex
mg	Milligrams
MI	Myocardial infarction
min	Minutes
MIP	Macrophage inflammatory protein
ml	Millilitres
MLP	Multilymphoid progenitor
mmol	Millimoles
MPTP	Mitochondrial permeability transition pore
MR	Magnetic resonance
MRI	Magnetic resonance imaging
mRNA	Messenger RNA
MVO	Microvascular obstruction
ng	Nanograms
NHS	Newcastle Health Service
NK cell	Natural killer cell
NKT cell	Natural killer T cell
NLR	Neutrophil to lymphocyte ratio
NRES	National Research Ethics Service
NSTEMI	Non-ST elevation myocardial infarction
O_2	Oxygen
$O_2^{\bullet-}$	Superoxide anion
PBMC	Peripheral blood mononuclear cell

PBS	Phosphate buffered saline
PCI	Percutaneous coronary intervention
PCR	Polymerase Chain Reaction
PE	Phycoerythrin
PerCP	Peridinin chlorophyll protein complex
PKC	Protein kinase C
PPCI	Primary percutaneous coronary intervention
PRR	Pattern-recognition receptor
PVD	Peripheral vascular disease
RANTES	Regulated upon activation, normal T-cell expressed and secreted
RCT	Randomised controlled trial
RISK	Reperfusion Injury Salvage Kinase
RNA	Ribonucleic acid
ROS	Reactive oxygen species
RT-PCR	Reverse transcription polymerase chain reaction
SD	Standard deviation
SDF	Stromal cell-derived factor
SEM	Standard error of the mean
sFKN	Soluble fractalkine
SI	Salvage index
SSC	Side scatter
SSFP	Steady-state free precession
STEMI	ST-elevation myocardial infarction
STIR	Short inversion time inversion recovery
SV	Stroke volume
TCE	T cell clonal expansion
T_{CM}	Central memory T cell
TCR	T cell receptor
TE	Echo time
T_{EM}	Effector memory T cells
T_{EMRA}	Terminally differentiated effector memory T cell

TGF	Transforming growth factor
T_H1	T helper 1 cell
T_H17	T helper 17 cell
T_H2	T helper 2 cell
TI	Inversion time
TIA	Transient ischaemic attack
TIMI	Thrombolysis in Myocardial Infarction
TLR	Toll-like receptor
T_N	Naive T cell
TNF-α	Tumour necrosis factor alpha
TR	Repetition time
T_{reg}	Regulatory T cell
WBC	White blood cell
µl	Microlitres

Chapter 1

Introduction

1.1 Myocardial Infarction

1.1.1 Preamble

Coronary artery disease (CAD) is the single largest cause of mortality in Europe, directly leading to 20% of deaths in men and 22% in women (Nichols et al., 2012). The most serious and acute manifestation is myocardial infarction (MI), which is characterised by irreversible myocardial damage caused by prolonged ischaemia. The most severe form of MI is ST-elevation myocardial infarction, generally caused by complete occlusion of a coronary artery, for which modern treatment involves the urgent reopening of the vessel. However, even with successful treatment, significant myocardial injury is sustained, some of which occurs as a direct consequence of reperfusion. The focus of this thesis will be the investigation of the role of the immune system, and in particular T lymphocytes, on this currently untreatable component of MI induced myocardial damage, ischaemia/reperfusion (I/R) injury.

1.1.2 Coronary Artery Disease

CAD is primarily caused by atherosclerosis within the coronary arteries. This is a chronic inflammatory condition, resulting in the development of multiple plaques within the intima of medium and large arteries (Camm et al., 2009; Lusis, 2000; Weber and Noels, 2011). These plaques are composed of a lipid rich core, containing extracellular lipids and large numbers of densely lipid-laden macrophages known as foam cells, capped by fibrous connective tissue (Falk, 2006; Weber and Noels, 2011). Leucocytes, including monocytes and T cells, as well as vascular endothelial cells release pro-inflammatory mediators and growth factors, which in addition to causing further leucocyte accumulation, result in proliferation of local smooth muscle cells (Galkina and Ley, 2009; Hansson and Libby, 2006; Weber and Noels, 2011). The resultant plaques initially develop a thick, stable fibrous cap, and if they become large enough can protrude into the vessel lumen sufficiently to restrict blood flow in the artery. It is these large stable plaques that result in one of the clinical manifestations of CAD, stable angina,

which is caused by transient myocardial ischaemia at times of increased myocardial oxygen demand such as during exercise (Bonow et al., 2011).

1.1.3 Acute Myocardial Infarction

While some atheromatous plaques remain stable, in others the fibrous cap can become degraded and liable to rupture. This is caused by chronic inflammatory processes including the release of proteases by activated leucocytes such as macrophages, mast cells and neutrophils (Falk et al., 2013; Sakakura et al., 2013). When plaque rupture occurs, highly thrombogenic substances within the core are exposed to blood within the vessel lumen, resulting in rapid and extensive formation of thrombus (Falk et al., 2013; Virmani et al., 2006). This can then cause partial or complete occlusion of the artery, restricting the blood flow and causing severe ischaemia in the myocardium distal to the blockage. After 15-20 minutes of ischaemia permanent myocardial damage ensues, resulting in MI (Camm et al., 2009). Initially, this affects the subendocardial region, spreading to involve the full thickness of the myocardial wall as the ischaemic time increases (Reimer and Jennings, 1979).

The vast majority of cases of MI are caused by unstable atheromatous plaques, as described above. The same pathological process can result in three different clinical scenarios: unstable angina, non-ST elevation myocardial infarction (NSTEMI), and STEMI, collectively termed 'acute coronary syndromes (ACS)' (Bonow et al., 2011). Which of these develops depends on the location, duration and extent of the coronary occlusion (Camm et al., 2009; Hamm et al., 2011; Steg et al., 2012). Unstable angina occurs when interruption to normal coronary flow results in clinical features such as chest pain and ECG changes, but the extent and/or duration of vessel occlusion are not sufficient to cause a detectable release of biomarkers indicative of myocardial necrosis, such as troponin I or T (Anderson et al., 2011). Myocardial infarction is defined as the presence of appropriate clinical features (such as typical chest pain), along with a detectable rise or fall of suitable biomarkers (Thygesen et al., 2012). MI can then be further divided into STEMI and NSTEMI based on the presence of ST segment elevation on the electrocardiogram (ECG). This ECG finding in the context of MI is usually indicative

of complete occlusion of the infarct related artery (Bonow et al., 2011; DeWood et al., 1980). The therapeutic significance of this is that patients with STEMI are best treated with rapid intervention to open the occluded vessel (reperfusion therapy), while those with NSTEMI are not (Hamm et al., 2011; Steg et al., 2012).

1.1.4 Clinical Consequences of Myocardial Infarction

Although the clinical outcome from MI has improved considerably in recent years, partly owing to new and more effective treatments, 6 month mortality from STEMI remains approximately 13% (Fox et al., 2006; Nallamothu et al., 2015). This is largely due to a number of short and long-term complications.

One of the most important sequelae is the development of left ventricular (LV) failure. This commonly occurs in the acute setting and can be secondary to a numbers of factors including loss of myocytes through infarction and stunning of viable tissue (Camm et al., 2009; Steg et al., 2012). LV dysfunction is the strongest predictor of mortality following STEMI (Camm et al., 2009; Reynolds and Hochman, 2008; Steg et al., 2012). In severe cases, acute LV dysfunction can result in cardiogenic shock, characterised by persistent hypotension and end organ hypoperfusion (Reynolds and Hochman, 2008). This occurs in 5-8% of cases of STEMI, and is a major cause of death, with mortality rates in the region of 50% (Reynolds and Hochman, 2008).

In addition to acute LV dysfunction, MI is a major cause of chronic heart failure (Mosterd and Hoes, 2007). Over a 7-8 year period after MI, 36% of patients experience cardiac failure (Hellermann et al., 2003). As well as the loss of myocytes directly damaged during the acute phase of MI, there follows a process of 'ventricular remodelling', which can be maladaptive and result in further decline of function (Sun, 2009). This process includes the formation of fibrous tissue, both at the site of infarction, resulting in scar formation, and at remote sites, impacting the function of viable areas of myocardium (Sun, 2009).

Arrhythmic complications can be another significant consequence of acute MI. Up to 20% of cases of STEMI are complicated by ventricular tachycardia or ventricular

fibrillation (Newby et al., 1998), which are life threatening and require immediate treatment with DC cardioversion (Steg et al., 2012). Supraventricular arrhythmias, including atrial fibrillation, are also common occurring in up to 28% of cases of acute MI (Steg et al., 2012). Atrial fibrillation in this context has been associated with adverse clinical outcomes, including increased mortality (Schmitt et al., 2009). In addition to acute rhythm disturbance, MI is also associated with a long-term risk of sudden cardiac death due to late ventricular arrhythmias (Behar et al., 1994; Dagres and Hindricks, 2013).

1.1.5 Management of Myocardial Infarction

The management of MI involves measures to re-establish/maintain myocardial perfusion, limit the myocardial damage sustained, and prevent complications. General measures include pain relief, with agents including opiates, and oxygen to correct hypoxaemia (Hamm et al., 2011; Steg et al., 2012).

Anti-thrombotic agents are crucial, given the contribution of thrombus to vessel occlusion. Dual antiplatelet therapy (DAPT), consisting of aspirin, together with a $P2Y_{12}$ receptor inhibitor (e.g. prasugrel) is standard therapy in both STEMI and NSTEMI (Hamm et al., 2011; Steg et al., 2012). In certain circumstances, highly potent parenteral antiplatelet agents, glycoprotein (GP) IIb/IIIa receptor inhibitors (e.g. abciximab) are also administered (Hamm et al., 2011; Steg et al., 2012). There is also a role for anticoagulants, including low molecular weight heparins, particularly in cases of NSTEMI (Hamm et al., 2011).

Anti-ischaemic therapies, aimed at either reducing myocardial oxygen demand or increasing supply, are also indicated in the acute treatment of certain cases of MI. Nitrates, such as glyceryl trinitrate, act by both reducing myocardial oxygen demand through venodilatation, causing a reduction in preload and end diastolic volume (EDV), as well as improving oxygen supply through coronary artery dilatation (Hamm et al., 2011). Other drugs used to limit ischaemia can include beta-blockers, which decrease myocardial oxygen demand through a reduction in heart rate and myocardial contractility (Hamm et al., 2011).

Other general measures in the treatment of MI include the detection and treatment of acute and chronic complications. Important examples include cardiac monitoring, allowing prompt recognition and treatment of potentially fatal arrhythmias (Steg et al., 2012). In addition, LV dysfunction and heart failure are common, and require recognition and appropriate management (Hamm et al., 2011; Steg et al., 2012).

1.1.6 Reperfusion Therapy

The most significant difference between the management of STEMI and NSTEMI is the urgent need to re-establish coronary blood flow in the former (Steg et al., 2012). The majority of cases of STEMI are due to complete occlusion of an artery, and opening the vessel is essential in salvaging viable myocardium. Consequently, reperfusion therapy has become the mainstay of treatment. The first form of this developed was thrombolysis, involving intravenous administration of fibrinolytic agents to dissolve intracoronary thrombus. Initial landmark trials in the use of the streptokinase in the 1980s established the efficacy of this treatment, showing an 18-25% reduction in early mortality compared to standard therapy at the time (Gray, 2006; GISSI, 1986; ISIS-2, 1988). Complications of fibrinolytic therapy, however, include risk of bleeding, particularly haemorrhagic stroke, and this must be considered in decisions to administer thrombolysis (Steg et al., 2012).

1.1.7 Primary Percutaneous Coronary Intervention

Over the last 15 years, reperfusion therapy for STEMI has progressed further with the development of primary percutaneous coronary intervention (PPCI). This involves the direct opening of the infarct related artery through a procedure known as an angioplasty. A wire is inserted into the coronary artery and past the occlusion, via a catheter inserted through a small puncture in either the radial or femoral artery. A wire-mounted balloon is then threaded over this angioplasty wire, and inflated at the site of the occlusion (Bonow et al., 2011; Camm et al., 2009). In the vast majority of cases a metallic stent is deployed, helping to maintain vessel patency. By definition, PPCI involves this procedure being

performed without prior or concurrent thrombolytic therapy (Steg et al., 2012). This method of reperfusion therapy has been shown to be superior to thrombolysis, both in terms of efficacy at re-establishing vessel patency, and clinical outcomes including reduced mortality (Keeley et al., 2003). However, PPCI requires the availability of suitable facilities and skilled personnel at the time of presentation, and delays in treatment can adversely affect outcome (De Luca et al., 2003; Nallamothu et al., 2007). Current recommendations are that reperfusion therapy is indicated in STEMI patients presenting within 12 hours of symptom onset, as well as those presenting at between 12 and 24 hours with evidence of ongoing ischaemia (Steg et al., 2012). PPCI is the recommended form of reperfusion therapy when possible within 120 minutes of first medical contact, otherwise thrombolytic therapy should be given in the absence of contraindications (Steg et al., 2012)

1.2 Myocardial Ischaemia/Reperfusion Injury

1.2.1 The Phenomenon of Myocardial Ischaemia/Reperfusion Injury

Achieving reperfusion is of critical importance in salvaging viable ischaemic myocardium in acute STEMI. However, reperfusion does come at a cost, and can actually cause damage to the reperfused myocardium, in a phenomenon known as ischaemia/reperfusion (I/R) injury (Yellon and Hausenloy, 2007; Braunwald and Kloner, 1985). This is thought to contribute up to 50% of the final infarct size, impacting subsequent left ventricular ejection fraction (LVEF) and clinical outcome (Hausenloy and Yellon, 2013).

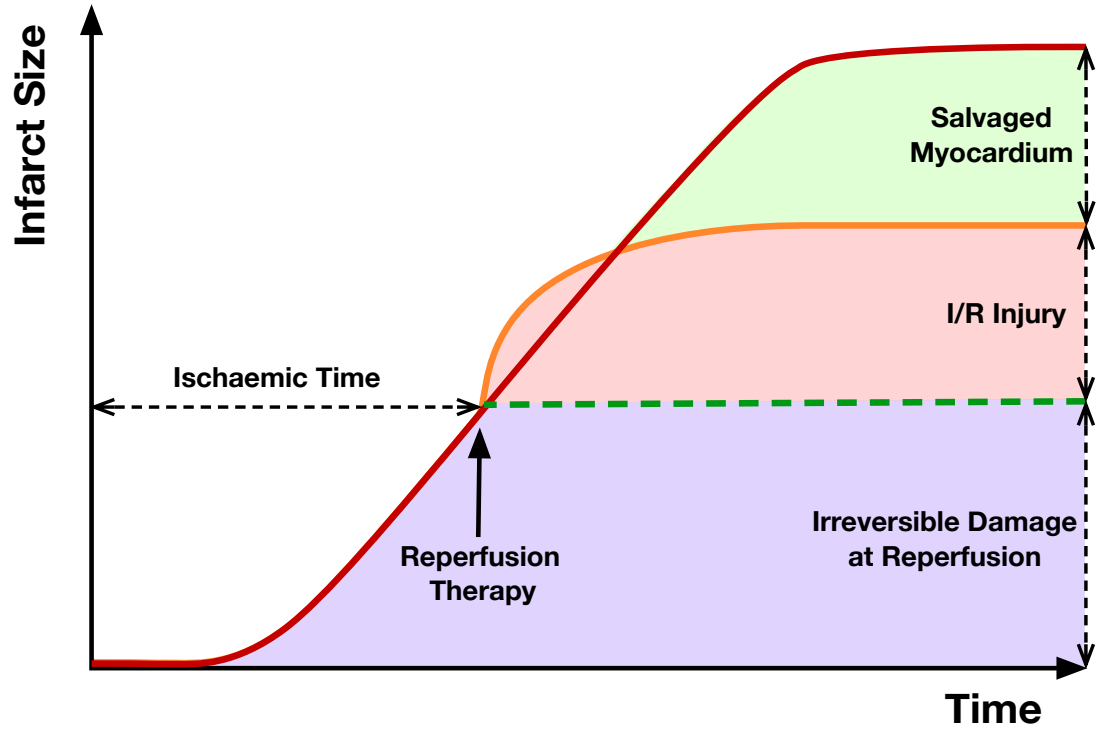

Figure 1.1: Schematic describing concept of I/R injury. The red line represents the development of the infarct over time in the absence of reperfusion. After a short period of ischaemia irreversible damage starts occur, increasing with time until the entire area at risk has undergone infarction. With reperfusion (orange line) there is an initial increase in myocardial damage before infarction ceases, with some of the area at risk salvaged. The total infarct size in cases of reperfusion, however, is greater than the irreversible damage sustained by the time of reperfusion (green broken line), because of I/R injury. Consequently, by limiting I/R injury, the extent of salvaged myocardium could be increased and overall infarct size reduced. Adapted from (Garcia-Dorado et al., 2014).

Four major components of myocardial I/R injury are recognised. These are reperfusion arrhythmias, myocardial stunning, microvascular obstruction (MVO) and lethal myocardial ischaemia/reperfusion injury (Yellon and Hausenloy, 2007). While the first two of these are transient and reversible, the latter two are irreversible and impact the final infarct size.

1.2.2 Reperfusion Arrhythmias

Reperfusion following myocardial ischaemia can directly trigger cardiac arrhythmias (Manning and Hearse, 1984). These are often ventricular in origin but are usually self limiting and harmless, as in the commonest such arrhythmia, accelerated idioventricular rhythm (Manning and Hearse, 1984; Steg et al., 2012). Although potentially dangerous sustained ventricular arrhythmias, such as ventricular tachycardia and fibrillation, can occur, they can be effectively treated with DC cardioversion (Steg et al., 2012).

1.2.3 Myocardial Stunning

Myocardial stunning refers to the transient impairment of myocardial function following ischaemia, despite adequate perfusion (Kloner et al., 1998). This form of I/R injury is reversible, with recovery of stunned myocardium occurring over days or weeks (Bolli and Marbán, 1999). It is thought that both oxidative stress and calcium overload play a role in this phenomenon (Kloner et al., 1998; Bolli and Marbán, 1999).

1.2.4 Microvascular Obstruction

MVO is defined as the inability to reperfuse areas of myocardium that have previously been ischaemic, despite adequate flow in the epicardial coronary vessel supplying the territory. It was first described in animal models involving transient ligation of coronary arteries (Kloner et al., 1974; Krug et al., 1966). Kloner et al. used a canine infarct model, in which dogs were subjected to coronary artery occlusion, followed by varying periods of reperfusion (Kloner et al., 1974). Using

thioflavin S, a fluorescent vital stain for endothelium, they were able to assess arterial flow within the myocardium. They demonstrated that after 90 minutes of ischaemia followed by reperfusion, the uptake of the tracer in the damaged myocardium was uneven, with areas of absent uptake the inner half of the infarct (Kloner et al., 1974). These areas represented parts of the myocardium that did not achieve adequate perfusion at the tissue level, despite flow in the corresponding epicardial vessel. Electron microscopy in this and subsequent studies has revealed characteristic findings shedding light on the multifactorial nature of MVO. At the level of the capillaries there is swelling of endothelial cells, with protrusion of blebs contributing to obstruction of the lumen (Kloner et al., 1974; Reffelmann and Kloner, 2006). Plugging of the capillaries with leucocytes, erythrocytes, and platelet thrombi is also typically seen (Durante and Camici, 2015; Reffelmann and Kloner, 2006). Furthermore, local myocyte swelling and subsarcolemmal blebs contribute further to capillary obstruction by external compression of the vessels (Kloner et al., 1974; Schwartz and Kloner, 2012; Wu, 2012).

The precise mechanisms and time course of development of MVO are not yet fully understood. Animal studies have suggested that it develops particularly rapidly within the first two hours following reperfusion (Reffelmann and Kloner, 2002). While some of the pathological findings can be explained in part by ischaemic injury itself, the process of reperfusion directly causes or can accentuate many of the proposed mechanisms (Ito, 2009; Durante and Camici, 2015). Ischaemic injury contributes to the observed swelling and protrusions from endothelial cells, resulting in reduction of the lumen size (Ito, 2009). The subsequent presence of erythrocytes, platelet thrombi, and leucocytes, however, suggests that there is then an initial phase of flow following reperfusion that is then impaired as the vessel becomes further obstructed (Reffelmann and Kloner, 2006; Wu, 2012). Furthermore, as well as mechanical obstruction, accumulated leucocytes can contribute by the release of reactive oxygen species (ROS), which can lead to further damage and impairment of endothelial function, vasoconstriction, and increased accumulation of fibrin/fibrinogen (Duilio et al., 2001). While all of the above mechanisms are thought to occur in both animal models and humans, additional factors including microembolisation of atherosclerotic plaque debris and platelet-fibrin complexes to the distal microvasculature can also contribute in

human patients undergoing PPCI (Limbruno et al., 2005). As well as contributing mechanically to MVO, microemboli can enhance the inflammatory reaction and vasoconstriction (Schwartz and Kloner, 2012).

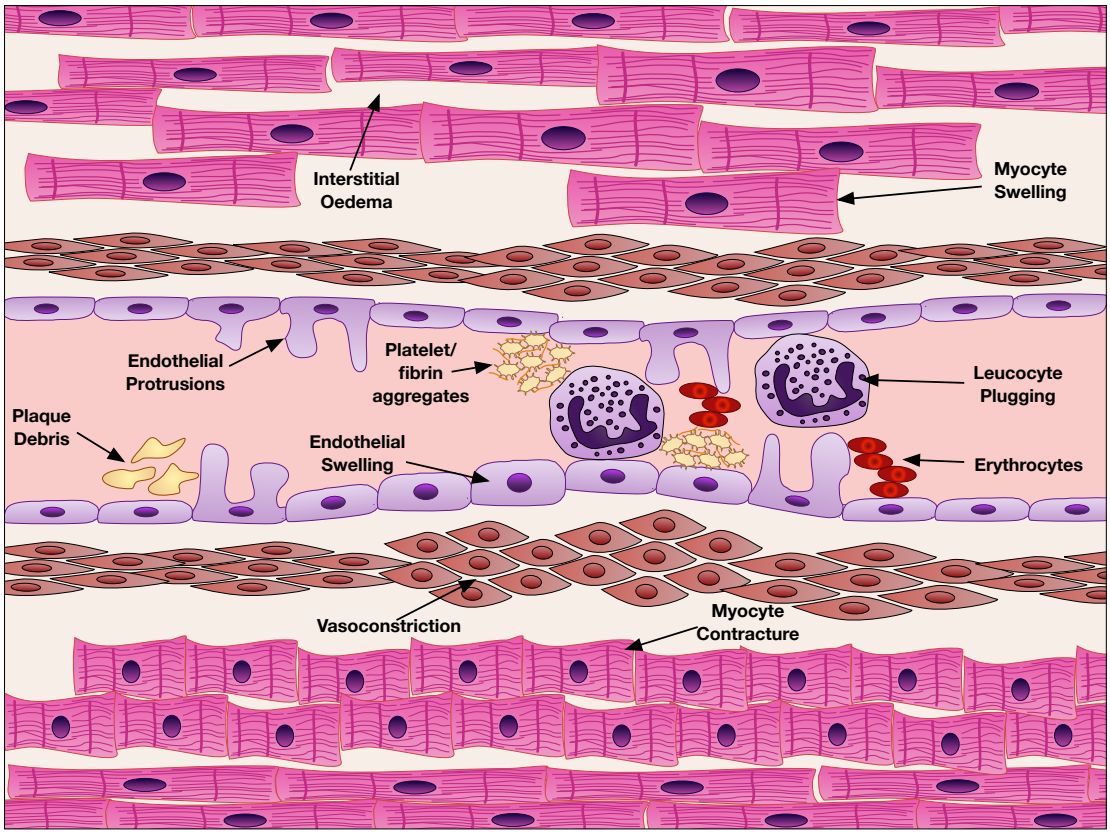

Figure 1.2: Known mechanisms of MVO in reperfused STEMI.

MVO following PPCI can result in characteristic changes on coronary angiography, including sluggish coronary flow (Iwakura et al., 1996). However, 30-50% of patients with apparently normal flow on angiography following reperfusion have evidence of MVO on further imaging, for instance by contrast echocardiography or magnetic resonance imaging (MRI) (Hombach et al., 2005; Ito et al., 1996). Cardiac MRI scanning, in particular, has become an increasingly useful method for identification of MVO, as will be discussed further below.

1.2.5 Prognostic Impact of MVO

The presence of MVO is of great clinical significance, as has been demonstrated by a number of studies showing relationships with adverse outcomes (Bolognese et

al., 2004; de Waha et al., 2010; Hombach et al., 2005; Ito et al., 1996; Wu et al., 1998b; Wu, 2012). It is known to be associated with larger infarct size, lower LVEF and adverse LV remodelling (Bolognese et al., 2004; Hombach et al., 2005; Ito et al., 1996; Wu et al., 1998b). Furthermore, it is a predictor of adverse clinical outcomes, including mortality and the composite end-point of death, MI and heart failure, independent of infarct size (de Waha et al., 2010; Hombach et al., 2005; Wu et al., 1998b; Eitel et al., 2014). Given its clinical significance and ease of measurability, MVO represents a useful end point for studies and clinical trials investigating reperfusion injury (Atar et al., 2009; Nazir et al., 2014; Wu, 2009).

1.2.6 Lethal Reperfusion Injury

This final component of myocardial I/R injury is defined as "reperfusion induced death of cardiomyocytes that were viable at the end of the index ischaemic event" (Hausenloy and Yellon, 2013). There are a number of potential contributory factors to this process.

1.2.7 Oxidative Stress

Shortly after myocardial reperfusion, a burst of oxidative stress occurs which results in cell death through several interacting mechanisms (Zweier et al., 1987). During ischaemia, myocardial cells switch their metabolism to anaerobic respiration. However, upon reperfusion, there is rapid restoration of aerobic metabolism, through reactivation of the mitochondrial electron transport chain. This results in excess production of reactive oxygen species (ROS), of which superoxide ($O_2^{\bullet -}$) is the most abundant (Monassier, 2008). This exceeds the capacity of the physiological anti-oxidant system that normally converts superoxide to hydrogen peroxide (H_2O_2) then to water (H_2O) and oxygen (O_2) (Raedschelders et al., 2012; Sanada et al., 2011). Furthermore, ROS generation also occurs through cellular xanthine oxidase, which catalyses the oxidation of xanthine and hypoxanthine to uric acid, coupled to the reduction of molecular oxygen to $O_2^{\bullet -}$ (Raedschelders et al., 2012). Hypoxanthine accumulates during ischaemia, and the above reaction then occurs upon reperfusion when oxygen supply is restored

(Raedschelders et al., 2012). The resultant ROS contribute to I/R injury through a number of mechanisms including direct damage to cellular structures, enzymes and DNA, acting as a neutrophil chemoattractant, and opening of the mitochondrial permeability transition pore (MPTP – see below) (Hausenloy and Yellon, 2013; Sanada et al., 2011).

1.2.8 Changes in Intracellular pH and Calcium Overload

During ischaemia, myocardial cells are forced to undergo anaerobic glycolysis in at attempt to maintain ATP availability. This results in accumulation of lactic acid and a drop in the intracellular pH. In an attempt to counter this, H^+ is excreted from the cell in exchange for Na^+ by the Na^+/H^+ exchanger channel in the cell membrane, resulting in intracellular Na^+ excess (Hausenloy and Yellon, 2013; Sanada et al., 2011). This, in turn, leads to reverse action of the $2Na^+/Ca^{2+}$ exchanger to facilitate excretion of Na^+ in exchange for Ca^{2+}, resulting in an excess of intracellular Ca^{2+} (Schafer et al., 2001). This is further compounded by the reduction in intracellular pH, which prevents functioning of the Na^+/K^+ ATPase and ATP dependent Ca^{2+} excretion and reuptake into the sarcoplasmic reticulum (Sanada et al., 2011).

Intracellular calcium overload mediates myocardial cell damage through multiple mechanisms including hypercontracture, opening of the MPTP, activation of proteases, and induction of apoptosis (Hausenloy and Yellon, 2013; Sanada et al., 2011). However, during ischaemia these processes are inhibited by the acidic intracellular pH. During reperfusion, however, correction of the pH occurs, reversing this protective inhibition (Sanada et al., 2011).

1.2.9 Mitochondrial Permeability Transition Pore Opening

One process that is thought to be a key effector in the early pathophysiology of I/R injury is opening of the MPTP. This is a channel in the inner mitochondrial membrane that it usually closed in the physiological state. However, opening of the pore can be induced by intracellular calcium excess (Di Lisa and Bernardi, 2006; Halestrap, 2009; Hausenloy et al., 2009). This has a number of deleterious effects

on the cell, culminating in cell death. Following opening, the mitochondrial membrane potential collapses, preventing further ATP synthesis through oxidative phosphorylation, leading to ATP depletion (Di Lisa and Bernardi, 2006; Halestrap, 2009; Hausenloy et al., 2009). Furthermore, pore opening causes mitochondrial swelling and eventual rupture, leading to the release of pro-apoptotic substances including cytochrome c (Halestrap, 2009; Heusch et al., 2010). Opening of the MPTP occurs following reperfusion-induced restoration of physiological pH (Hausenloy et al., 2009; Hausenloy and Yellon, 2013; Sanada et al., 2011). Moreover, production of ROS and intracellular Ca^{2+} excess triggered by reperfusion further promote this process (Sanada et al., 2011). MPTP opening has been the target of a number of potential treatments intended to reduce myocardial I/R injury, as will be discussed below (Hausenloy and Yellon, 2013).

1.2.10 Inflammation

Following reperfusion in MI, there is a marked inflammatory response characterised by the influx of neutrophils into the reperfused myocardium (Behar et al., 1994; Matusik et al., 2012; Monassier, 2008; Vinten-Johansen, 2004). This process begins immediately and proceeds over the subsequent 6 hours, with a second phase occurring after 24 hours (Monassier, 2008). The exact relationship between inflammation and myocardial I/R injury is not fully understood, but there is strong evidence to support a role for leucocytes in reperfusion-induced myocardial damage (Vinten-Johansen, 2004). In the case of ischaemia without reperfusion, neutrophil accumulation occurs slowly, peaking at 2-4 days, with their presence largely confined to the periphery of the ischaemic area (Vinten-Johansen, 2004). In contrast, with reperfusion the recruitment of neutrophils occurs more rapidly and in greater numbers, localised primarily in the centre of the infarct zone (Chatelain et al., 1987). Within the reperfused myocardium there is extensive release of ROS and inflammatory mediators, which attract neutrophils and drive inflammation (Vinten-Johansen, 2004; Matusik et al., 2012). Accumulated neutrophils release further ROS, as well as proteases, resulting in tissue damage (Vinten-Johansen, 2004). Furthermore, the influx of large numbers of these leucocytes leads to plugging of the capillary network, contributing to MVO (Vinten-Johansen, 2004).

Direct evidence for the role of this inflammatory response in I/R injury comes from animal studies demonstrating reduced infarct size with anti-inflammatory agents delivered at the time of reperfusion (Hausenloy and Yellon, 2013; Vinten-Johansen, 2004). These have included the use of antibodies blocking cell adhesion molecules, including P-selectin (Hayward et al., 1999) and CD18 (Ma et al., 1991; Baran et al., 2001; Faxon et al., 2002; Granger et al., 2003). Evidence for a link between inflammation and I/R injury in humans includes independent associations between systemic inflammatory markers and mediators, notably TNF-α and C-reactive protein (CRP), with both MVO and persistent ST-elevation after reperfusion in STEMI, findings thought to be related to I/R injury (Blancke et al., 2005; Durante and Camici, 2015; Ndrepepa et al., 2010).
Given their role in inflammation, induction and modification of the inflammatory response to reperfusion may be one potential mechanism through which lymphocytes, the principal focus of this project, could influence myocardial I/R injury. This will be discussed in more detail in subsequent sections.

1.2.11 Pharmacological Treatment of Myocardial Ischaemia/Reperfusion Injury

In spite of the considerable potential of myocardial I/R injury as a therapeutic target, successful treatment remains elusive and no specific therapies have reached routine clinical use (Garcia-Dorado et al., 2014; Hausenloy and Yellon, 2013). The failure to date to establish effective treatment strategies is in spite of extensive research and numerous clinical trials (Dirksen et al., 2007; Hausenloy and Yellon, 2013; Piper and Garcia-Dorado, 2012; Sharma et al., 2012).
Pharmacological strategies have included the use of anti-inflammatory agents, including pexelizumab, a monoclonal antibody to the C5 complement component (Armstrong et al., 2007), and CD11/CD18 integrin receptor blockers (Faxon et al., 2002), as well as anti-oxidants, aiming to reduce oxidative stress (Chan et al., 2012; Flaherty et al., 1994; EMIP-FR, 2000). However, randomised controlled trials (RCTs) assessing these treatments have been generally disappointing, failing to show any clear evidence of benefit (Dirksen et al., 2007; Hausenloy and Yellon, 2013; Sharma et al., 2012). One possible reason for the lack of positive clinical

outcomes could be that in many of the animal studies positive findings were apparent only after relatively short periods of ischaemia (generally <90 minutes) (Vinten-Johansen, 2004). In human clinical trials, however, ischaemic times have generally been generally significantly longer (up to either 6 or 12 hours), and may have missed the therapeutic window for such agents to be effective (Vinten-Johansen, 2004).

Attempts have also been made to reduce I/R injury though prevention of intracellular calcium overload using calcium channel blocking agents. While some smaller RCTs have suggested beneficial effects (Pizzetti et al., 2001; Sheiban et al., 1997; Theroux et al., 1998), these have not been upheld by larger studies (Bar et al., 2006).

Recently, pharmacological agents utilising naturally occurring protective mechanisms, such as the reperfusion injury salvage kinase (RISK) pathway, have been studied. This pathway consists of a series of protein kinases known to be activated during myocardial I/R, and is thought to exert beneficial effects at the level of the MPTP, preventing opening of the channel (Hausenloy et al., 2005). One such drug that has been tried is adenosine, which activates the pathway through the protein kinases extracellular-signal-regulated kinase (ERK)-1/2 and protein kinase C (PKC) (Morel et al., 2012; Sharma et al., 2012). However, the large AMISTAD II trial (n=5745) failed to show any overall positive findings with the use of this agent in the context of PPCI treated STEMI (Ross et al., 2005), although there was evidence of benefit in a subgroup analysis of anterior MI patients presenting early (Kloner et al., 2006). Another attempt to reduce I/R injury by targeting this pathway has been the use of insulin (Hausenloy and Yellon, 2007). Unfortunately, despite initially promising results from some small studies (Sharma et al., 2012; Zhang et al., 2005), the large CREATE-ECLA trial (n=20201) failed to show any significant benefit with glucose-potassium-insulin infusion in STEMI patients receiving reperfusion therapy (Mehta et al., 2005). A more promising agent utilizing the RISK pathway is the glucagon-like-peptide 1 (GLP-1) analogue exenatide (Lonborg et al., 2012; Morel et al., 2012). An RCT of 172 STEMI patients demonstrated a significant improvement in infarct size and myocardial salvage index with administration of this drug prior to reperfusion (Lonborg et al., 2012).

This encouraging result requires further study in larger trials evaluating clinical end points.

Another pharmacological strategy has been the use of drugs that directly inhibit opening of the MPTP (Morel et al., 2012). Of these agents the most promising has been cyclosporin, which also has immunosuppressive effects through inhibition of T cell activation (Azzi et al., 2013). Piot et al. conducted a small pilot RCT of 58 STEMI patients randomised to receive an intravenous bolus of cyclosporin or normal saline placebo prior to PPCI (Piot et al., 2008). They demonstrated a reduction in infarct size of 20% with cyclosporin measured by late gadolinium enhancement in a subset of the patients undergoing cardiac MRI (Piot et al., 2008). Since then, a further small trial has reported reduced adverse LV remodelling with administration of cyclosporin (Mewton et al., 2010). However, a similar sized study investigating the use of this drug along with thrombolytic therapy failed to find any benefit (Ghaffari et al., 2013). Unfortunately, a recent large clinical trial involving almost 800 patients has failed to show any improvement in clinical outcome measures at one year with cyclosporin treatment prior to PPCI (Cung et al., 2015). However, although the rationale for its use in these trials was inhibition of MPTP opening, it is conceivable that any biological effects of cyclosporin could also be in part due to its immunosuppressive properties. None of these trials were designed to assess immunological parameters.

1.2.12 Mechanical Treatment of Myocardial Ischaemia/Reperfusion Injury

It has long been established from animal models that periods of transient ischaemia prior to complete vessel occlusion protect the heart from subsequent I/R injury and reduce infarct size, a concept known as ischaemic preconditioning (Murry et al., 1986). It was subsequently demonstrated by Zhao et al. that the same is true of post conditioning (iPost), where a sustained period of vessel occlusion with subsequent reperfusion is followed shortly by brief periods of alternating vessel occlusion and reperfusion, before the vessel is opened a final time (Zhao et al., 2003). Both ischaemic pre and post conditioning are thought to exert their protective function through activation of the RISK pathway (Hausenloy and Yellon, 2007; Sanada et al., 2011).

Significantly, ischaemic post conditioning is very achievable in the STEMI population undergoing PPCI, as the vessel can be readily re-occluded through re-inflation of the angioplasty balloon. This has been tested in a number of clinical trials, with variable findings. While some early smaller trials have appeared to show a benefit with this treatment (Lonborg et al., 2010; Staat et al., 2005), others have shown no benefit or even evidence of harm (Freixa et al., 2012; Tarantini et al., 2012). Unfortunately, in recent years large clinical trials have not found any consistent benefit with iPost in human patients with STEMI treated by PPCI (Hahn et al., 2013; Hahn et al., 2015; Limalanathan et al., 2014).

1.3 Basic Immunology

This research project focuses on the role of immune cells, and specifically T lymphocytes, in myocardial I/R injury. It is, therefore, necessary to briefly outline the basic concepts behind the development and function of these cells.

1.3.1 The Immune System

At the most fundamental level, the immune system refers to the various systems that have evolved to protect us from infection. However, it has become clear that it also has involvement in huge variety of disease processes. It is intrinsically linked with the process of inflammation, which, as described above, is known to contribute to MI and I/R injury.

Traditionally, the immune system has been divided into innate and adaptive immunity. Innate immunity refers to relatively primitive pre-existing mechanisms able to defend the host against pathogens immediately at the time of exposure. Adaptive immunity, on the other hand, consists of more evolutionarily sophisticated defences against specific pathogens that take time to develop (Owen et al., 2013). However, as our understanding of the immune system has developed it has become clear that there is considerable overlap between the two systems (Iwasaki and Medzhitov, 2015). Nevertheless, it provides a useful framework to begin to consider the cells and mechanisms of the immune system.

1.3.2 Innate Immunity

The mechanisms of the innate immune system are the first stage of a host organism's defences upon pathogen exposure (Hoffmann and Akira, 2013). These include simple barrier defences, such as the skin, and more complicated processes such as inflammation, through which leucocytes, including neutrophils, monocytes and natural killer (NK) cells are recruited to sites of injury. There they exert a number of important antimicrobial functions as well as contributing to healing (Male et al., 2006; Owen et al., 2013). The innate immune system consists of both

humoral (secreted) components, including the complement system, and cell mediated components, such as the killing of abnormal cells by phagocytes (Owen et al., 2013).

1.3.3 Adaptive Immunity

The adaptive immune system consists of more evolutionarily advanced defence mechanisms, and is characterised by the ability to recognise and respond to specific threats. This specificity is one of the hallmarks of adaptive immunity, and involves the recognition of particular biological molecules, usually proteins or peptides, termed antigens, using specific receptors (Boehm, 2011). The principal cells of this system are B and T lymphocytes (B and T cells), each of which is able to recognise a specific antigen and mount a tailored response (Boehm, 2011). The other characteristic feature of the adaptive immune system is that it is able to learn from exposure to a particular pathogen, responding more rapidly and effectively on repeated exposure. This second hallmark of the adaptive immune system is termed immunological 'memory' (Zinkernagel et al., 1996).

As with innate immunity, the adaptive immune system has both a humoral arm, including the production and secretion of antibody by B cells, and a cell mediated arm, through the targeting and destruction of abnormal or infected cells by $CD8^+$ T cells (Owen et al., 2013).

1.3.4 Cells of the Immune System

Most of the principal cells of the immune system are derived from haematopoietic stem cells found in the bone marrow, which are able to divide and differentiate to form any type of blood cell (Akashi et al., 2000; Doulatov et al., 2012). These cells initially form two main lineage precursor cells; common myeloid precursors (CMPs), committed to the myeloid lineage, and multilymphoid progenitors (MLPs) (Doulatov et al., 2012). The MLP cells primarily differentiate to form the three types of lymphocytes, although at this stage they are also thought to retain some myeloid potential (Doulatov et al., 2012). The major populations of lymphoid cells

formed are T cells and B cells, which are the main cells of the adaptive immune system, and NK cells, which traditionally are viewed as part of the innate immune system (Doulatov et al., 2012; Owen et al., 2013). The CMP cells differentiate to form three separate lineages: the erythroid lineage, which forms red blood cells; the megakaryocytic lineage, which forms platelets, and the granulocyte/monocyte lineage, which forms many of the leucocytes of the innate immune system (Akashi et al., 2000; Passegue et al., 2003). In addition to these subsets, dendritic cells, which are antigen presenting cells (APCs), crucial in the initiation of adaptive immune responses, are thought to be formed by both myeloid and lymphoid progenitors (Doulatov et al., 2012).

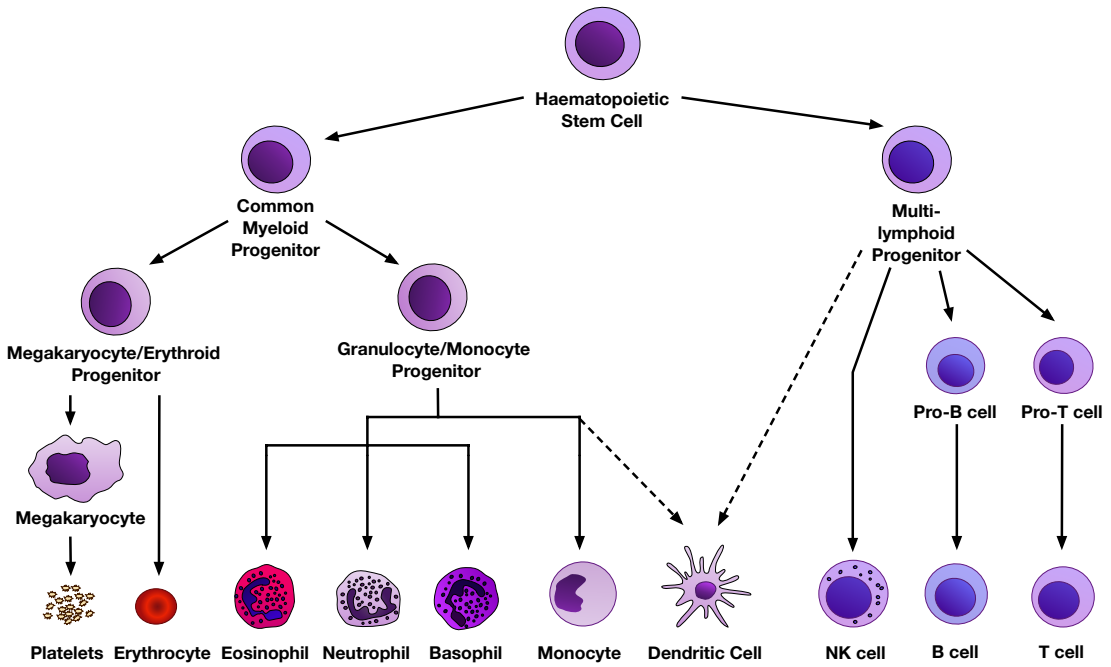

Figure 1.3: Simplified model of haematopoiesis. Based on models outlined in (Akashi et al., 2000; Doulatov et al., 2012; Passegue et al., 2003).

1.3.5 Lymphocytes

The principal cell type in the adaptive immune system is the lymphocyte. These can be divided into T cells, B cells and NK cells, each of which has wide ranging and very different functions.

The main function of B cells is the production of immunoglobulin (antibody). Each B cell expresses a single form of antibody, which is able to recognise a specific antigen (Boehm, 2011; Pieper et al., 2013). When expressed on the cell surface, this immunoglobulin forms the B cell receptor (BCR). Upon exposure to their specific antigen under appropriate circumstances, B cells are activated to proliferate and secrete large quantities of antibody, which has a number of functions in defence against pathogens (Nutt et al., 2015; Owen et al., 2013).

NK cells are traditionally considered to be part of the innate immune system. They are not able to recognise a specific antigen, but have a role in destruction of abnormal cells, for instance tumour cells or those infected with intracellular pathogens (Vivier et al., 2008).

The third type of lymphocyte, and the focus of this research project is the T cell.

1.3.6 T Lymphocytes

T cells have a wide variety of functions in the adaptive immune system and can be divided into a number of subsets. The characteristic feature of all T cells, however, is the possession of the T cell receptor (TCR).

The TCR is a cell surface receptor, consisting of a heterodimer of two different polypeptide chains (Andreu-Ballester et al., 2012; Owen et al., 2013). Each TCR is able to recognise a specific antigenic peptide, displayed on the surface of another cell in conjunction with a major histocompatibility complex (MHC) molecule (Male et al., 2006; Owen et al., 2013). Although each T cell displays only a single specific type of TCR, there is such enormous diversity in the T cell pool that each individual possesses T cells able to recognise countless different antigens. This allows the organism to mount an adaptive immune response to a huge variety of pathogens. To be capable of signalling following antigen exposure, the TCR chains must associate with a further series of polypeptide molecules known as the CD3 complex. This is expressed on all mature T cells and at various stages of T cell development (Dave, 2009; Kuhns and Badgandi, 2012).

1.3.7 T Cell Development

The key stages in T cell development occur in the thymus and involve gene rearrangement to produce the TCR, as well as differentiation into one of the main T cell subsets (Male et al., 2006; Owen et al., 2013; Spits, 2002). The vast majority of T cells are characterised as either $CD4^+$ or $CD8^+$ T cells, depending on which of these markers they express. These two additional cell surface molecules are co-receptors, essential for the recognition and response to antigen by the TCR. CD4 is necessary for successful TCR binding to MHC class II/peptide complexes, while CD8 is required for binding to MHC class I/peptide complexes (Owen et al., 2013).

Early in the process of T cell development, lymphoid precursor cells not yet committed to the T cell lineage migrate to the thymus from the bone marrow. There they progress into the T cell developmental pathway, at which point they are known as thymocytes, and undergo gene rearrangement to express a TCR (Blom and Spits, 2006; Koch and Radtke, 2011). They then undergo two selection stages throughout which the vast majority die. During positive selection, the thymocytes must receive survival signals from weak interaction with self-peptide/MHC complexes (Klein et al., 2009; Spits, 2002). The surviving cells then undergo negative selection, through which all cells that interact strongly with self-peptide/MHC are deleted (Klein et al., 2009). These processes ensure that the final surviving cells are able to interact strongly enough with self MHC to allow them to screen for foreign antigenic peptides displayed by APCs, yet they should not interact strongly enough to lead to activation and an inappropriate autoimmune response.

1.3.8 $CD4^+$ T Cells

Mature T cells expressing CD4 on their surface are known as T helper cells. They are so-named because following activation they exert their effects by secretion of cytokines and directly interacting with other cell types, assisting them in their functions. $CD4^+$ T helper cells can be further characterised, depending on the cytokines they secrete and types of responses they facilitate (Jiang and Dong, 2013; Owen et al., 2013).

The first two T helper cell subsets to be discovered are known as T_H1 and T_H2 cells (Abbas et al., 1996; Jiang and Dong, 2013). T_H1 cells produce inflammatory cytokines including IFN-γ and TNF- α, and their principal role is in protection against intracellular pathogens (Abbas et al., 1996; Jiang and Dong, 2013). They do this predominantly by helping macrophages and $CD8^+$ T cells to eliminate infected cells, and by helping B cells to produce classes of antibody that are effective against these types of pathogens (Jiang and Dong, 2013). However, this cytokine profile also promotes inflammation, and T_H1 cells are known to have a pathological role in both autoimmune and delayed-type hypersensitivity reactions (Owen et al., 2013). At this point, it is also worth considering that IFN-γ production by $CD4^+$ T cells has been shown to have an important role in myocardial I/R injury in a mouse model, as will be discussed further below (Yang et al., 2006).

T_H2 cells, on the other hand, are characterised by the production of IL-4, IL-5, IL-10 and IL-13 (Abbas et al., 1996; Jiang and Dong, 2013). These cells principally help B cells to produce antibodies effective against extracellular pathogens (Jiang and Dong, 2013).

Several other $CD4^+$ T cell subsets have now been identified. These include regulatory T cells (T_{reg} cells), which express CD25, and are known to have immunoregulatory properties, helping to suppress inflammation and autoimmune disease (Jiang and Dong, 2013). Other recently discovered subsets include T_H17 cells, which produce the pro-inflammatory cytokine IL-17 and are thought to contribute to autoimmune disease (Jiang and Dong, 2013).

1.3.9 $CD8^+$ T Cells

As mentioned previously, $CD8^+$ T cells are able to recognise antigenic peptides expressed in conjunction with MHC class I molecules. In contrast to MHC class II, which is only expressed by certain specialised APCs, MHC class I is found on the surface of all cell types (Male et al., 2006; Owen et al., 2013). Cells infected with intracellular pathogens can present foreign peptides in conjunction with these molecules (Male et al., 2006; Owen et al., 2013). The main role of $CD8^+$ T cells is to

detect such infected cells and destroy them by inducing apoptosis, helping to eliminate the pathogen (Wong and Pamer, 2003). Owing to this ability to induce cell death, $CD8^+$ T cells are also known as cytotoxic T lymphocytes (CTLs).

As well as inducing the death of cells through direct interaction with them, $CD8^+$ T cells also produce and secrete cytokines (Harty et al., 2000; Mosmann et al., 1997). These are primarily pro-inflammatory cytokines such as IFN-γ and TNF-α, a profile similar to that produced by T_H1 cells, although a subset of $CD8^+$ T cells can produce T_H2 type cytokines (Mosmann et al., 1997).

1.3.10 γδ T Cells

Brief mention should be given to a further subset of T cells that, while not the principal focus of this thesis, may nevertheless be relevant in MI and I/R injury. While the majority of T cells have a TCR composed of an α and a β chain, γδ T cells have a structurally different TCR, consisting of γ and δ polypeptide chains. In humans they constitute approximately 4% of total T cells (Chien et al., 2014). In contrast to the more common αβ T cells, antigen recognition is not restricted to those presented in conjunction with MHC molecules (Carding and Egan, 2002). The majority of γδ T cells do not express either CD4 or CD8, although a minority are positive for CD8 expression (Carding and Egan, 2002). This heterogeneous group of cells comprise several further subsets, and have a variety of effector functions including cytokine production and cytotoxicity (Carding and Egan, 2002; Prinz et al., 2013). One subset of γδ T cells, for instance, are known to be major producers of the pro-inflammatory cytokine IL-17 (Carding and Egan, 2002).

1.3.11 T Cell Activation and Development of Effector Cells

Under most circumstances in order for a T cell to proliferate and mount an immune response, it must first be exposed to its specific antigenic peptide/MHC complex on the surface of another cell. The engagement of the TCR results in a signalling cascade necessary for T cell activation (Smith-Garvin et al., 2009). However, this alone is insufficient and a second signal is required for activation,

without which the T cell enters a non-functional state known as anergy (Smith-Garvin et al., 2009). This second signal is provided by the APC in circumstances where an immune response is deemed appropriate, through a process known as costimulation. This involves interaction between costimulatory receptors on the surface of the T-cell, the best characterised of which are CD27 and CD28, with their corresponding ligands on the surface of the APC (CD80 or CD86) (Smith-Garvin et al., 2009). In the presence of these two signals the T cell becomes activated and starts to secrete IL-2, a pro-proliferative cytokine. The T cell then undergoes multiple rounds of division, producing a large number of daughter cells. During this phase the eventual phenotype of the cell is determined by the local cytokine environment (Pepper and Jenkins, 2011).

It is also important to note, however, that in other circumstances T cell activation can occur without specific antigen recognition. It has been shown that certain danger associated molecular patterns (DAMPs), as well as combinations of cytokines, are able to induce proliferation and differentiation of T cells to develop effector functions without antigen exposure (Imanishi et al., 2007; Unutmaz et al., 1994). In the case of DAMPs this occurs through binding to another group of cell surface molecules, pattern-recognition receptors (PRRs), including toll-like receptors (TLRs) (Imanishi et al., 2007). It is thought that these mechanisms of T cell activation may be important in circumstances of sterile inflammation, such as that seen in MI and I/R injury (Huang et al., 2007; Rao et al., 2014).

1.3.12 Generation of T Cell Memory

An adaptive immune response results in rapid proliferation of activated T cells and generation of large numbers of effector cells directed against the initiating antigen. Once the initial insult has been cleared the vast majority of these cells die by apoptosis. However, a small number of memory T cells are generated and persist after antigen clearance, being maintained for many years, most likely by homeostatic proliferation (Farber et al., 2014). These cells are phenotypically different from naïve T cells (T_N cells), expressing an altered pattern of cell surface molecules (Sallusto et al., 1999). They are able to respond quickly to subsequent re-exposure to the same antigen, leading to a more rapid and robust secondary

immune response. It is the generation and maintenance of these cells that forms the basis for immunological memory, one of the characteristics of the adaptive immune response.

1.3.13 T Cell Subpopulations

It is possible to sub-classify both $CD4^+$ and $CD8^+$ T-cells on the basis of surface molecules that are known to reflect different stages in T cell differentiation. I will, therefore, discuss some of these markers, and describe a well-recognised classification model used in this project.

1.3.14 CD45RA/RO Expression

CD45, also known as common leucocyte antigen, is a glycoprotein found on the surface of all myeloid and lymphoid cells (Clement, 1992). It exists in a number of isoforms, which are differentially expressed on the surface of lymphocytes. Although the exact function of this molecule is not fully understood, it is known that prior to antigen exposure, T_N cells express the CD45RA isoform (Clement, 1992; Henson et al., 2012). Upon activation, this isoform is downregulated and replaced with the smaller CD45RO molecule (Clement, 1992; Henson et al., 2012). Consequently, it was initially thought that expression of CD45RA identified T_N cells, while the presence of CD45RO (or absence of CD45RA) characterised the antigen experienced primed/memory pool (Akbar et al., 1988). It has subsequently become apparent, however, that a subset of memory cells switch back from CD45RO to CD45RA expression at an advanced stage of differentiation (Henson et al., 2012).

1.3.15 CCR7 and CD62L Expression

One of the characteristic features of different T cell sup-populations is that they exhibit different patterns of migration. T_N cells, for example, continually circulate through secondary lymphoid tissues, which they enter from the blood via specialised high endothelial venules (HEV) (Masopust and Schenkel, 2013). These

cells express a number of surface molecules that facilitate this migration, including CD62L (L-selectin), an adhesion molecule that mediates leucocyte rolling in the HEV (Grailer et al., 2009). The chemokine receptor CCR7 is then critical in mediating transmigration into the lymphoid tissue through interaction with its ligands, the chemokines CCL19 and CCL21 (Moschovakis and Forster, 2012). T cells with immediate effector function do not need to migrate to lymph nodes, and do not express these lymph node homing molecules (Masopust and Schenkel, 2013; Sallusto et al., 2004). Instead such cells circulate through non-lymphoid tissues, where they are potentially able to encounter pathogenic antigen at the sites of infection or injury (Masopust and Schenkel, 2013).

1.3.16 A Model of T Lymphocyte Subpopulations

In 1999, in a seminal paper, Sallusto et al. proposed a T cell classification model based on the expression of CCR7 and CD45RA (Sallusto et al., 1999). It is known that naïve T cells (T_N) cells express both of these molecules, but lose expression of CD45RA following antigen exposure and activation. The absence of CD45RA expression was, therefore, taken to identify an antigen experienced memory phenotype. These CD45RA negative cells, however, were shown to represent two different subpopulations based on the expression of CCR7 (Sallusto et al., 2004). $CCR7^+CD45RA^-$ cells lack immediate effector cell function, but home to secondary lymphoid tissues, where they are able to rapidly differentiate and form effector cells following further antigen exposure (Sallusto et al., 2004). This population of cells was termed central memory (T_{CM}) cells (Sallusto et al., 1999). T cells lacking both CCR7 and CD45RA, however, maintain immediate effector functions and home to inflamed non-lymphoid tissues (Sallusto et al., 2004). Consequently these cells were termed effector memory (T_{EM}) cells (Sallusto et al., 1999).

In addition, Sallusto et al. also identified a further subset of $CD8^+$ T cells that did not express CCR7, but did express CD45RA (Sallusto et al., 1999). These cells displayed high levels of effector functions, including perforin expression (Sallusto et al., 1999). It has since become clear that this $CCR7^-CD45RA^+$ population does exist in small numbers in the $CD4^+$ as well as $CD8^+$ T cell pool, and that it represents a highly differentiated subset that has been termed terminally

differentiated effector memory T cells (T_{EMRA}) (Henson et al., 2012; Koch et al., 2008).

The subclassification of $CD4^+$ and $CD8^+$ T cells into T_N, T_{CM}, T_{EM} and T_{EMRA} cells based on expression of CCR7 and CD45RA is now well established (Koch et al., 2008; Sallusto et al., 1999; Sallusto et al., 2004) and is the method I have used in this project.

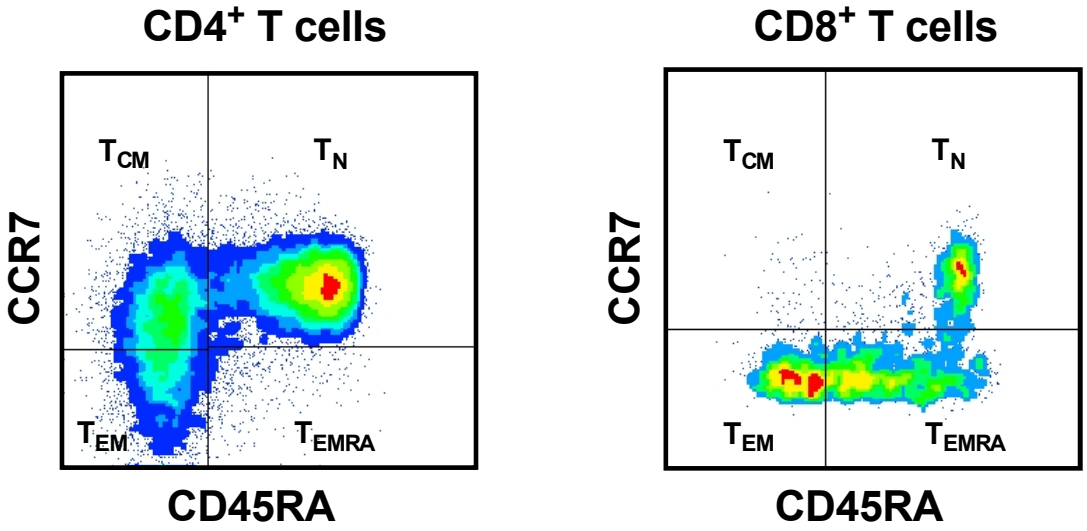

Figure 1.4: T cell subclassification model, using expression of CD45RA and CCR7. Based on model proposed by Sallusto et al. (Sallusto et al., 1999; Sallusto et al., 2004)

1.3.17 CD28 and CD27 Expression

As discussed previously, CD27 and CD28 are important costimulatory molecules on the surface of T cells. Moreover, their expression is regulated during the stages of T cell differentiation, and consequently they provide additional information concerning T cell phenotype (Appay et al., 2008). T_N cells ($CCR7^+CD45RA^+$) express both CD27 and CD28, allowing them to respond to costimulation in the context of antigen exposure (Appay et al., 2008). These molecules are then downregulated as differentiation of antigen experienced cells progresses (Appay et al., 2002). Consequently, some models of T cell subpopulations have used expression of these molecules, rather than CCR7 to classify cells (Appay et al., 2008). In reality,

however, there is considerable overlap in expression of each of these alternatives, and the resultant classification models (Appay et al., 2008). In the case of antigen experienced $CD8^+$ T cells, the T_{CM} population tend to express both CD28 and CD27, but the more differentiated populations lose expression of CD28, followed by CD27 (Appay et al., 2002; Appay et al., 2008). $CD4^+$ T cells, on the other hand, lose expression of CD27 followed by CD28 (Okada et al., 2008). In both cases the cells lacking expression of these costimulatory molecules appear to represent a highly differentiated population with potent effector functions, largely overlapping with the T_{EMRA} population in the model described above (Appay et al., 2002; Appay et al., 2008; Okada et al., 2008; Sallusto et al., 2004). In order to provide additional information concerning the differentiation stage of T cells in my own studies, I have assessed CD27 expression in each of the subpopulations in addition to the classification model described above.

1.4 Leucocytes in Myocardial Infarction

1.4.1 Introduction

Leucocytes are known to be critical cells in coronary artery disease, playing a key role in the pathogenesis of atherosclerosis, as well as in the destabilisation of plaques leading to MI. Increasingly, their importance in both myocardial injury and healing is becoming appreciated. While the majority of research in this area has been devoted to monocytes, it is now becoming clear that other leucocytes, including lymphocytes, are recruited to the myocardium during and following MI. Comparatively little work has been conducted investigating the role of these cells, although this is now recognised as an important and underinvestigated area requiring further research (Hofmann and Frantz, 2015).

1.4.2 Myocardial Leucocyte Recruitment Following MI – Data From Animal Models

To date few studies have sought to characterise myocardial leucocyte recruitment following MI in humans and most available data comes from murine models. One study by Yan et al. used a mouse model of MI with or without reperfusion, quantifying leucocyte subsets within the myocardium using flow cytometry at various time points (Yan et al., 2013). They found that the predominant leucocytes present were macrophages, although neutrophils, T cells, B cells and NK cells all show highly significant recruitment compared to mice exposed to a sham procedure (Yan et al., 2013). In MI without reperfusion, myocardial neutrophil numbers peaked at day 3, while those of macrophages, T cells, B cells and NK cells all peaked later at day 7 (Yan et al., 2013). In spite of this late peak, there was highly significant recruitment of most leucocyte subsets, including T cells, by day 1 post-MI (Yan et al., 2013). In contrast, in MI with reperfusion the total number of leucocytes recruited was reduced compared to non-reperfused MI, with the lymphocyte peak occurring earlier after only 3 days (Yan et al., 2013).

In addition to studying myocardial leucocyte numbers, Yan et al. also characterised the cells phenotypically. With regard to the T cells recruited following MI with reperfusion, they found that that $CD4^+$ T cells displayed a primarily pro-inflammatory T_H1 phenotype, with far fewer T_H2 cells (Yan et al., 2013). Moreover, they found that the expression of the T_H1 promoting cytokine IL-12 peaked strongly in the heart early after MI (Yan et al., 2013). There were also relatively high numbers of T_{reg} cells found in the myocardium, and this was associated with expression of the anti-inflammatory cytokine IL-10, which peaked later at day 7 (Yan et al., 2013). While this detailed study does shed considerable light on the temporal evolution of myocardial leucocyte recruitment following MI, it may not accurately reflect the situation in human patients. Furthermore, the earliest time point studied was at 1 day post-MI, telling us very little about the very early events occurring during ischaemia and immediately following reperfusion.

Two further studies have addressed the question of lymphocyte recruitment into the myocardium in mouse models of MI without reperfusion. Zouggari et al. demonstrated infiltration of B cells with a peak at day 5 (Zouggari et al., 2013). In the same study T cells were present when first measured at 0.5 days, before peaking after 1 day and declining thereafter. This represents a significantly earlier peak in T cell infiltration than that found by Yan et al. (Yan et al., 2013). Another study by Hofman et al. has investigated recruitment of $CD4^+$ T cells. They found these cells to be present in the myocardium by day 3, peaking at day 7 after MI, before their numbers declined (Hofmann et al., 2012). Unfortunately, they did not report any findings for any cellular recruitment at earlier time points. Both of these studies, however, involved permanent coronary artery ligation without reperfusion, and therefore no I/R injury will have been induced. It is feasible that $CD4^+$ T cells could have quite different recruitment patterns in infarcts with and without reperfusion.

Several other studies investigating leucocyte recruitment following MI have primarily focussed on monocytes. Using a mouse MI model involving permanent coronary artery ligation (i.e. without reperfusion), Nahrendorf et al. demonstrated bimodal recruitment of different monocyte subsets (Nahrendorf et al., 2007). There was early recruitment of inflammatory Ly-$6C^{hi}$ monocytes with substantial

numbers present at 1 day post-MI and peaking at day 3, followed by a later phase of anti-inflammatory Li-6C^{lo} cells peaking at day 7 (Nahrendorf et al., 2007). Ly-6C^{hi} monocytes are thought to differentiate into inflammatory M1 macrophages, while Ly-6C^{lo} cells correspond to the M2 phenotype. It is thought that M1 cells have an important role in phagocytosis and removal of necrotic debris, while M2 cells guide myocardial repair and healing (Nahrendorf et al., 2010; Swirski and Nahrendorf, 2013). The same study also demonstrated substantial neutrophil influx beginning almost immediately post-infarct, although recruitment of lymphocytes was not investigated (Nahrendorf et al., 2007). Another murine study has shown similar bimodal recruitment of monocytes, as well as demonstrating that this also occurred in smaller numbers in remote areas of myocardium not directly involved in the infarct (Lee et al., 2012). Furthermore, another study has reported that inflammation and leucocyte recruitment were seen at distant sites including the kidney in a mouse model of MI, although the leucocyte subsets involved were not characterised (Ruparelia et al., 2013).

A recent study by Jung et al. utilised real-time imaging of labelled cells in a murine MI model using a minimally invasive endoscope, allowing in vivo investigation of leucocyte recruitment in the very early stages of MI (Jung et al., 2013). They demonstrated rapid recruitment of cells expressing the chemokine receptor CX3CR1, which were primarily monocytes, within 30 minutes of the onset of ischaemia (Jung et al., 2013). At this very early stage, recruitment of CX3CR1 positive cells actually outstripped that of neutrophils, which peaked after a day (Jung et al., 2013). However, as with many other studies, there was no reperfusion component, and lymphocyte recruitment was not specifically investigated.

1.4.3 Myocardial Leucocyte Recruitment Following MI in Human Patients

Characterisation of myocardial leucocyte recruitment following MI in human patients is extremely challenging given the difficulty in obtaining tissue specimens from living patients. One study has investigated the infiltration of monocytes into the myocardium of patients who had died following MI, dividing cases into early (~3-12h post-MI), inflammatory (12h-5 days) and proliferative (5-15 days) phases based on time of death (van der Laan et al., 2014). They found that in early phase

hearts, the number of monocytes in the myocardium did not differ from control cases, although it must be noted that none of the patients had undergone successful reperfusion therapy (van der Laan et al., 2014). They identified significant recruitment of monocytes in the two later phases, with $CD14^+CD16^-$ monocytes dominating in the inflammatory phase, while $CD14^+CD16^-$ and $CD14^+CD16^+$ cells were later present in equal numbers (van der Laan et al., 2014). The human $CD14^+CD16^-$ subset is thought to correspond to the inflammatory Ly-$6C^{hi}$ subset in mice, whereas the $CD14^+CD16^+$ are analogous to Ly-$6C^{lo}$ cells.

Two studies by Abbate et al. have specifically investigated lymphocyte infiltration into the myocardium of patients who had died from cardiovascular disease (Abbate et al., 2004; Abbate et al., 2008). They demonstrated a T cell infiltrate in infarct regions and remote myocardium in patients with recent MI (1 to 12 weeks before death) that was not seen in control cases who had died from non-cardiac causes (Abbate et al., 2004). At that stage the infiltrate was greater in patients whose infarct related artery had remained occluded (Abbate et al., 2004). They subsequently demonstrated less marked myocardial T cell infiltration in patients who had died suddenly, between 0 and 0.25 days after MI onset, as well as in those who had died at a much later stage several months following MI (Abbate et al., 2008). However, while these studies do point to a role for T cells during and after MI, they are not able to clarify the temporal evolution of lymphocyte recruitment in the early stages of infarction. Moreover, they include patients treated by different strategies, with and without reperfusion, and in the context of concurrent pathologies including sepsis (Abbate et al., 2004; Abbate et al., 2008). Consequently, they provide little insight into the involvement of T cells in MI and I/R injury after successful reperfusion therapy.

1.4.4 Mechanisms of Leucocyte Recruitment

As outlined above, a marked inflammatory response occurs in the myocardium during myocardial ischaemia and directly following reperfusion. This is triggered initially by necrosis of cardiomyocytes, leading to release of intracellular contents (Christia and Frangogiannis, 2013). Such cellular debris contains a wide variety of DAMPs, which are recognised by other cell types through ligation of PRRs

including TLRs (de Haan et al., 2013). This leads to the release of various inflammatory mediators, triggering inflammatory cell infiltration. Furthermore, production of reactive oxygen species (ROS) by ischaemic tissue promotes activation of inflammatory cascades and mediator release (Lakshminarayanan et al., 2001; Nossuli et al., 2001). Myocardial gene expression studies in a mouse model of MI with reperfusion revealed rapid upregulation of the inflammatory cytokines TNF-α, IL-1β and IL-6, which then declined from 6-24 hours post-reperfusion (Christia et al., 2013). DAMPs liberated by necrotic cells and damaged extracellular matrix also cause activation of the complement cascade, resulting in production of anaphylatoxins, which are potent neutrophil chemoattractants, as well as upregulation of adhesion molecules on endothelial cells (Monsinjon et al., 2001). Exposure to ROS and complement components triggers degranulation of resident mast cells, causing release of preformed mediators including histamine and TNF-α (Frangogiannis, 2014). This contributes to further upregulation of chemokines and adhesion molecules by endothelial cells (Christia and Frangogiannis, 2013).

The process of leucocyte extravasation from the bloodstream to the tissues occurs in several stages. Firstly, there is an initial phase of rolling along the endothelial surface, which is mediated by adhesion molecules known as selectins (Ley, 1996). Exposure to immobilised chemokines on the endothelium then contributes to activation of another group of adhesion molecules, called integrins, which mediate firm binding and leucocyte arrest (Christia and Frangogiannis, 2013). Transmigration through the vascular wall is then directed by exposure to chemokine gradients. The particular milieu of chemokines and adhesion molecules present determines the subsets of leucocytes recruited, and varies throughout the process of ischaemia and reperfusion (Frangogiannis and Entman, 2005). Once present in the infarct zone, leucocytes help to sustain inflammation through release of mediators and cytokines, although they also have important roles in healing and resolution of inflammation (Frangogiannis, 2014; Nahrendorf and Swirski, 2013).

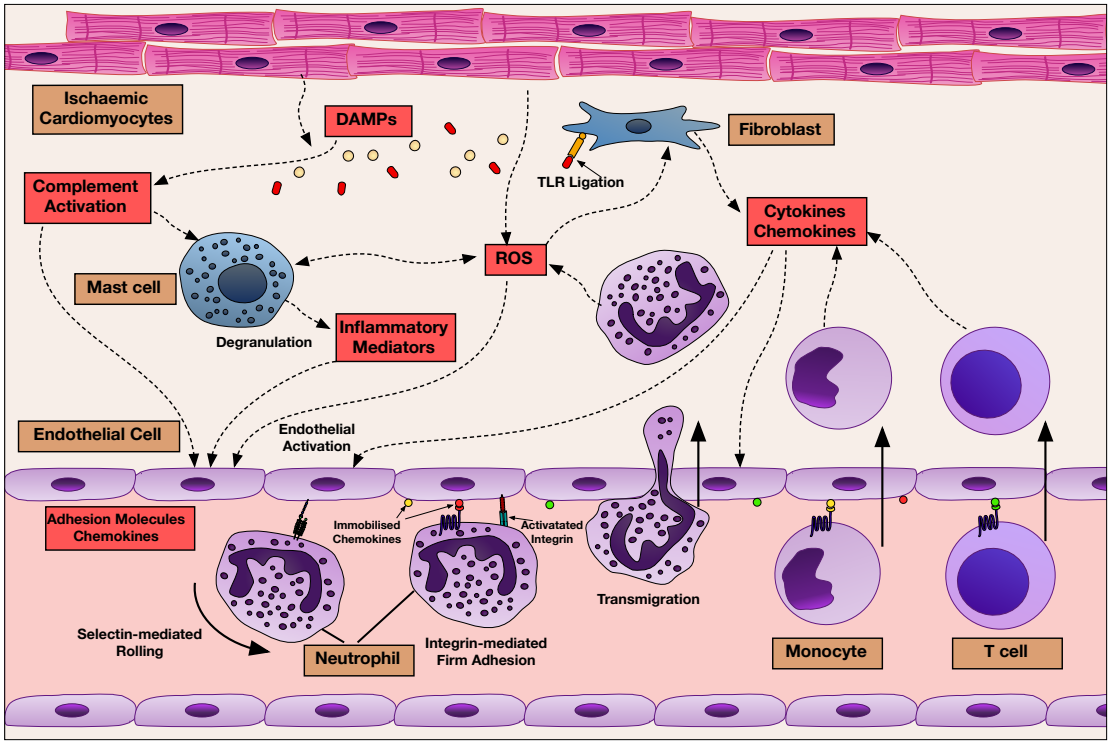

Figure 1.5: Inflammation and leucocyte recruitment in MI. Ischaemia induced cardiomyocyte stress and damage leads to release of DAMPs and ROS. Ligation of TLRs causes activation of inflammatory cascades in cells including resident fibroblasts, triggering release of cytokines and chemokines. The complement system is also activated. Resident mast cells degranulate, releasing a host of inflammatory mediators. These events induce endothelial cell activation, expression of adhesion molecules and production of chemokines. Leucocytes are recruited in response to these stimuli. Initial interaction with the endothelium occurs through selectin mediated rolling. Ligation of chemokine receptors by immobilised chemokines triggers integrin activation and firm adhesion, prior to transmigration. This process results in infiltration of various leucocyte populations, most notably neutrophils, monocytes and T cells, which further sustain the inflammatory process.

1.4.5 Chemokines in Leucocyte Recruitment

The chemokines are a group of small proteins that play a crucial role in leucocyte migration in health and disease. They do this through interaction with receptors found on the surface of leucocytes, directing movement of the cell towards an increasing chemokine concentration gradient. The chemokines themselves share a number of characteristics, including the presence (in most cases) of four cysteine residues, which form two disulphide bonds, resulting in three-dimensional folding of the molecule (Baggiolini, 2001). A total of over 50 chemokines have been identified, which can be divided into 4 groups based on the number and position of the cysteine residues in the N-terminal region (Le et al., 2004). The two main groups are CC (e.g. CCL1) chemokines, which have two adjacent N-terminal cysteines, and CXC chemokines (e.g. CXCL1), which have two cysteines separated

by another amino acid (Le et al., 2004). The remaining groups are C chemokines, which uniquely contain only two cysteines in total (one in the N-terminal region, one downstream), and CX3C chemokines, which have two N-terminal cysteines separated by three amino acids. The only known example of the latter group is fractalkine (CX3CL1), which exists both as a secreted and membrane bound form (Imai et al., 1997). Each chemokine is able to bind to one or more receptor, all of which share a characteristic structure consisting of seven transmembrane domains, with most coupled to a G-protein through which they signal (Bachelerie et al., 2014; Murphy et al., 2000). In addition to influencing migration, chemokines can have a number of other effects on cells, including activation and altered gene expression (Frangogiannis and Entman, 2005). Moreover, as well as their effects on leucocytes, chemokines are able to influence the function of non-immune cells, including endothelial cells and fibroblasts (Frangogiannis and Entman, 2005).

As outlined above, leucocyte recruitment to the myocardium following MI occurs in two main stages. These consist of an inflammatory phase, dominated by neutrophils and inflammatory monocytes, followed by a proliferative phase in which less inflammatory monocytes are predominant. Chemokines play a key role throughout these processes (Liehn et al., 2011a).

During the early inflammatory phase, several members of the CXC chemokine group are the principal inducers of neutrophil migration (Frangogiannis, 2007). The neutrophil chemotactic effect of these molecules appears to be dependent on the presence of a tripeptide glutamic acid-leucine-arginine (ELR) motif (Clark-Lewis et al., 1995), and they act by binding to one or both of the receptors CXCR1 and CXCR2 (Le et al., 2004). The prototypic neutrophil chemokine is CXCL8 (IL-8), which has been shown to be upregulated in myocardial I/R in a rabbit model (Kukielka et al., 1995). Moreover, blockade of IL-8 with a neutralising antibody reduces myocardial I/R injury in rabbits (Boyle et al., 1998). A number of other chemokines share similar features. One study in a rat model found that myocardial I/R induces expression of the ELR motif containing chemokines CXCL1, CXCL2 and CXCL6 (Chandrasekar et al., 2001). Neutralisation studies confirmed that all three of these molecules contribute to neutrophil infiltration (Chandrasekar et al., 2001).

Recruitment of monocytes during the inflammatory phase appears to be primarily dependant on another chemokine, CCL2 (MCP-1) (Frangogiannis, 2007; Liehn et al., 2011a). This molecule is upregulated in animal models of MI (Tarzami et al., 2002), and its production is accentuated by reperfusion (Kumar et al., 1997). Blockade of CCL2 in a mouse myocardial I/R model resulted in reduced monocyte infiltration and attenuated infarct size (Liehn et al., 2010). However, it is known that besides inflammatory leucocyte infiltration CCL2 has a number of other functions that may be important in myocardial healing (Cavalera and Frangogiannis, 2014; Frangogiannis, 2007; Morimoto and Takahashi, 2007). These include regulation of fibroblast activity and scar formation, as well as angiogenesis and anti-apoptotic effects on cardiomyocytes (Dewald et al., 2005; Morimoto and Takahashi, 2007). Indeed, there are reports of cardioprotective effects of CCL2 in myocardial I/R injury (Morimoto et al., 2008). This highlights the complex nature of the molecular events occurring in I/R injury, with multiple studies targeting particular molecules often yielding conflicting results.

After the initial phase dominated by neutrophils and monocytes, cells of a less inflammatory phenotype infiltrate the myocardium. These include a subset of monocytes whose recruitment is dependent on the chemokine receptors CX3CR1 and CCR5 interacting with the respective ligands, CX3CL1 (fractalkine) (Nahrendorf et al., 2007) and CCL5 (RANTES) (Liehn et al., 2011a). Other monocyte chemoattractants known to be expressed in MI include CCL3 (MIP-1α), CCL4 (MIP-1β) (Dewald et al., 2004) and CCL7 (MCP-3) (Schenk et al., 2007), although their specific roles in this setting are poorly understood.

Little is known about the mechanisms of lymphocyte recruitment following ischaemia and reperfusion. One group of T cells thought to contribute to infarct healing are T_{reg} cells (Dobaczewski et al., 2010; Weirather et al., 2014). They appear to be recruited through ligation of the chemokine receptor CCR5 (Dobaczewski et al., 2010), whose ligands include CCL3, CCL4 and CCL5 (Bachelerie et al., 2014). However, no convincing data exist concerning the molecular events involved in recruitment of other T cell subsets, notably IFN-γ producing T_H1 $CD4^+$ T cells. Chemokine receptors expressed by these cells include CCR5 (Bonecchi et al., 1998), CXCR3 (Yamamoto et al., 2000) and CX3CR1

(Bachelerie et al., 2014; Combadière et al., 2003). In addition to the CCR5 ligands mentioned above, this raises the possibility of the CXCR3 ligands (CXCL9, CXCL10 and CXCL11) as well as CX3CL1 (fractalkine) as possible candidates. Of these molecules CCL3 and CCL4 (Dewald et al., 2004; Nossuli et al., 2001), CXCL10 (Frangogiannis et al., 2001) and CX3CL1 (Njerve et al., 2014) have all been shown to be regulated following myocardial I/R. In addition, CCL5 is known to contribute to I/R injury in the renal system through T_H1 cell recruitment (Fiorina et al., 2006). It is worth noting that while CX3CR1 is found on highly differentiated T cells in humans, expression on murine T cells is negligible (Bachelerie et al., 2014; Jung et al., 2000), limiting the use of mouse models when studying this receptor in lymphocytes

Chemokine	Synonyms	Receptors	Main Target Leucocytes	Notes
CC Chemokines				
CCL2	- Monocyte chemotactic protein (MCP)-1	CCR2	Monocytes	- Recruitment of inflammatory monocytes in MI (Liehn et al., 2010).
CCL3	- Macrophage inflammatory protein (MIP)-1α	CCR1 CCR5	Monocytes T cells	- Upregulated following myocardial I/R (Dewald et al., 2004). - May have a role in neutrophil recruitment to myocardium and ventricular remodelling in mice (Liehn et al., 2008; Liehn et al., 2011a).
CCL4	- MIP-1β	CCR5 CCR8	Monocytes, T cells, Dendritic cells (DCs)	- Upregulated following myocardial I/R (Dewald et al., 2004). - Role in leucocyte recruitment in MI unknown (Frangogiannis, 2007).
CCL5	- Regulated upon activation, normal T-cell expressed and secreted (RANTES)	CCR1 CCR3 CCR5	Monocytes T cells DCs	- Administration of CCL5 antagonist reduced myocardial monocyte and neutrophil infiltration, and diminished infarct size in a mouse I/R model (Braunersreuther et al., 2010).
CCL7	- MCP-3	CCR1 CCR2 CCR3	Monocytes T cells (T_H2>T_H1)	- Contributes to homing of mesenchymal stem cells to infarcted myocardium in mice (Schenk et al., 2007). - Probable role for B cell derived CCL7 in monocyte recruitment to myocardium post-MI (Zouggari et al., 2013).
CX3C Chemokines				
CX3CL1	- Fractalkine	CX3CR1	Monocytes NK cells T cells (highly differentiated)	- Known to be regulated in human patients with STEMI treated by reperfusion therapy (Njerve et al., 2014). - Migration of CX3CR1 expressing leucocytes occurs very early (within 30 minutes) of MI (Jung et al., 2013). - Involved in recruitment of a subset of monocytes during the proliferative phase following MI (Nahrendorf et al., 2007). - Contributes to T cell migration (including T_H1) in other systems (Bachelerie et al., 2014; Fiorina et al., 2006), role in lymphocyte migration in MI unknown.

Table 1.1. Chemokines in leucocyte recruitment in myocardial infarction. Continued on next page.

Chemokine	Synonyms	Receptors	Main Target Leucocytes	Notes
CXC Chemokines				
CXCL1	- Growth regulated oncogene (GRO)-1 - Keratinocyte derived chemokine (KC)	CXCR1 CXCR2	Neutrophils	- Neutrophil infiltration in a rat model of myocardial I/R (Chandrasekar et al., 2001).
CXCL2	- MIP-2	CXCR2	Neutrophils	- Neutrophil infiltration in a rat model of myocardial I/R (Chandrasekar et al., 2001).
CXCL6	- LPS induces CXC chemokine (LIX)	CXCR1 CXCR2	Neutrophils	- Key role in neutrophil infiltration in a rat model of myocardial I/R (Chandrasekar et al., 2001).
CXCL8	- IL-8	CXCR1 CXCR2	Neutrophils	- Upregulated in a rabbit myocardial I/R model (Kukielka et al., 1995). - Inhibition reduced myocardial I/R injury in a rabbit model (Boyle et al., 1998).
CXCL9	- Monokine induced by interferon-γ (MIG)	CXCR3	T cells (T_H1>T_H2)	- Known T_H1 chemokine (Bachelerie et al., 2014), but impact on leucocyte recruitment in MI unknown. - Not significantly regulated in a mouse model of myocardial I/R (Saxena et al., 2014a).
CXCL10	- Interferon-γ induced protein (IP-10)	CXCR3	T cells (T_H1>T_H2)	- Known T_H1 chemokine (Bachelerie et al., 2014), but impact on leucocyte recruitment in MI unknown. - Limits adverse remodelling in a mouse model of myocardial I/R through CXCR3-independent anti-fibrotic effects (Bujak et al., 2009; Saxena et al., 2014a). - Role in preventing angiogenesis in early inflammatory phase of wound healing through angiostatic effects (Frangogiannis, 2007).
CXCL11	- Interferon inducible T-cell alpha chemoattractant (ITAC)	CXCR3	T cells (T_H1>T_H2)	- Known T_H1 chemokine (Bachelerie et al., 2014), but impact on leucocyte recruitment in MI unknown. - Not significantly regulated in a mouse model of myocardial I/R (Saxena et al., 2014a).
CXCL12	- Stromal cell-derived factor (SDF)-1	CXCR4	Progenitor Cells Monocytes	- Role in myocardial healing through recruitment of progenitor cells (Cavalera and Frangogiannis, 2014). - CXCR4 deficient mice show reduced neutrophil and delayed monocyte recruitment (Liehn et al., 2011b).

Table 1.1. Chemokines in leucocyte recruitment in myocardial infarction. Continued from previous page.

1.4.6 Innate Leucocytes in Myocardial Infarction and Healing

In order to understand the roles of leucocyte subsets recruited following MI it is necessary to outline the major processes involved in myocardial injury and healing. This can be broadly divided into three phases. In addition to the inflammatory and proliferative phases described above there follows a maturation phase in which mature scar is formed (Cavalera and Frangogiannis, 2014; van der Laan et al., 2012b).

The neutrophils and pro-inflammatory monocytes recruited during the first phase promote matrix breakdown, and phagocytose and remove non-viable tissue (van der Laan et al., 2012b). This important step is necessary before healing can occur (van der Laan et al., 2012b). However, this inflammatory response can be harmful if it is excessive or prolonged, leading to enhanced myocardial cell death and matrix degradation (Cavalera and Frangogiannis, 2014; Frangogiannis, 2012; Marchant et al., 2012). Numerous studies in animal models aimed at reducing inflammation during this phase have shown attenuated infarct size with this strategy, although these have not successfully led to beneficial human treatments (Braunersreuther et al., 2010; Hayward et al., 1999; Jolly et al., 1986; Liehn et al., 2008; Ma et al., 1991).

The proliferative phase is characterised by regulation of inflammation and formation of granulation tissue. During this stage, non-classical monocytes ($CD14^+CD16^+$ in humans, Li-$6C^{lo}$ in mice) and M2 macrophages secrete anti-inflammatory cytokines (e.g. IL-10 and TGF-β) as well as growth factors that encourage fibroblast proliferation and angiogenesis (van der Laan et al., 2012b). As a result, new blood vessels and extracellular matrix are formed, stabilising the developing scar. Neutrophils undergo apoptosis, delivering signals to macrophages resulting in their ingestion and removal. This triggers anti-inflammatory pathways within the macrophages, inducing further release of IL-10 and TGF-β (Frangogiannis, 2012). As such, inflammation subsides and repair takes over. During the final maturation phase fibroblasts undergo apoptosis and extracellular matrix is remodelled, ultimately forming a mature, collagen based scar (van der Laan et al., 2012b). These stages of infarct healing are inextricably linked and the

balance between inflammation and repair is key to determining a successful outcome or otherwise. In addition to causing direct myocardial damage in the early stages, failure to appropriately regulate inflammation can lead to infarct expansion, ventricular dilatation and deterioration of ventricular systolic function, contributing to excess long-term morbidity and mortality (Frangogiannis, 2012). Excessive matrix deposition during the proliferative phase, on the other hand, can contribute to ventricular stiffening and diastolic failure (Shinde and Frangogiannis, 2014). The leucocytes present have a critical role in regulating this delicate balance.

1.4.7 Lymphocytes in Myocardial Infarction and Healing

While a great deal of research has been conducted into the effects of monocytes and neutrophils in MI, there is a comparative paucity of data regarding the role of lymphocytes. However, some solid evidence exists of a key contribution by T_H1 cells in myocardial I/R injury, as well as several other lymphocyte subsets during healing and repair.

In addition to a role in I/R injury, which will be considered separately in the next section, recent studies have demonstrated an emerging contribution for T cells in the later stages of MI and infarct healing. Hofman et al., using a model of MI without reperfusion, showed that two types of $CD4^+$ T cell deficient mice (CD4 knockout [KO] and MHC class II deficient [$MHC^{\Delta/\Delta}$]) had reduced collagen deposition and neovascularisation in the infarct zone compared to wild-type mice at day 7 (Hofmann et al., 2012). Moreover, The CD4 KO mice showed increased left ventricular dilatation, while $MHC^{\Delta/\Delta}$ mice had excess mortality (Hofmann et al., 2012). Both of these groups displayed deranged collagen deposition and scar formation. These findings were associated with elevated numbers of granulocytes and $Ly6C^{hi}$ monocytes in the myocardium at day 7, indicating that $CD4^+$ T cells may be important in limiting inflammation at this stage during the healing process (Hofmann et al., 2012). However, in the same study no differences were seen in the number or composition of innate leucocytes in the myocardium at day 3, suggesting that such effects may be time specific (Hofmann et al., 2012).

Several researchers have suggested an important role for T_{reg} cells in myocardial healing following infarction. Two studies have shown that depletion of these cells resulted in enhanced inflammation in mouse models of MI (Saxena et al., 2014b; Weirather et al., 2014). T_{reg} depletion resulted in greater numbers of neutrophils and Ly-6C^{hi} monocytes, as well as total CD4$^+$ and CD8$^+$ T cells, in the myocardium compared to wild type mice (Weirather et al., 2014). Moreover, there was increased infarct size (Weirather et al., 2014), and greater ventricular dilatation and remodelling (Saxena et al., 2014b) in T_{reg} cell depleted mice. These mice also showed enhanced inflammatory M1 macrophage polarisation, while in wild type mice therapeutic T_{reg} cell activation resulted in greater anti-inflammatory M2 macrophage function and improved survival (Weirather et al., 2014). This is in keeping with two other studies in both rats and mice that have shown attenuated post-infarct myocardial inflammation and reduced adverse remodelling with T_{reg} cell activation or adoptive transfer (Matsumoto et al., 2011; Tang et al., 2012). In summary, there is strong evidence that T_{reg} cells contribute positively to myocardial healing following MI through reduction of inflammation during the proliferative phase, preventing excessive matrix degradation. It has also been suggested that they may have stimulatory effects on fibroblasts, promoting matrix deposition and stable scar formation (Hofmann and Frantz, 2015).

One study has shown a potential pathogenic role for γδ T cells (Yan et al., 2012). In a mouse model of MI without reperfusion, mice deficient in these cells were protected from adverse ventricular remodelling and had reduced infarct size at 28 days compared to wild type mice (Yan et al., 2012). This protection was associated with reduced sustained infiltration of inflammatory leucocytes, including neutrophils and macrophages, at day 7 post-MI. The mechanism of this appeared to be loss of production of the pro-inflammatory cytokine IL-17A by γδ T cells (Yan et al., 2012). In addition to increased inflammatory cell infiltration, IL-17A also has pro-apoptotic and pro-fibrotic effects, contributing to adverse cardiac remodelling (Yan et al., 2012).

Another study, on the other hand, has suggested a protective role during post-MI healing for a further minor T cell subset, called invariant NKT (iNKT) cells (Sobirin et al., 2012). Administration of a specific activator of these cells in a mouse model

of MI resulted in their increased infiltration into the myocardium at 7 days. This was associated with improved cardiac function and attenuated remodelling at 28 days. There was also increased expression of the anti-inflammatory cytokine IL-10 in the treated group (Sobirin et al., 2012).

Finally, one major study has investigated the role of B cells in a mouse model of MI without reperfusion (Zouggari et al., 2013). The investigators found that B cell depleted mice had reduced myocardial monocyte infiltration and inflammatory cytokine expression, as well as improved cardiac function and reduced ventricular remodelling at 14 days post-MI (Zouggari et al., 2013). Through a series of reconstitution experiments they demonstrated that B cell production of CCL7 contributed to monocyte infiltration and had an adverse effect on ventricular function post-MI (Zouggari et al., 2013). Moreover, the use of mice with leucocytes unable to respond to TLR signalling suggested that CCL7 production by B cells was, at least in part, dependent on this mechanism of stimulation (Zouggari et al., 2013). To date, this is the only study to perform an extensive mechanistic investigation of the role of B cells in MI. However, as with most of the studies discussed in this section, this animal model did not include a reperfusion component, limiting the value in the context of modern treatment in humans.

1.5 Evidence for a Role for Lymphocytes in Ischaemia/Reperfusion Injury

1.5.1 Myocardial I/R Injury

Most of the published research addressing the role of lymphocytes in MI has focussed on injury and healing in the absence of reperfusion. However, given the importance if I/R injury with modern reperfusion therapy, further understanding of the involvement of lymphocytes in this process is essential. There is a wealth of evidence implicating T cells, in particular, in I/R injury in various organ systems (Huang et al., 2007; Linfert et al., 2009). Surprisingly, myocardial I/R injury has received comparatively little attention in this regard. As briefly alluded to above, however, there is robust evidence from mouse models for an important role for $CD4^+$ T cells in this context.

This issue has been clearly evaluated in two studies by Yang et al. (Yang et al., 2005; Yang et al., 2006). They used a model involving transient occlusion of the left anterior descending (LAD) artery followed by reperfusion. They demonstrated that in wild type mice T cells, as well as neutrophils, accumulated in the previously ischaemic myocardium within minutes of reperfusion, and that this was associated with a drop in the peripheral blood lymphocyte count (Yang et al., 2006). Rag 1 KO mice, which lack mature lymphocytes, had reduced myocardial neutrophil accumulation as well as an absence of T cells in the heart following reperfusion (Yang et al., 2005; Yang et al., 2006). Furthermore, these mice were protected from I/R injury, developing smaller infarcts than wild type mice, and this protection was lost following adoptive transfer of $CD4^+$ T cells (Yang et al., 2006). Similar levels of protection were achieved with $CD4^+$ T cell depletion in wild type mice, while $CD8^+$ T cell depletion had no effect (Yang et al., 2006). Consequently, this provides clear evidence for a critical role for $CD4^+$ T cells in myocardial I/R injury in the mouse, likely due to pro-inflammatory effects. Moreover, adoptive transfer of $CD4^+$ T cells from IFN-γ KO mice to Rag 1 KO mice failed to abolish the protection from I/R injury, suggesting a critical role for this pro-inflammatory cytokine produced by T_H1 cells (Yang et al., 2006).

A number of studies have investigated the role of other T cell subsets in murine myocardial I/R injury. A study assessing the involvement of the T cell derived cytokine IL-17A found that it was primarily produced by γδ T cells in the reperfused myocardium (Liao et al., 2012). Inactivation of IL-17A with a neutralising antibody, or deletion using IL-17 KO mice, resulted in reduced infarct size and improved ventricular function compared to wild type mice (Liao et al., 2012). Moreover, administration of recombinant IL-17A prior to reperfusion further increased infarct size (Liao et al., 2012). As previously observed in MI without reperfusion (Yan et al., 2012), IL-17A was shown to have pro-apoptotic effects in cardiomyocytes in murine myocardial I/R, as well as increasing neutrophil infiltration through accentuated production of chemokines including CXCL1, CXCL2 and CXCL6 (Liao et al., 2012). Furthermore, in a study in rats the IL-17 pathway was shown to be activated following myocardial I/R, while blockade with an IL-17 neutralising antibody resulted in reduced cardiomyocyte apoptosis (Barry et al., 2013). Consequently, there is strong evidence that this cytokine contributes pathologically to myocardial I/R injury, and that in this situation it is primarily derived from γδ T cells.

Another group has investigated the role of iNKT cells in murine myocardial I/R injury (Homma et al., 2013). They found that administration of an activator of these cells prior to reperfusion reduced infarct size at 24 hours. This was associated with upregulation of the anti-inflammatory cytokine IL-10, although IFN-γ production also increased. Protection from I/R injury was abrogated by neutralisation of IL-10, while IFN-γ blockade reduced infarct size (Homma et al., 2013). This suggests that iNKT cells mediate protective effects through IL-10 production, in spite of the concurrent release of harmful IFN-γ.

A recently published paper by Xia et al. has addressed the role of T_{reg} cells in murine myocardial I/R injury (Xia et al., 2015). It was reported that selective depletion of T_{reg} cells prior to I/R increased infarct size. Moreover, adoptive transfer of in vitro activated T_{reg} cells significantly reduced infarct size and improved myocardial function (Xia et al., 2015). Mechanisms of these effects included activation of the RISK pathway protein kinases Akt and ERK, and reduced cardiomyocyte apoptosis. Furthermore, adoptive transfer of T_{reg} cells reduced

neutrophil infiltration following I/R, and that this was associated with diminished expression of the chemokines CXCL1 and CXCL6 (Xia et al., 2015).

These studies confirm the importance of T cells in myocardial inflammation and injury following I/R in mice. Moreover, there are clearly opposing subset-specific effects, with IFN-γ-producing T_H1 cells being detrimental, while T_{reg} cells appear to be protective.

1.5.2 Other Organ Systems

In addition to the situation in the heart, there is a wealth of evidence pointing to a critical role for lymphocytes, and particularly $CD4^+$ T cells, in I/R injury in other organ systems (Huang et al., 2007; Ioannou et al., 2011; Linfert et al., 2009; Rao et al., 2014; Zuidema and Zhang, 2010). Of these, the renal system has been the most extensively investigated. Rabb et al. demonstrated that mice deficient in both $CD4^+$ and $CD8^+$ T cells showed significantly less damage than wild type mice in a model of kidney I/R injury (Rabb et al., 2000). As well as lower serum creatinine and improved histological appearance, these mice had significantly less neutrophil infiltration into the post-ischaemic kidney (Rabb et al., 2000). Yakota et al. went on to demonstrate that T cell depletion in mice using a combination of antibodies to CD3, CD4 and CD8 also resulted in protection from renal I/R injury (Yokota et al., 2002). The same group then established that $CD4^+$ T cells, in particular, were key effector cells in this process. They demonstrated that $CD4^+$ T cell deficient mice were protected, and that adoptive transfer of these cells abolished this protection (Burne et al., 2001). Furthermore, as with the myocardial model discussed above (Yang et al., 2006), adoptive transfer of $CD4^+$ T cells unable to produce IFN-γ was insufficient to re-establish I/R injury (Burne et al., 2001). Further studies by other groups have replicated this finding, emphasising the importance of IFN-γ (Day et al., 2006). Moreover, one study in a mouse model of renal I/R injury demonstrated that mice deficient in the chemokine receptor CXCR3 had reduced recruitment of IFN-γ producing $CD4^+$ T cells, and reduced I/R injury (Fiorina et al., 2006). Adoptive transfer of wild type T cells able to express CXCR3 restored injury, suggesting an important role for this chemokine receptor through recruitment of IFN-γ producing cells (Fiorina et al., 2006).

Several different T cell subsets have been shown to be important in renal I/R injury in mouse models. Two studies using wild type, αβ-TCR deficient and γδ-TCR deficient mice have demonstrated a pathogenic role for both conventional $CD4^+$ T cells and γδ T cells, although the former appeared most significant (Hochegger et al., 2007; Savransky et al., 2006). Furthermore, as with myocardial injury, T_{reg} cells have been found to have a protective effect, with their depletion resulting in exacerbated renal damage (Jun et al., 2014; Kinsey et al., 2009). Adoptive transfer experiments have indicated that this protection is mediated through the anti-inflammatory cytokine IL-10 (Kinsey et al., 2009).

In addition to the renal system, numerous studies have demonstrated the involvement of T cells in hepatic I/R injury (Khandoga et al., 2006; Kuboki et al., 2009; Zwacka et al., 1997). This was first shown by Zwacka et al., who found that athymic nude mice lacking T cells were protected, displaying reduced injury and neutrophil accumulation in a hepatic I/R model compared to wild type mice (Zwacka et al., 1997). Khandoga et al. subsequently showed that $CD4^+$ T cells were recruited to the hepatic microvasculature following I/R, where they were frequently co-localised with platelets (Khandoga et al., 2006). Moreover, this was associated with reduced sinusoidal perfusion in the post-ischaemic liver (Khandoga et al., 2006). $CD4^+$ T cell deficient mice, however, were markedly protected from I/R injury, showing improved microvascular function and diminished neutrophil infiltration (Khandoga et al., 2006). Consequently, they hypothesised that $CD4^+$ T cells contribute to hepatic I/R injury by promoting microvascular dysfunction (Khandoga et al., 2006). This could be potentially highly relevant in human myocardial I/R injury, given the importance of MVO. However, in contrast to myocardial and renal I/R injury, several other studies have suggested that IFN-γ does not play a significant role in $CD4^+$ T cell mediated hepatic damage following I/R (Shen et al., 2009; Zhai et al., 2008).

As with the myocardial system, there is strong evidence demonstrating diverse T cell subset specific roles in hepatic I/R injury in murine models. T cells recruited include conventional $CD4^+$ T cells, iNKT cells and γδ T cells (Caldwell et al., 2005). One study by Kuboki et al. investigated the role of each of these cell types using

combinations of mice with T cell subset specific deficiencies (Kuboki et al., 2009). They found that $CD4^+$ T cells and iNKT cells contributed to liver damage, while γδ T cells were crucial in neutrophil recruitment. The pathogenic involvement of iNKT cells in hepatic I/R injury is supported by several other studies (Lappas et al., 2006; Shimamura et al., 2005). Blockade of T_{reg} cells with an anti-CD25 antibody, however, had no significant effect, suggesting that these cells do not confer protection from I/R injury in this organ system (Kuboki et al., 2009).

Other organs in which T cells have been shown to contribute to I/R injury include the brain and the lung. Yilmaz et al. demonstrated that mice deficient in either $CD4^+$ or $CD8^+$ T cells have reduced infarct size in an I/R injury model of ischaemic stroke (Yilmaz et al., 2006). In a rat syngeneic lung transplant model, de Perrot et al. found that recipient T cells migrated into the lungs where they contributed to I/R injury and diminished lung function, while nude rats lacking T cells were protected (de Perrot et al., 2003). This protection was associated with significantly lower levels of IFN-γ in the lung tissue. Reconstitution of nude rats with T cells re-established I/R injury (de Perrot et al., 2003). Similarly, in a murine lung I/R model involving transient hilar occlusion, antibody mediated depletion of $CD4^+$ T cells or neutrophils, but not $CD8^+$ T cells, was shown to be protective (Yang et al., 2009). Furthermore, $CD4^+$ T cell depletion significantly reduced neutrophil infiltration (Yang et al., 2009). As such $CD4^+$ T cells once again appear to mediate lung I/R injury through pro-inflammatory effects.

1.6 Significance of Leucocyte Counts in Human Patients with STEMI

1.6.1 Total Leucocyte and Monocyte Counts in STEMI

While providing clear evidence of a role for specific leucocyte populations in myocardial I/R injury in humans is challenging, several studies give indirect evidence that allows us to generate hypotheses.

It has long been known that the total leucocyte count following acute MI is of prognostic relevance, with an elevated count predicting higher mortality (Cannon et al., 2001; Furman et al., 1996). In the era of thrombolysis it was found that a raised leucocyte count was associated with failure of restoration of epicardial coronary flow (Barron et al., 2000). Importantly, Kirtane et al. also demonstrated that a higher percentage of neutrophils among leucocytes was independently associated with reduced microvascular perfusion (Kirtane et al., 2004). One possible mechanism for this could be neutrophil plugging contributing to MVO. However, this observed association does not prove whether an elevated neutrophil count is a direct cause of, or merely a marker for reduced microvascular perfusion.

More recently, studies have confirmed that the negative impact of elevated leucocyte counts persists in the era of PPCI. Pellizon et al. found that a raised admission leucocyte count was associated with larger infarct size and lower LVEF, and this finding was independent of the infarct territory (Pellizzon et al., 2003). Mariani et al. went on to assess the significance of total and differential leucocyte counts throughout admission following PPCI for STEMI, rather than solely admission counts (Mariani et al., 2006). They demonstrated that that the peak total leucocyte count was inversely associated with achievement of myocardial blush grade (MBG) 2-3 (a measure of adequate microvascular perfusion) and recovery of left ventricular function at 6 months (Mariani et al., 2006). Furthermore, peak neutrophil and monocyte counts were also inversely related to microvascular reperfusion as determined by MBG (Mariani et al., 2006). These data suggest a possible role for these cell types in the failure to achieve microvascular reperfusion, potentially contributing to I/R injury. However, it must again be

stressed that these findings are associations and do not provide clear evidence of a mechanistic link.

Tsujoika et al. have gone on to further assess the impact of monocyte counts following PPCI. They demonstrated that the two main monocyte subsets, $CD14^+CD16^-$ and $CD14^+CD16^+$ cells, are mobilized sequentially following reperfusion, peaking at 2.6 and 4.8 days respectively (Tsujioka et al., 2009). The peak of $CD14^+CD16^-$, but not $CD14^+CD16^+$ cells, was negatively correlated with extent of myocardial salvage as assessed by cardiac MRI (Tsujioka et al., 2009). In a further study, they also found that that peak $CD14^+CD16^-$ count was positively associated with the presence of MVO (Tsujioka et al., 2010). Taken together, these studies indicate a potential role for monocytes in myocardial I/R injury and MVO.

1.6.2 Significance of Lymphocyte Counts in STEMI

Evidence suggesting prognostic significance for lymphocyte counts in STEMI patients comes from a number of studies assessing the neutrophil to lymphocyte ratio (NLR). Several groups have reported increased mortality in patients in whom this ratio is high (Arbel et al., 2014; Cho et al., 2011; Núñez et al., 2008; Shen et al., 2010). These findings imply potential prognostic significance for both high neutrophil and low lymphocyte counts. Furthermore, in recent years positive associations have been identified between elevated NLR and slow coronary flow post-PPCI (Turkmen et al., 2013), as well as major adverse cardiovascular events (MACE) (Han et al., 2013; He et al., 2014). These findings are of relevance in I/R injury, given that slow flow after PPCI is often related to microvascular damage and MVO. Further direct evidence for the prognostic significance of lymphopaenia in MI comes from a large study of 1037 patients in whom a lymphocyte count in the lowest quartile, obtained 12-24 hours after symptom onset, was an independent predictor for increased mortality (Dragu et al., 2008). This study, however, included both STEMI and NSTEMI patients, in whom the treatment strategy was variable. The relevance of lymphopaenia in STEMI treated specifically by PPCI had not been investigated prior to the work conducted for this thesis (see Chapter 4).

It is worth noting that some of the studies mentioned in the section 1.6.1 concerning leucocyte counts in STEMI did not find any significant correlations between lymphocyte count and outcome measures. Mariani et al., for instance, found no association between lymphocyte peak and any of the variables they assessed (including MBG and LV functional recovery), in contrast to their findings for neutrophils and monocytes (Mariani et al., 2006). Similarly, in contrast to $CD14^{+}CD16^{-}$ monocytes, Tsujoika et al. did not find any correlation between peak lymphocyte count and MVO (Tsujioka et al., 2010). However, both of these studies looked at the peak lymphocyte count, which may not be the most relevant measure. Moreover, both studies analysed blood taken on admission and then the following day, potentially missing any acute changes that could have occurred in the intervening period.

Husser et al. have studied temporal changes in differential leucocyte counts following PPCI for STEMI, analysing blood on admission, then at 12, 24, 48, 72 and 96 hours after revascularisation (Husser et al., 2011). They found an early peak in the neutrophil count at 12 hours, coinciding with a drop in the lymphocyte count, which subsequently recovered over the next 36 hours (Husser et al., 2011). They did not, however, find any significant relationship between the minimum lymphocyte count and infarct size, in contrast to the peak neutrophil count, which was higher in large infarcts (Husser et al., 2011). The timings of blood tests in this study, however, would also have missed any acute changes occurring very rapidly after reperfusion.

One study by Bodi et al. has assessed the temporal changes in lymphocyte counts at 0, 2, 12, 24, 48 and 96 hours after reperfusion therapy (PPCI or thrombolysis) (Bodi et al., 2009). They found an early drop in the lymphocyte count between 0 and 2 hours. Furthermore, a lymphocyte count of less than 1800 cells/μl at 2 hours was significantly associated with a higher risk of MVO on cardiac MRI (Bodi et al., 2009). Although this does not explain the pathophysiology of this phenomenon, these data provide the first suggestion of a link between the drop in lymphocyte count following reperfusion therapy, and the development of MVO. Further research is required to characterise the behaviour of lymphocytes in the acute phase following reperfusion. In particular, lymphocyte subsets have yet to be

investigated in this setting, as have their relationships with myocardial I/R injury. This forms the basis of the research described subsequently in this thesis.

Prior to my own work in this field, one small pilot study conducted by my PhD supervisor investigated the change in lymphocyte subsets in the blood following PPCI for STEMI (Hoffmann et al., 2012). In 17 patients peripheral blood was taken at the start of the procedure, then at 30 minutes, 120 minutes, and at 24 hours post-reperfusion. There was a 35% drop in T cell count over the first 30 minutes, followed by 6% and 60% increases respectively in the next two time intervals (Hoffmann et al., 2012). Importantly, there were no significant changes in the monocyte or granulocyte counts over these intervals, suggesting a specific process involving T cells, rather than a reflection of general leucocyte kinetics. Although this study did not include any clinical or imaging outcome measures, it did demonstrate acute changes in T cell numbers occurring rapidly after reperfusion in humans, highlighting their likely involvement in the post-reperfusion process. The loss of these cells from the circulation raises the possibility of sequestration into the reperfused myocardium, where they could potentially contribute to I/R injury.

1.7 Cytomegalovirus

1.7.1 Human Cytomegalovirus Infection

Cytomegalovirus (CMV), also known as human herpes virus type 5, is a highly prevalent pathogen, with between 30 and 90% of the population in developed countries showing serological evidence of prior infection (Crough and Khanna, 2009). Primary infection in the immunocompetent host is usually mild or asymptomatic, but the infection is never completely cleared and enters a period of latency that persists for life. Throughout this time there is periodic reactivation, characterised by recurrent viral replication. This typically occurs at times of immunosuppression, inflammation, infection or stress (Crough and Khanna, 2009).

1.7.2 The Immune Response to CMV

CMV exposure elicits a robust adaptive immune response that is crucial in controlling the acute infection as well suppressing viral reactivation during latency (Griffiths et al., 2015). The T cell response is characterised by the development of large numbers of memory cells, particularly of the T_{EMRA} subsets, with a highly differentiated phenotype lacking expression of CD27 and CD28 (Appay et al., 2002; Crough and Khanna, 2009; Kuijpers et al., 2003). The CMV-specific T cell response is highly immunodominant and increases with age, with CMV directed cells generally constituting approximately 10% of the total $CD8^+$ T cell pool, but up to 50% in elderly individuals (Blackman and Woodland, 2011; Crough and Khanna, 2009). These CMV specific cells are largely oligoclonal, due to repeated division of individual cells resulting in the development of T cell clonal expansions (TCEs) (Blackman and Woodland, 2011). Although less dramatic than in $CD8^+$ cells, CMV seropositivity also has a significant effect on the $CD4^+$ T cell compartment (Chidrawar et al., 2009; Pourgheysari et al., 2007; Solana et al., 2012). The proportion of $CD4^+$ T cells specific for CMV again increases with age, from 2.2% in individuals under 50 years of age, to 4.7% in those over 65 in one study (Pourgheysari et al., 2007).

The development of TCEs is also accompanied by age-associated involution of the thymus, leading to a reduction in the number of T_N cells and contraction of the overall T cell repertoire (Blackman and Woodland, 2011; Khan et al., 2002). This leads to an impairment of the immune response to new antigens, and development of a set of features known as the immune risk phenotype (Blackman and Woodland, 2011; Moss, 2010). This is characterised by reversal of the usual $CD4^+$ to $CD8^+$ T cell ratio (i.e. development of higher numbers of $CD8^+$ than $CD4^+$ T cells) and a predominance of $CD8^+$ T_{EMRA} cells (Wikby et al., 2002). There is an associated increase in mortality in elderly individuals with this phenotype, compared to those without (Strindhall et al., 2007; Wikby et al., 1998).

1.7.3 Chronic CMV Infection and Vascular Disease

In a recent cohort study of individuals aged 65 or over, CMV seropositivity was associated with a 42% increase in mortality after correction for confounding variables (Savva et al., 2013). Interestingly, this was driven by a large increase in vascular deaths, with no difference in the mortality rate from other causes (Savva et al., 2013). Prior to the publication of this study, it has long been proposed that chronic CMV infection may have a role in the development of vascular disease. Initial evidence for this came from the identification of CMV antigens within arterial smooth muscle cells from individuals with atherosclerosis (Melnick et al., 1983). Many epidemiological studies have subsequently confirmed this link (Stassen et al., 2008). It is known that atherosclerosis itself is an inflammatory condition, and it is thought that chronic CMV infection may contribute to its development by promoting a pro-inflammatory environment within the vascular wall (Stassen et al., 2008). Although latent CMV infection is thought to have a role in the initial development of vascular disease, little is known about the impact of CMV seropositivity during and after MI.

One study by Spyridopoulos et al. involving individuals with a recent MI found an accelerated decrease in telomere length in $CD8^+$ T cells compared to other cell populations in these patients (Spyridopoulos et al., 2009). Given that telomere length declines with each cell division, it can be seen as a marker for a cell's proliferative history, in this case suggesting increased turnover of $CD8^+$ T cells

following MI. Furthermore, the decrease in telomere length in these cells was driven primarily by the presence of shorter telomeres in highly differentiated cells in CMV positive individuals (Spyridopoulos et al., 2009). Interestingly, the decrease in telomere length in $CD8^+CD45RA^+$ T cells (primarily T_{EMRA} cells) correlated strongly with LV dysfunction, suggesting a possible link between CMV driven $CD8^+$ T cell senescence and myocardial functional impairment after MI (Spyridopoulos et al., 2009).

As described in detail in section 1.5.1, there is robust evidence for a role for T cells in myocardial I/R injury, although subset specific effects are likely to exist. Given the profound impact of latent CMV infection on T cell phenotype, this raises the possibility that CMV serostatus could potentially influence I/R injury by affecting the T cell response. Consequently, this question will be investigated further in my studies by assessing CMV serostatus, as well as T cell kinetics in STEMI patients treated with PPCI.

1.8 Cardiac Magnetic Resonance Imaging

1.8.1 Introduction

Over the last decade cardiac MRI (CMR) has become increasingly widely used, both in clinical and research settings. This technique offers many distinct advantages over more traditional imaging modalities, such as echocardiography, following MI. As well as producing highly reproducible data on cardiac chamber size and function, CMR offers the ability to conduct detailed tissue characterisation, differentiating between areas of normal myocardium, oedematous myocardium, infarct and MVO (Hundley et al., 2010; Perazzolo Marra et al., 2011). This ability makes CMR particularly useful in the study of myocardial I/R injury (Perazzolo Marra et al., 2011; Saeed et al., 2010).

1.8.2 Assessment of Left Ventricular Size and Function

CMR provides an extremely reliable and reproducible method of assessing left ventricular dimensions and function (Hundley et al., 2010). In order to do this, an MRI sequence technique known as steady-state free precession (SSFP) is usually used. This allows both high spatial and temporal resolution, permitting production of moving 'cine' images of the heart. In order to assess ventricular volumes a series of sequences are obtained, each producing a cine image of a short axis slice through the heart. The high temporal resolution (less that 50ms) allows accurate determination of end-systolic and end-diastolic frames (Hundley et al., 2010; Perazzolo Marra et al., 2011). Internal and external dimensions of the left ventricle can then be measured on each slice by planimetry around the endocardial and epicardial borders, allowing calculation of chamber volumes. These can then be used to calculate the stroke volume (SV) and LVEF. For a detailed description of how this was done in this project see section 3.4.

1.8.3 Assessment of Infarct Size and MVO

One of the greatest benefits of CMR over other modalities is the ability to characterise different tissues. This is possible because the various tissues have differing characteristics affecting two of the components of the MR signal, namely T1 (T1 relaxation time) and T2 (T2 relaxation time) (Biglands et al., 2012; Ridgway, 2010; Rodgers and Robson, 2011).

In the case of tissue assessment in MI, the intravenous administration of a contrast agent called gadolinium is required. This substance has a short T1, resulting in a high MR signal on T1 weighted images in tissues where it is concentrated (Florian et al., 2011; Hundley et al., 2010; Perazzolo Marra et al., 2011). Gadolinium is an extracellular agent, and follows clear kinetics following administration. After a matter seconds it passes through the coronary arteries and into the myocardium. After a further 10-15 minutes, the gadolinium has largely passed through the normal myocardium, where it is then found at a low concentration. However, in areas of acute infarction the extracellular space is comparatively expanded due to necrosis. This results in an elevated gadolinium concentration in these areas, producing a higher T1 MR signal (Hundley et al., 2010; Perazzolo Marra et al., 2011). Consequently, in order to image infarcted myocardium, a technique called late gadolinium enhancement (LGE) is used, whereby T1 weighted images are obtained approximately 10-15 minutes after administration of the contrast agent. The imaging parameters are set to null the signal from normal myocardium, leading to a dark appearance in these regions, but a bright hyperenhanced image in areas of scar (Hundley et al., 2010; Pennell et al., 2004; Perazzolo Marra et al., 2011). The infarct area can then be measured accurately using sophisticated analysis software.

In the context of reperfused infarcts, LGE CMR imaging also offers the considerable benefit of being able to detect and quantify MVO, which appears as dark areas within the infarct core (Perazzolo Marra et al., 2011; Saeed et al., 2010; Wu, 2012). The reason for this appearance is that entry of gadolinium into regions of MVO occurs very slowly, relying on passive diffusion rather than perfusion, given the obstruction of microvascular flow (Saeed et al., 2010; Wu, 2012). Consequently, at

the time of imaging the concentration of gadolinium remains very low, producing a dark signal (Perazzolo Marra et al., 2011; Saeed et al., 2010). It has been demonstrated that these areas of hypoenhancement correlate with regions of MVO seen histologically in animal models (Judd et al., 1995).

1.8.4 Area At Risk and Myocardial Salvage

A further use of CMR in the acute phase following PPCI for STEMI can be quantification of the area at risk (AAR) (Florian et al., 2011; Perazzolo Marra et al., 2011; Saeed et al., 2010). This represents the total area affected by ischaemia prior to reperfusion, providing an indirect measure of the hypothetical infarct size should the vessel have remained occluded (Hausenloy and Yellon, 2013). The CMR assessment of this involves acquisition of T2-weighted images, such as the short inversion time (TI) inversion recovery (STIR) images used in this study (see section 3.4 for full methodology). Increased water content within the myocardial AAR, due to myocardial oedema, results in a high signal and a comparatively bright appearance on the MRI images (Florian et al., 2011; Perazzolo Marra et al., 2011; Saeed et al., 2010). Several studies in animal models have found that this area of brightness corresponds to the histologically measured AAR (Aletras et al., 2006; García-Dorado et al., 1993).

In the context of PPCI for STEMI, once AAR and infarct size have been determined, it is possible to calculate how much myocardium has been rescued, or salvaged, by opening the occluded vessel. This is done by simply subtracting the infarct size from the AAR (Berry et al., 2010; Friedrich et al., 2008). The salvaged area can also be expressed as a proportion of the total AAR, producing a parameter known as the salvage index (SI). I/R injury contributes to the final infarct size and, along with the irreversible damage sustained prior to reperfusion, is one of the two factors limiting the amount of myocardium salvaged (Hausenloy and Yellon, 2013). Consequently, SI been utilised as a primary end point in studies assessing the impact of agents intended to limit I/R injury (Lonborg et al., 2012).

Although there is no single measure that can determine exactly what proportion of an infarct has occurred as a direct consequence of reperfusion, CMR is an

extremely valuable tool in assessing I/R injury. MVO, infarct size, salvage area and salvage index provide useful information of proven prognostic significance, which can be used to give an impression of I/R injury (Hausenloy and Yellon, 2013; Saeed et al., 2010).

1.8.5 Disadvantages of CMR

Despite the major benefits of CMR as an imaging modality in studies investigating myocardial I/R injury, there are some factors that can limit its use. The scan is time consuming, taking up to an hour to perform, and requires a considerable amount of patient cooperation throughout the process. Given the effect of respiratory motion on the position of the heart, each sequence must be obtained during a breath hold of around ten seconds (Pennell et al., 2004; Ridgway, 2010). Consequently, this requires the patient to be capable of repeated breath holding, without which images are significantly degraded and of limited use (Ferreira et al., 2013). This restricts the number of patients who are suitable for any study involving CMR, as pre-existing conditions severely affecting breathing are likely to result in an inability to complete the scan.

A number of other contraindications to this type of scan must be taken into account. One of the most important of these is claustrophobia. The scan involves a prolonged period of time within the enclosed space of the scanner, which a number of people find intolerable. It has been reported that approximately 2% of patients have significant claustrophobia during CMR (Pennell et al., 2004), although in the context of recent MI this percentage is likely to be higher, as I have discovered through my own experience in this study. Additional contraindications include permanent pacemakers, as well as any recent metallic implant susceptible to magnetic forces. Consequently, these factors were considered exclusion criteria for recruitment to the prospective study conducted for this thesis, as discussed further in section 3.2.1.

Chapter 2

Aims

2.1 Aims

The overall aim of this PhD project was to investigate the role of T lymphocytes in myocardial I/R injury following PPCI for STEMI.

Specifically, my aims were:

- Firstly, to clarify the prognostic significance of lymphocyte counts in a large retrospectively analysed cohort of STEMI patients treated by PPCI.
- To establish a flow cytometric analysis assay for characterisation and enumeration of detailed human lymphocyte subpopulations in fresh whole blood.
- Using this assay, to clarify the kinetics of lymphocyte, and in particular T cell subsets, in the blood of STEMI patients following reperfusion.
- To study trans-coronary gradients in cell counts, aiming to establish whether T cells are sequestered into the myocardium in the reperfusion phase after PPCI.
- To assess whether T cell kinetics following reperfusion in STEMI show any relationship to cardiac MRI derived markers of myocardial injury, namely infarct size, microvascular obstruction (MVO) and myocardial salvage index.
- To assess the impact of CMV serostatus on T cell dynamics following reperfusion, and myocardial I/R injury.
- To investigate the mechanisms of lymphocyte kinetics following reperfusion in STEMI.

Chapter 3

Methods

3.1 Retrospective STEMI Cohort

3.1.1 Clinical Database of STEMI Patients

For retrospective analysis of mortality outcome data from STEMI patients, I was able to access a database of 1531 consecutive patients admitted to the Freeman Hospital, Newcastle upon Tyne, and treated with PPCI between April 2008 and February 2010. Entry criteria for this study were based on standard STEMI diagnostic criteria, namely chest pain of onset within 12 hours associated with persistent ST segment elevation of 0.1mV in at least two contiguous leads or new left bundle branch block (LBBB) on electrocardiogram (ECG). Baseline clinical data and procedural characteristics were available, having been recorded in the local PPCI database and updated on discharge. Mortality data up to July 2011 had been included in the database, giving maximum follow up of 40 months (mean 25.2 months). These data were provided by the Office of National Statistics and linked to the PPCI data through the NHS number for each patient. Leucocyte counts (total white blood cells (WBC), neutrophils, monocytes, lymphocytes, and eosinophils) were also available, having been identified and recorded from the full blood count (FBC) tests carried out in hospital via the local pathology database. These were combined with the hospital PPCI and mortality data to produce the study database.

The initial work to develop the database had been conducted by a collaborator, Nicholas Howard, prior to my involvement in analysis. In particular, Mr Howard identified and recorded the available pathology results. The FBC with the lowest lymphocyte count during the PPCI admission was recorded in each case, as well as the timing of this sample in relation to the procedure. Where available, FBC results were also recorded from day 1 post-PPCI (within and closest to 24 hours post-PPCI), as well as day 2 (within and closest to 48 hours). In addition, the most recent FBC results prior to admission were also recorded, as were the next results after discharge. These 'prior' and 'post' admission results were available in cases where there had been previous or subsequent blood tests conducted by Newcastle University Hospitals laboratories, for instance from other admissions or clinic appointments.

3.1.2 Exclusion Criteria

The principal exclusion criteria for this retrospective study were unavailability of data, and concurrent illness likely to affect life expectancy or leucocyte counts. A total of 91 cases were excluded for the following reasons: unavailable blood results (n=29), acute inflammatory or infectious disease (n=4), organ transplantation (n=5), and previous inclusion from a prior admission (n=29). This left a total of n=1440 cases for further analysis.

The main parameter I wished to assess in relation to lymphocyte counts was mortality. However, given that a large proportion of early mortality from MI is directly related to the acute infarction (e.g. cardiogenic shock, arrhythmias prior to reperfusion etc.) rather than I/R injury, long-term rather than early mortality was more relevant in this study. For this reason my analysis focussed on patients who were discharged alive (n=1377), excluding n=63 patients with in hospital mortality.

3.1.3 Statistical Analysis

All analysis was carried out in SPSS version 22 and graphs were produced in GraphPad Prism version 6. As the principal data did not pass normality testing by Shapiro-Wilk test, non-parametric tests were used. Unmatched groups were compared using the Mann-Whitney U test (2 groups) or Kruskal-Wallis test with Dunn's multiple comparisons test (3 or more groups). Leucocyte counts were not normally distributed and are expressed in chapter 4 as median with interquartile range. Where multiple comparisons tests were used, reported p values are those corrected for multiple tests. A p value of less than 0.05 was considered significant. Multivariate analysis for prognostic dissection of data was performed using backwards conditional stepwise Cox regression. Two different models were used. In model 1 the minimum lymphocyte quartile was entered as a categorical variable, while in model 2 the counts of neutrophils, monocytes and lymphocytes at the time of the minimum lymphocyte count were entered as continuous variables. In both models, all variables that differed significantly between

minimum lymphocyte quartiles or mortality groups were entered as covariates (for full list see **Table 3.1**).

Covariates Included	
Model 1	**Model 2**
Sex	Sex
Age (per 10 years)	Age (per 10 years)
BMI	BMI
Diabetes mellitus	Diabetes mellitus
Family history of CAD	Family history of CAD
Hypertension	Hypertension
Current or ex smoker	Current or ex smoker
Previous angina	Previous angina
Previous PCI	Previous PCI
Previous MI	Previous MI
Previous stroke/TIA	Previous stroke/TIA
Door to balloon time (min)	Door to balloon time (min)
Total ischemic time (min)	Total ischemic time (min)
Cardiogenic shock Pre-PPCI	Cardiogenic shock Pre-PPCI
Anterior MI	Anterior MI
Haemoglobin (per 10g/l)	Haemoglobin (per 10g/l)
Creatinine (per 100μmol/l)	Creatinine (per 100μmol/l)
Statin	Statin
ACE-inhibitor/ARB	ACE-inhibitor/ARB
Beta-blocker	Beta-blocker
Clopidogrel	Clopidogrel
Aspirin	Aspirin
GP IIb/IIIa inhibitor	GP IIb/IIIa inhibitor
Lymphocyte Quartiles	**Cell Counts**
Quartile 1 vs. Quartile 4	Lymphocytes (per 1000 cells/μl)
Quartile 2 vs. Quartile 4	Monocytes (per 1000 cells/μl)
Quartile 3 vs. Quartile 4	Neutrophils (per 1000 cells/μl)

Table 3.1: Full list of covariates entered in each Cox regression model.

3.2 Prospective Patient Recruitment and Sample Collection

3.2.1 Patient Recruitment

Ethical approval was obtained from the National Research Ethics Service (NRES) North East Ethics Committee, and NHS permissions granted by Newcastle University Hospitals NHS Trust.

A total of 60 patients presenting with acute STEMI to the Freeman Hospital, Newcastle upon Tyne, where they were treated with PPCI, were recruited to the study having given informed consent. Inclusion criteria were chest pain of onset within 6 hours, with new ST segment elevation on ECG of 0.1mV in at least two contiguous leads.

Exclusion criteria were as follows:

- Cardiogenic shock
- Previous MI or coronary artery bypass grafting (CABG)
- Known active malignant process or infection
- Any chronic inflammatory condition requiring treatment with immunosuppressive agents (e.g. steroids, methotrexate)
- Patent arterial flow [Thrombolysis in Myocardial Infarction (TIMI) grade 2 or 3] in the infarct related artery on initial angiography
- Presence of collateral circulation supplying infarct region
- Any pre-existing contraindication to MRI scanning (e.g. pacemaker or internal cardiodefibrillator, severe claustrophobia, breathlessness or frailty likely to limit tolerability of scan)
- Inability or unwillingness to give informed consent.

A control group of 15 patients admitted with NSTEMI undergoing non-emergency angiography ± PCI were also enrolled in the study. Exclusion criteria for this group were the same as for the STEMI group, with the exception of MRI contraindications (as no scan was obtained in this group), TIMI flow grade, previous MI/CABG and

total ischemic time. The rationale for inclusion of this group was to provide evidence that any cellular changes seen in the STEMI group were likely to be related to acute ischaemia/reperfusion, rather than merely a procedurally induced phenomenon related to PCI itself. A further 5 NSTEMI patients undergoing PCI were subsequently recruited for analysis of lymphocyte chemokine receptor expression.

3.2.2 Percutaneous Coronary Intervention and Blood Sample Collection

Coronary angiography and PPCI were performed as per standard clinical care. Arterial access was achieved via the radial or femoral artery, and diagnostic coronary angiographic images were obtained using the operator's catheter of choice. PPCI was performed, including the insertion of drug eluting and/or bare metal stents as deemed appropriate by the operator. All patients received dual antiplatelet therapy (300mg aspirin + one of 60mg prasugrel, 600mg clopidogrel, or 180mg ticagrelor) prior to the procedure. Decisions regarding the use of additional parenteral antithrombotic therapy and aspiration catheters were left to the discretion of the operator.

In the STEMI patients, at the start of the procedure, coinciding with arterial sheath insertion, arterial blood was drawn into 4x9ml heparinised tubes for peripheral blood mononuclear cell (PBMC) isolation (Becton Dickinson (BD) Biosciences, catalogue no. 367526), 1x4ml EDTA tube for leucocyte quantification (BD Biosciences, cat. no. 367862), and 1x5ml serum tube for serum separation (BD Biosciences, cat. no. 367986). These samples were taken to represent the pre-reperfusion time point. The procedure then continued as per standard care, and the exact time of reperfusion was recorded. This was determined by the re-establishment of TIMI II or III flow and/or development or reperfusion arrhythmias. Subsequent arterial blood samples were then taken at 15 and 30 minutes post-reperfusion (both 1x4ml EDTA and 1x5ml serum tube), either through the angioplasty guide catheter or the arterial sheath. A final arterial sample was taken at 90 minutes, prior to removal of the sheath (1x4ml EDTA, 1x5ml serum and 2x9ml heparinised tubes). A further blood sample was obtained by venepuncture in all STEMI patients at 24 hours, and at 3-6 months in a subset of

23 patients (both 1x4ml EDTA, 1x5ml serum and 4x9ml heparinised tubes). A summary of the study design for STEMI patients, outlining blood sampling timings etc. is given in **Figure 3.1**.

In the 15 NSTEMI patients in the control group, arterial blood samples were acquired at the start of the procedure, and at 15, 30 and 90 minutes (each 1x4ml EDTA, 1x5ml serum tube). These timings were taken from the moment of culprit vessel instrumentation (i.e. angioplasty wire insertion), or the initial pre-PCI sampling in cases of no intervention. In the 5 NSTEMI patients included for chemokine receptor analysis, arterial blood was taken only at the start of the procedure (1x4ml EDTA, 1x5ml serum tube).

After obtaining the 90 minute samples, all blood samples were transported at room temperature to the laboratory to undergo immediate processing. This was conducted within 4 hours of sample acquisition. For details on which assays were carried out in each group see **Figure 3.2**.

3.2.3 Coronary Sinus Sampling and Trans-Coronary Gradients

In a subset of 12 STEMI patients, upon completion of the PPCI procedure and as close to 30 minutes following reperfusion as possible, blood was obtained from deep within the coronary sinus (CS), at or close to the level of the great cardiac vein. This was conducted via catheterisation of the femoral or brachiocephalic vein following insertion of a haemostatic venous sheath. The CS was engaged using a catheter of the operator's choice under fluoroscopic guidance. Catheter position deep within the CS was confirmed radiographically by contrast injection, and blood drawn (4ml EDTA, 5ml serum tube). 'Simultaneous' aortic blood (4ml EDTA, 5ml serum tube) was obtained via the angioplasty catheter within 30 seconds of CS sampling.

The rationale behind CS blood sampling was to determine whether cells were being lost from the blood as it passed through the myocardial vasculature. The CS is the main venous vessel draining blood into the right atrium from the myocardium, with the great cardiac vein one of its major tributaries draining the

anterior left ventricular wall (Loukas et al., 2009). Consequently, a higher cell count in the aortic sample than a sample from this location would indicate loss of cells between these two points (i.e. within the myocardial circulation), suggesting sequestration of cells within this region. This method has previously been used to detect uptake of $CD4^+CD25^+$ regulatory T cells into the myocardium of heart transplant recipients, proving its ability to detect gradients in T cell subsets (Schmidt-Lucke et al., 2007). Furthermore, the inferior wall of the heart, supplied by the right coronary artery, generally does not drain into the upper coronary sinus, but instead drains into the distal CS or directly into the right atrium (Roberts et al., 1976; Spencer et al., 2013). Consequently, coronary sinus blood from inferior infarcts should not have passed through the reperfused myocardium prior to sampling deep in the CS. Trans-coronary gradients from inferior infarct cases were therefore used as a negative control, for comparison with those from anterior infarcts caused by LAD occlusion.

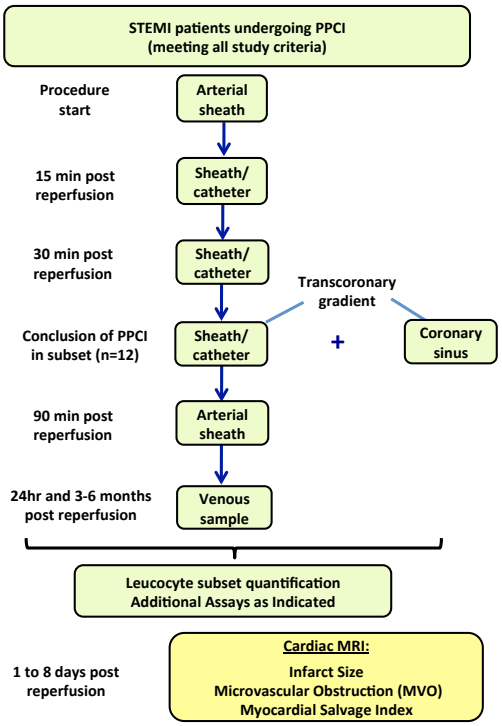

Figure 3.1: Study design for STEMI patients in prospective study. Blood was taken at the indicated time points, as well as from the coronary sinus to determine trans-coronary gradients. Cardiac MRI was used to assess the end points of infarct size, MVO and myocardial salvage index.

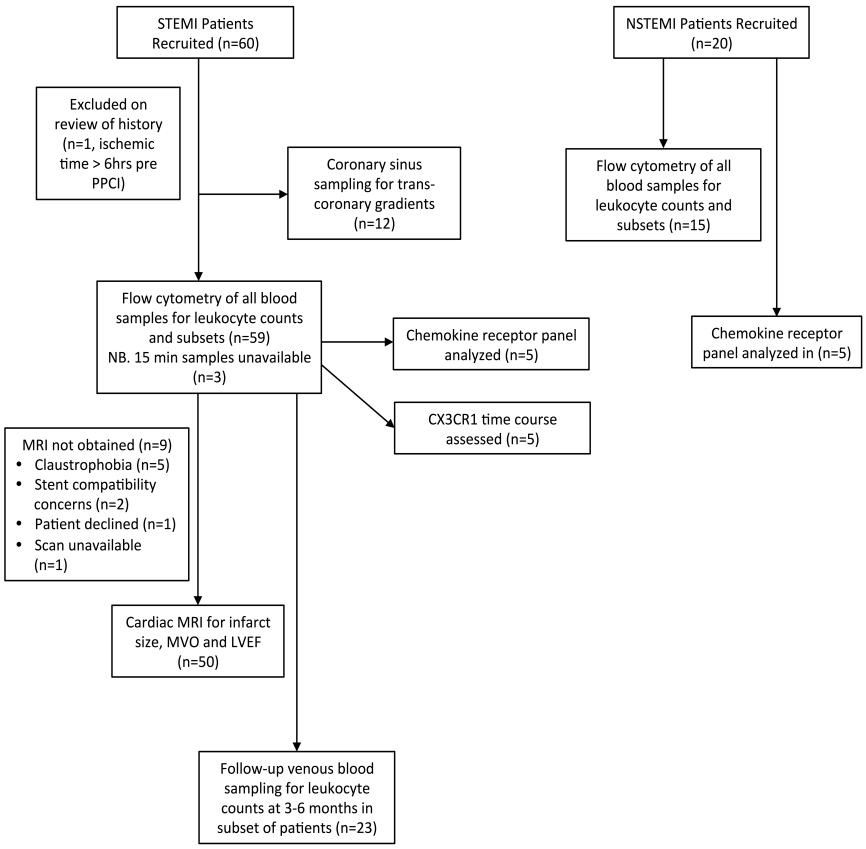

Figure 3.2: Flow chart for prospective study, outlining the study groups recruited and the investigations carried out in each.

3.3 Leucocyte Multicolour Flow Cytometry

Blood samples in EDTA tubes obtained as described above were used for quantification of leucocyte subpopulations by flow cytometric analysis.

3.3.1 Quantification of Major Leucocyte Populations (TruCount Assay)

Following transport of samples from the hospital to the laboratory the blood tubes for leucocyte quantification were immediately placed on a roller for 10 minutes to ensure adequate mixing. 50µl of whole blood was then carefully added to labelled BD TruCount tubes (BD Biosciences, cat. no 340334) prior to addition of 10µl BD Multitest TruCount antibody mix (CD3-FITC, CD8-PE, CD45-PerCP, CD4-APC, BD Biosciences, cat. no. 342447). The tubes were gently vortexed to mix for 5 seconds then incubated at room temperature in the dark for 25 minutes. Red cell lysis was then performed by addition of 1.5ml of Pharmlyse FACS lysis buffer (BD Biosciences, cat. no. 555899) to each tube, prior to mixing by vortexing, and incubating at room temperature in the dark for a further 20 minutes. The tubes were then placed on a roller under foil (to keep in the dark) for 5 minutes prior to analysis.

3.3.2 Flow Cytometry Analysis and Gating Hierarchy For TruCounts

Each tube was analysed on a BD FACS Canto cytometer, using BD FACSDiva acquisition software (BD Biosciences). Each sample was run with a stop gate of 10000 T cells, to ensure adequate numbers for representative quantification of leucocyte subsets.

The gating of the leucocyte populations was carried out as follows:

1. An initial plot of forward scatter (FSC) against side scatter (SSC) was produced to ensure a normal appearance for a whole blood sample.
2. All events were plotted by CD45-PerCP against side scatter (SSC), and a gate drawn around all leucocytes.

3. A further scatter plot of all events by CD45-PerCP expression against side-scatter (SSC) was created and gates drawn around the granulocyte, monocyte and lymphocyte populations, as determined by their characteristic scatter properties.
4. The lymphocyte population was then displayed as a scatter plot of CD3-FITC against CD45-PerCP, and gates placed around the $CD3^+$ (T cells) and $CD3^-$ (NK and B cells combined) populations.
5. The T cell population was displayed as a scatter plot of CD4-APC fluorescence against CD8-PE, and a 4 quadrant gate set to divide into the four subpopulations $CD8^+CD4^-$ ($CD8^+$ T cells), $CD8^+CD4^+$ (double positive T cells), $CD8^-CD4^-$ (double negative) and $CD8^-CD4^+$ ($CD4^+$ T cells).
6. Finally, all recorded events were then displayed by CD45-PerCP against CD4-APC expression (top right plot in **Figure 3.3**). The TruCount beads appear in this plot as a distinct population with very high fluorescence for both fluorochromes. A gate was then placed around this population in order to quantify the TruCount beads.

This process resulted in an event count for each leucocyte population as well as the TruCount beads. Given that the number of TruCount beads in each tube is accurately calibrated by the manufacturer and was known in each case, the absolute cell count (cells/µl) for each leucocyte subset could be determined by comparing the number of positive events in the population, with the number of TruCount bead events. This was calculated using the formula:

$$\text{cell count (cells/µl)} = \frac{\#\text{events in cell population}}{\#\text{TruCount bead events}} \times \frac{\#\text{beads/tube}}{\text{volume blood/test(µl)}}$$

These calculations gave a count for each of the major leucocyte subsets. These values were then also used to determine the absolute numbers of the detailed subpopulations identified in the 8 colour assay below.

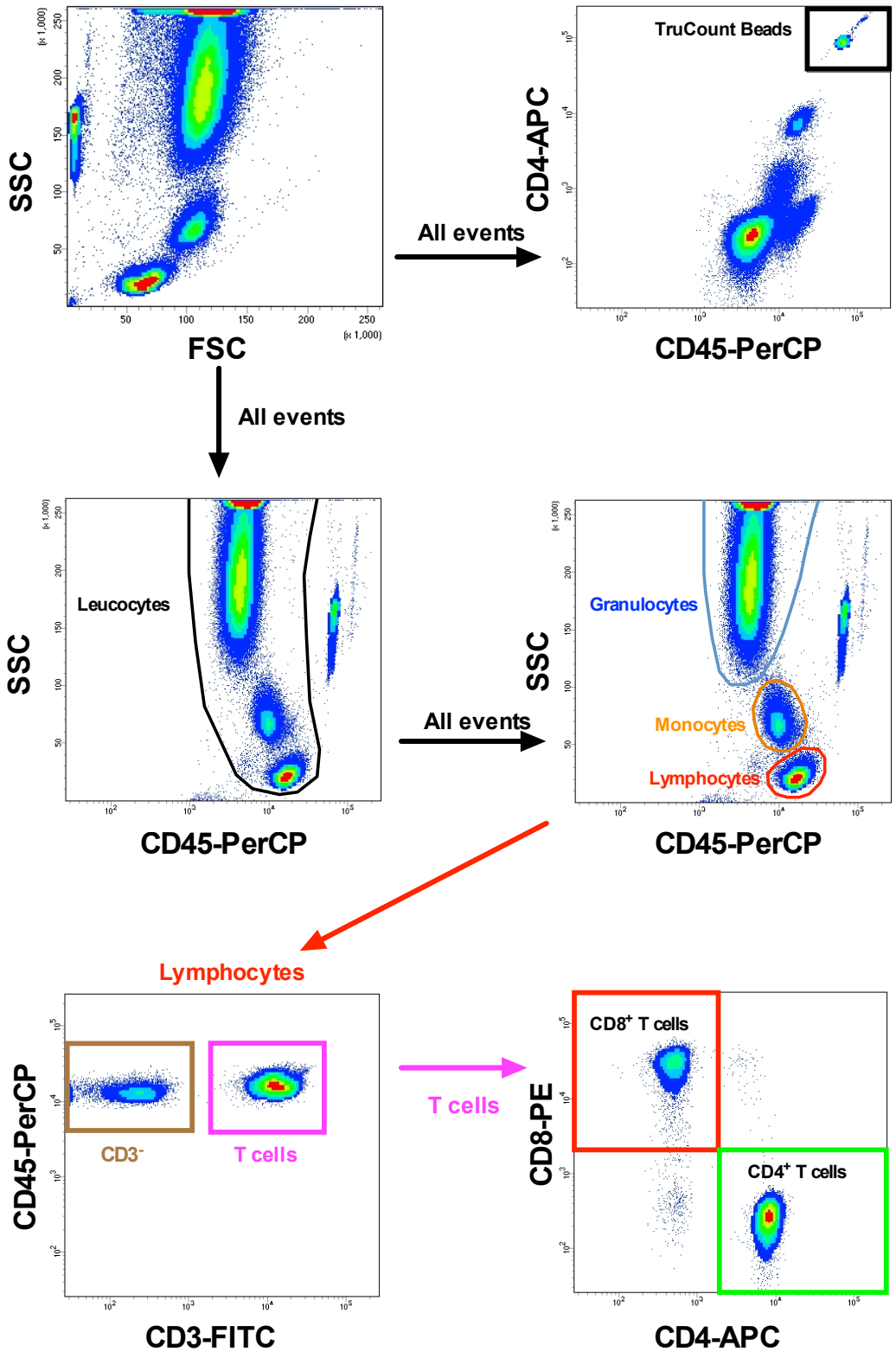

Figure 3.3. Gating strategy for TruCount analysis. See section 3.3.2 for full description of this gating procedure.

3.3.3 Quantification of Leucocyte Subpopulations (8 Colour Assay)

Staining for quantification of detailed leucocyte subsets was conducted simultaneously with the TruCount assay described above. For each blood sample analysed, 50µl of whole blood was added to a labelled FACS tube. Flourochrome labelled monoclonal antibodies were added to each tube as follows:

Anti CD3-FITC (BD Biosciences, cat. no 555332)	5µl
Anti CD4-V500 (BD Biosciences, cat. no. 560768)	5µl
Anti CD8-APC-H7 (BD Biosciences, cat. no. 641400)	5µl
Anti CD45RA-Pacific Blue (Invitrogen, CA, USA, cat. no. MHCD45RA28)	5µl
Anti CCR7-PeCy7 (BD Biosciences, cat. no. 557648)	5µl
Anti CD27-APC (BD Biosciences, cat. no. 337169)	5µl
Anti CD16-PE (BD Biosciences, cat. no. 561313)	5µl
Anti CD56-PerCP-eFluor710 (eBioscience, CA, USA cat. no. 46-0567-42))	5µl

The samples were then gently vortexed to mix for 5 seconds, before being incubated in the dark at room temperature for 30 minutes. 1ml of Pharmlyse FACS lysis buffer was then added to each sample, before gently vortexing to mix. The tubes were then incubated again in the dark at room temperature for a further 10 minutes before washing 3 times using a BD FACS lyse/wash assist machine (BD Biosciences). The samples were then analysed as described below.

Additional fluorescence minus one (FMO) control samples were prepared containing all antibodies except one. This was done for the CCR7, CD45RA, CD16 and CD56 antibodies. The rationale for this was to guide setting of the gates for positive fluorescence for each of these markers.

3.3.4 FACS Analysis and Gating Hierarchy for 8 Colour Flow Cytometry

Each sample was analysed on a BD FACS Canto II cytometer with BD FACSDiva acquisition software. The samples were run until 20000 T cell events had been detected, or until just before the sample ran dry in cases with low T cell numbers.

A simplified gating hierarchy is shown in **Figure 3.4**. This can be summarised in the following steps:

1. Lymphocytes and monocytes were gated based on their typical forward and side scatter characteristics.
2. Monocytes were then classified into $CD16^+$ and $CD16^-$ subsets, with the level of the CD16 gate determined using the CD16 FMO sample.
3. Lymphocytes were plotted by CD3-FITC fluorescence against side scatter, and classified into T cells ($CD3^+$) and $CD3^-$ lymphocytes.
4. The $CD3^-$ lymphocytes were then plotted by CD16-PE against CD56-PerCP-eFluor710 fluorescence. Cells negative for both markers were classified as B cells, while those positive for either or both were NK cells. The CD16 and CD56 positivity cut-offs were guided by the respective FMO samples. The NK cells could be further classified based on CD16 and CD56 expression, with the majority being CD56 dim and a smaller number CD56 bright.
5. T cells ($CD3^+$ lymphocytes) were plotted by CD4-V500 against CD8-APC-H7, allowing classification of $CD4^+$ and $CD8^+$ T cells. Each of these major subsets was further divided into T_N, T_{CM}, T_{EM} and T_{EMRA} based on expression of CCR7 and CD45RA, as previously described in section 1.3.16 and shown in **Figure 3.4**.
6. These detailed T cell subsets were then further classified based on their expression of the co-stimulatory molecule CD27 (e.g. $CD8^+$ T_{EM} $CD27^+$ and $CD8^+$ T_{EM} $CD27^-$ etc.)

However, a technical issue relating to the gating for CCR7 positivity resulted in the necessity for a slightly more complex gating hierarchy than this simplified description. Infrequently, some individuals' T cells included a high proportion of $CD56^+$ cells. Unfortunately, in spite of optimal compensation for spectral overlap,

$CD56^+$ T cells had higher background fluorescence levels for CCR7 than $CD56^-$ T cells, as revealed by scatter plots from FMO CCR7 samples (i.e. no CCR7 antibody present in tube) and shown in **Figure 3.5A**. It can be seen in these images that the $CD4^+CD56^+$ and $CD8^+CD56^+$ T cells (shown as grey dots) appear as separate populations with higher fluorescence on the PECy7 channel than the $CD4^+CD56^-$ and $CD8^+CD56^-$ T cells (green and red dots respectively). When the CCR7 gates were set based on fluorescence for typical $CD56^-$ T cells in the FMO CCR7 sample, this could result in misidentification of some of the $CD56^+$ T cells as $CCR7^+$, when they were in fact $CCR7^-$ (**Figure 3.5B**). In order to resolve this problem, prior to any T cell subset gating, total T cells ($CD3^+$ lymphocytes), were divided into $CD56^-$ and $CD56^+$ cells, and the full subset gating hierarchy (steps 5 and 6 in the summary above) was conducted separately for each, with different gates for CCR7 positivity. The numbers for each subset within the $CD56^-$ and $CD56^+$ cells were then combined to give the total number of events for each T cell subset (**Figure 3.5C**). The methodology for placement of CCR7 and CD45RA gates for T cell subset classification is shown in **Figure 3.6**. This involved placement of the gates at the upper limits of fluorescence in the relevant FMO samples, separately for $CD4^+CD56^-$, $CD4^+CD56^+$, $CD8^+CD56^-$ and $CD8^+CD56^+$ T cells, in order to ensure correct gating in each of the major subsets.

The data obtained from this assay alone (event counts) were not absolute cell counts but relative numbers. However, the absolute cell counts for each subset could be calculated using these figures and the counts for the major populations derived from the TruCount assay. This was conducted using the formula:

Absolute count (subset) = (Subset events/Parent events) * Parent absolute count (TruCount)

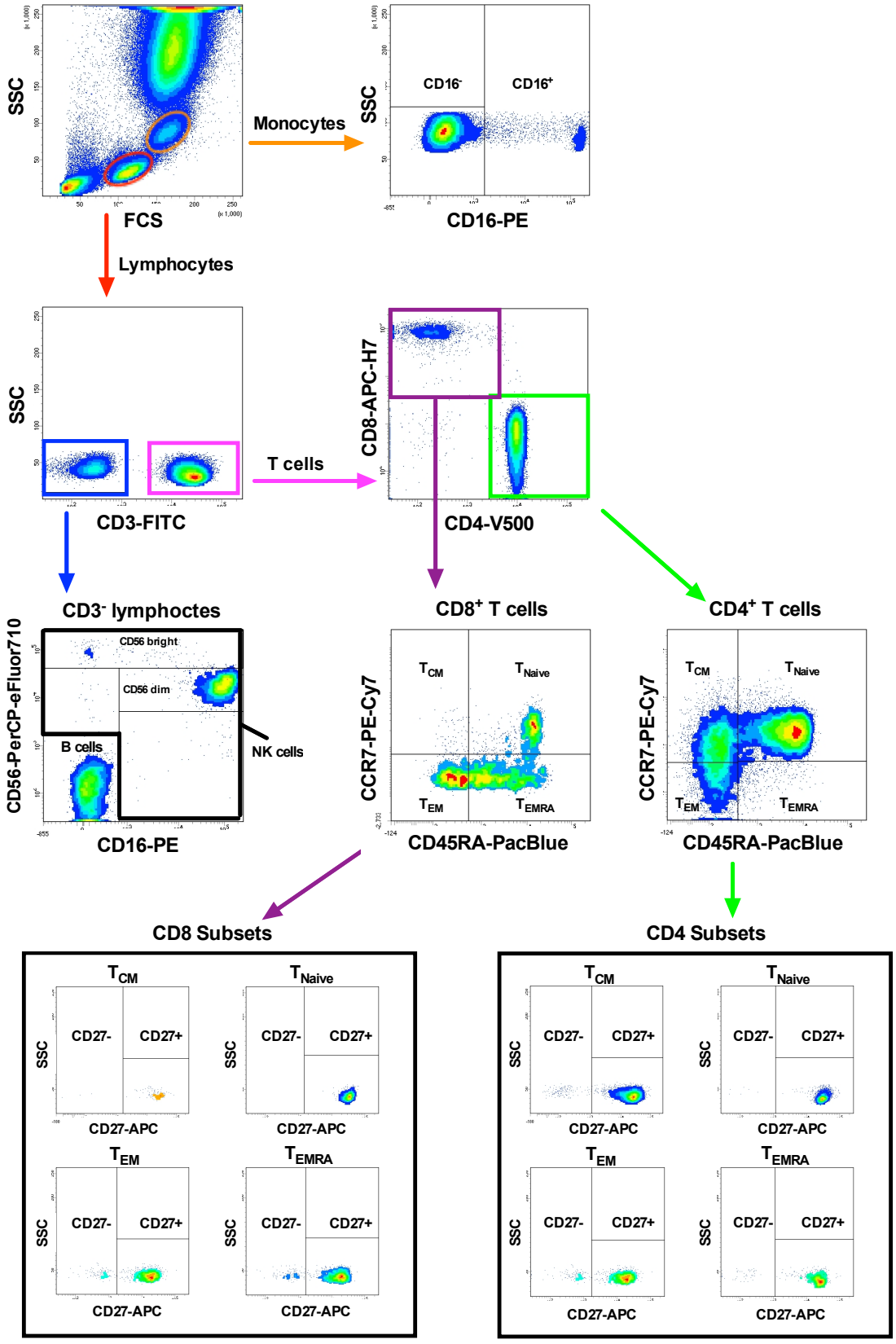

Figure 3.4. Simplified gating strategy for 8 colour assay. See main text for explanation of gating hierarchy.

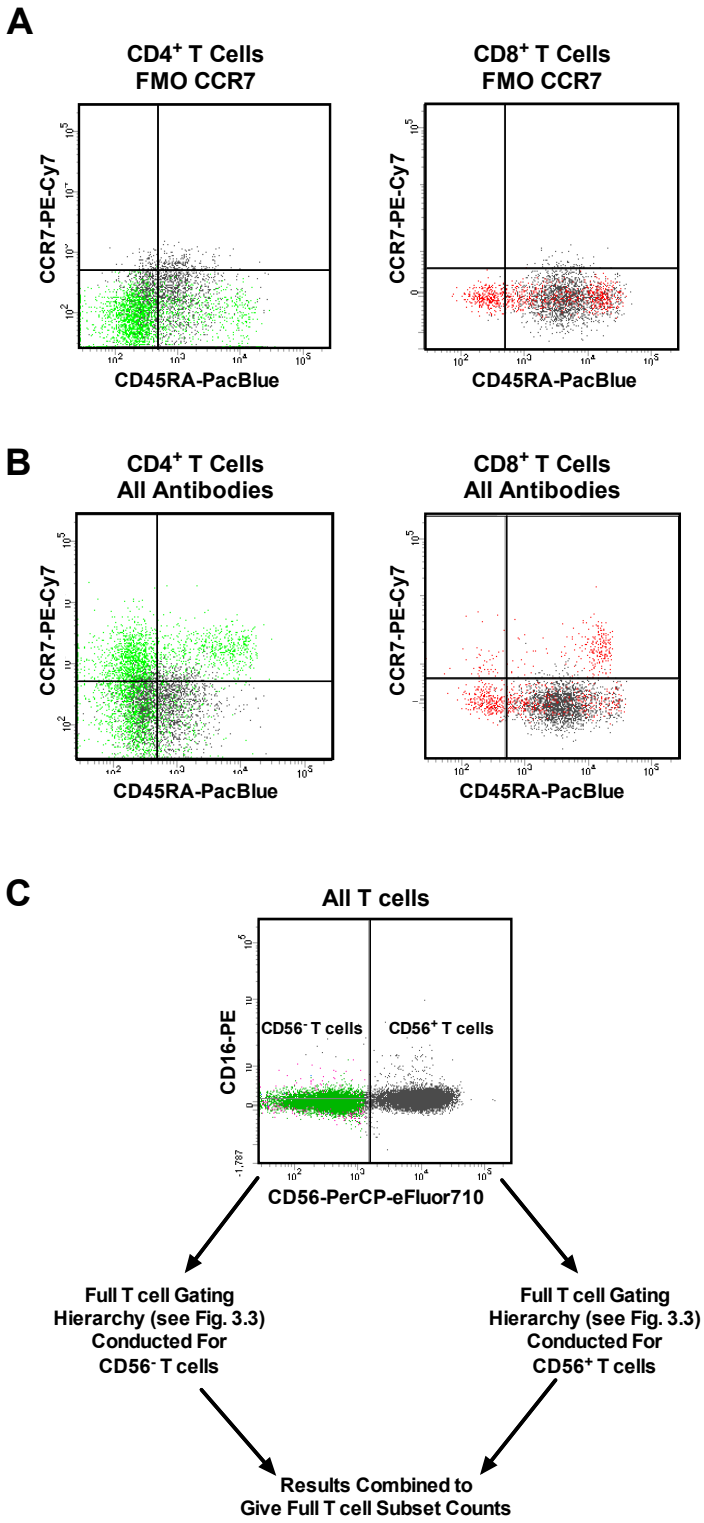

Figure 3.5. Technical issue regarding CD56 and CCR7 fluorescence. **A:** CD45 vs. CCR7 plots for CD4+ T cells and CD8+ T cells from FMO CCR7 sample (no CCR7 antibody) in an individual with many CD56+ T cells (shown as grey dots). Artefactual elevation of CCR7 fluorescence in CD56+ T cells causes difficulty placing CCR7 gates, as seen in **B:** similar plots from equivalent tube containing all antibodies. **C:** Difficulty resolved by dividing T cells into CD56- and CD56+ cells prior to T cell subset gating, then conducting full subset hierarchy (as in **Figure 3.3**) separately for each before recombining to give total T cell subset numbers.

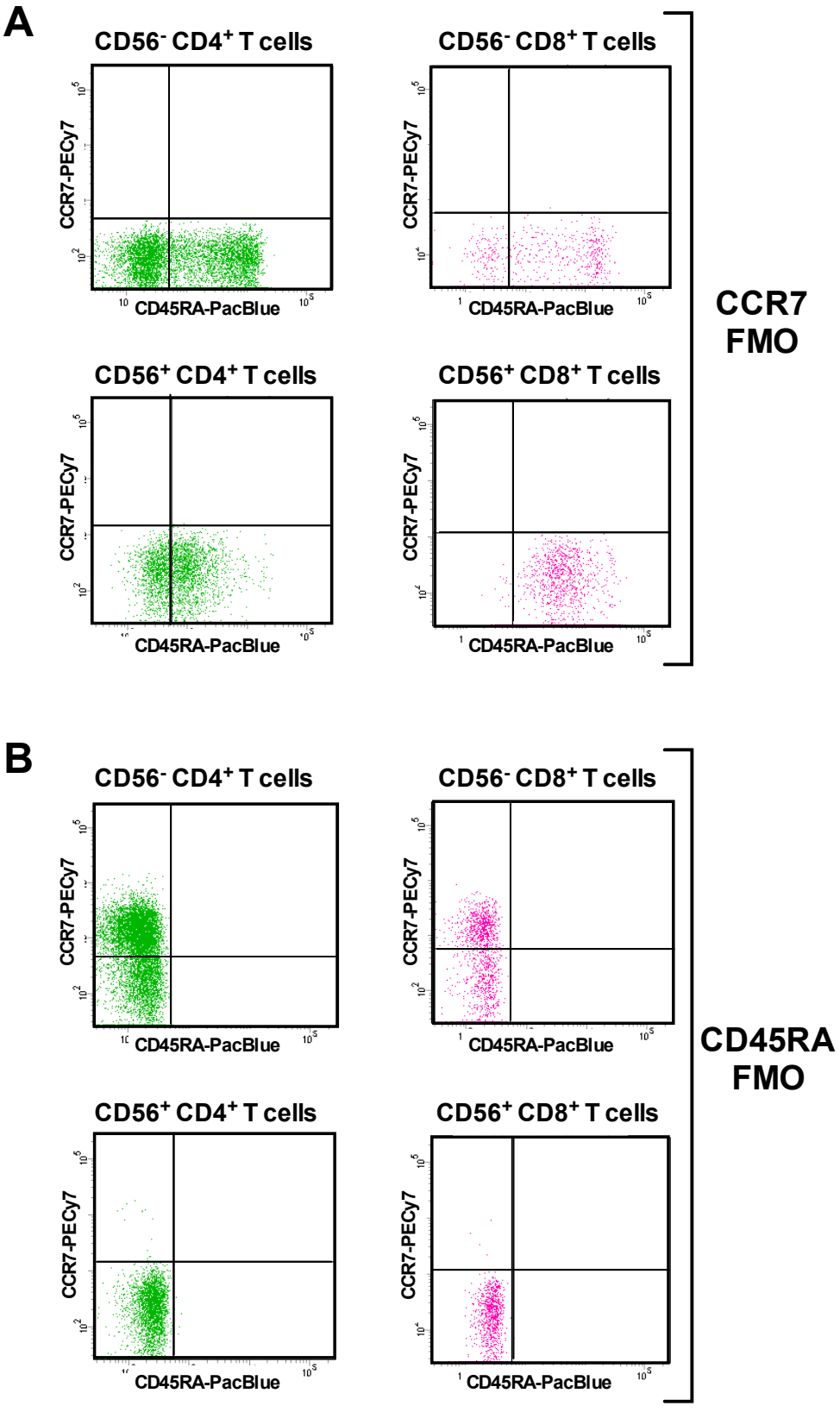

Figure 3.6. Placement of gates for CCR7 and CD45RA for T cell subset categorisation. **A:** Positioning of CCR7 gate using CCR7 FMO (sample missing CCR7 antibody). Gate for CCR7 positivity placed at limit of CCR7 fluorescence on FMO sample (i.e. background fluorescence) for $CD56^{+}CD4^{+}$, $CD56^{-}CD4^{+}$, $CD56^{+}CD8^{+}$, and $CD56^{-}CD8^{+}$ T cells separately. **B:** Similarly, positioning of CD45 gates using upper limit of fluorescence on CD45RA FMO sample.

3.3.5 Reproducibility of Flow Cytometry Assays

In order to assess the reliability and reproducibility of the TruCount and 8 colour assays used in this project, in the early stages of the study all analysis was performed in duplicate, with two FACS tubes being prepared and analysed for each blood sample. The final results obtained from these (absolute cell counts in cells/μl) were recorded and the mean value for each blood sample used in the final analysis. In addition, the coefficient of variation (CV) was calculated for each sample using the formula:

$$\text{CV} = \text{Standard deviation (SD)} \div \text{mean}$$

The CVs varied between the different leucocyte subsets as a result of the different methods of gating and levels within the hierarchy for each population. The mean CVs for the major leucocyte counts obtained from the TruCount assay are shown in **Table 3.2**. Similarly, the CVs for the detailed subsets quantified using the 8 colour assay varied between populations, and were higher for the less numerous subsets. These are shown in **Table 3.3**.

Cell Population	n (of duplicates)	Mean CV (%)
Leucocytes	23	1.4
Lymphocytes	23	1.5
T cells	23	1.5
$CD8^+$ T cells	23	2.0
$CD4^+$ T cells	23	1.6
$CD3^-$ Lymphocytes	23	1.7
Granulocytes	23	1.5
Monocytes	23	2.3

Table 3.2: Mean CV for TruCount assay for each major cell population quantified, during testing of duplicates for 23 separate blood samples.

Cell Population	n (of duplicates)	Mean CV (%)
$CD16^-$ Monocytes	30	0.8
$CD16^+$ Monocytes	30	4.7
$CD8^+$ T_N cells	31	4.9
$CD8^+$ T_{CM} cells	31	10.2
$CD8^+$ T_{EM} cells	31	3.0
$CD8^+$ T_{EMRA} cells	31	1.7
$CD4^+$ T_N cells	31	2.0
$CD4^+$ T_{CM} cells	31	2.7
$CD4^+$ T_{EM} cells	31	2.4
$CD4^+$ T_{EMRA} cells	31	7.4
B cells	30	1.4
NK cells	30	2.0

Table 3.3: Mean CV for 8 colour assay for each cell population quantified.

The CVs for the TruCount assay were generally low, at approximately 2% or less, indicating excellent reproducibility. Of the major cell populations, the highest mean CV was for monocytes (2.3%), while for $CD4^+$ and $CD8^+$ T cells it was only 1.6% and 2% respectively.

The most relevant CVs for the 8 colour assay in this project are those of the T cell subsets. Among the $CD4^+$ T cell subpopulations, the least numerous cells, $CD4^+$ T_{EMRA} cells, had the highest mean CV, at 7.4%. The CVs for the other $CD4^+$ subpopulations were small and similar, at 2%, 2.7% and 2.4% for T_N, T_{CM} and T_{EM} cells respectively. This assay, therefore, showed good reproducibility for the major $CD4^+$ T cell subpopulations.

Regarding the $CD8^+$ T cell subsets, the mean CV was high for $CD8^+$ T_{CM} cells, at 10.2%, although these represent only a small proportion of total $CD8^+$ T cells. Given the scarcity of these cells, relatively high variability in the assay would be expected for this subset. The mean CV was lower for the other $CD8^+$ T cell subsets at 4.9%, 3.0% and 1.7% for T_N, T_{EM} and T_{EMRA} cells respectively. The T_{EMRA} cells were the most numerous of these cell subpopulations, and notably had the lowest CV. The CVs for B cells and NK cells were also reassuringly low, at 1.4% and 2.0% respectively.

3.3.6 T Cell Chemokine Receptor Expression

The surface expression of chemokine receptors in T cells was assessed using a 6-colour flow cytometric assay. A cocktail of the following four antibodies was added to aliquots of 100µl whole blood, while one sample (FMO CCR7) was also prepared without the anti-CCR7 antibody:

- 20µl anti-CD3-PE (clone UCH-T1, BD Biosciences, #555333)
- 5µl anti-CD4-V400 (clone RPA-T4, BD Biosciences, #560768)
- 20µl anti-CD8-FITC (clone RPA-T8, BD Biosciences, #555366)
- 5µl anti-CCR7-BV421 (clone G043H7, Biolegend, #353208,),

In addition, 5µl of an APC-labelled antibody of one of the following specificities was added:

- Anti-CCR1 (clone 5F10B29, Biolegend, #362908)
- Anti-CCR3 (clone 5E8, Biolegend, #310708)
- Anti-CCR9 (clone L053E8, Biolegend, #358908)

- Anti-CXCR1 (clone 8F1/CXCR1, Biolegend, #320612)
- Anti-CXCR2 (clone 5E8/CXCR2, Biolegend, #320710)
- Anti-CXCR3 (clone G025H7, Biolegend, #353708)
- Anti-CX3CR1 (clone 2A9-1, Biolegend, #341610)

Finally 5µl of a PE-Cy7-labelled antibody of one of the following specificities was also added to each tube:

- Anti-CCR2 (clone K036C2, Biolegend, #357212)
- Anti-CCR4 (clone L291H4, Biolegend, #359420)
- Anti-CCR5 (clone J418F1, Biolegend, #359108)
- Anti-CCR6 (clone G034E3, Biolegend, #353418)
- Anti-CXCR4 (clone 12G5, Biolegend, #306518)
- Anti-CXCR5 (clone J252D4, Biolegend, #356924)
- Anti-CXCR6 (clone K041E5, Biolegend, #356012)

The tubes were then gently vortexed to mix, and incubated at room temperature in the dark for 25 minutes to permit antibody binding. Red cell lysis was performed using Pharmlyse (BD Biosciences) followed by three wash steps using a BD lyse/wash assist machine. Analysis was then performed on a BD FACS Canto II cytometer. The gating protocol used for this assay is shown in **Figure 3.7**. In short, lymphocytes were gated on scatter characteristics, followed by identification of T cells by CD3 expression. These were then subclassified as $CD4^+$ or $CD8^+$ T cells, based on expression of these two markers. Each major T cell subset was then further divided based on CCR7 expression into $CCR7^+$ (T_N and T_{CM} combined) and $CCR7^-$ (T_{EM} and T_{EMRA} combined). Placement of the CCR7 positivity gates was guided by the upper limit of fluorescence from the FMO CCR7 sample. Expression of each chemokine receptor in these subsets was determined using mean fluorescence intensity (MFI) on the appropriate channel.

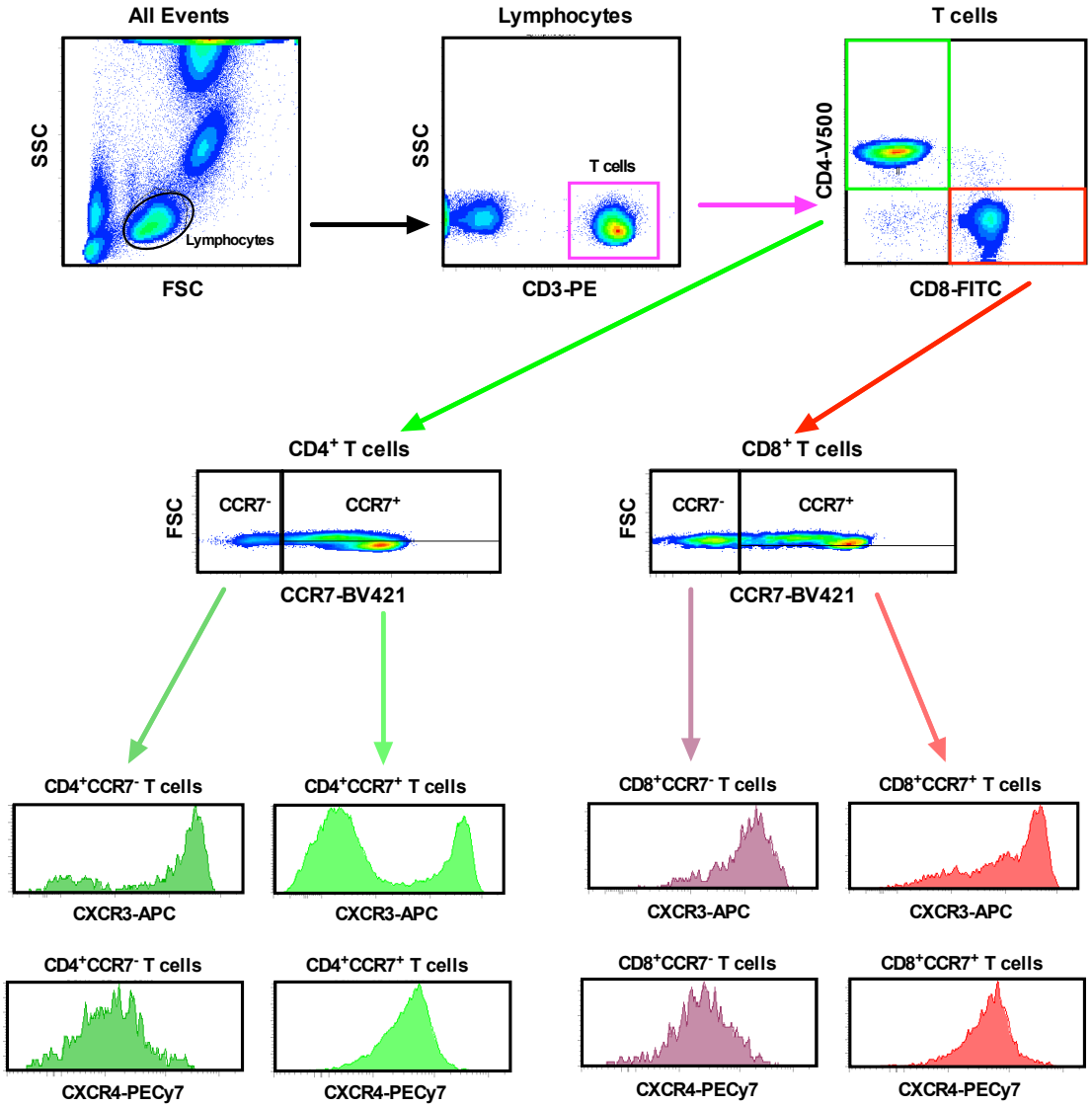

Figure 3.7: Gating strategy for chemokine receptor expression assay. Example shown displays the gating for a tube containing anti-CXCR3-APC and anti-CXCR4-PECy7 antibodies. The top two rows show T cell subset gating, while the bottom two rows show histograms for expression of these two receptors in each T cell subset studied in this assay. Expression was quantified using mean fluorescence intensity (MFI) on the relevant channel (APC or PE-Cy7) for each subset. Additional tubes with alternative combinations of chemokine receptor antibodies were used for each blood sample to quantify expression of other chemokine receptors.

3.3.7 Leucocyte Surface CX3CR1 Expression in STEMI Time Course Assay

The time course of expression of CX3CR1 on leucocyte subsets in STEMI was determined using another 6 colour flow cytometric assay, this time including anti-CD16-PE and anti-CD56-PE to allow assessment of $CD3^-$ lymphocyte subsets (B cells and NK cells). Aliquots of 100µl whole blood were stained with a cocktail of the following antibodies:

- 20µl anti-CX3CR1-APC (clone 2A9-1, Biolegend, #341610)
- 20µl anti-CD3-FITC (clone UCH-T1, BD Biosciences, #555332)
- 5µl anti-CD4-V500 (clone RPA-T4, BD Biosciences, #560768)
- 5µl anti-CD8-APC-H7 (clone SK1, BD Biosciences, #641400)
- 5µl anti-CD16-PE (clone B73.1, BD Biosciences, #561313)
- 5µl anti-CD56-PE (clone B159, BD Biosciences, #555516)
- 5µl anti-CCR7-PE-Cy7 (clone 3D12, BD Biosciences, #557648)

The tubes were mixed by vortexing prior to incubation at room temperature in the dark for 25 minutes. Red cell lysis followed by two wash steps was then performed as described above. Analysis was conducted using a BD FACS Canto II machine. The gating strategy for this assay is shown in **Figure 3.8**. As before, the cut-offs for CCR7 positivity in $CD4^+$ and $CD8^+$ T cells were determined using the upper limit of fluorescence on an FMO CCR7 sample. The expression of CX3CR1 for each population was determined using MFI on the APC channel.

This assay was also used to assess the impact of pre-incubation of blood with recombinant soluble fractalkine (sFKN) on CX3CR1 expression. On these occasions, aliquots of 100µl of donor blood was incubated for 1 hour at room temperature with varying concentrations of the recombinant fractalkine standard included with the fractalkine ELISA kit (R&D Systems, #DCX310), prior to surface antibody staining as above.

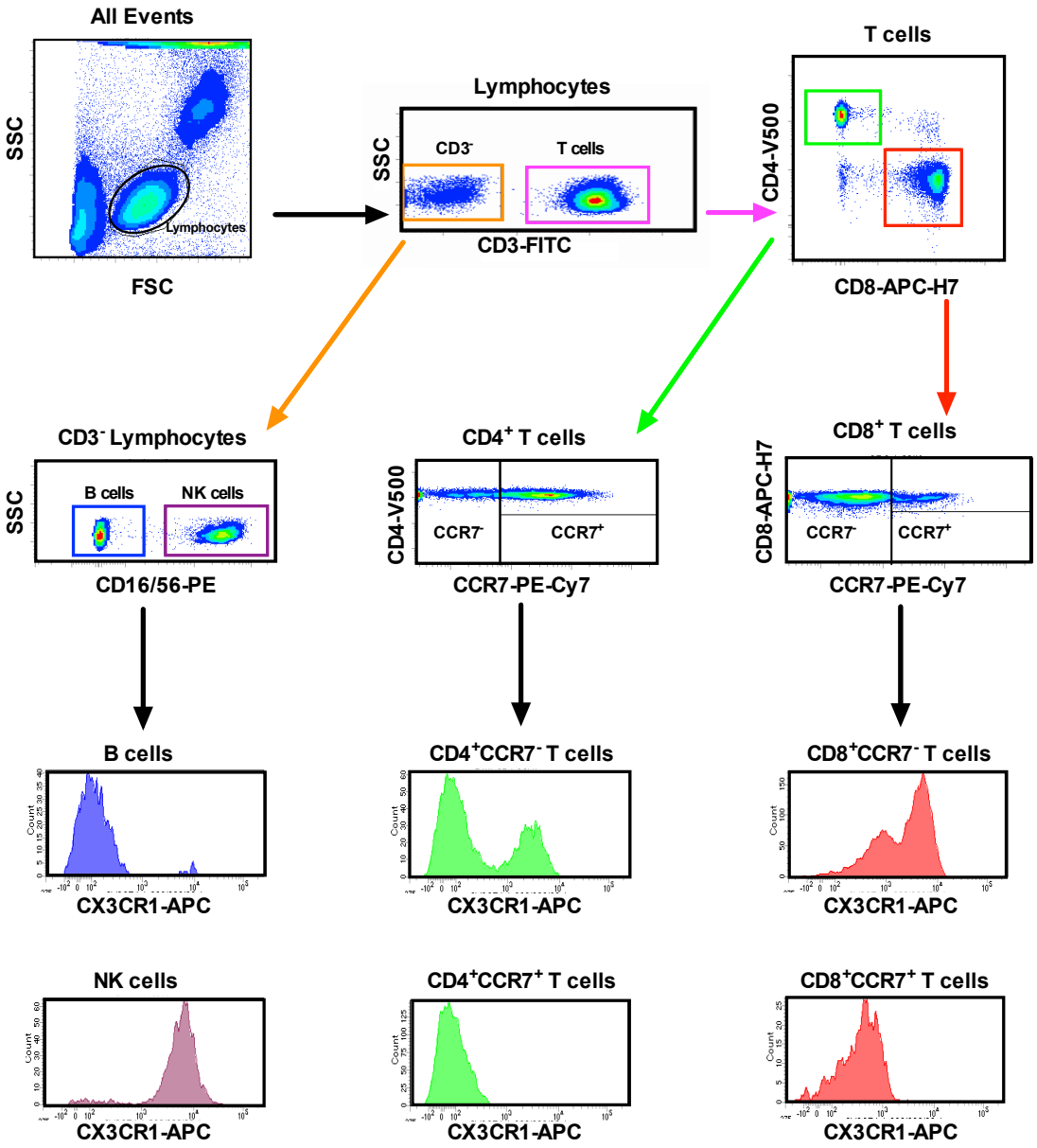

Figure 3.8: Gating strategy for CX3CR1 time course assay. The top two rows show lymphocyte subset gating, while the bottom two rows show histograms for expression CX3CR1 in each lymphocyte subset studied in this assay. Expression was quantified using MFI on the APC channel for each subset.

3.4 Cardiac Magnetic Resonance Imaging

3.4.1 Image Acquisition

CMR scans were obtained at 1-8 days post-MI with a Siemens Avanto 1.5 Telsa MRI scanner, using a phased array body coil combined with a spine coil. All images were obtained during breath holding. Localiser images were acquired as well as axial black blood HASTE images to define anatomy. Cine images of the heart in 2, 3 and 4 chamber views were obtained using a SSFP sequence (repetition time [TR]: set according to heart rate, image matrix 144x192, echo time (TE): 1.19ms, flip angle: 80°). T2 weighted STIR images were then obtained in the same projections, using a black-blood segmented turbo spin echo technique (TR according to heart rate, TE 47ms, flip angle 180°, TI 140ms, image matrix 208x256). Further sequential end-diastolic STIR images were then acquired along the short axis of the heart, covering the full extent of the left ventricle in parallel slices (each 6mm with 2mm gap). Corresponding short axis SSFP cine images were then obtained to allow quantification of chamber volumes and function. Intravenous Gadobutrol contrast (Gadovist, Bayer Schering Pharma AG, Berlin, Germany) was then administered at a dose of 0.1mmol/kg, and after 10 minutes short axis end-diastolic LGE images (in corresponding locations to cine and STIR images) were obtained using an inversion recovery (IR) segmented gradient echo sequence (TR: according to heart rate, TE: 3.41ms, flip angle: 25°, image matrix: 196x256). The inversion time (TI) for LGE imaging was selected in order to null normal myocardium (giving it a dark appearance), and adjusted throughout acquisition (increased approximately every second slice) to maintain nulling.

3.4.2 Image Analysis

All analysis was performed using validated cardiac MRI analysis software (cvi42, Circle Cardiovascular Imaging Inc., Calgary, Canada). This was conducted by myself following training in CMR analysis and cvi42 software. In order to prevent bias, anonymised scans were analysed blindly in batches, and were subsequently linked back to the relevant clinical and flow cytometric data. LV volumes and function were determined using the short axis SSFP cine images, following determination of the longitudinal extent of the chamber by cross referencing with the 4 and 2 chamber images, as previously described and validated (Childs et al., 2011). Epicardial and endocardial borders were traced automatically on each end-systolic and end-diastolic short axis cine frame with manual correction where necessary, allowing automated calculation of LV mass, dimensions and ejection fraction (**Figure 3.9**).

In order to quantify infarct size and MVO, the short axis LGE images were used, all of which were taken at end diastole. Epicardial and endocardial borders were then traced on each slice, and a reference region of normal myocardium identified using an automated method with manual correction where necessary. Areas of enhancement (infarction) were then identified and quantified automatically using a signal intensity threshold of 5 SD above normal remote myocardium, as previously described and validated (Vermes et al., 2013). Regions of hypoenhancement within the enhanced zone (MVO), were identified and quantified using semi-automatic thresholding following manual border delineation of areas of interest, and included in the calculated infarct mass (**Figure 3.10**).

In order to allow calculation of myocardial salvage index, the AAR was quantified using the short axis T2 weighted STIR images (**Figure 3.11**). Epicardial and endocardial borders, and a reference area of normal myocardium were identified as before. AAR was identified and quantified using a signal intensity threshold of 2 SD above normal remote myocardium, as previously described and validated (O h-Ici et al., 2012). Myocardial salvage and salvage index were then determined using the following calculations:

$$\text{Myocardial Salvage (g)} = \text{AAR (g)} - \text{ Infarct size (g)}$$

$$\text{Salvage Index} = \frac{\text{Myocardial Salvage}}{\text{AAR}}$$

Unfortunately, in some cases, particularly of non-anterior infarcts, the STIR images suffered from artefact related to the position of the coil. This technical limitation restricted the use of these images and the myocardial salvage index data. This issue will be described in detail section 6.2.3.

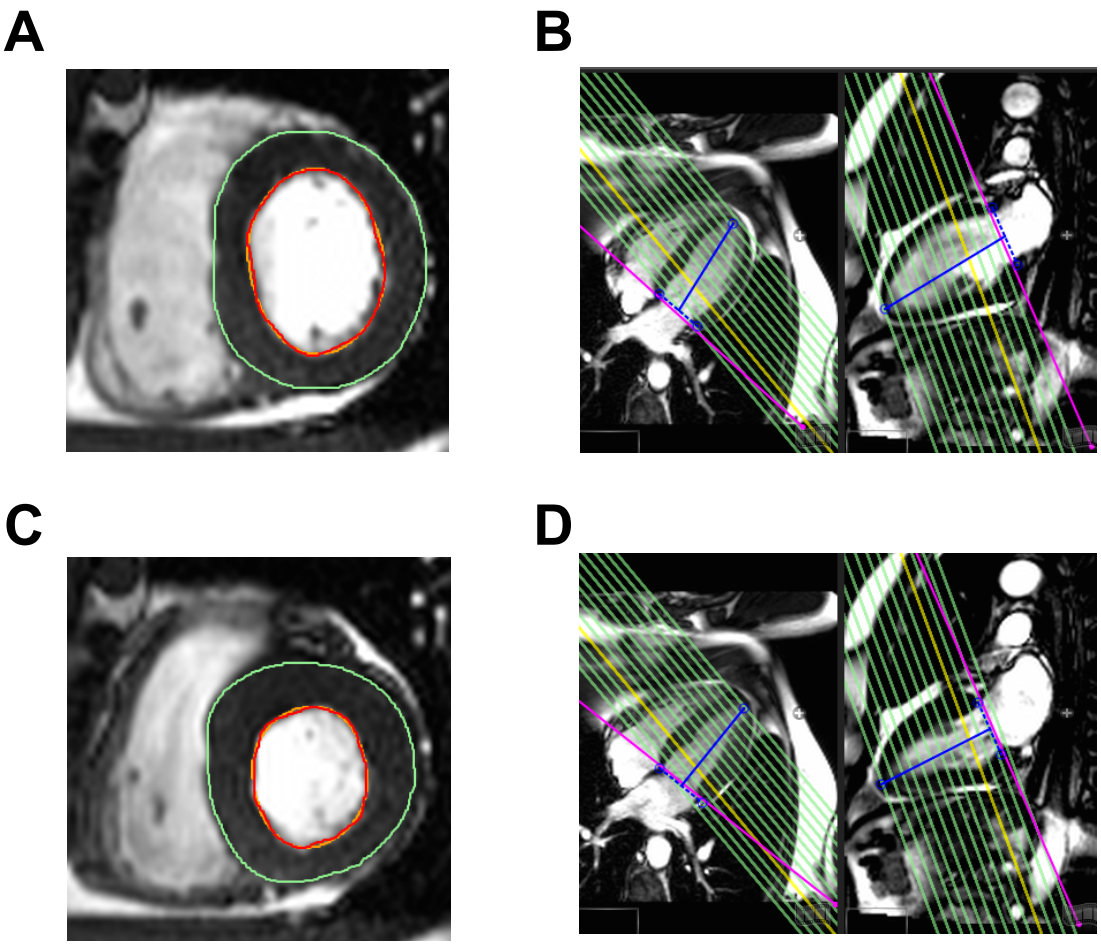

Figure 3.9: LV dimensions and function assessment by CMR. **A**: Basal ventricular short axis slice at end diastole showing endocardial border (red), epicardial border (green) **B**: Corresponding long axis reference image in both 4 and 2 chamber views, showing the slice position (highlighted in yellow). **C**: Equivalent short axis slice (**C**) and long axis reference images (**D**) at end systole.

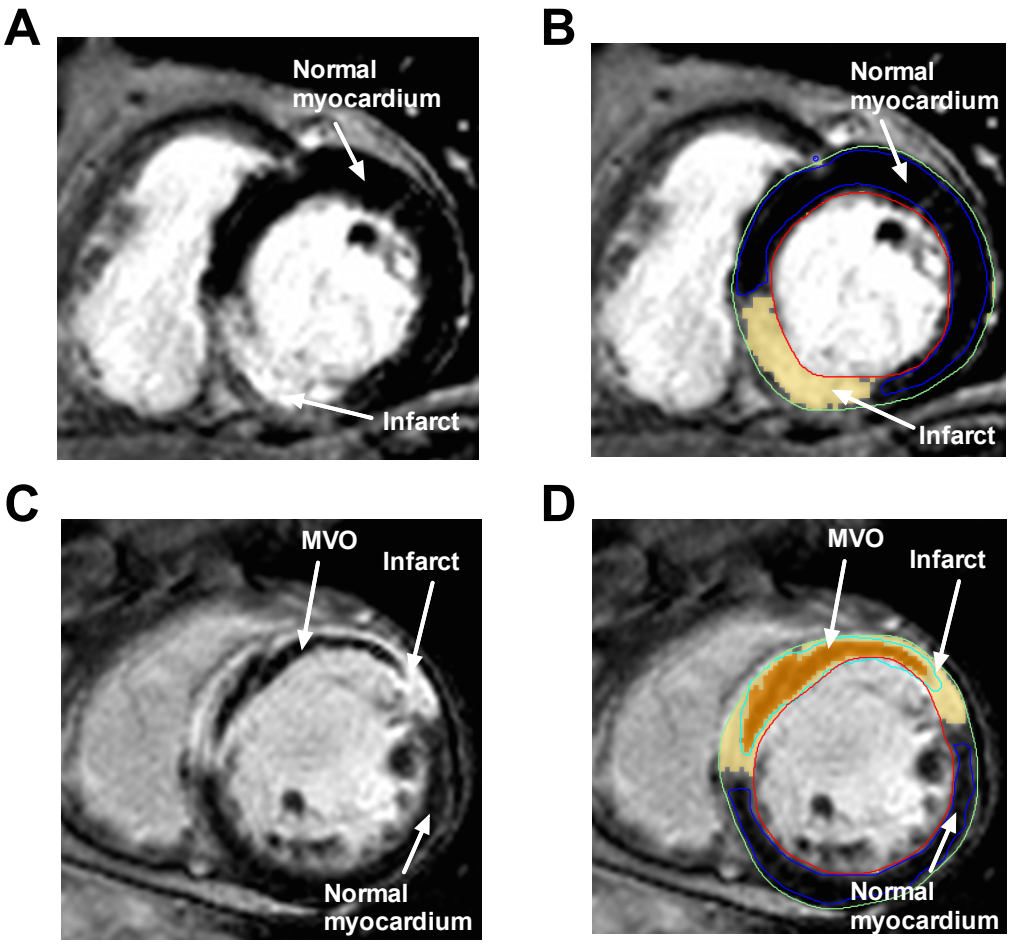

Figure 3.10: Analysis of LGE images for infarct size and MVO quantification. **A+B:** Short axis LGE image showing inferior infarct. **A:** Raw image without analysis, in which normal myocardium appears dark and infarct zone shows enhanced (white) appearance **B:** Corresponding analysed image showing myocardial borders (red: endocardial, green: epicardial) as well as normal myocardium reference area (blue border) and region of enhancement (infarct, yellow shading). **C+D**: Short axis LGE images showing anteroseptal infarct with extensive MVO **C:** Raw image in which dark core of MVO can be clearly seen within hyperenhanced infarct. **D** Corresponding analysed image shows all contours and analysis, with infarct area shown in yellow and MVO shaded orange.

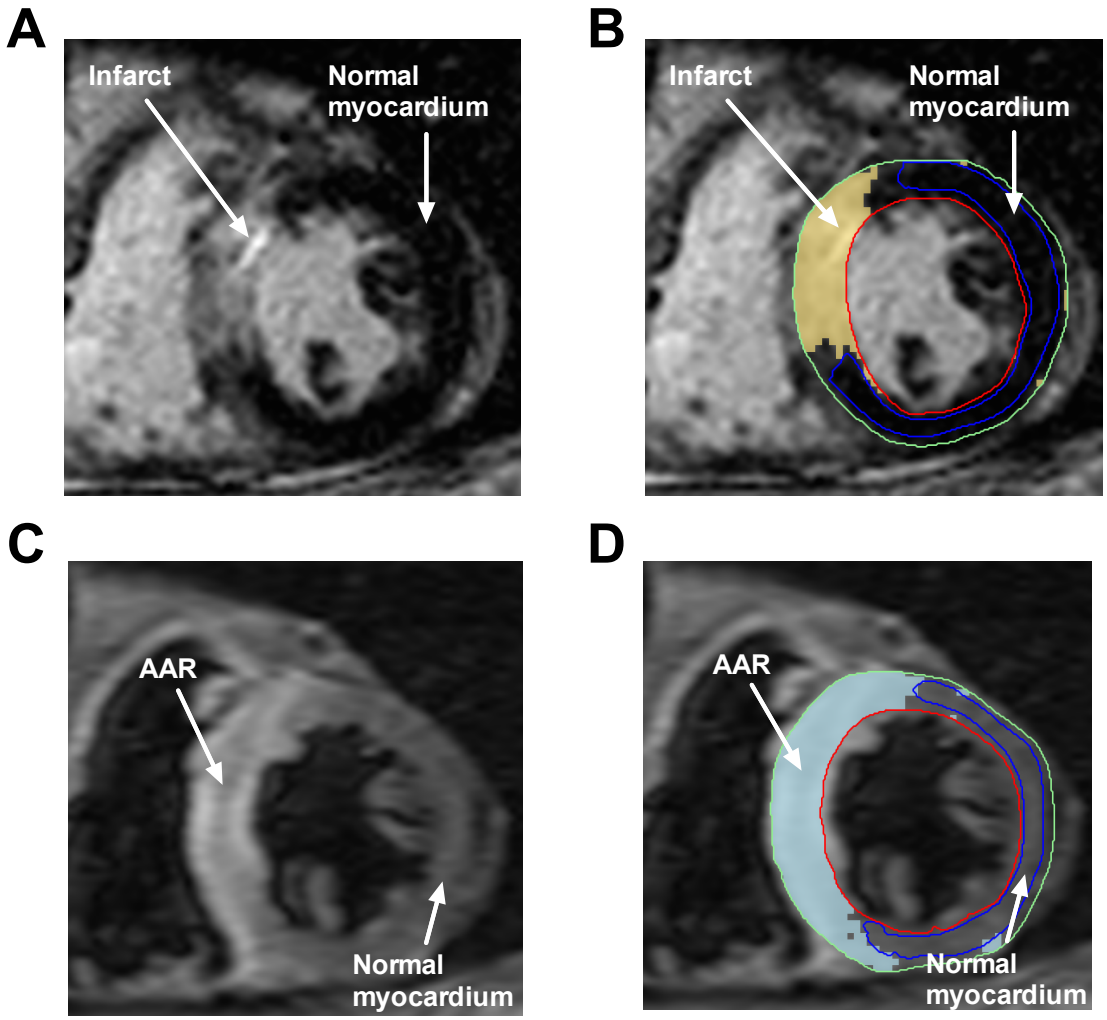

Figure 3.11: Analysis of LGE and STIR images for salvage index quantification. **A+B**: Short axis LGE slice showing anteroseptal infarct. **A**: Raw image without contours or analysis. **B**: Analysed image showing endocardial (red) and epicardial (green) borders, normal myocardial reference region (blue outline) and infarct area (yellow shading). **C+D**: Corresponding STIR images of the same infarct slice. **B:** Raw image with AAR appearing enhanced (brighter) compared to normal myocardium. **D** Analysed image with normal myocardial reference region (blue outline) and detected AAR shaded light blue.

3.5 Additional Methods

3.5.1 Peripheral Blood Mononuclear Cell Isolation

PBMC isolation was carried out by density gradient centrifugation, with blood from each of the 0min, 90min, 24hr and 3-6 month time points. Whole blood was obtained in heparinised tubes as described above. The blood was transferred to 50ml Falcon tubes (15-20ml blood in each tube), and 15ml phosphate buffered saline (PBS) (Gibco, Invitrogen, CA, USA, cat. no. 18912-014) added and mixed. The blood/PBS mixture was then layered gently over 15ml of Biocoll separating solution (Biochrom AG, Berlin, Germany, cat. no. L6115) prior to centrifugation at 800g for 20 minutes at room temperature with no brake. This resulted in the separation of the mixture into distinct layers, with the PBMC layer clearly present between the serum/PBS on top, and the separating solution underneath. This layer was then carefully aspirated, and placed in a separate tube, before making up to a volume of 50ml with PBS. The resultant tubes containing PBMC/PBS suspension were centrifuged again at 800g for 10 minutes with full brake to wash the cells. The supernatant was then discarded, the cell pellets resuspended in 50ml PBS, and the wash step repeated. The cells were then resuspended, counted with a Neubauer haemocytometer, and a final wash step carried out. They were then resuspended at a concentration of 10 million cells/ml in medium made up as follows: Roswell Park Memorial Institute (RPMI) 1640 medium (Invitrogen, cat. no. 21875034) + 10% foetal bovine serum (PAA laboratories, Austria, cat. no. A15-151) + 0.002% penicillin/streptomycin (Invitrogen, cat. no. 15070063) + 10% Dimethyl sulfoxide (DMSO) (Sigma-Aldrich, St Louis, USA, cat. no. D2650). The cells were then stored as aliquots of 2 million or 10 million cells in cryogenic vials (Fisher Scientific, UK, cat no CRY-960-070B) at -80°C until required for further experiments, following controlled cooling in a freezing chamber (Nalgene “Mr Frosty”, Thermoscientific, MA, USA, cat. no. 5100-0001).

3.5.2 Serum Isolation and Freezing

Blood was collected into serum separation tubes (BD Biosciences, cat. no 367986) at each time point as previously described. The tubes were mixed by gently inverting 5 times, and the blood allowed to clot. Following transportation to the research laboratory (and within 4 hours of collection) these tubes were centrifuged at 1000g at room temperature for 10 minutes. This resulted in the separation of the contents into a top layer of serum, overlying a second layer of the separation gel in the tubes and a final third layer on the bottom containing the clotted cellular contents of the blood. Aliquots of 200μl of the serum were then transferred to cryogenic vials (Fisher Scientific, cat. no. CRY-960-070B), before storing at -80°C until required for further experiments.

3.5.3 Serum Fractalkine Quantification

Following thawing of stored frozen serum samples soluble fractalkine levels were measured using an enzyme-linked immunosorbent assay (ELISA). This assay was conducted by my laboratory colleague, Dr Evgeniya Shmeleva, using serum samples that I had prepared from study patients' blood. The fractalkine ELISA kit (Human CX3CL1/Fractalkine Immunoassay, #DCX310, R&D Systems, USA) was used for this purpose, according to the manufacturer's instructions.

3.5.4 Real-Time Reverse Transcription Polymerase Chain Reaction (RT-PCR)

This assay was conducted by another laboratory colleague, Dr Karim Bennaceur, using cryopreserved PBMCs that I had prepared as described above. After thawing of PBMC aliquots, total RNA was extracted with Trizol solution (Life Technologies, UK). Total RNA (up to 1 μg) was reverse transcribed using The High Capacity cDNA Reverse Transcription Kit (Life Technologies, USA) according to the manufacturer's instructions. The resulting cDNA samples were stored at -80°C until further use. For TaqMan reverse transcription (RT)-PCR of each gene up to 400ng of cDNA was used for each reaction. The following TaqMan Gene Expression Assays (Life Technologies) were mixed with patients' cDNA: 18s

(Hs03003631_g1), CX3CR1 (Hs01922583_s1), CXCR1 (Hs01921207_s1), CXCR3 (Hs01847760_s1), CXCR4 (Hs00607978_s1), CCR4 (Hs00747615_s1), CCR5 (Hs99999149_s1), CCR7 (Hs01013469_m1), CD11a (Hs00158218_m1), CD11b (Hs00355885_m1), CD62L (Hs01046459_m1). RT-PCR reactions were carried out in 96-well reaction plates in a volume of 20μL using TaqMan Universal Master Mix (Life Technologies). Reaction plates were run on the Applied Biosystems 7500HT Fast Real-Time PCR System with the following profile: 95°C for 20 seconds followed by 40 cycles of 95°C for 3 seconds and 60°C for 30 seconds. The relative expression of each gene in the different samples was calculated by the ΔΔCT comparative expression method and the ΔCT values for all the genes in each sample were calculated by subtracting the mean CT values for the housekeeping gene (18s) from the CT value for each target gene.

3.5.5 Statistical Analysis

All statistical analysis was performed using SPSS (version 21), and graphs produced in GraphPad Prism (version 6). Where data did not pass normality testing by Shapiro-Wilk test, non-parametric tests were used. Non-parametric correlations between parameters were assessed using Spearman correlation coefficient. Unmatched groups were compared using Mann-Whitney U test (2 groups) or Kruskal-Wallis test with Dunn's multiple comparisons test (3 or more groups). Matched groups (3 or more) were compared using Friedman's test with Dunn's multiple comparisons test. Where normality testing criteria were met, 3 or more groups were compared using one way ANOVA with Holm–Sidak multiple comparisons test and correlations between parameters assessed using Pearson correlation coefficient. Data are expressed as mean ± standard error of the mean (SEM) except where otherwise stated. Where multiple comparisons tests were used, reported p values are those corrected for multiple tests. A p value of less than 0.05 was considered significant.

Chapter 4

Prognostic Significance of Leucocyte Counts in STEMI

4.1 Introduction

Clear evidence exists from animal models supporting a role for T lymphocytes in myocardial I/R injury, as well as multiple other organ systems (see section 1.5). Given the importance of I/R injury in human STEMI patients undergoing PPCI, the role of T cells in this context represents an important question in need of clarification. The principal aims of this study were to address this question. However, investigation of cellular disease mechanisms in humans is challenging, in part because of the unavailability of tissue specimens. The most accessible and ethically acceptable tissue available in human patients is blood. Consequently, most studies investigating T cell distribution and function in humans primarily utilise this compartment (Koch et al., 2008; Okada et al., 2008; Sathaliyawala et al., 2013). All STEMI patients undergoing PPCI require vascular access as part of routine clinical care, allowing easy access to blood samples. However, one potential limitation of blood is that lymphocytes found in this tissue compartment account for only a small proportion of total body lymphocytes, while most reside in lymph nodes, the spleen or the gut (Ganusov and De Boer, 2007; Thome et al., 2014; Trepel, 1974). It is, therefore, important to know that peripheral blood lymphocyte counts are truly relevant in clinical cases of STEMI, before using blood samples to further investigate disease mechanisms.

While there is some existing evidence for the prognostic impact of lymphocyte counts in cardiovascular disease, most studies have either included a diverse cohort of patients (e.g. both STEMI and NSTEMI) or focussed on NLR (see section 1.6.2). The prognostic relevance of lymphocyte counts alone in STEMI has not previously been investigated. Consequently, I planned to do so in a well-defined population of STEMI patients treated by PPCI, prior to further investigating the role of T cells in particular. Given the previously known association between high NLR and mortality in STEMI (Arbel et al., 2014; Núñez et al., 2008; Shen et al., 2010), and between lymphopaenia and poor outcome in other cardiac presentations (Núñez et al., 2009b; Núñez et al., 2009a), I hypothesised that low lymphocyte counts would predict elevated mortality in STEMI patients.

In order to address this question I was able to utilise a database of 1531 consecutive patents admitted with STEMI and treated with PPCI at a single UK tertiary centre. Of these, 1377 patients who were discharged alive and met all entry criteria were included in the analysis. Available in the database were blood sample results including differential leucocyte counts from the sample with the lowest lymphocyte count recorded during the admission for each patient, as well as from day 1 and day 2 post-PPCI, and pre- and post-admission where available. For full details of the methodology for this chapter, including entry/exclusion criteria, further information on the database, and statistical analysis see section 3.1.

4.2 Results

4.2.1 Leucocyte Counts in Retrospectively Analysed STEMI Cohort

In the 1377 patients included in the analysis and discharged alive, data were available for all cases for the full blood count with the lowest lymphocyte count during the admission. The mean timing of this sample was 19.6±1.4 hours post-PPCI. The day 1 sample was available in 1363 cases (mean timing 11.8±0.2 hours), and the day 2 sample in 666 cases (mean timing 35.7±0.3 hours). In addition, a sample was available at some point prior to admission in 452 cases (mean timing 940±47 days pre-PPCI), and post-discharge in 556 cases (864±25 days post-PPCI). The latter two time points provided a crude measure of pre-morbid and post-morbid baseline cell counts respectively, although it must be borne in mind the timing of those tests was highly variable and the clinical circumstances unknown.

Analysis of the data revealed characteristic temporal evolution in cell counts, as shown in **Figure 4.1**. The median pre-admission leucocyte count was 8100 cells/μl, with an interquartile range (IQR) of 6525–9800 cells/μl, but was significantly elevated in comparison on day 1 post-PPCI at 10800 cells/μl (IQR 8800; 13200 cells/μl) ($p<0.001$). There then followed a decline to 10100 cells/μl (8300; 12600) ($p=0.008$ vs. day 1). The later post-discharge white cell count had declined further to 7720 cells/μl (6255; 9423) ($p<0.001$ vs. day 1 and day 2). There was no significant difference between the pre-admission and post-discharge 'baseline' values ($p=1.0$), indicating that the values during the admission were indeed significantly elevated compared to normal.

Distinct characteristic patterns were also seen in the temporal evolution of the leucocyte subsets. Unsurprisingly, the neutrophil counts broadly followed the pattern seen in the total white cell count with no difference between the pre and post-admission 'baseline' levels (4685 cells/μl [IQR: 3785; 6130] and 4565 cells/μl [3683; 5935] respectively, $p=1.0$). There was a significant elevation at day 1 post-PPCI (7760 cells/μl [6090-9870], $p<0.001$ vs. pre-admission) followed by a decline. The monocyte count also showed elevation during admission compared to the 'pre' and 'post' levels. In this case, the highest level occurred at day 2 post-PPCI

(820 cells/μl [610; 1060]) compared to 630 cells/μl (500; 790) pre-admission ($p<0.001$) and 650 cells/μl (520; 820) post-discharge ($p<0.001$). Again, there was no significant difference between the pre-admission and post-discharge levels ($p=1.0$).

In contrast to the neutrophil and monocyte counts, lymphocyte counts displayed a different pattern, with a drop in cell counts during the PPCI admission compared to pre and post 'baseline' levels. The day 1 count was 1910 cells/μl (IQR: 1370; 2520), compared to 2170 cells/μl (1700; 2775) ($p<0.001$) before-admission and 1990 cells/μl (1500; 2498) ($p=0.017$) after discharge. In contrast to the other leucocytes subsets, there was a significant difference between the pre-admission and post-discharge levels, with the latter count being significantly lower ($p=0.042$).

The median value for the lowest lymphocyte count recorded during admission was 1580 cells/μl (IQR: 1150; 2670), occurring at 19.6±1.4 hours following PPCI. These samples (i.e. the one from each patient with the lowest lymphocyte count) also had a higher neutrophil count (8220 cells/μl [6260; 10500]) than any of the other time points, suggesting that the lymphocyte count nadir and neutrophil peak approximately coincided in this cohort of patients. The monocyte count on these samples (680 cells/μl [510-898]) was lower than that seen on the day 1 and day 2 samples, indicating that monocytes were yet to peak when lymphocyte counts were at their lowest.

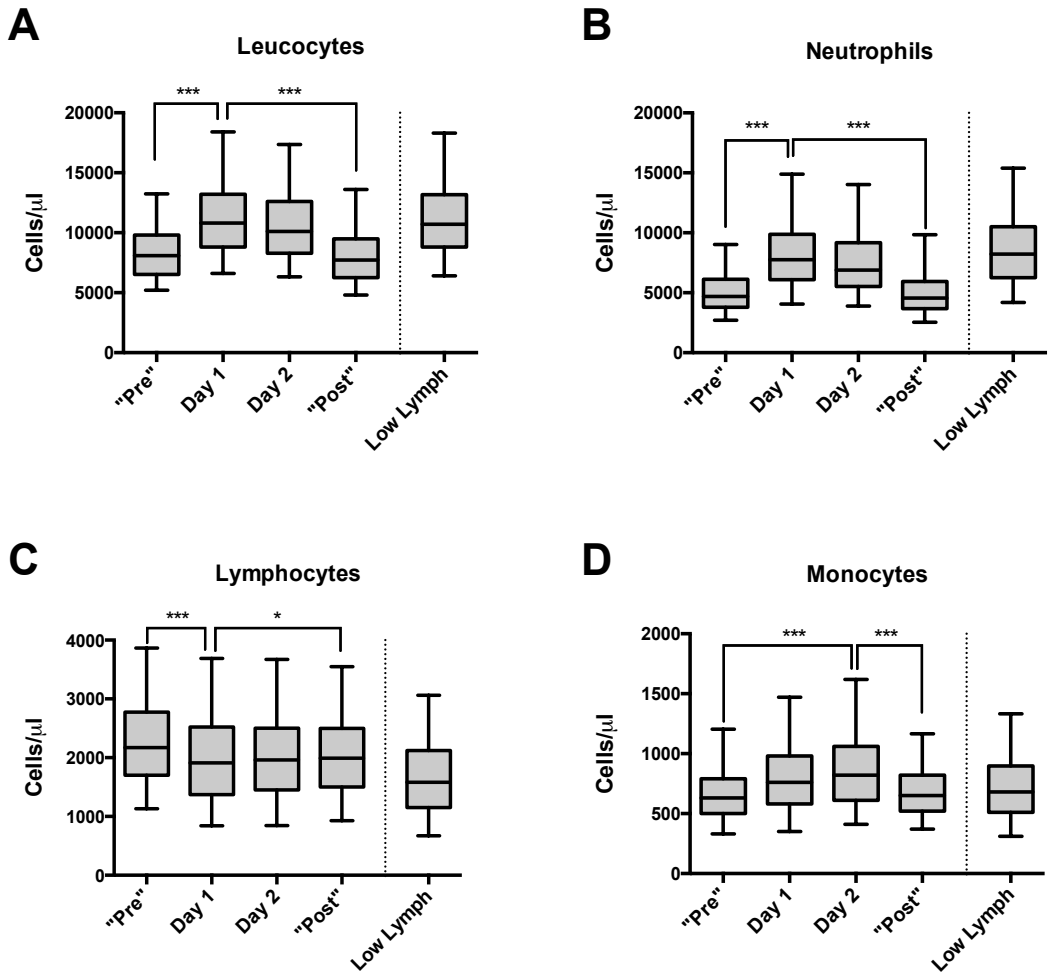

Figure 4.1: Cell counts for total leucocytes (A), neutrophils (B), lymphocytes (C) and monocytes (D) in STEMI patients treated with PPCI and discharged alive (total n=1377). Box plots display median (central line), 25th and 75th centiles (limits of box) and 5th and 95th centiles (error bars). "Pre" refers to closest available FBC prior to admission (mean 940±47 days pre-PPCI), "post" to the closest available FBC post-discharge (mean 864±25 days post-PPCI). The "low lymph" sample refers to the sample from each case during the admission with the lowest lymphocyte count (mean timing 19.6±1.4 hours post-PPCI). The mean timings for the day 1 samples were 11.8±0.2 hours, and 35.7±0.3 hours for the day 2 samples. Note: not all samples were available in each case, hence different 'n's for each time point (pre-admission: n=452, day 1: n=1363, day 2: n=666, post-admission: n=556, "low lymph": n=1377). Statistics refer to Friedman Test with Dunn's multiple comparisons test. * $p<0.05$, ** $p<0.01$, ***$p<0.001$, ns = not significant

4.2.2 Baseline Variables and Mortality Post-Discharge in STEMI Patients

Baseline variables for the cohort of STEMI patients treated with PPCI and discharged alive are shown in **Table 4.1**, along with the data divided by the presence of the primary outcome measure, mortality during follow up. Of these 1377 patients, a total of 128 died during the follow up period, while 1249 did not. There were many striking differences between patients who died and those who survived. Unsurprisingly, those who died were on average significantly older. Other baseline variables that significantly differed between these groups were gender (lower percentage of males in those who died) and BMI (lower mean BMI in non-survivors). The percentages with a positive smoking history and family history of ischaemic heart disease were lower in those who died. A number of factors in the past medical history also varied between survivors and non-survivors. A significantly higher proportion of individuals who died had a history of previous angina, and this was also the case for previous MI and diabetes.

There were several characteristics relating to the PPCI procedure that differed between survivors and non-survivors. As may be expected, those who died had a significantly longer total ischaemic time, as well as door to balloon time. These patients were also more likely to have had multivessel PCI, or failure to establish normal arterial flow (TIMI 3) in the culprit vessel at the end of the procedure. There was no significant difference in the occurrence of cardiogenic shock pre-procedure, perhaps reflecting the fact that all patients included in this analysis survived to discharge, while cardiogenic shock is an extremely poor short term prognostic feature and the main cause of early death post-PPCI (Pedersen et al., 2014). Admission blood parameters differed between survivors and non-survivors, with the latter having significantly lower haemoglobin and cholesterol, but higher creatinine levels. Finally, the medical treatment during admission also differed, with significantly lower percentages of those who died receiving statins, ACE-inhibitors/angiotensin receptor blockers (ARBs), beta-blockers, aspirin, clopidogrel and GP IIb/IIIa inhibitors. This striking finding may be a reflection of the fact that patients who died were generally older with more comorbidities (e.g. renal dysfunction) and therefore more likely to have drug contraindications.

4.2.3 Cell Counts Varied Between Survivors and Non-Survivors

Next, I analysed the total leucocyte, as well as neutrophil, lymphocyte and monocyte counts separately for survivors and non-survivors (**Figure 4.2**). In the case of the total leucocyte count, there was no difference between these groups at day 1, but at day 2 the count was significantly higher in those who died (median 11600 cells/μl [IQR: 8700; 15500] vs. 10000 cells/μl [8300; 12300], p=0.001). At the time of the lowest lymphocyte count there was no difference in the total leucocyte count between these groups. A similar pattern was present for both neutrophils and monocytes, with no difference on day 1 or at the low lymphocyte time point, but significantly higher counts on day 2 in patients who died. The monocyte count at day 2, for example, was 930 cells/μl [645; 1360] in those who died, compared to 810 cells/μl [610; 1040] in those who survived (p<0.001).

The lymphocyte count was significantly different between survivors and non-survivors at all time points during the admission. At day 1 the median count was 1940 cells/μl [1430; 2540] in those who survived, and 1460 cells/μl [1010; 2060] in those who died (p<0.001). This difference, with lower counts in those who died, was maintained at day 2 and was also present at the time of the lowest lymphocyte count (survivors: 1630 cells/μl [1200; 2170] vs. non-survivors: 1145 cells/μl [760; 1578], p<0.001).

	Overall	Primary Outcome Status		n (for variable)	p value
		No Mortality (n=1249)	Mortality in Follow-up (n=128)		
Age (years)	62.8 ± 13.3	61.6 ± 12.8	74.6 ± 12.6	1377	**<0.001**
Male sex	992 (72.0)	911 (72.9)	47 (63.3)	1377	**0.020**
BMI	27.6 ± 5.3	27.7 ± 5.2	25.8 ± 5.5	1222	**<0.001**
Diabetes mellitus	144 (10.5)	120 (9.6)	24 (18.8)	1375	**0.001**
Family history of CAD	553 (44.6)	519 (45.7)	34 (32.7)	1240	**0.011**
Hypertension	553 (40.2)	492 (39.4)	61 (47.7)	1377	0.069
Hypercholesterolemia	406 (29.5)	366 (29.3)	40 (31.3)	1377	0.646
Current or ex-smoker	964 (73.6)	888 (74.4)	76 (65.0)	1310	**0.026**
Previous angina	228 (21.3)	235 (19.1)	53 (41.4)	1352	**<0.001**
Previous PCI	93 (6.8)	81 (6.5)	12 (9.4)	1374	0.218
Previous MI	194 (14.4)	157 (12.8)	37 (31.1)	1347	**<0.001**
Previous stroke or TIA	67 (4.9)	57 (4.6)	10 (7.8)	1377	0.126
PVD	46 (4.9)	39 (3.1)	7 (5.5)	1377	0.189
Door to balloon time (min)	29.6 ± 18.2	29.3 ± 18.4	31.9 ± 16.2	1348	**0.009**
Total ischemic time (min)	269.1 ± 378	266.8 ± 371.2	293.0 ± 445.2	1329	**0.011**
Cardiogenic shock pre-PPCI	40 (2.9)	33 (2.7)	7 (5.5)	1367	0.089
Anterior MI	534 (39.0)	475 (38.3)	59 (46.5)	1368	0.072
Multivessel PCI	146 (10.6)	124 (9.9)	22 (17.2)	1377	**0.011**
TIMI 3 post-PCI	1203 (92.5)	1102 (93.3)	101 (84.2)	1301	**<0.001**
Haemoglobin (g/l)	139.5 ± 16.5	140.7 ± 15.9	128.1 ± 17.9	1374	**<0.001**
Serum cholesterol (mmol/l)	5.0 ± 1.3	5.1 ± 1.3	4.4 ± 1.3	1283	**<0.001**
Serum creatinine (μmol/l)	102.8 ± 44.7	99.0 ± 30.4	138.8 ± 105.4	1373	**<0.001**
Statin	1238 (89.9)	1130 (90.5)	108 (84.4)	1377	**0.029**
ACE-inhibitor/ARB	1191 (86.5)	1093 (87.5)	98 (76.6)	1377	**0.001**
Beta-blocker	1158 (84.1)	1065 (85.3)	93 (72.7)	1377	**<0.001**
Clopidogrel	1252 (90.9)	1142 (91.4)	110 (85.9)	1377	**0.039**
Aspirin	1256 (91.2)	1146 (91.8)	110 (85.9)	1377	**0.027**
GP IIb/IIIa inhibitor	1151 (84.0)	1075 (86.5)	76 (59.4)	1371	**<0.001**

Table 4.1: Baseline data for 1377 consecutive STEMI patients treated with PPCI and discharged alive. Continuous variables expressed as mean ± SD and compared using Mann-Whitney U test for presence of primary outcome (mortality during follow up). Categorical variables expressed as n (% of valid n for relevant variable) and compared using chi-square (χ^2) test. Note: missing data in database led to lower n numbers for certain variables, hence values given for each variable in column 5.

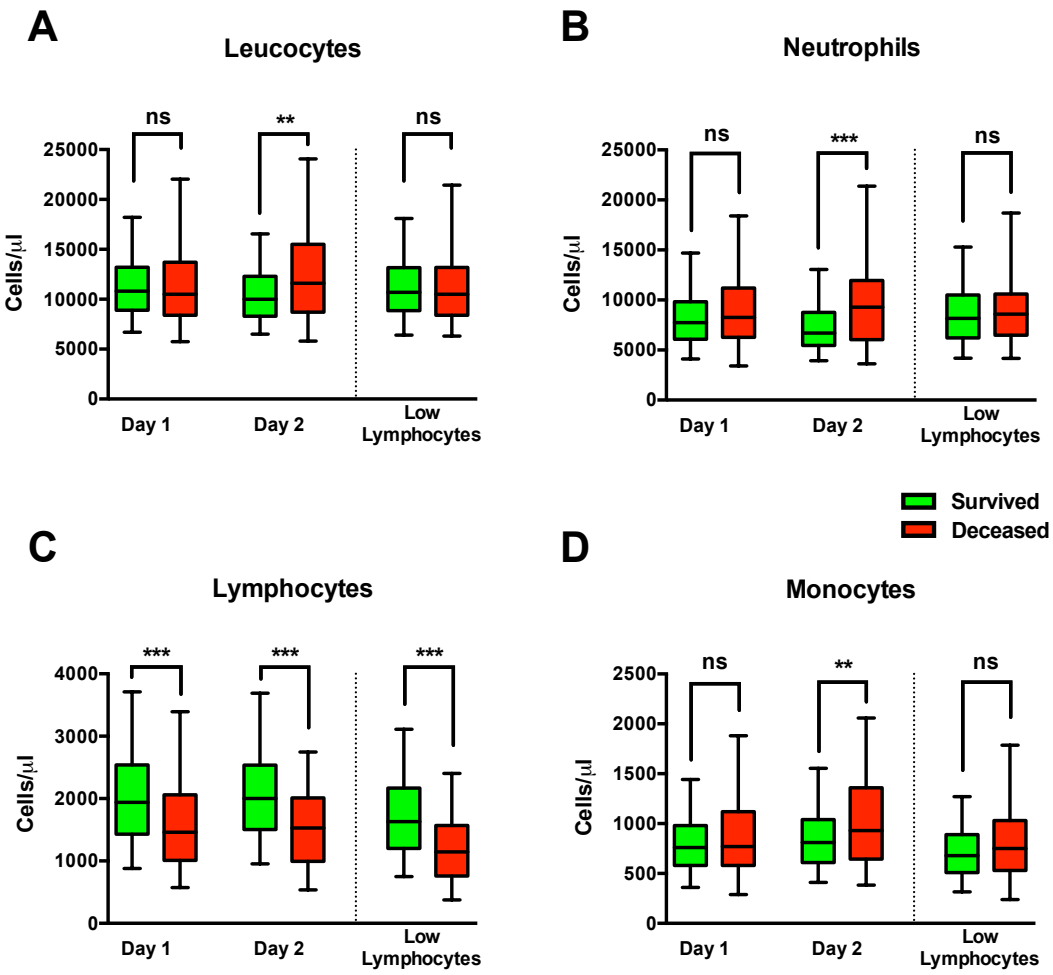

Figure 4.2: Cell counts according to primary outcome measure of mortality during follow-up, for total leucocytes (A), neutrophils (B), lymphocytes (C) and monocytes (D) in STEMI patients (total n=1377). Box plots display median (central line), 25th and 75th centiles (limits of box) and 5th and 95th centiles (error bars). The "low lymphocytes" sample refers to the sample from each case during the admission with the lowest lymphocyte count. Day 1: n=1363, day 2: n=666, "low lymphocytes": n=1377. Statistics refer to Mann-Whitney U Test for survived vs. deceased during follow-up. * $p<0.05$, ** $p<0.01$, ***$p<0.001$, ns = not significant

4.2.4 Grouping of Patients by Lowest Lymphocyte Count Quartiles Reveals Relationship with Mortality

Given that lymphocytes were the primary cells of interest in this study, and there were significant differences in their counts between survivors and non-survivors, patients were subsequently categorised into quartiles for further analysis based on their minimum lymphocytes counts. As with the mortality groups (**Table 4.1**), there were considerable differences between the low lymphocyte quartile groups (**Table 4.2**). The mean age decreased incrementally from quartile 1 (lowest lymphocyte counts, mean age: 69±13.3 [SD]) to quartile 4 (highest counts, mean age: 57.7±11.6) ($p<0.001$). Individuals with lower lymphocyte counts also tended have a lower BMI ($p<0.001$), and interestingly, a lower percentage of them had a positive smoking history than those in the higher quartiles ($p<0.001$). Analysis of the past medical history and admission blood parameters also revealed striking differences between the groups, again echoing the differences between mortality groups. Individuals in the lower quartiles tended to have greater comorbidities, with higher rates of hypertension, previous ischaemic heart disease (both angina and MI) and stroke/transient ischaemic attack (TIA), as well as lower haemoglobin and higher creatinine levels. Moreover, use of all recorded medical treatments during admission differed significantly between the groups, with lower rates in the lower quartiles. Once again, this may well be due to greater drug contraindications given the higher frequency of comorbidities in these patients. All of these findings are in keeping with generally older and more unwell patients occupying the lower lymphocyte count quartiles.

	Minimum-Lymphocyte Count Quartile					
	Q1 (≤1140 cells/μl)	**Q2** (1141-1565 cells/μl)	**Q3** (1566-2120 cells/μl)	**Q4** (>2120 cells/μl)	**n**	**p value**
Age (years)	69.0 ± 13.3	63.8 ± 12.9	60.9 ± 12.9	57.7 ± 11.6	1377	**<0.001**
Male sex	247 (72.2)	244 (72.4)	245 (68.8)	256 (74.9)	1377	0.361
BMI	26.8 ± 5.4	26.7 ± 4.6	28.3 ± 5.6	28.3 ± 5.2	1222	**<0.001**
Diabetes mellitus	36 (10.6)	39 (11.6)	33 (9.3)	36 (10.5)	1375	0.804
Family history of CAD	112 (38.4)	149 (49.7)	130 (39.9)	162 (50.3)	1240	**0.002**
Hypertension	153 (44.7)	152 (45.1)	129 (36.2)	119 (34.8)	1377	**0.005**
Hypercholesterolemia	97 (28.4)	100 (29.7)	103 (28.9)	106 (31.0)	1377	0.887
Current or ex-smoker	198 (63.5)	206 (64.4)	275 (79.7)	285 (85.6)	1310	**<0.001**
Previous angina	92 (27.5)	68 (20.2)	60 (17.3)	68 (20.1)	1352	**0.009**
Previous PCI	33 (9.7)	25 (7.4)	19 (5.3)	16 (4.7)	1374	**0.039**
Previous MI	66 (20.0)	49 (14.8)	45 (13.0)	34 (10.0)	1347	**0.003**
Previous stroke or TIA	25 (7.3)	20 (5.9)	8 (2.2)	14 (4.1)	1377	**0.012**
PVD	12 (3.5)	12 (3.6)	13 (3.7)	9 (2.6)	1377	0.869
Door to balloon time (min)	32.5 ± 20.2	28.7 ± 17.0	28.6 ±18.0	28.5 ± 17.1	1348	**0.005**
Total ischemic time (min)	289.6 ± 399.5	259.5 ± 250.4	251.5 ± 410.3	276.5 ± 423.4	1329	**0.001**
Cardiogenic shock Pre-PPCI	18 (5.3)	10 (3.0)	4 (1.1)	8 (2.4)	1367	**0.012**
Anterior MI	161 (47.4)	118 (35.1)	136 (38.6)	119 (35.0)	1368	**0.002**
Multivessel PCI	51 (14.9)	35 (10.4)	31 (8.7)	29 (8.5)	1377	**0.021**
TIMI 3 post-PCI	278 (87.7)	300 (94.3)	314 (93.5)	311 (94.2)	1301	**0.003**
Haemoglobin (g/l)	135.5 ± 17.5	137.9 ± 17.5	140.3 ± 15.1	144.2 ± 14.7	1374	**<0.001**
Serum cholesterol (mmol/l)	4.6 ± 1.3	5.0 ± 1.3	5.1 ± 1.2	5.4 ± 1.3	1283	**<0.001**
Serum creatinine (μmol/l)	113.6 ± 68.6	103.8 ± 46.1	98.2 ± 23.7	95.6 ± 22.4	1373	**<0.001**
Statin	298 (87.1)	294 (87.2)	330 (92.7)	316 (92.4)	1377	**0.012**
ACE-inhibitor/ARB	281 (82.2)	281 (83.4)	325 (91.3)	304 (88.9)	1377	**0.001**
Beta-blocker	273 (79.8)	274 (81.3)	311 (87.4)	300 (87.7)	1377	**0.005**
Clopidogrel	300 (87.7)	298 (88.4)	335 (94.1)	319 (93.3)	1377	**0.004**
Aspirin	303 (88.6)	298 (88.4)	335 (94.1)	320 (93.6)	1377	**0.007**
GP IIb/IIIa inhibitor	256 (75.3)	285 (84.8)	311 (87.9)	299 (87.7)	1371	**<0.001**

Table 4.2: Baseline data for 1377 consecutive patients treated with PPCI and discharged alive, divided into quartiles based on lowest lymphocyte count recorded during admission. Continuous variables expressed as mean ± SD and compared using Kruskal-Wallis test. Categorical variables expressed as n (% of valid n for relevant variable) and compared using chi-square (χ^2) test. The total n for each variable is shown in column 6. Discrepancy in this number between variables was due to missing values, which had not been recorded in the database at the time of admission.

Next, the survival rates for the minimum lymphocyte count quartile groups were analysed using the Kaplan Meier method, and compared with the log rank test (**Figure 4.3**). This revealed early divergence of the curves, with incrementally diminished survival in the lower lymphocyte quartiles. This was most striking in quartile 1 (lowest lymphocyte counts), with markedly lower early survival than the other groups. The divergence in survival rates between quartiles continued throughout the follow up period. Similar findings were revealed when the mortality data for these groups were compared using the chi-square (χ^2) test (**Table 4.3**). A total of 128 patients out of the full cohort of 1377 died during the follow up period. Of these, 64 patients were from quartile 1 (18.7% of that quartile), 32 from quartile 2 (9.5%), 23 from quartile 3 (6.5%), and only 9 (2.6%) from quartile 4 ($p<0.001$). As such, it is very clear that mortality was higher in the quartiles with lower lymphocyte counts. However, this analysis does not take into account the impact of confounding variables, which will almost certainly have been relevant given the numerous differences between the quartile groups (**Table 4.2**), and the obvious parallels with the differences between the mortality groups (**Table 4.1**).

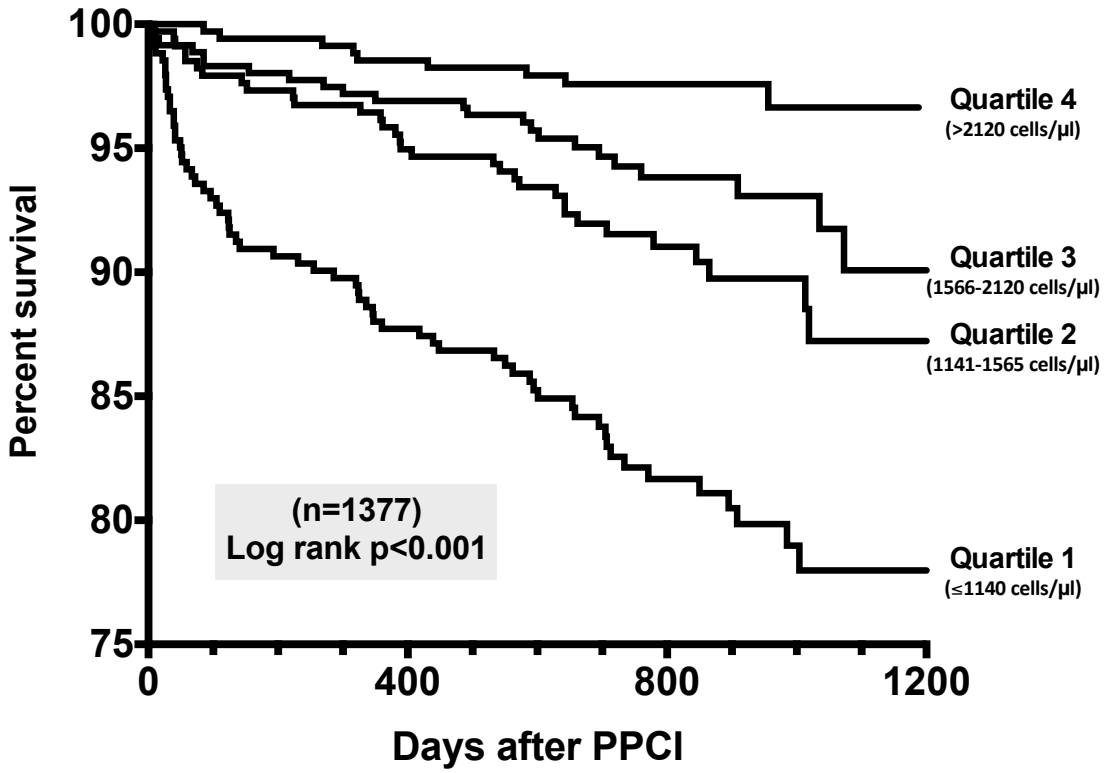

Figure 4.3: Kaplan Meier survival curves of 1377 consecutive patients discharged alive following PPCI (follow up time 1200 days). Patients were divided into 4 quartiles according to their minimum peripheral blood lymphocyte counts obtained during their admission. Curves compared using log rank test.

	Minimum-Lymphocyte Count Quartile					
	Q1 (≤1140 cells/µl)	Q2 (1141-1565 cells/µl)	Q3 (1566-2120 cells/µl)	Q4 (>2120 cells/µl)	Total	p value
n	342	337	356	342	1377	n/a
Mortality during follow up (%)	64 (18.7)	32 (9.5)	23 (6.5)	9 (2.6)	128 (9.3)	**<0.001**

Table 4.3: Mortality during follow up for STEMI patients discharged alive, according to minimum lymphocyte count quartile. Quartiles compared using chi squared (χ^2) test.

4.2.5 Multivariate Analysis Reveals Independent Predictive Effect of Lymphopaenia for Mortality in STEMI Patients Post-PPCI

In order to address the issue of confounding in the mortality data for lymphocyte count quartiles, multivariate stepwise Cox regression analysis was performed. This was done with two different models. In the first of these, model 1 (**Figure 4.4A**), the lymphocyte count quartile was entered as a categorical variable. In the second, model 2 (**Figure 4.4B**), the counts of lymphocytes, monocytes and neutrophils obtained at the time of the lowest lymphocyte count were entered as continuous variables. In both cases, known prognostic variables, as well as all other measured baseline, procedural or treatment variables that differed significantly between mortality groups (**Table 4.1**) or lymphocyte quartiles (**Table 4.2**) were entered as covariates.

Using model 1, the minimum lymphocyte quartile was independently predictive of mortality, with a hazard ratio (HR) of 2.88 (95% confidence interval (CI): 1.24-6.7) for quartile 1 vs. quartile 4 (p=0.014), and 2.81 (1.21-6.54) for quartile 2 vs. quartile 4 (p=0.017). Other variables independently associated with increased mortality in this model were increasing age, previous angina, diabetes mellitus and increasing serum creatinine (**Figure 4.4A** and **Table 4.4**). The use of a GP IIb/IIIa inhibitor during PPCI, on the other hand, was associated with reduced mortality. The complete list of variables entered into the analysis is shown in **Table 4.4**.

When leucocyte subset counts were entered into the Cox regression analysis as continuous variables (model 2, **Figure 4.4B** and **Table 4.4**), the lymphocyte count was again identified as an independent significant predictor for outcome. Increasing lymphocyte count was associated with a reduced risk of mortality (HR 0.56, 95% CI: 0.37-0.84 per 1000 cells/μl, p=0.005). Other significant variables in this model were increasing monocyte count, age, previous angina and increasing creatinine, all of which were associated with elevated mortality, while use of a GP IIb/IIIa inhibitor was again protective. Importantly, both of these Cox regression models clearly indicate that lymphopaenia was independently predictive of increased mortality in the STEMI cohort studied.

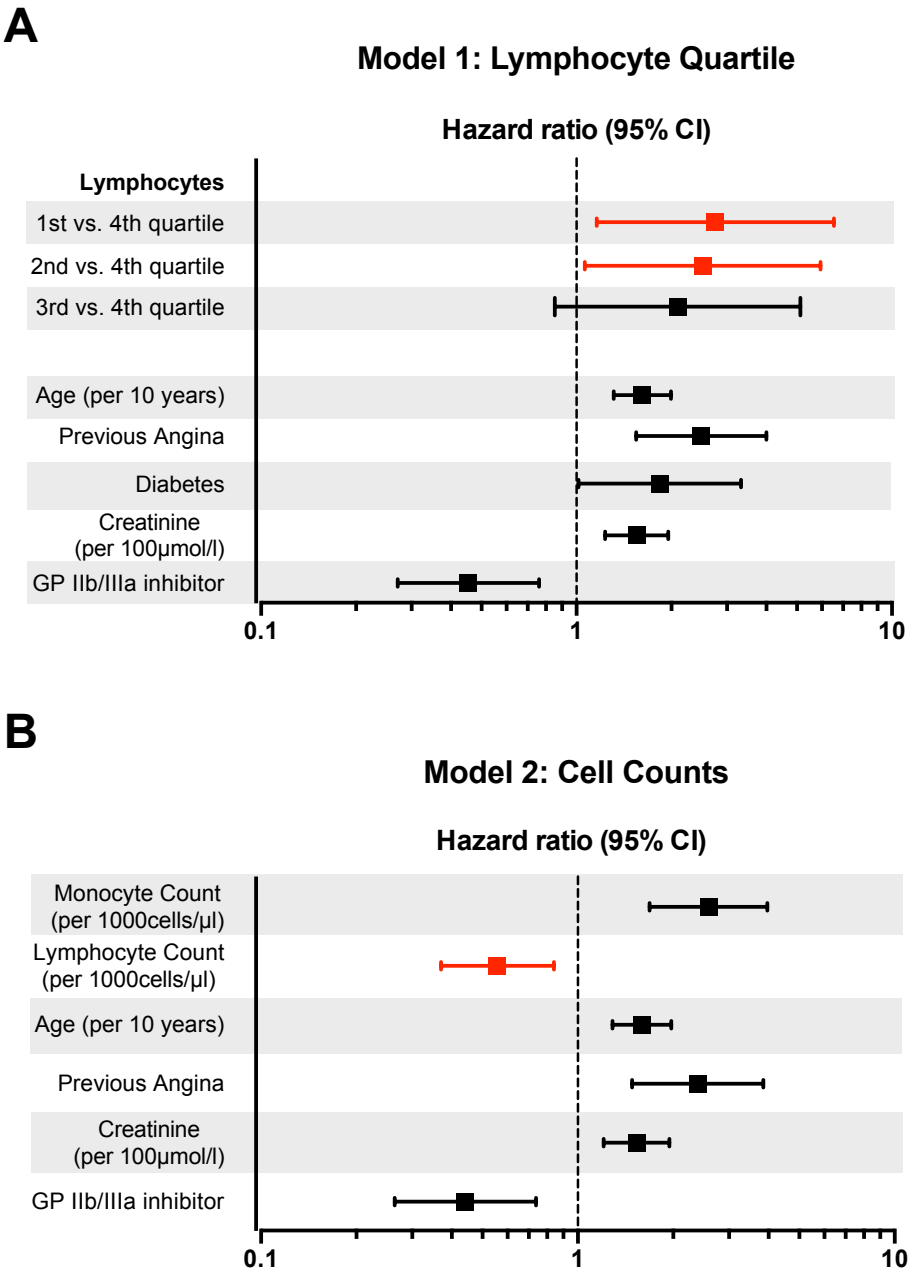

Figure 4.4: Multivariate analysis (backwards conditional stepwise Cox regression) for primary outcome (mortality during follow-up up to 1200 days) in STEMI patients discharged alive following PPCI. **A:** Model 1 in which lymphocyte quartile was entered as a covariate, along with all baseline variables that significantly varied between lymphocyte quartiles or primary outcome status. All significant predictors of mortality in this model are shown in the Forest plot, with hazard ratio indicated by the central square, and 95% CI by the error bars. **B:** Model 2 in which lymphocyte, monocyte and neutrophil counts at the time of the lowest lymphocyte count during admission were entered as continuous variables, along with covariates as in model 1. (n=934 for both models due to loss of 434 cases from total 1377 due to missing data for at least one variable).

Variable	Model 1		Model 2	
	Hazard Ratio (95% confidence interval)	**p value**	**Hazard Ratio (95% confidence interval)**	**p value**
Sex	N/A	0.633	N/A	0.796
Age (per 10 years)	1.62 (1.31 – 1.99)	**<0.001**	1.59 (1.29 – 1.97)	**<0.001**
BMI	N/A	0.622	N/A	0.986
Diabetes mellitus	1.84 (1.02 – 3.33)	**0.045**	N/A	0.151
Family history of CAD	N/A	0.675	N/A	0.858
Hypertension	N/A	0.406	N/A	0.632
Current or ex smoker	N/A	0.821	N/A	0.878
Previous angina	2.49 (1.55 – 4.00)	**<0.001**	2.39 (1.48 – 3.85)	**<0.001**
Previous PCI	N/A	0.800	N/A	0.976
Previous MI	N/A	0.685	N/A	0.880
Previous stroke/TIA	N/A	0.808	N/A	0.818
Door to balloon time (min)	N/A	0.761	N/A	0.775
Total ischemic time (min)	N/A	0.995	N/A	0.788
Cardiogenic shock Pre-PPCI	N/A	0.119	N/A	0.330
Anterior MI	N/A	0.499	N/A	0.517
Haemoglobin (per 10g/l)	N/A	0.199	N/A	0.102
Creatinine (per 100µmol/l)	1.55 (1.23 – 1.96)	**<0.001**	1.53 (1.21 – 1.95)	**<0.001**
Statin	N/A	0.341	N/A	0.349
ACE-inhibitor/ARB	N/A	0.800	N/A	0.989
Beta-blocker	N/A	0.697	N/A	0.527
Clopidogrel	N/A	0.466	N/A	0.461
Aspirin	N/A	0.525	N/A	0.522
GP IIb/IIIa inhibitor	0.45 (0.27 – 0.76)	**0.003**	0.44 (0.26 – 0.74)	**0.002**
Lymphocyte Quartiles				
Quartile 1 vs. Quartile 4	2.75 (1.16 – 6.55)	**0.022**	Not in Model	N/A
Quartile 2 vs. Quartile 4	2.51 (1.06 – 5.94)	**0.036**	Not in Model	N/A
Quartile 3 vs. Quartile 4	2.09 (0.85 – 5.13)	0.106	Not in Model	N/A
Cell Counts				
Lymphocytes (per 1000 cells/µl)	Not in Model	N/A	0.56 (0.37 – 0.84)	**0.005**
Monocytes (per 1000 cells/µl)	Not in Model	N/A	2.59 (1.69 – 3.97)	**<0.001**
Neutrophils (per 1000 cells/µl)	Not in Model	N/A	N/A	0.298

Table 4.4: Full list of variables entered into both stepwise Cox regression models (model 1 and model 2). P values are shown for all variables, as well as multivariate hazard ratios with 95% confidence intervals for all those included in final step of analysis. (n=934 for both models due to loss of 434 cases from total 1377 due to missing data for at least one variable).

4.3 Discussion

This study has provided helpful new information regarding the prognostic significance of lymphocyte counts following PPCI for STEMI. Analysis of the leucocyte counts available from before, during and after admission has also allowed assessment of temporal dynamics of the major leucocyte subsets in the bloodstream. As well as identifying an easily accessible marker of prognosis in STEMI, this result also justifies the use of circulating lymphocyte subset counts to investigate the role of T cells in myocardial I/R injury in the chapters that follow.

4.3.1 Temporal Changes in Leucocyte Counts in STEMI Treated by PPCI

Total leucocyte and major leucocyte subset counts were analysed at four main time points in this study, namely pre-admission, day 1 and day 2 post-PPCI, and post-discharge, as well as the time of the minimum lymphocyte count during the admission. This allowed assessment of the temporal evolution of cell counts following PPCI for STEMI.

Total leucocyte count and neutrophil count were both elevated during admission, peaking at day 1 following PPCI. This is in keeping with a marked inflammatory response occurring secondary to both acute infarction and reperfusion. Lymphocyte counts, on the other hand, were low compared to baseline after PPCI. In individuals with a post-discharge result the lymphocyte count had increased although not back to preadmission levels. These findings are in keeping with two studies that have previously investigated temporal evolution of leucocyte subsets following PPCI, both of which showed a marked drop of lymphocytes following reperfusion (Bodi et al., 2009; Husser et al., 2011). In contrast, monocyte counts were elevated during admission, but unlike neutrophils, the peak occurred later on day 2 post-PPCI. This is also in keeping with published data showing mobilisation of classical monocytes approximately 2 days after PPCI (Tsujioka et al., 2009). There are, however, limitations to the use of this data in assessing leucocyte temporal dynamics. This analysis was retrospective, with blood results recorded at the times they were taken for clinical reasons. Consequently, none of the sample timings were standardised, and there was variability for all of the time points.

Moreover, for the same reason not all samples were available in each patient, and in the case of the pre-admission and post-discharge results they were only available in a minority. Furthermore, the pre-admission and post-discharge samples were taken for clinical reasons at remote times. This meant that the timing was extremely variable, and clinical circumstances at the time of sampling were unknown. As such, the data in this chapter provides only a relatively crude assessment of leucocyte temporal dynamics. These limitations could be avoided by prospective recruitment and analysis of STEMI patients, with blood sampling occurring at standardised times specifically for the study. Such work has now been conducted and will form the basis of the subsequent chapters in this thesis.

4.3.2 Lymphocyte Counts and Clinical Outcome in STEMI Patients

Until now, the importance of lymphocyte counts in STEMI patients undergoing PPCI has not been fully elucidated. Lymphopaenia has previously been shown in a study of 1037 patients by Dragu et al. to be an independent predictor of long-term mortality in acute MI (Dragu et al., 2008). However, this study included both STEMI and NSTEMI patients, managed with a variety of treatment modalities. Furthermore, numerous studies have assessed the prognostic value of NLR in STEMI patients treated with PPCI, finding it to be an independent predictor of outcome, both in terms of mortality (Arbel et al., 2014; He et al., 2014; Núñez et al., 2008; Shen et al., 2010) and MACE (Han et al., 2013; Kaya et al., 2013). Moreover, an elevated NLR has been shown to be associated with no reflow post-PPCI, a finding related to MVO, one component of myocardial I/R injury (Akpek et al., 2012; Turkmen et al., 2013).

Very few previous studies have directly assessed the importance of lymphocyte counts in STEMI. One study by Núñez et al. has shown that lymphopaenia following PPCI is associated with increased risk of reinfarction within 3 years (Nunez et al., 2010). In another study by Bodi et al., lymphopaenia at 2 hours post-reperfusion in STEMI treated by PPCI was independently associated with MVO identified on cardiac MRI (Bodi et al., 2009). This important observation is suggestive of a potential link between lymphocytes and myocardial I/R injury in humans. However, one recent study appears to contradict this finding, demonstrating an

association between higher lymphocyte counts and poor microvascular reperfusion post-PPCI, as measured indirectly by angiographic myocardial blush grade and ECG ST segment resolution (Karahan et al., 2015). It is worth noting, however, that in the latter study the blood tests analysed were obtained prior to PPCI, as opposed to after reperfusion, as was the case in the study by Bodi et al.

The data described in this chapter add significantly to the existing literature described above. In keeping with findings of Núñez et al. regarding lymphopaenia and reinfarction risk, this study specifically used the minimum lymphocyte count obtained during admission, rather than initial or peak levels. This is of particular relevance given the temporal evolution of lymphocyte counts. Unlike neutrophils and monocytes, lymphocytes characteristically drop after PPCI, prior to recovery in their numbers. As such, focussing on admission or peak counts discounts the period of maximal lymphocyte reaction. This could lead to missing potentially important prognostic relationships. The use of peak lymphocyte counts, for example, may explain why Mariani et al. failed to find any relationship between these cells and their outcome measures of LV function recovery and myocardial blush grade (Mariani et al., 2006). In my study, however, the use of minimum lymphocyte counts has allowed me to demonstrate that lymphopaenia following PPCI is an independent predictor of long-term mortality.

By using the cell counts from the time of minimum lymphocyte count, this study was designed to primarily address the involvement of those cells after PPCI. Nevertheless, other leucocyte subsets, namely monocytes and neutrophils, were also included in the analysis. The availability of blood results, however, dictated that the data from the time of minimum lymphocyte count were also used for the other leucocyte subsets, as values were available in all subjects at that time point. As such, the criticism applied above to other studies investigating lymphocyte counts, can be applied to this study when considering other leucocyte subsets. Specifically, the monocyte and neutrophil counts included in the multivariate analysis may not accurately reflect the peak responses of those cells. However, Cox regression model 2, in which counts of each leucocyte subset were entered as continuous variables, also revealed a significant association between higher monocyte counts and increased mortality. Elevated monocyte counts, and in

particular those of the classical monocyte subset, are known to be associated with adverse outcomes from STEMI, in terms of LV salvage (Tsujioka et al., 2009) and MVO (Tsujioka et al., 2010), as well as regional (van der Laan et al., 2012a) and overall (Hong et al., 2007; Mariani et al., 2006) LV functional recovery. This study, however, is the first to demonstrate that monocyte count is an independent predictor of long-term mortality following PPCI for STEMI.

4.4 Conclusions

The data presented in this chapter provide valuable new information on the prognostic relevance of lymphocytes in STEMI treated by PPCI. However, while the findings suggest the involvement of these cells in the processes of myocardial injury in this context, such mechanisms are yet to be elucidated. As discussed in section 1.5.1, there is considerable evidence from animal models supporting a role for T lymphocytes in myocardial I/R injury. Although I have identified the prognostic relevance of total lymphocyte counts in this chapter, lymphocyte subset counts, however, were not available in the retrospective cohort described here. Moreover, cardiac MRI scanning, which would allow quantification of MVO, was not performed in these patients. In order to address these issues the subsequent chapters of this thesis will go on to describe a comprehensive analysis of detailed lymphocyte subset dynamics in a prospectively recruited cohort of STEMI patients. One important benefit of the study described so far, however, is that it justifies the use of circulating lymphocyte counts in the subsequent prospective study, given their clear prognostic significance.

Chapter 5

Leucocyte Dynamics Following Reperfusion in STEMI

5.1 Introduction

In the previous chapter retrospective analysis of a cohort of 1377 STEMI patients allowed a crude assessment of major leucocyte subset kinetics following PPCI. However, there were several limitations to the use of this retrospective data in this regard. Most notably, the timings for blood tests were not standardised, and depended on clinical need in the cases analysed. For the same reason, only a small number of blood results for each patient were available during the admission. In particular, blood sampling had not been conducted on multiple occasions in the early period after PPCI, therefore not allowing any assessment of leucocyte dynamics directly after reperfusion. Clearly, this immediate post-reperfusion time period is of greatest interest when considering the involvement of cells in I/R injury. Moreover, the use of standard hospital pathology blood results limited the available data to major leucocyte subsets. Consequently, no distinction was possible between lymphocyte subsets, such as T cells, B cells and NK cells. As such, no inference was possible regarding T cell kinetics in the retrospectively studied patient cohort. This is clearly of relevance given the previously discussed evidence for a role for T cells in myocardial I/R injury in murine studies (Liao et al., 2012; Yang et al., 2005; Yang et al., 2006).

At the time of starting this project, existing knowledge of lymphocyte, and in particular lymphocyte subset kinetics following PPCI in humans was extremely limited. The previously discussed studies by Bodi et al. and Husser et al. had established that, in contrast to total leucocytes, neutrophils and monocytes, circulating lymphocyte counts drop following reperfusion prior to a subsequent recovery (Bodi et al., 2009; Husser et al., 2011). The only published data on more detailed lymphocytes subsets in this setting came from a small pilot study conducted by Hoffman et al., led by my PhD supervisor, Prof I Spyridopoulos. This showed that in a group of 17 STEMI patients treated by PPCI, $CD4^+$ T cells were depleted in the bloodstream within 30 minutes of reperfusion (Hoffmann et al., 2012). In the present study, however, I intended to clarify this phenomenon further, and provide the first detailed analysis of lymphocyte and T cell subset dynamics following reperfusion in STEMI.

In order to achieve this, I prospectively recruited a cohort of 60 STEMI patients undergoing PPCI in the Freeman Hospital, Newcastle upon Tyne, between September 2012 and March 2015, as well as 15 NSTEMI patients undergoing non-emergency PCI. The rationale for the latter group was to provide a control group of patients undergoing the same PCI procedure, but without the acute ischaemia/reperfusion process associated with vessel opening in STEMI. All patients had blood taken for detailed leucocyte characterisation at the start of the procedure (prior to reperfusion or intervention), and at specified time points thereafter. On subsequent review of the clinical history, one STEMI case was identified as having an onset to reperfusion time of greater than 6 hours, and was therefore excluded from the analysis, leaving 59 patients in this group. For a detailed description of all methodologies involved in this prospective study please see Chapter 3. The baseline characteristics of both groups included in this part of the study are shown in **Table 5.1**.

	STEMI (n=59)	NSTEMI (n=15)	p value
Age	59.3 ± 10.7	61.1 ± 11.8	0.742
Male sex	44 (74.6)	11 (73.3)	1.000
BMI	26.8 ± 4.6	30.9 ± 6.0	**0.006**
Diabetes mellitus	6 (10.2)	0 (0)	0.337
Family history of CAD	23 (39.0)	7 (46.7)	0.697
Active smoker	31 (52.5)	4 (26.7)	0.089
Hypertension	19 (32.2)	10 (66.7)	**0.020**
Anterior MI	28 (47.5)	N/A	N/A
Serum cholesterol (mmol/l)	5.3 ± 1.1	4.3 ± 1.1	**0.036**
Serum creatinine (µmol/l)	80.2 ± 17.0	84.9 ± 21.4	0.472
Peak troponin T (ng/l)	4899 ± 3385	207 ± 214	**<0.001**
Procedural Characteristics			
Door-to-balloon time (minutes)	26.8 ± 14.3	N/A	N/A
Onset-to-reperfusion time (minutes)	164.6 ± 81.3	N/A	N/A
Onset-to-procedure time (days)	N/A	5.01± 2.78	N/A
Pre-PCI flow (TIMI 0/1/2/3)	55/4/0/0	2/1/0/12	**<0.001**
Post-PCI flow (TIMI 0/1/2/3)	0/0/0/59	1/0/0/14	0.203
Vascular access (radial/femoral)	56/3	13/2	0.265
Pre-admission Medication			
Statin therapy	10 (16.9)	6 (40.0)	0.077
B-blocker	2 (3.4)	3 (20.0)	0.054
Aspirin	5 (8.5)	2 (13.3)	0.624
ACE-inhibitor/ARB	6 (10.2)	7 (46.7)	**0.003**

Table 5.1: Baseline data for STEMI and NSTEMI patients. Continuous variables expressed as mean ± SD and compared using Mann-Whitney U test. Categorical variables expressed as n (%) and compared using chi-square (χ^2) or Fisher's exact test as appropriate.

5.2 Results

5.2.1 Acute Dynamic Changes in Major Leucocyte Subsets Following Reperfusion

Leucocyte subsets were quantified in STEMI and NSTEMI patients undergoing PCI at the start of the procedure and at 15, 30 and 90 minutes following reperfusion/intervention. Further blood samples were analysed in the STEMI patients only at 24 hours, and then in a subset of STEMI patients at a remote follow up time of 3-6 months. Characteristic patterns were seen in the STEMI patients, with early depletion of lymphocyte counts compared to pre-PPCI (2295±129 [SEM] cells/μl) occurring until 90 minutes (1317±78 cells/μl), with recovery by 24 hours (2153±101 cells/μl) (p for trend <0.001, **Figure 5.1A**). In contrast, comparable changes were not seen in the NSTEMI group. This resulted in significantly lower lymphocyte counts in the STEMI group compared to NSTEMI at 90 minutes (p=0.012).

The temporal evolution of other leucocyte subsets in the STEMI group also showed distinct dynamics. There was a small drop in monocyte counts by 90 minutes (635±36 to 522±28 cells/μl, p<0.001), followed by a peak at 24 hours (776±36 cells/μl, p<0.001 vs. 90min, **Figure 5.1B**). The monocyte count did not change significantly between pre-PCI and 90 minutes in the NSTEMI group. No significant differences were observed in monocyte counts between STEMI and NSTEMI patients over the time points studied in both groups. Granulocyte counts were unsurprisingly significantly higher in the STEMI group at each comparable time point (p<0.001, **Figure 5.1C**). There was no significant change in the granulocyte count from the start of the procedure to 90 minutes in either group, although it then declined in the STEMI patients between 90 minutes and 24 hours (p<0.001).

Within the lymphocyte population, the transient depletion observed after reperfusion in the STEMI group was primarily due to loss of T cells and NK cells. The total T cell count dropped from 1508±95 cells/μl pre-reperfusion to 898±58 cells/μl at 90 minutes (p<0.001, **Figure 5.1D**), prior to recovery by 24 hours. In contrast, no significant decline was seen in the NSTEMI group. Amongst the T cells,

there was a more marked decline in $CD8^+$ T cells than $CD4^+$ T cells following reperfusion in STEMI. The $CD4^+$ T cells dropped from 935±65 to 653±47 cells/μl at 90 minutes ($p<0.001$), before recovering completely to 1076±58 cells/μl at 24 hours ($p<0.001$). $CD8^+$ T cells, however, declined from 494±48 cells/μl at the start of the procedure to 216±17 cells/μl at 90 minutes post-reperfusion ($p<0.001$), before recovering to 463±33 cells/μl at 24 hours ($p<0.001$). Neither $CD4^+$ nor $CD8^+$ T cells changed significantly between the start of the procedure and 90 minutes in the NSTEMI group.

As with T cells, NK cells showed a large drop in the STEMI group, from 501±33 cells/μl to 203±18 cells/μl at 90 minutes ($p<0.001$, **Figure 3G**), although they did not significantly recover by 24 hours. Unlike in T cells, however, the drop in the STEMI group was paralleled by a similar, albeit slightly smaller, drop in the NSTEMI group (397±65 to 216±24 cells/μl at 90 minutes, $p=0.004$). In the STEMI patients, B cells exhibited a smaller drop than T cells or NK cells between pre-reperfusion and 90 minutes post-reperfusion (286±24 to 216±17 cells/μl, $p<0.001$). In contrast, there was no significant change in the NSTEMI group.

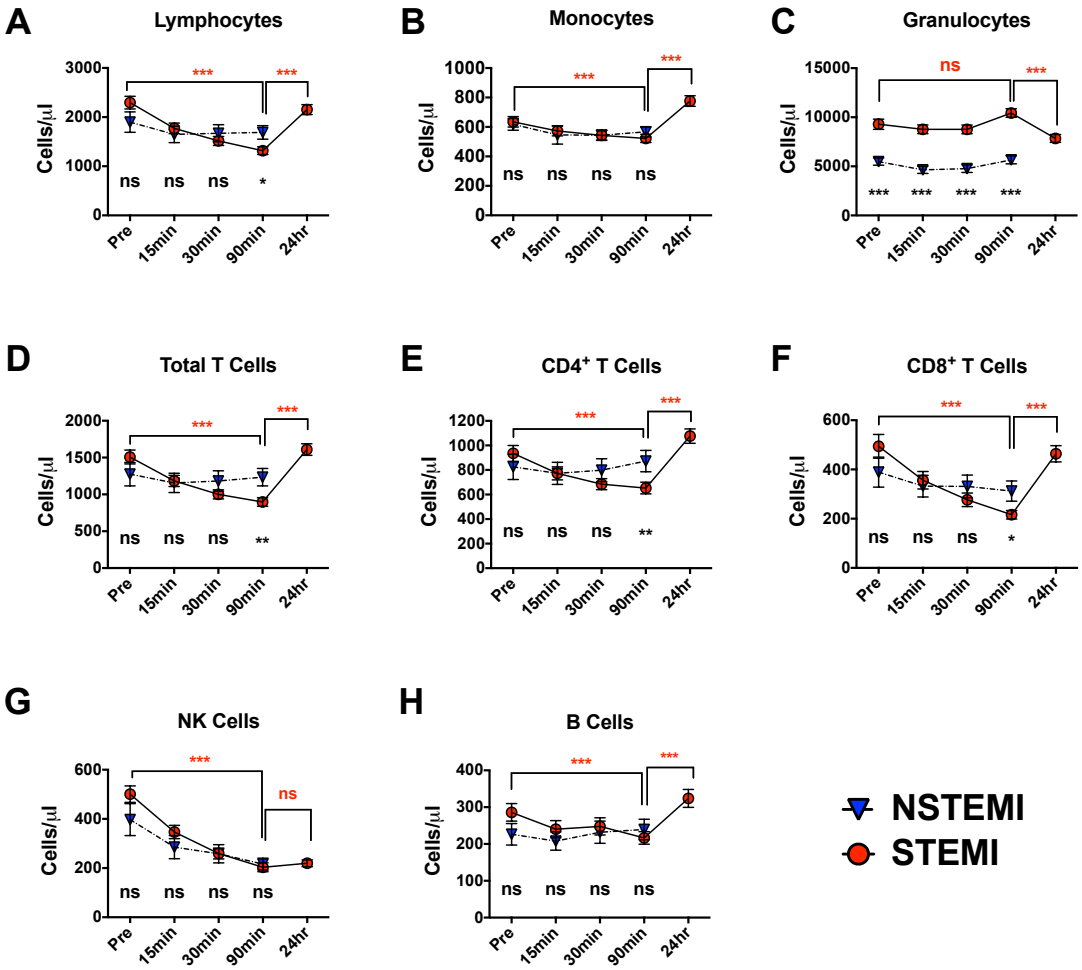

Figure 5.1: Acute time courses in circulating leucocyte subset counts**. A-C:** Major leucocyte subsets of (A) lymphocytes, (B) monocytes and (C) granulocytes, showing change in cell counts over time. Time points were measured from reperfusion in STEMI group (red circles), and from first culprit vessel instrumentation (or initial 'pre' blood sampling if no intervention) in NSTEMI group (blue triangles). **D-F**: T lymphocyte cell counts, including (D) total, (E) $CD4^+$ T cells and (F) $CD8^+$ T cells. **G-H:** $CD3^-$ (non-T) lymphocyte subset counts: (G) NK cells and (H) B cells. Upper statistics (red) refer to difference in counts between indicated time points in the STEMI group (Friedman test, with Dunn's multiple comparisons test), while lower (black) refer to difference between STEMI and NSTEMI at corresponding time points (Mann-Whitney U test) (STEMI n=59, NSTEMI n=15). * $p<0.05$, ** $p<0.01$, ***$p<0.001$, ns = not significant.

5.2.2 Highly Differentiated Effector T Cell Subsets Show Greater Decline Following Reperfusion in STEMI

Having established the transient loss of circulating T cells following reperfusion in STEMI, I next focused on the distribution and behaviour of the subpopulations. At the initial time point, there were no statistical differences between the absolute counts of any of the principal $CD4^+$ or $CD8^+$ T cell subsets, namely T_N, T_{CM}, T_{EM} and T_{EMRA} for each, between the STEMI and the NSTEMI patients (**Figure 5.2A+B**). Within the $CD4^+$ T cell compartment, T_N cells were most numerous (370±33 cells/μl in the STEMI group), with T_{CM} cells the next most abundant at 256±18 cells/μl. Of the two $CD4^+$ effector T cell populations, T_{EM} were most plentiful at 251±23 cells/μl, while $CD4^+$ T_{EMRA} cells were comparatively rare at only 59±11 cells/μl in STEMI patients. In the $CD8^+$ T cell compartment, on the other hand, the vast majority of cells were effector cells (295±33 cells/μl for $CD8^+$ T_{EMRA} and 124±14 cells/μl for $CD8^+$ T_{EM}). There were comparatively fewer $CD8^+$ T_N cells at 59±7 cells/μl, while $CD8^+$ T_{CM} cells were infrequent at only 16±2 cells/μl. When the subpopulations were expressed as a percentage of their parent population (i.e. $CD4^+$ or $CD8^+$ T cells), there were also no differences between STEMI and NSTEMI patients at the pre-PCI time point (**Figure 5.2C+D**).

By the 90 minute time point, the distribution of T cell subsets had changed considerably. Although there was no significant difference in the $CD4^+$ T_N count between the groups, the counts of $CD4^+$ T_{CM} (194±14 vs. 233±17 cells/μl, p=0.043), $CD4^+$ T_{EM} (147±9 vs. 227±20 cells/μl, p<0.001) and $CD4^+$ T_{EMRA} (27±4 vs. 32±4 cells/μl, p=0.019) were all lower in STEMI compared to NSTEMI patients (**Figure 5.2E**). Amongst the $CD8^+$ T cells, there were no significant differences in the T_N or T_{CM} cell counts between the groups. Both effector cell populations, however, were now significantly lower in the STEMI patients (54±4 vs. 95±15 cells/μl, p=0.001 for $CD8^+$ T_{EM} cells, 102±10 vs. 147±22 cells/μl, p=0.038 for $CD8^+$ T_{EMRA} cells) (**Figure 5.2F**).

In order to control for the variations in cell counts between different individuals, I next considered the percentage changes in cell counts over time for each population. To address the earliest changes post-reperfusion, the 15-30 minute

time period was used (**Figure 5.3A+B**). The reason that this period was chosen, rather than pre-15 or pre-30min, was that the "pre-reperfusion" time point was variable in its relation to reperfusion. The other timings were taken from the point of reperfusion precisely, whereas the initial "pre-reperfusion" sample was taken at the start of the procedure, and the time to reperfusion from that point varied. As such, the 15-30 minute time period provided a more clearly defined interval, all of which occurred after reperfusion. The total change occurring acutely, on the other hand, was best represented by the pre-reperfusion to 90 minute time period (**Figure 5.3C+D**), at the end of which T cell counts reached their nadir.

Between pre-reperfusion and 90 minutes post-reperfusion in STEMI patients total $CD4^+$ T cells dropped by a median of -29% (interquartile range (IQR): -43; -15%) and $CD8^+$ T cells by -55% (IQR: -66; -29). Comparable drops were not observed in the NSTEMI patients. Within these two major T cell subsets, depletion in STEMI patients varied between the subpopulations, with a greater drop in the more differentiated cells (**Figure 5.3C+D**). In the case of $CD4^+$ T cells, the median drop for T_N cells was -24% (-39; -13) and T_{CM} cells -22% (-37; -9), compared to -39% (-54; -15) for T_{EM} and -41% (-61; -17) for T_{EMRA} cells ($p<0.001$ for overall Friedman test) (**Figure 5.3C**). A similar pattern was seen over this time period in the $CD8^+$ T cell subsets. The $CD8^+$ T_{EM} cells declined by -52% (-67; -37) and the $CD8^+$ T_{EMRA} cells by -66% (-74; -44), compared to only -26% (-40; -5) for $CD8^+$ T_N cells and -26% (-43; -6) for $CD8^+$ T_{CM} cells (**Figure 5.3D**). An analogous picture was observed in the very early post-reperfusion period between 15 and 30 minutes (**Figure 5.3A+B**). Again, a progressively greater drop was seen as cellular differentiation levels increased. In the case of $CD4^+$ T cells the median changes were -4% (-12; -1), -7% (-14; -1), -14.5% (-23; -4) and -14.5% (-29; -5) for T_N, T_{CM}, T_{EM} and T_{EMRA} cells respectively, while the equivalent changes in $CD8^+$ T cell subsets were -7% (-16; 0), -8.5% (-21; -5), -20% (-27; -10) and -24.5% (-35; -11). As such, the $CCR7^-$ effector subsets (T_{EM} and T_{EMRA}) declined by significantly more than the $CCR7^+$ cells (T_N and T_{CM}) in both $CD4^+$ and $CD8^+$ T cells ($p<0.001$, for both 15-30min and pre-90min periods). Moreover, when the effector T cell subsets were further divided by expression of the co-stimulatory molecule CD27, which is downregulated in highly differentiated T cells, the drop was greater still in cells lacking expression (**Figure 5.3E+F**).

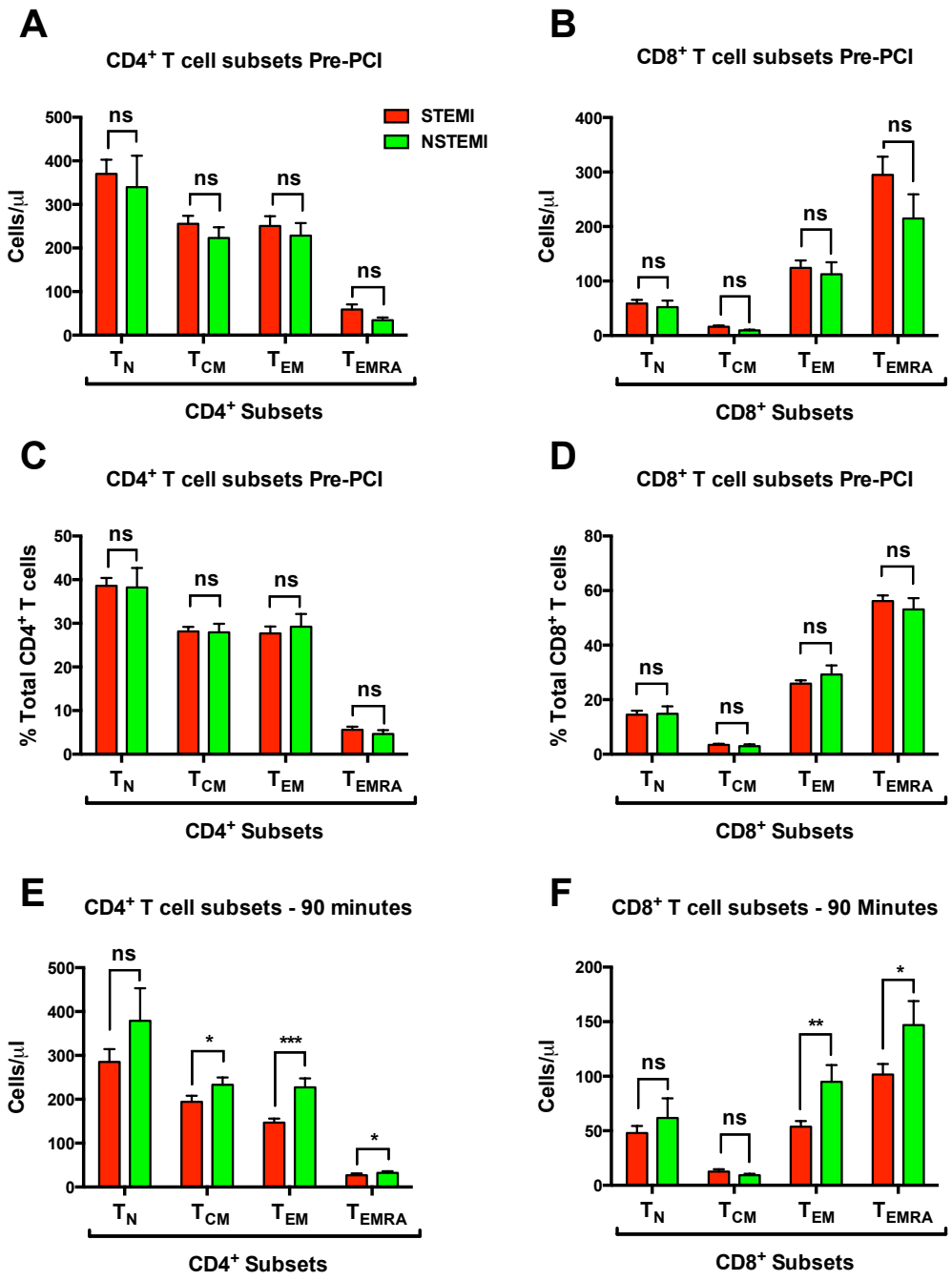

Figure 5.2: Absolute counts and percentages of T cell subsets in STEMI and NSTEMI**. A** and **B** show CD4+ and CD8+ T cell subsets counts respectively in both STEMI (n=59) and NSTEMI (n=15) groups at the pre-PCI time point. **C** and **D** show the percentages of CD4+ and CD8+ T cell subsets respectively at the pre-PCI time point. **E** and **F** show CD4+ and CD8+ T cell subsets counts respectively at 90 minutes (time measured from reperfusion in STEMI group and from first culprit vessel instrumentation, or initial 'pre' blood sampling if no intervention, in NSTEMI group). Groups compared using Mann-Whitney U test. * $p<0.05$, ** $p<0.01$, ***$p<0.001$, ns = not significant.

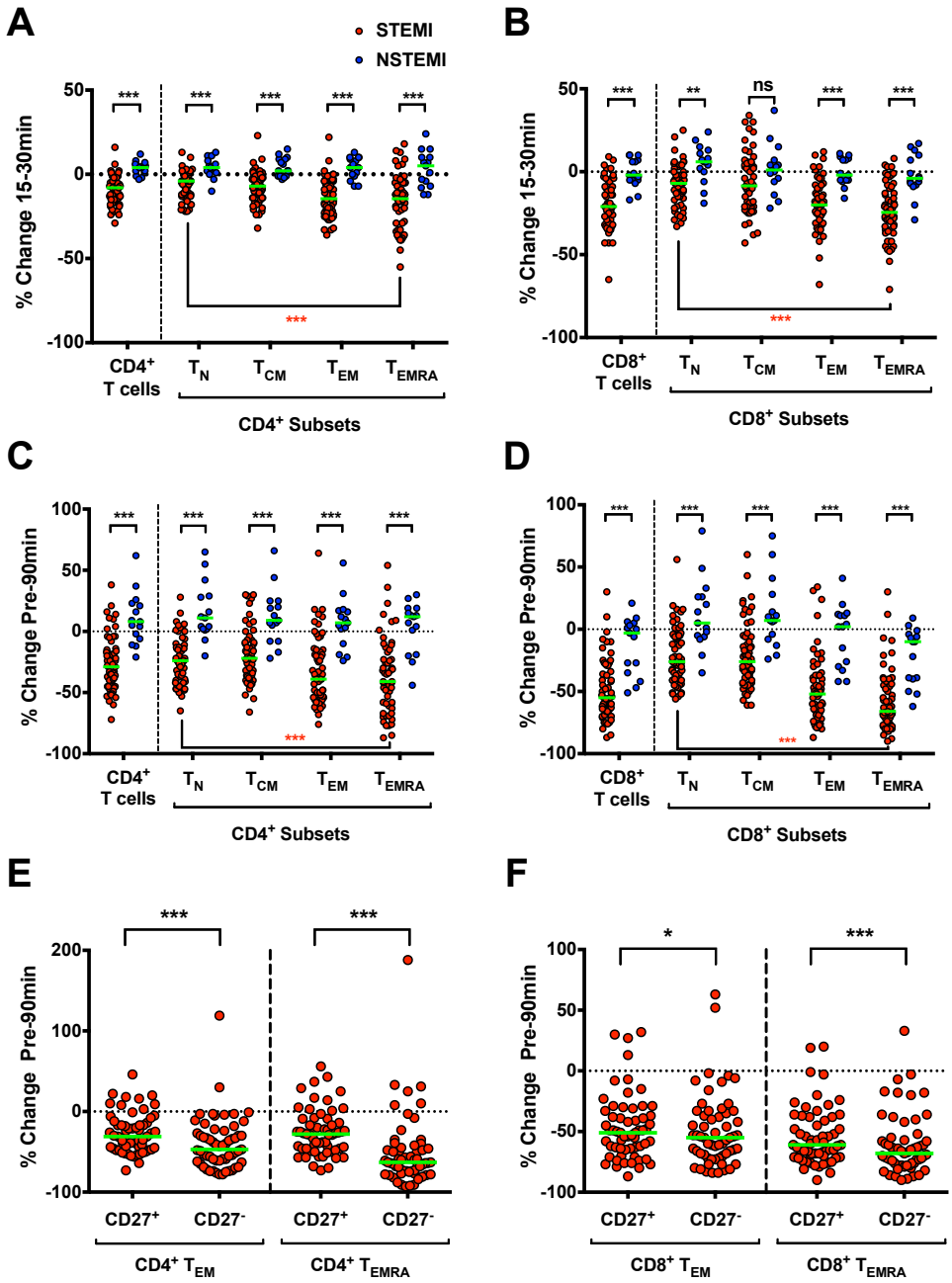

Figure 5.3: Percentage change in counts of circulating T cell subsets. **A and B:** Percentage change in T cell subset counts in STEMI (red) and NSTEMI (blue), shown as scatter plots of percentage change between 15 and 30 minutes post-reperfusion, in **A:** CD4+ T cells and subsets, and **B:** CD8+ T cells and subsets. **C and D:** Percentage change in T cell subset counts between pre-reperfusion and 90 minutes in **C:** CD4+ T cells and subsets, and **D:** CD8+ T cells and subsets. Upper statistics (black) refer to differences between groups (STEMI and NSTEMI) for each subset (Mann-Whitney U test), lower (red) indicate differences between subsets in the STEMI group (Friedman test) (STEMI n=59 NSTEMI n=15). **E and F:** Percentage change in effector T cell subsets between pre-reperfusion and 90 minutes in STEMI patients, in **E**: CD4+ T cell subsets and **F**: CD8+ T cell subsets, with effector (T_{EM} and T_{EMRA}) subsets further divided based on expression of the co-stimulatory molecule CD27.. Statistics refer to Wilcoxon signed rank test for indicated populations, * $p<0.05$, *** $p<0.001$, ns = not significant. (n=56 in **A+B**, n=59 in **C-F**, disparity due to lack of 15 min samples in 3 patients due to concurrent clinical circumstances)

5.2.3 Differential Recovery of T Cell Subsets Following Reperfusion-Induced Depletion

Next, I considered the recovery of the various T cell subpopulations following their acute depletion after reperfusion. In order to address this, both the overall changes between pre-reperfusion and 24 hours (**Figure 5.4A+B**) and the change between 90 minutes and 24 hours (**Figure 5.4C+D**) were considered. Within the $CD4^+$ compartment, all subsets recovered to beyond their pre-reperfusion starting point by 24 hours, with median pre-reperfusion to 24 hour changes of +19.5% (-6; +50), +31% (+12.5; +64), +12% (-11; +44) and +30.5 (-7.5; +85.5) for T_N, T_{CM}, T_{EM} and T_{EMRA} cells respectively. The T_{CM} and T_{EMRA} populations both had significantly greater overall increases in this time period than either of the T_N or T_{EM} populations ($p<0.001$ for each comparison) (**Figure 5.4A**). When the 90 minute to 24 hour period alone was considered, the $CD4^+$ T_{EMRA} cells showed greater recovery than any of the other $CD4^+$ subsets (**Figure 5.4C**), although it must be remembered that this was from a lower nadir, as they had also dropped more than the other subsets following reperfusion (**Figure 5.3C**).

A slightly different pattern was seen in the $CD8^+$ subsets. In this case, over the entire pre-reperfusion to 24 hour period, all subsets except T_{EM} cells increased in circulating numbers, with the median changes being +33.5% (+3.5; +63), +32% (+8; +78), -8.5% (-25; +17) and +6% (-25.5; +35) for T_N, T_{CM}, T_{EM} and T_{EMRA} cells respectively. Of these subsets, the overall change in T_N and T_{CM} cells was significantly more positive than either of the T_{EM} and T_{EMRA} cells ($p<0.001$ in each comparison) (**Figure 5.4B**). Over the 90 minute to 24 hour period alone, all $CD8^+$ T cell subsets showed a positive change, although this was significantly greater in the T_{EMRA} cells than any other subset ($p<0.001$ for each comparison) (**Figure 5.4D**).

In summary, in both $CD4^+$ and $CD8^+$ T cells, the subsets that most consistently showed an overall percentage increase over the full 24 hour period were the T_{CM} cells, while the T_{EMRA} cells showed the strongest percentage recovery from the 90 minute levels. It is unclear whether this latter finding was due to expansion of the existing circulating T_{EMRA} pool, accelerated differentiation of other subsets to take

up a more senescent phenotype, or a return of cells lost immediately following reperfusion to the circulation over the next 24 hours.

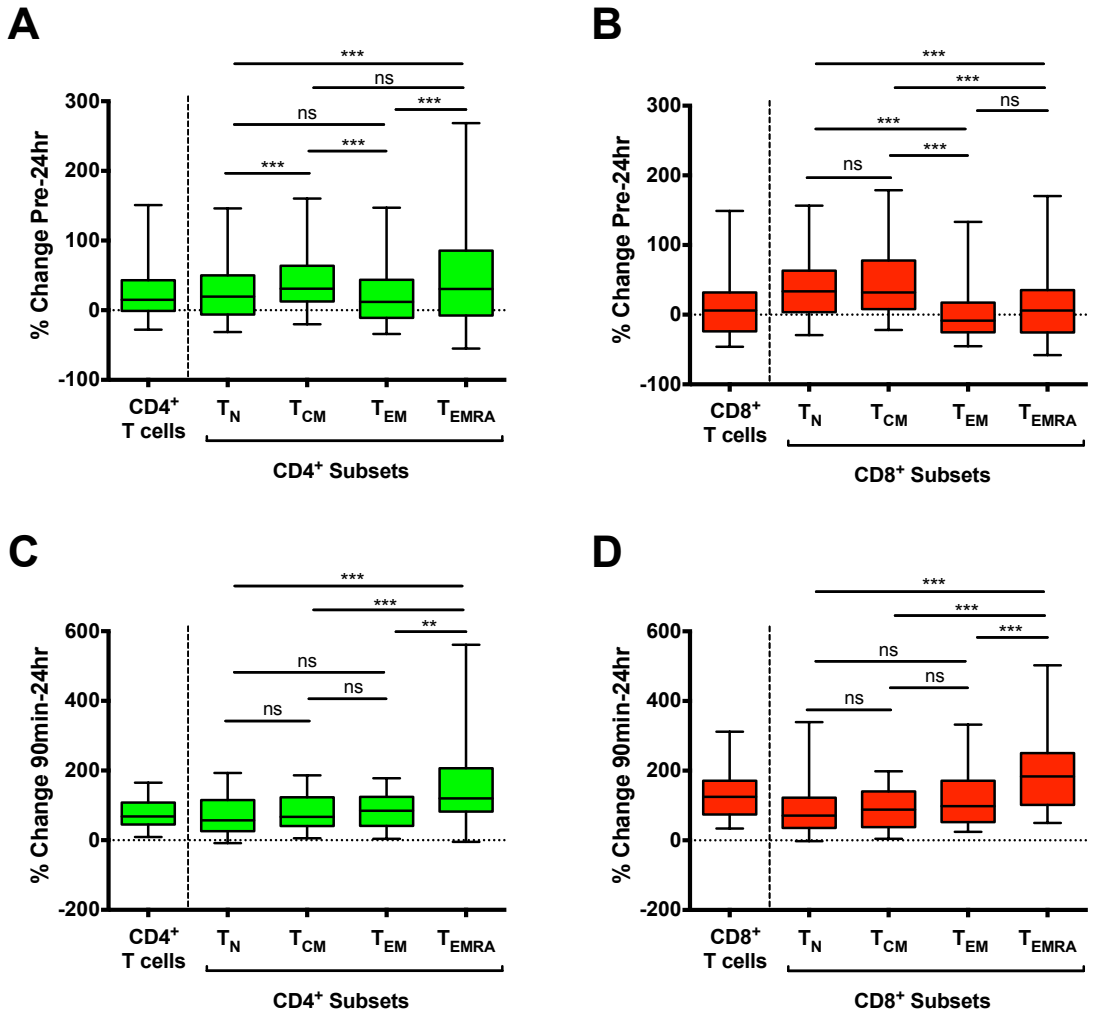

Figure 5.4: Percentage change in counts of circulating T cell subsets over 24 hours post-reperfusion in STEMI patients. **A and B:** Percentage change in T cell subset count in STEMI between pre-reperfusion and 24 hours post-reperfusion in **A:** CD4+ T cells and subsets, and **B:** CD8+ T cells and subsets. **C and D:** Percentage change in T cell subset count in STEMI between 90 minutes and 24 hours post-reperfusion in **C:** CD4+ T cells and subsets, and **D:** CD8+ T cells and subsets. Data shown as box and whisker plots, in which central line shows median value, limits of box the 25th and 75th percentiles, and error bars the 5th and 95th percentiles. Statistics show results of Friedman test with Dunn's multiple comparisons test for each pair of subsets as indicated. ** $p<0.01$, *** $p<0.001$, ns = not significant

5.2.4 The Effect of Pre-Admission Statins on Leucocyte Counts and Post-Reperfusion Dynamics

Next I considered whether the regular medication received by a patient prior to admission with STEMI would affect the admission leucocyte counts and subsequent post-reperfusion dynamics. In particular, I was interested in the impact of statins, given their well-documented anti-inflammatory properties (Antonopoulos et al., 2012). Of the 59 patients in the STEMI group, 10 were receiving statins preadmission. Interestingly, these patients did have significantly higher lymphocyte and T cell counts at presentation (**Table 5.2**). However, the subsequent percentage changes in leucocyte counts following reperfusion were no different between cases with or without statins (**Table 5.3)**, indicating that the data relating to dynamic changes in cell counts post-reperfusion were unlikely to have been affected by this therapy.

Cell Count (cells/μl ± SEM)			
Leucocyte Subset	**No Statin Pre-admission (n=49)**	**Statin Pre-admission (n=10)**	**P value**
Granulocytes	9243 ± 510	9507 ± 1790	0.840
Monocytes	638 ± 41	621 ± 62	0.832
Lymphocytes	2187 ± 140	2822 ± 285	**0.045**
B cells	287 ± 28	283 ± 39	0.671
NK cells	484 ± 36	585 ± 84	0.308
T cells	1417 ± 102	1954 ± 203	**0.019**
$CD4^+$ T cells	878 ± 69	1215 ± 157	**0.025**
$CD4^+ CCR7^+$ T cells	586 ± 48	821 ± 112	0.055
$CD4^+ CCR7^-$ T cells	292 ± 34	395 ± 62	**0.041**
$CD8^+$ T cells	462 ± 55	648 ± 83	**0.005**
$CD8^+ CCR7^+$ T cells	74 ± 9	79 ± 25	0.960
$CD8^+ CCR7^-$ T cells	388 ± 50	570 ± 84	**0.005**

Table 5.2: Baseline (pre-PPCI) leucocyte counts in STEMI patients with and without preadmission statin therapy. Data expressed as mean ± SEM. Groups compared using Mann-Whitney U test.

Percentage Change in Cell Count Pre-reperfusion to 90 minutes (median [IQR])			
Leucocyte Subset	**No Statin Pre-admission (n=49)**	**Statin Pre-admission (n=10)**	**p value**
Granulocytes	+3 (-11; +44.5)	+19.5 (-7.5; +105)	0.317
Monocytes	-10 (-35.5; -0.5)	-7.5 (-27; +4)	0.353
Lymphocytes	-44 (-52.5; -24)	-43.5 (-51.5; -14)	0.686
B cells	-22 (-34; -12)	-15.5 (-28.5; -1)	0.203
NK cells	-62 (-73.5; -45)	-62.5 (-70; -6)	0.473
T cells	-40 (-54; -20)	-44 (-51.5; -18)	0.864
$CD4^+$ T cells	-29 (-42.5; -15.5)	-32 (-45; -7)	0.887
$CD4^+ CCR7^+$ T cells	-25 (-38; -12)	-25.5 (-42; -3)	0.944
$CD4^+ CCR7^-$ T cells	-38 (-56.5; -17)	-44 (-53; -21.5)	0.762
$CD8^+$ T cells	-55 (-65; -32)	-55 (-71; -29)	0.716
$CD8^+ CCR7^+$ T cells	-24 (-39.5; -2)	-25.5 (-39; -15)	0.887
$CD8^+ CCR7^-$ T cells	-62 (-69.5; -41.5)	-59 (-76; -38.5)	0.936

Table 5.3: Change in leucocyte counts between pre-reperfusion and 90 minutes in STEMI patients with and without preadmission statin therapy. Data expressed as median (IQR). Groups compared using Mann-Whitney U test.

5.2.5 Trans-Coronary Gradients Suggest Loss of T-Lymphocytes Within the Myocardial Circulation

Having established the depletion of T cells from the circulation in the acute period following reperfusion, I next aimed to investigate whether any of these cells might be recruited to the post-ischaemic myocardium. In order to do this, I studied trans-coronary gradients, comparing cell counts from blood taken simultaneously from the aorta (proximal to the myocardial vascular tree), and from deep within the coronary sinus (CS) (distal, draining the anterior myocardial bed). The trans-coronary gradient was obtained by subtracting the aortic cell count from the CS cell count, and expressed as a percentage of the aortic count. As such, a negative value suggested loss of cells between these sites (i.e. within the myocardial vasculature draining primarily the anterior portion of the left ventricle). Significance of the trans-coronary gradient in each population was determined by comparing aortic with CS cell counts using the Wilcoxon signed rank test. Inferior STEMI cases were included as control in this analysis, as blood draining the inferior wall would not be sampled deep within the CS, and, therefore, no gradient would be expected in these cases. Only the major leucocyte populations quantified using the TruCount assay (see section 3.3.2) were included in this analysis, given the requirement for highly accurate cell counts, and the increased variability associated with the additional 8 colour assay to quantify the finer subpopulations.

There was a significant drop in total T cells (-3.8±0.8%, p=0.028), $CD4^+$ T cells (-3.9±0.8%, p=0.028), and $CD8^+$ T cells (-3.5±1%, p=0.027) across the myocardial circulation in anterior MI when the samples were taken within 45 minutes of reperfusion (**Figure 5.5A**). Although these drops in cell counts were small, they occurred consistently and were well above the coefficient of variation (CV) of the measurement (1.5%, 1.6% and 2% for total T cells, $CD4^+$ and $CD8^+$ T cells respectively, **Table 3.2** in section 3.3.5), indicating that they were within the range detectable with this assay. Significant gradients were not seen for granulocytes (-3.8±4.3%, p=0.53) or monocytes (-1.4±0.9%, p=0.25). In contrast, in anterior MI cases where the samples were taken later than 45 minutes, and in inferior MI (all sampled at less than 45 minutes) no significant T cell trans-coronary gradients were seen (**Figure 5.5B**). As such, this indicates that T cells were likely to have

been sequestered into the anterior myocardium or microvasculature in cases of reperfused anterior MI, although this was only detectable early after reperfusion.

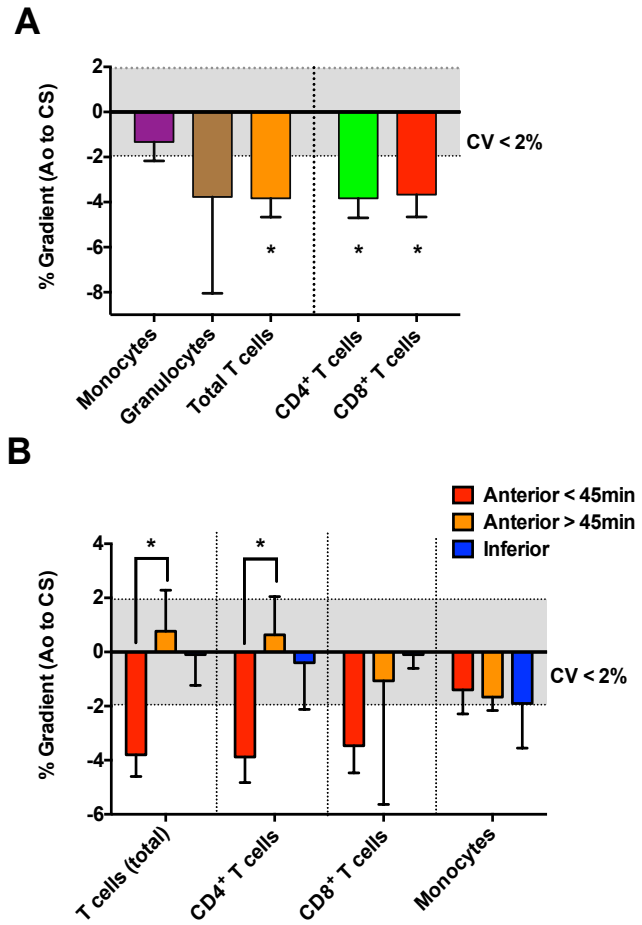

Figure 5.5: Trans-coronary gradients in cell counts, indicating loss of some cells across the myocardial circulation. Blood was taken simultaneously from the aortic root and CS at the end of PPCI in a subset of STEMI patients (n=12). Of these, n=9 were anterior STEMI (samples taken at <45 minutes post-reperfusion in n=6, >45 minutes post-reperfusion in n=3) and n=3 were inferior STEMI (all sampled at <45 minutes). **A:** Percentage change in cell counts of leucocyte subsets between aorta and CS for anterior MI with sampling at <45 minutes (n=6). Negative values indicate a drop across myocardial circulation. Statistics refer to Wilcoxon signed rank test of aorta vs. CS counts for indicated populations. **B:** Impact of sample timing and infarct location on trans-coronary gradients. Statistics refer to difference between anterior infarcts with sampling before (n=6) or after (n=3) 45 minutes (Mann-Whitney U test). **Note**: Mean troponin T for anterior infarcts with sampling < 45min: 4814±1811ng/l, anterior infarcts with sampling > 45min: 9705±2409ng/l; inferior infarcts: 5462±2890ng/l, excluding larger infarcts in the anterior sampling <45min cases as a possible cause for these findings. * $p<0.05$.

5.2.6 Longer-Term Impact of Myocardial Infarction on T Cell Subsets

Finally, I planned to investigate the longer-term impact of MI on T cell subsets in STEMI patients treated with PPCI. This was to determine whether STEMI with reperfusion resulted in any determinable sustained change in the T cell compartment of the immune system. The first variable compared in this regard was the $CD4^+$ to $CD8^+$ T cell ratio, a figure that is known to be associated with immunological ageing. A low $CD4^+$ to $CD8^+$ ratio is associated with immunosenescence, particularly when it is less than 1 (an 'inverted' $CD4^+$ to $CD8^+$ ratio), where it forms part of what is known as the "immune risk profile" (Wikby et al., 1998). In the subset of STEMI patients who underwent follow-up blood tests at 3-6 months (n=23), there was no difference in the $CD4^+$ to $CD8^+$ T cell ratio between pre-reperfusion and this time point (2.46±0.26 vs. 2.57±0.25, p=0.52) (**Figure 5.6A**).

I next considered the distribution of the subsets within the $CD4^+$ and $CD8^+$ T cell compartments. When absolute cell counts from pre-reperfusion and 3-6 months were compared, there were no differences for any of the subsets, with the exception of $CD8^+$ T_{CM} cells, for which counts were very low at both time points (pre-reperfusion: 13±4 cells/μl vs. 3-6 months: 15±4 cells/μl, p=0.018) (**Figure 5.6B+C**). When the percentage distribution of T_N, T_{CM}, T_{EM} and T_{EMRA} cells within each of the $CD4^+$ and $CD8^+$ compartments were compared, there were no differences between pre-reperfusion and follow-up samples (**Figure 5.6D+E**). As such, from this data there did not appear to have been a significant long-term impact of STEMI treated by PPCI on T cell subset distributions.

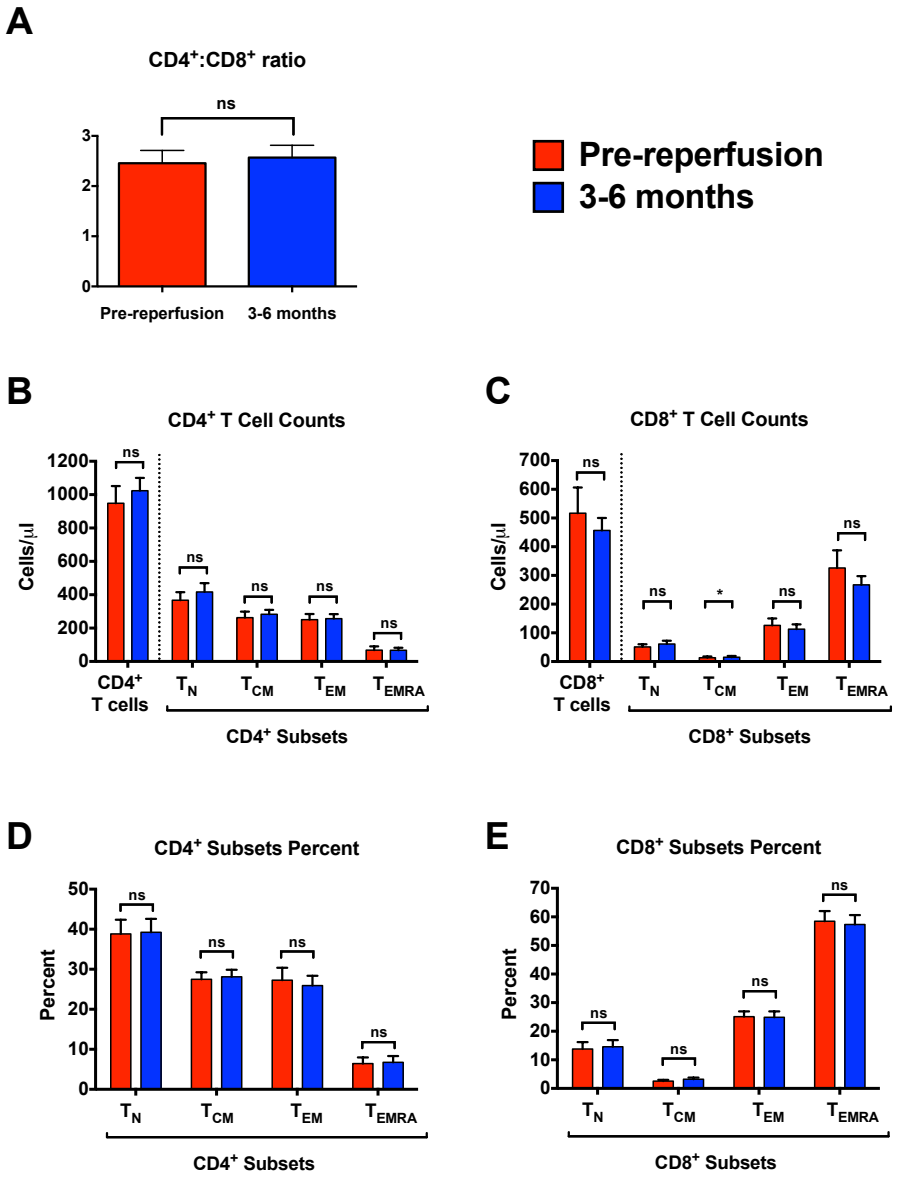

Figure 5.6: Longer term impact of STEMI treated by PPCI on the circulating T cell compartment. **A:** CD4+ to CD8+ T cell ratio in circulating blood in STEMI patients pre-reperfusion (red) and at remote follow up between 3 and 6 months later (blue). **B and C:** Absolute counts of CD4+ T cells and subsets (**B**), and CD8+ T cells and subsets (**C**) in blood pre-reperfusion and at 3-6 month follow up. **D and E:** Percentage distribution of CD4+ T cell subsets (**D**) and CD8+ T cell subsets (**E**) in blood, expressed as percentage of parent population. All statistics refer to pre-reperfusion vs. 3-6 month levels compared using Wilcoxon signed rank test (n=23).

5.3 Discussion

5.3.1 Transient Lymphocyte Depletion From the Bloodstream Occurs Following Ischaemia/Reperfusion

My data provide clear evidence of lymphocyte depletion from circulating blood following reperfusion in STEMI, and a detailed analysis of the specific subsets involved. In contrast, no overall loss of lymphocytes from the blood occurred in NSTEMI cases within 90 minutes of PCI. These findings are in keeping with previous studies that have reported transient loss of lymphocytes following reperfusion in STEMI, although these studies did not include any control group (Bodi et al., 2009; Husser et al., 2011). The NSTEMI and STEMI groups in this study do undoubtedly represent different clinical scenarios, with significantly larger infarcts in the STEMI group, and primarily open infarct related arteries at presentation in the NSTEMI group. Given this latter characteristic, the NSTEMI patients will not have experienced acute ischaemia/reperfusion. They did, however, undergo the same procedure, and consequently, I believe that this indicates that the characteristic cellular changes seen in the STEMI group were not merely procedurally induced, but were secondary to the I/R process, which was a central difference between these two groups. There were, however, other differences between the groups, limiting the use of the NSTEMI group as a control in this setting. Most notable was the markedly different infarct size, as indicated by the peak troponin T (**Table 5.1).** However, the only potential experiment that could avoid this problem would be to compare STEMI patients undergoing reperfusion with similar cases without reperfusion, which would clearly not be ethically acceptable in a human population. As such, the NSTEMI patients provided the best available control, although it remains important to acknowledge the limitations indicated above.

Another interesting finding was that although there was no overall depletion of lymphocytes in the NSTEMI cases, there was a significant drop in the counts of NK cells following PCI, in contrast to those of T cells and B cells. In this respect, NK cells appeared to behave similarly post-PCI in the two groups, while the dynamics of T cells, in particular, were markedly different. As such, it may well be that the

mechanisms involved in T cell depletion and NK cell depletion in these circumstances differ, as the former appeared to be a specific process occurring following I/R, while the latter occurred after PCI in both patient groups.

5.3.2 Transient T Cell Depletion From the Bloodstream Is Due to Selective Loss of Effector T Cells with Recovery Occurring Within 24 Hours

In the case of both $CD4^+$ and $CD8^+$ T cells, depletion from circulating blood following reperfusion in STEMI was primarily due to loss of effector cells (T_{EM} and T_{EMRA}). This was in contrast to the less differentiated T cell subsets (T_N and T_{CM}), which showed comparatively smaller drops. Moreover, when effector subsets were further divided by CD27, those without expression, signifying greater cellular differentiation status, declined by more than those expressing this marker. These findings are of relevance because of the known functional differences between these groups of cells. Effector T cells possess potent effector functions, such as cytokine production in the case of $CD4^+$ cells and cytotoxicity in $CD8^+$ cells (Sallusto et al., 2004). Moreover, lack of CD27 expression is associated with a higher proportion of IFN-γ producing cells in $CD4^+$ T_{EM} and T_{EMRA} cells (Okada et al., 2008), and with greater cytotoxic functions in $CD8^+$ T cells (Takata and Takiguchi, 2006; Hamann et al., 1997). Consequently, the cells that could potentially contribute to the pathological processes of I/R injury are the same populations that display the greatest dynamic changes following reperfusion.

It is noteworthy that circulating T cell numbers recovered rapidly over the 24 hours following their initial depletion. Although this recovery varied between the subpopulations, all showed marked increases after 90 minutes following reperfusion. There could be a number of potential reasons for this. One possible explanation could be a simple return to the circulation of the cells that had previously been depleted. However, some subsets, in particular the T_{CM} cells of both $CD4^+$ and $CD8^+$ lineages, recovered to beyond their initial levels. A possible explanation for this could be replacement of cells lost from the circulation with those from other parts of the T cell pool, for instance, the lymph nodes or spleen. Finally, a third possibility could be clonal expansion of circulating cells to replace those lost. It has been shown in vitro that human T_{CM} cells, in particular, are

capable of cytokine induced proliferation and differentiation to produce T_{CM}, T_{EM}, T_{EMRA}, and, surprisingly, phenotypically T_N cells (Geginat et al., 2003). It is also entirely possible, however, that a combination of these potential mechanisms could be responsible for the recovery of T cells following their initial depletion.

5.3.3 Trans-Coronary Gradients Suggest Loss of Some T cells Within the Myocardial Circulation Following Reperfusion in STEMI

The trans-coronary gradient data reported in this chapter suggest that some T cells are lost within the reperfused myocardial circulation during their depletion from the bloodstream post-PPCI in STEMI. Consequently, the changes in T cell counts seen in these patients are likely indicative of recruitment of at least some of these cells into the reperfused myocardium. Moreover, the fact that a significant trans-coronary gradient was only seen in anterior STEMI patients when the coronary sinus sample was taken within 45 minutes of reperfusion suggests that this sequestration occurs early after reperfusion. Inferior STEMI cases served as a control to demonstrate that trans-coronary gradients in T cell counts were only seen when the infarct area vasculature was drained via the CS. However, one limitation of this methodology that must be acknowledged is that while the inferior wall is primarily not drained via the CS, there is considerable anatomical variation (Roberts et al., 1976; Spencer et al., 2013). Consequently, in some individuals, blood draining from the inferior wall may reach the coronary sinus. Although blood sampling was conducted from deep within the CS to minimise this limitation, it is impossible to exclude the possibility that a small proportion of the CS blood may have passed through the inferior myocardial wall prior to sampling in some cases. Nevertheless, no significant T cell trans-coronary gradient was seen in the inferior MI cases, in spite of a similar infarct size to the anterior cases with early coronary sinus sampling, supporting the conclusion regarding myocardial sequestration of these cells.

One issue that must be considered is that while the data described here do suggest loss of some T cells within the reperfused myocardial vasculature, the total number of these cells lost from the circulation is enormous. The drop in circulating T cells following reperfusion constituted 29% and 55% of $CD4^+$ and $CD8^+$ T cells

initially present respectively. It seems unlikely that such vast numbers could possibly be sequestered into the heart alone. Consequently, it is my belief that while some T cells are indeed recruited to the reperfused myocardium following PPCI, many others must be lost elsewhere. The destination for these 'missing' cells remains obscure, although given the rapidity of the recovery of T cell numbers over the following 24 hours, one possibility could be that cells are marginated from the circulation through adhesion to the endothelium. It would seem feasible that this process could occur both within the myocardial microvasculature and elsewhere, at sites of endothelial activation. Given the selective loss of potent effector T cells from the circulation following reperfusion, it is easy to imagine that these cells could contribute to inflammation and, potentially, tissue damage at their destination. Within the myocardial microvasculature, for instance, such activity could contribute I/R injury through vascular plugging and MVO.

5.3.4 Myocardial Infarction with Ischaemia/Reperfusion Did Not Affect Long-Term T Cell Subset Distribution

Finally, the data in this chapter also addressed the residual effect of STEMI with reperfusion on the T lymphocyte compartment after recovery. There was no convincing evidence from this study of any significant long-term effects in this regard. This is of importance because there is compelling evidence to suggest that the relative composition of the T cell compartment of the immune system has prognostic relevance. A series of cohort studies conducted in Sweden have identified a particular set of characteristics, collectively referred to as the "immune risk profile" which predict mortality in older individuals (Strindhall et al., 2013; Wikby et al., 1998; Wikby et al., 2008). One key component of this phenotype is a reduced $CD4^+$ to $CD8^+$ T cell ratio, and in particular its reversal to less than 1 (i.e. higher $CD4^+$ than $CD8^+$ T cell numbers). This particular parameter has also been shown to predict mortality in a further UK based study (Huppert et al., 2003). Consequently, it was of interest whether MI affected such parameters in the long-term in STEMI patients. Two small studies have previously reported reduced $CD4^+$ to $CD8^+$ T cell ratios in MI patients, which returned to normal prior to discharge (Al-Ahmad et al., 2004; Syrjälä et al., 1991). My results confirm that acute changes appear to be transient, and that the $CD4^+$ to $CD8^+$ T cell ratio remains unaltered at

remote follow-up at 3-6 months. As such, from this parameter alone, this study provides no evidence of MI-induced alteration of the T cell compartment towards findings in keeping with the immune risk profile.

Additional alterations to the T cell compartment occur with ageing of immune system, beyond merely changes in the $CD4^+$ to $CD8^+$ T cell ratio. Thymic involution results in decreased production of new T cells, and there is a progressive loss of T_N cells, accompanied by expansion of the T_{EMRA} cell pool and narrowing of the T cell repertoire (Blackman and Woodland, 2011; Koch et al., 2008; Nikolich-Zugich, 2008). Consequently, I also wished to determine whether STEMI treated with PPCI induced evidence of immune 'ageing' within the $CD4^+$ or $CD8^+$ T cell compartments by changing the distribution of subsets within each. Again, the data from this study did not show any evidence of such an effect. However, it must be considered that changes could occur not only in the counts and distribution of cells, but also in their functional characteristics at a per cell level. As no functional assays were conducted directly as part of this study, I am unable to conclude whether any such alterations could have occurred.

5.4 Conclusions

The dynamic changes in leucocyte, and in particular, T cell counts following reperfusion in STEMI have been characterised in detail here for the first time. Trans-coronary gradients have provided evidence for sequestration of some of these depleted cells into the reperfused myocardium/microvasculature in the early post-reperfusion period. In the next chapter I will go on to investigate the relationship between these findings and MRI parameters, including MVO, an important component of myocardial I/R injury.

Chapter 6

Cardiac MRI and Leucocyte Dynamics in Reperfused STEMI

6.1 Introduction

Having characterised the cellular changes that occur in the blood following reperfusion in STEMI, I next considered how these findings relate to cardiac MRI outcome measures. This form of imaging provides an invaluable tool to researchers as well as clinicians, allowing detailed analysis and quantification of myocardial and microvascular injury in the acute setting post-STEMI. Importantly, the ability to measure microvascular obstruction (MVO) provides a non-invasive assessment of one component of myocardial I/R injury. Consequently, this measure is now used as a study end-point in major clinical trials assessing treatment measures targeting I/R injury (Atar et al., 2009; Nazir et al., 2014; Wu, 2009).

Prior to this study, very little was known about the relationship between leucocyte dynamics and imaging findings in STEMI. As previously discussed, one study demonstrated an association between post-reperfusion lymphopaenia and MVO (Bodi et al., 2009). However, this study investigated only total lymphocyte counts, rather than any of the finer subpopulations. Similarly, two studies have demonstrated an association between elevated peak numbers of $CD14^{+}CD16^{-}$ monocytes and the presence of MVO (Tsujioka et al., 2010), as well as reduced myocardial salvage (Tsujioka et al., 2009). This study, however, is the first to address the relationship between very early post-reperfusion leucocyte dynamics and MRI findings. Moreover, it is the first to include detailed lymphocyte subset dynamics, rather than counts of this entire leucocyte family combined.

6.2 Results

6.2.1 Baseline Characteristics and MRI Outcomes of STEMI Patients Undergoing Cardiac MRI

Cardiac MRI was conducted in the STEMI patients recruited to the study. For details of the MRI protocols and analysis techniques used, please see section 3.4. Of the 59 STEMI patients, 50 successfully completed imaging, while 9 patients did not undergo a full scan (due to claustrophobia in 5, stent compatibility concerns in 2, unavailability of scan slot in 1 and patient declining in 1). The overall baseline data and MRI parameters from these 50 patients are summarised in **Table 6.1**. With regards baseline parameters, there were no statistically significant differences between the patients who successfully completed an MRI scan and those who did not, with the exception of gender (more females did not complete a scan).

For further analysis, the patients were subsequently divided into groups based on the presence and extent of MVO (MVO group, **Table 6.2**) and infarct size (infarct size group, **Table 6.3**). There were no significant differences amongst either of these sets of groups with regard to pre-admission baseline characteristics or treatment (both pre-admission and during PPCI). In the case of the MVO groups, there were a number of significant differences between them relating to the infarct characteristics (**Table 6.2**). There was an incremental increase in the mean values for peak troponin T as the extent of MVO increased (i.e. from the zero, to low, to high MVO groups). Similarly, the infarct size measured by LGE on MRI (expressed as % of LV) also increased incrementally throughout these groups ($p<0.001$). In keeping with these findings, individuals in the higher MVO groups tended to have greater end diastolic and end systolic LV volumes than those without MVO ($p=0.025$ and $p=0.004$ respectively), as well as lower LVEF ($p=0.002$).

A similar pattern was seen when the cases were divided into infarct size groups (**Table 6.3**). Peak troponin T was higher in the larger infarct groups, increasing incrementally from small, to medium, then large infarcts ($p<0.001$). There was also a significant association between infarct size group and infarct territory, with more anterior MI cases amongst the larger infarcts ($p=0.006$). Furthermore, the large

infarct groups had greater LV end diastolic and systolic volumes (p=0.035 and p=0.001 respectively), lower LVEF (p=0.001) and more MVO (p<0.001) than smaller infarcts.

	MRI (n=50)	No MRI (n=9)	p value
Age	58.5 ± 10.1	64 ± 13.0	0.164
Male sex	41 (82.0)	3 (33.3)	**0.006**
BMI	26.9 ± 4.6	26.3 ± 4.2	0.958
Diabetes mellitus	4 (8.0)	2 (22.2)	0.224
Family history of CAD	20 (40.0)	3 (33.3)	0.742
Active smoker	26 (52.0)	5 (55.6)	1.000
Hypertension	16 (32.0)	3 (33.3)	1.000
Anterior MI	26 (52.0)	2 (22.2)	0.150
Serum cholesterol (mmol/l)	5.2 ± 1.0	5.6 ± 1.5	0.681
Serum creatinine (μmol/l)	81.6 ± 16.9	72.4 ± 16.2	0.194
Peak troponin T (ng/l)	5086 ± 3435	4515 ± 3234	0.627
Door-to-balloon time (minutes)	27.2 ± 14.9	24.6 ± 11.0	0.834
Onset-to-reperfusion time (minutes)	160.4 ± 79.1	187.9 ± 94.6	0.376
Pre-admission Medication			
Statin therapy	8 (16.0)	2 (22.2)	0.641
B-blocker	1 (2.0)	1 (11.1)	0.284
Aspirin	4 (8.0)	1 (11.1)	0.577
ACE-inhibitor/ARB	5 (10.0)	1 (11.1)	1.000
MRI Parameters			
Time to MRI (days)	2.7 ± 1.7	N/A	n/a
End diastolic volume (EDV, ml)	131.9 ± 37.4	N/A	n/a
End systolic volume (ESV, ml)	63.4 ± 28.4	N/A	n/a
Stroke volume (SV, ml)	67.1 ± 19.9	N/A	n/a
LV ejection fraction (LVEF, %)	53.3 ± 10.5	N/A	n/a
Infarct size (% of LV)	20.1 ± 11.1	N/A	n/a
MVO mass (g)	3.8 ± 5.8	N/A	n/a

Table 6.1: Baseline data for STEMI patients with and without completed MRI scans. MRI parameters included for the former group. Continuous variables expressed as mean ± SD and compared using Mann-Whitney U test, categorical variables as n (%) and compared using chi-square (χ^2) or Fisher's exact test as appropriate.

	MVO group			p value
	None (0g)	Low (0.1-2.7g)	High (>2.7g)	
n	19	14	17	n/a
Age	57.5 ± 7.3	61.0 ± 12.1	57.5 ± 11.3	0.698
Male sex	15 (78.9)	12 (85.7)	14 (82.4)	0.882
BMI	28.0 ± 5.0	25.0 ± 4.0	27.2 ± 4.4	0.087
Diabetes mellitus	0 (0)	1 (7.1)	3 (17.6)	0.148
Family history of CAD	9 (47.4)	3 (21.4)	8 (47.1)	0.455
Active smoker	12 (63.2)	6 (42.9)	8 (47.1)	0.453
Hypertension	8 (42.1)	1 (7.1)	7 (41.2)	0.063
Anterior MI	6 (31.6)	9 (64.3)	11 (64.7)	0.077
Serum cholesterol (mmol/l)	5.2 ± 1.0	5.4 ± 0.8	5.2 ± 1.1	0.826
Serum creatinine (μmol/l)	77.6 ± 13.6	79.4 ± 15.4	87.8 ± 20.2	0.244
Peak troponin T (ng/l)	2493 ± 2197	4213 ± 1853	8703 ± 2318	**<0.001**
Door-to-balloon time (minutes)	29.8 ± 18.2	26.1 ± 13.1	25.1 ± 12.1	0.738
Onset-to-reperfusion time (minutes)	173.2 ± 85.6	158.5 ± 66.8	147.6 ± 83.1	0.455
Pre-admission Medication				
Statin therapy	4 (21.1)	1 (7.1)	3 (17.6)	0.545
B-blocker	1 (5.3)	0 (0)	0 (0)	0.435
Aspirin	1 (5.3)	0 (0)	3 (17.6)	0.169
ACE-inhibitor/ARB	2 (10.5)	0 (0)	3 (17.6)	0.264
Treatment During PPCI				
Aspirin	19 (100)	14 (100)	17 (100)	n/a
Additional antiplatelet (prasugrel/clopidogrel/ticagrelor)	17/2/0	12/1/1	15/0/2	0.430
Heparin	18 (94.7)	14 (100)	17 (100)	0.435
Abciximab	9 (47.4)	3 (21.4)	10 (58.8)	0.105
Tirofiban	5 (26.3)	5 (35.7)	4 (23.5)	0.738
Bivalirudin	2 (10.5)	5 (35.7)	3 (17.6)	0.193
Aspiration catheter	16 (84.2)	11 (78.6)	14 (82.4)	0.916
MRI Parameters				
Time to MRI (days)	3.1 ± 2.3	2.8 ± 1.6	2.3 ± 0.8	0.896
End diastolic volume (ml)	118.7 ± 36.9	122.4 ± 23.9	154.3 ± 38.2	**0.025**
End systolic volume (ml)	48.5 ± 19.0	58.8 ± 17.2	83.7 ± 33.3	**0.004**
Stroke volume (ml)	70.2 ±22.4	63.6 ± 16.7	66.5 ± 20.1	0.768
LV ejection fraction (%)	59.6 ± 8.1	51.8 ± 9.6	47.4± 10.2	**0.002**
Infarct size (% of LV)	11.5 ± 6.6	18.7 ± 7.1	30.9 ± 8.5	**<0.001**
MVO mass (g)	0.0 ± 0.0	1.0 ± 0.7	10.3 ± 1.4	**<0.001**

Table 6.2: Baseline data for prospective cohort patients undergoing cardiac MRI, divided by MVO groups. Continuous variables expressed as mean ± SD and compared using Kruskal-Wallis test. Categorical variables as n (%) unless otherwise stated, and compared using chi-square test (χ^2).

	Infarct Size Group			p value
	Small (<13.3%)	**Medium (13.3-23.8)**	**Large (>23.8%)**	
n	16	18	16	n/a
Age	60.1 ± 9.6	57.6 ± 10.1	57.8 ± 11.1	0.783
Male sex	12 (75.0)	15 (83.3)	14 (87.5)	0.644
BMI	27.5 ± 4.8	27.3 ± 5.4	25.9 ± 3.4	0.687
Diabetes mellitus	0 (0.0)	2 (11.1)	2 (12.5)	0.356
Family history of CAD	6 (37.5)	8 (44.4)	6 (37.5)	0.857
Active smoker	9 (56.3)	9 (50.0)	8 (50.0)	0.918
Hypertension	7 (43.8)	5 (27.8)	4 (25.0)	0.467
Anterior MI	4 (25.0)	9 (50.0)	13 (81.3)	**0.006**
Serum cholesterol (mmol/l)	5.2 ± 1.1	5.3 ± 1.0	5.3 ± 0.8	0.929
Serum creatinine (μmol/l)	76.6 ± 13.2	84.1 ± 20.7	83.8 ± 15.3	0.369
Peak troponin T (ng/l)	2027 ± 1936	5112 ± 2335	8115 ± 2976	**<0.001**
Door-to-balloon time (minutes)	26.9 ± 13.2	29.4 ± 18.4	24.9 ± 12.2	0.652
Onset-to-reperfusion time (minutes)	170.1 ± 47.1	175.2 ± 104.5	133.9 ± 68.7	0.103
Pre-admission Medication				
Statin therapy	3 (18.8)	2 (11.1)	3 (18.8)	0.779
B-blocker	1 (6.3)	0 (0.0)	0 (0.0)	0.338
Aspirin	1 (6.3)	1 (5.6)	2 (12.5)	0.721
ACE-inhibitor/ARB	1 (6.3)	2 (11.1)	2 (12.5)	0.825
Treatment During PPCI				
Aspirin	16 (100)	18 (100)	16 (100)	n/a
Additional antiplatelet (prasugrel/clopidogrel/ticagrelor)	12/3/0	13/2/3	14/1/1	0.359
Heparin	15 (93.8)	18 (100)	16 (100)	0.338
Abciximab	7 (43.8)	7 (38.9)	8 (50.0)	0.809
Tirofiban	5 (31.3)	4 (22.2)	5 (31.3)	0.792
Bivalirudin	3 (18.8)	5 (27.8)	2 (12.5)	0.533
Aspiration catheter	11 (68.8)	15 (83.3)	15 (93.8)	0.181
MRI Parameters				
Time to MRI (days)	3.1 ± 2.1	2.4 ± 1.4	2.8 ± 1.6	0.653
End diastolic volume (ml)	144.5 ± 29.7	128.2 ± 32.4	153.3 ± 40.8	**0.035**
End systolic volume (ml)	46.7 ± 17.3	58.9 ± 20.4	85.0 ± 32.3	**0.001**
Stroke volume (ml)	67.8 ± 17.6	69.3 ± 18.6	63.9 ± 24.0	0.942
LV ejection fraction (%)	59.7 ± 8.4	54.7 ± 8.1	45.3 ± 10.1	**0.001**
Infarct size (% of LV)	8.2 ± 3.1	19.1 ± 3.3	33.1 ± 6.8	**<0.001**
MVO mass (g)	0.3 ± 0.6	2.4 ± 3.3	8.9 ± 7.3	**<0.001**

Table 6.3: Baseline data for prospective cohort patients undergoing cardiac MRI, divided by infarct size groups. Continuous variables expressed as mean ± SD and compared using Kruskal-Wallis test. Categorical variables as n (%) unless otherwise stated, and compared using chi-square test (χ^2).

6.2.2 The Relationship Between Timing of MRI Scanning Post-Reperfusion and MRI Outcomes

One potential source of inaccuracy and confounding within the MRI data from STEMI patients was the variability in timing of the scan (range 1 to 8 days post-PPCI). For this reason, I investigated whether there were any identifiable relationships between this parameter and the MRI outcomes of interest. Firstly, there were no significant differences between either the MVO groups, or the infarct size groups in terms of scan timing (p=0.896 and p=0.653 respectively, **Tables 6.2 and 6.3**). Next, I studied whether there were any significant correlations between scan timing and the continuous variables of MVO mass, infarct size (as % of LV), and LVEF (**Figure 6.1**). There were no significant correlations for either MVO (r=-0.06, p=0.70) or infarct size (r=-0.04, p=0.77). However, there was a significant positive correlation between scan timing and LVEF (r=0.36, p<0.01), i.e. as the time to scan post-reperfusion increased, there was a trend towards higher LVEF.

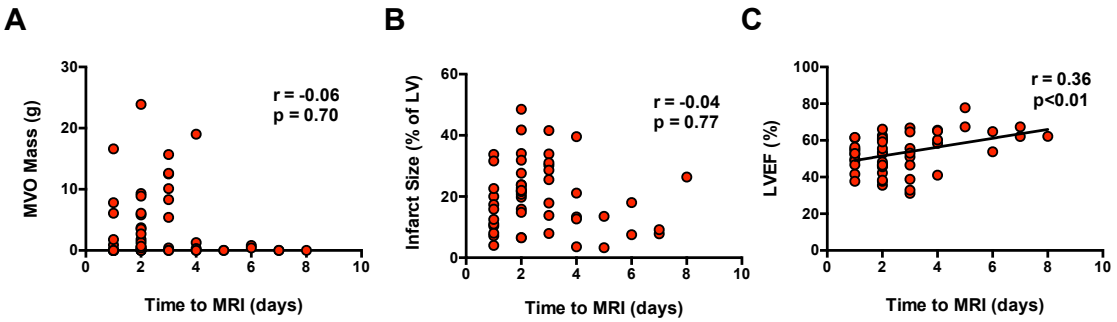

Figure 6.1. Relationship between MRI findings and timing of MRI scan. **A**: MVO. No significant relationship was seen between the timing of MRI scanning and the presence and extent of MVO. **B**: Infarct size expressed as % of left ventricle. No significant relationship was seen between the timing of MRI scanning and infarct size. **C**: LVEF. The LVEF determined by CMR increased significantly with an increase in time from reperfusion to MRI scan. Statistics refer to Spearman correlation coefficient (n=50).

6.2.3 Technical Issues With Assessment of Area At Risk and Myocardial Salvage Index

One of the MRI parameters intended to help give an indication of I/R injury was myocardial salvage index. This is a measure of the proportion of ischaemic myocardium (area at risk) that has been successfully rescued by PPCI and prevented from forming part of the infarct. As outlined in section 3.4.2, salvaged myocardium can be measured by subtracting the infarct area on LGE images from the AAR identified on STIR images as a zone of hyperenhancement. Unfortunately, in practical terms this assessment was hampered by technical issues with the STIR images, particularly in cases of inferior STEMI (**Figure 6.2**). I found that in cases of anterior STEMI, the AAR was almost always successfully identified on these images as a hyperenhanced zone including but extending beyond the limits of the infarct zone on the corresponding LGE image (**Figure 6.2A+B**). However, when the infarct was not in the anterior territory, analysis of signal intensity of the T2-weighted STIR images often misidentified the AAR, falsely categorising some of the anterior wall as AAR, due to comparatively higher signal intensity (**Figure 6.2C+D**). Consequently, with the exception of the relationship with other cardiac MRI outcomes in cases of anterior STEMI with interpretable STIR images (**Figure 6.3D-F**), I have elected not to report the myocardial salvage index data acquired in this study.

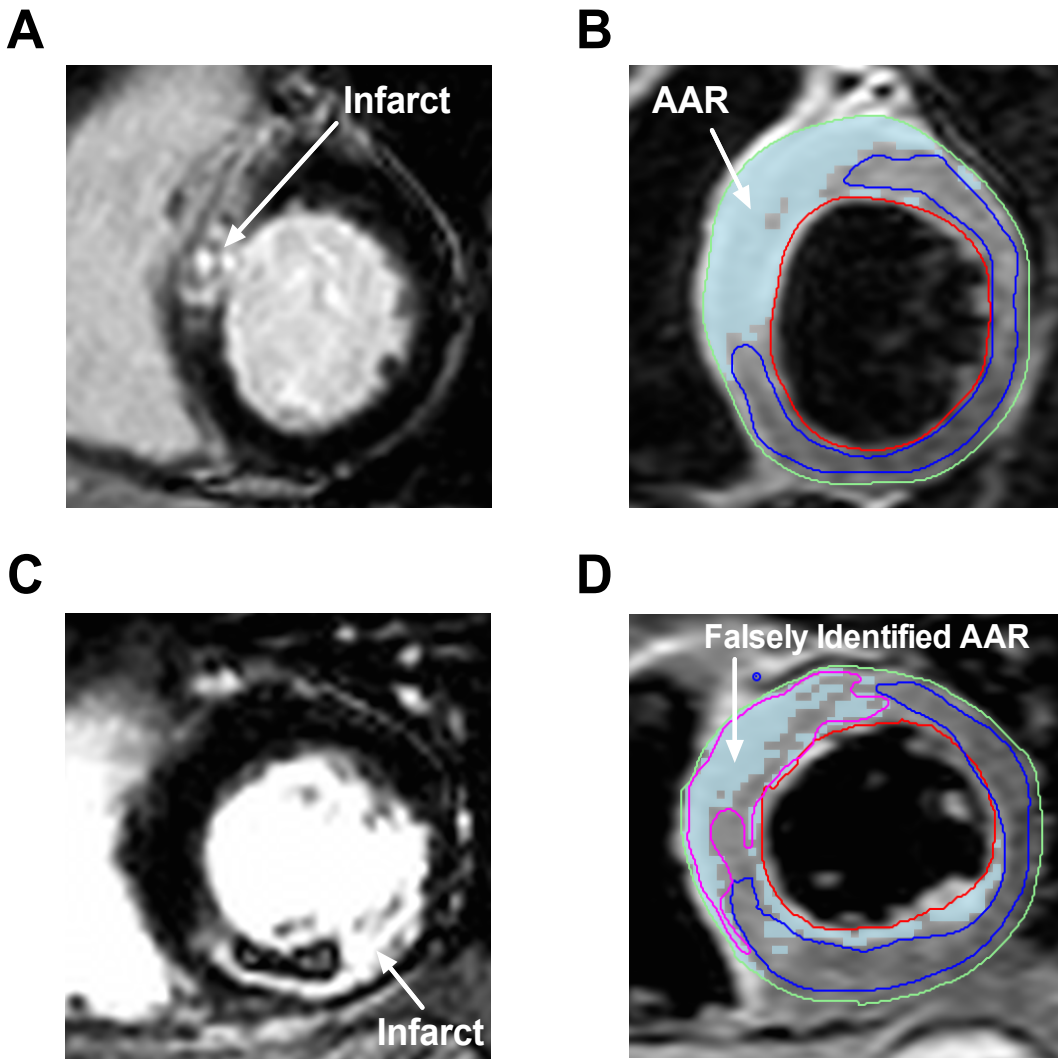

Figure 6.2. Technical issues with area at risk and salvage index quantification. **A+B:** Corresponding LGE and T2-weighted STIR images respectively for an anteroseptal STEMI. The region of infarction is indicated by the white hyperenhanced area in **A**, while the corresponding AAR is indicated by light blue shading in the analysed image in **B**. **C+D** show corresponding LGE and T2-weighted STIR images respectively for an inferior STEMI with extensive MVO. The region of infarction is indicated by the hyperenhanced area in **C,** with a hypoenhanced zone (MVO) within core of the infarct. In the analysed STIR image (**D**), however, the analysis software has misidentified the AAR, due to comparatively stronger signal from the anterior wall, making salvage index quantification unreliable.

6.2.4 The Relationship Between MRI Outcome Measures in STEMI Patients Post-Reperfusion

Next I considered the relationship between the major cardiac MRI outcomes measures, namely infarct size (as % of LV), MVO mass, LVEF and, with the caveats outlined above, myocardial salvage index (**Figure 6.3**). There was a strong positive correlation between infarct size and MVO mass, with more MVO occurring in larger infarcts ($r=0.76$, $p<0.001$, **Figure 6.3A**). Left ventricular systolic function, as measured by LVEF, was negatively correlated with both infarct size ($r=-0.58$, $p<0.001$, **Figure 6.3B**) and MVO mass ($r=-0.50$, $p<0.001$, **Figure 6.3C**) (i.e. poorer LV function with larger infarcts and more MVO).

In terms of myocardial salvage index in anterior MI cases with interpretable STIR images, there were significant correlations with each of the other major MRI outcomes. There was a strong negative correlation with infarct size ($r=-0.93$, $p<0.001$, **Figure 6.3D**). Thus, the larger infarcts tended to take up a comparatively greater proportion of the AAR. There was a positive correlation between salvage index and LVEF ($r=0.47$, $p=0.020$, **Figure 6.3D**), with better LV function in those cases with more salvaged myocardium. Finally, there was a significant negative correlation between MVO mass and salvage index ($r=-0.68$, $p<0.001$, **Figure 6.3E**), with a tendency towards lower salvage in infarcts with more MVO.

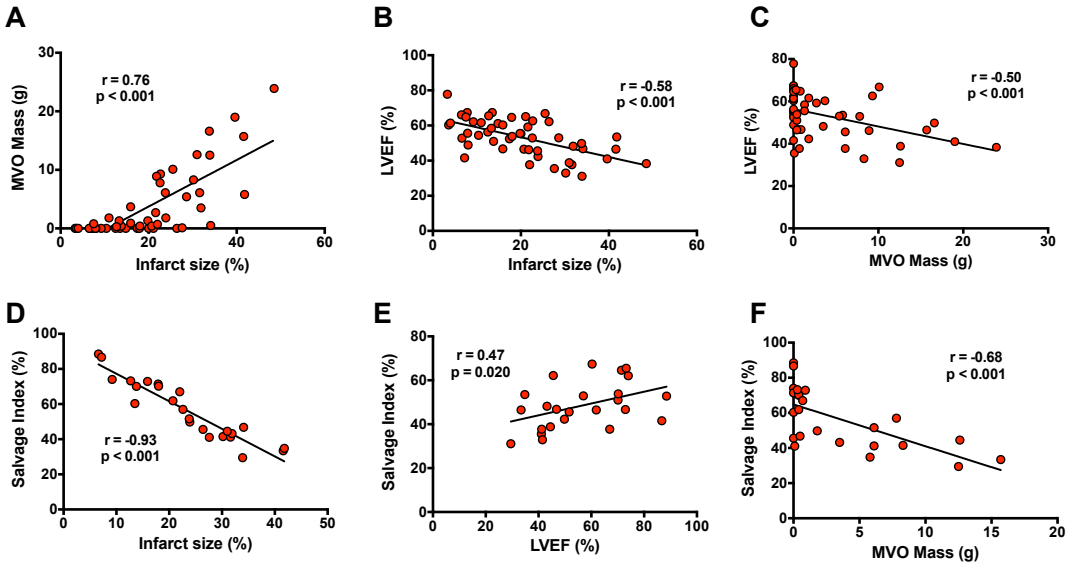

Figure 6.3: Relationship between different MRI outcomes. **A:** Infarct size (expressed as % of left ventricle) and MVO mass (g), **B**: Infarct size and LVEF (%), **C**: MVO mass and LVEF, **D**: Infarct size and salvage index (expressed as % of AAR), **E**: LVEF and salvage index, **F**: MVO mass and salvage index (n=50 for **A-C**, while n=24 for **D-F**, due to the inclusion of only anterior MI cases with sufficient quality STIR images for AAR quantification). Statistics refer to Spearman correlation coefficient for each pair of parameters.

6.2.5 The Extent of Effector T Cell Depletion Early After Reperfusion Is Associated With Myocardial Ischaemia/Reperfusion Injury

The main purpose of conducting cardiac MRI in the STEMI cases in this study was to assess for any relationship between the cellular changes outlined in chapter 5 and the MRI outcome measures, particularly MVO, a component of myocardial I/R injury. In order to investigate this, the cellular kinetics observed were compared for each of the three MVO groups (zero [0g], low [0.1-2.7g] and high [>2.7g]). These comparisons were conducted for the changes in cell counts occurring over the total acute post-reperfusion period (ΔPre-90min), the early post-reperfusion period (Δ15-30min), and the late post-reperfusion period (Δ90min-24hr).

For the changes occurring in the main leucocyte subsets over the pre-reperfusion to 90 minute time period (ΔPre-90min) there were no significant differences between the MVO groups (**Figure 6.4**). There were also no significant differences between the MVO groups for late post-reperfusion changes (Δ90min-24hr) in any of the major leucocyte populations (data not shown).

The early post-reperfusion period, however, showed a different pattern, with significant variation between the MVO groups for Δ15-30min in some leucocyte subsets (**Figure 6.5**). Most notably, the drop in T cell counts over this period was highly significantly greater in the high MVO group (-17% [-26.5; -12.5]) compared to the zero MVO group (-8% [-13; -3.5]) (p=0.003, **Figure 6.5C**). In contrast, there was a weak relationship between MVO group and Δ15-30min for monocytes, and none for granulocytes, NK cells or B cells (**Figure 6.5**).

When the variation in Δ15-30min between MVO groups was considered separately for T cell subsets, a striking pattern was revealed (**Figure 6.6**). For both $CD4^+$ and $CD8^+$ T cells (**Figure 6.6A+B** respectively), Δ15-30min did not vary significantly among the MVO groups for $CCR7^+$ (T_N and T_{CM}) cells (p=0.11 for $CD4^+CCR7^+$, p=0.26 for $CD8^+CCR7^+$). However, when the $CCR7^-$ effector subsets (T_{EM} and T_{EMRA}) were considered, the drop was greater in the higher MVO groups. In the case of $CD8^+CCR7^-$ T cells the median drop in the high MVO group was -28% (-37; -20.5) compared to -18% (-25.5; -6.5) in the zero MVO group (p=0.030), while the difference was more striking in the $CD4^+CCR7^-$ T cells (high MVO: -24% [-31; -14] vs. zero MVO -8% [-15; -3], p=0.002). Within the $CD4^+$ T cell subsets, the strongest relationship between MVO group and Δ15-30min was seen for the scarce $CD4^+$ T_{EMRA} cells, with a median drop of -29% (-37.5, -16) in the high MVO group, compared to -12% (-15.5; -1.5) in the zero MVO group (p<0.001). As such, significant associations between early post-reperfusion cellular changes and MVO were only seen in the effector T cell subsets, and in particular $CD4^+$ T_{EMRA} cells. These cells are known to be potent producers of inflammatory cytokines including IFN-γ (Henson et al., 2012).

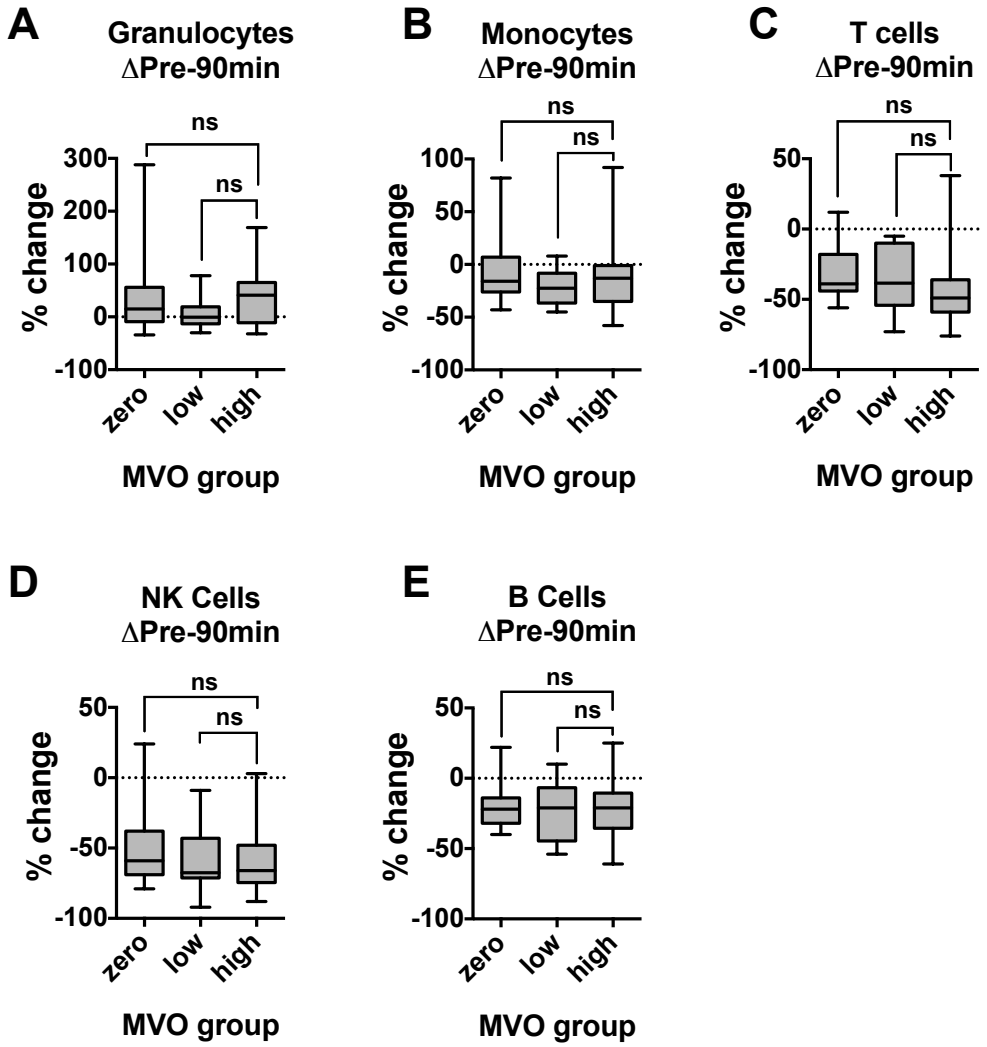

Figure 6.4: Relationship between MVO group and total acute post-reperfusion change (Δpre-90min) in major leucocyte subsets in STEMI patients undergoing cardiac MRI for **A**: Granulocytes, **B**: Monocytes, **C**: T cells, **D**: NK cells and **E**: B cells. Box plots display median (central line), 25th and 75th (limits of box), and range (error bars). Statistics refer to differences between MVO groups as indicated (Kruskal-Wallis test with Dunn's multiple comparisons test) (n=50, by MVO group: zero: n=19, low: n=14, high: n=17). * $p<0.05$, ** $p<0.01$, ***$p<0.001$, ns = not significant.

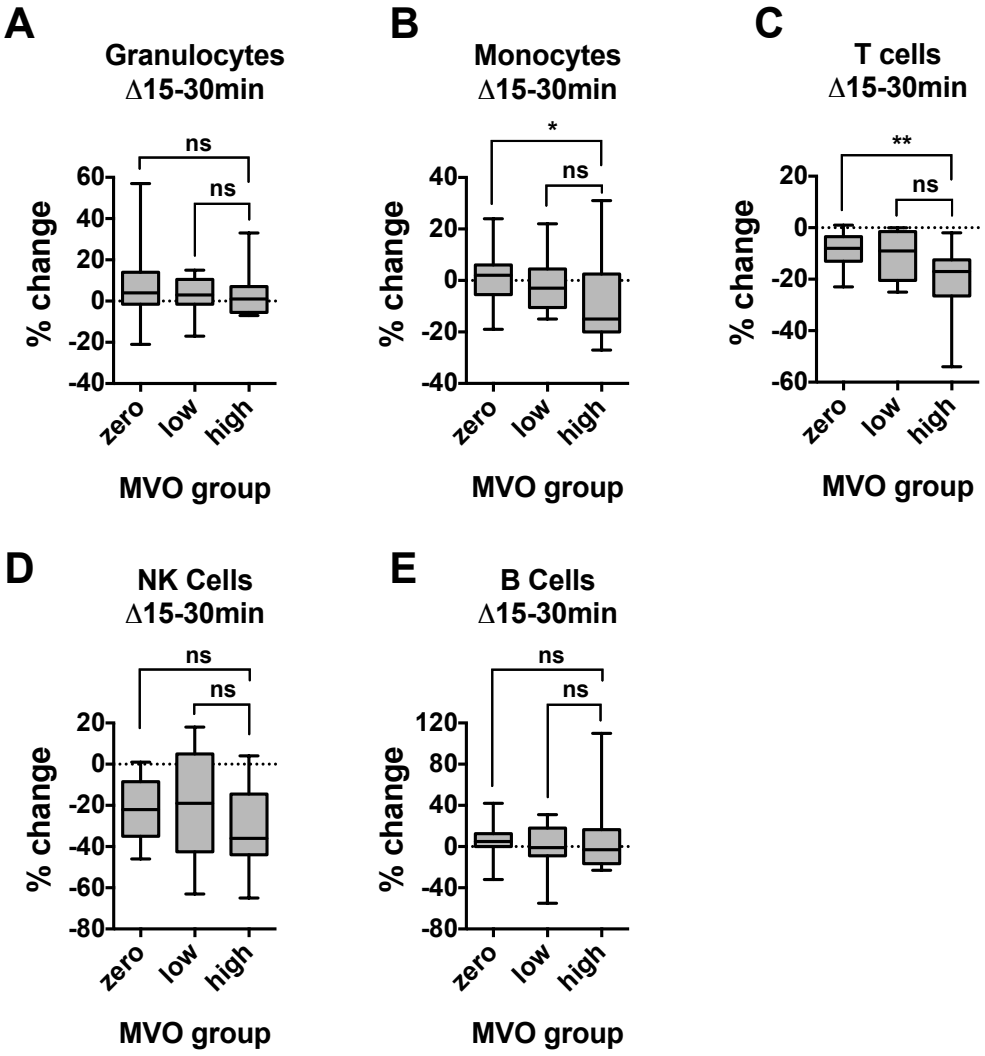

Figure 6.5: Relationship between MVO group and early post-reperfusion change (Δ15-30min) in major leucocyte subsets in STEMI patients undergoing cardiac MRI for **A**: Granulocytes, **B**: Monocytes, **C**: T cells, **D**: NK cells and **E**: B cells. Box plots display median (central line), 25th and 75th (limits of box), and range (error bars). Statistics refer to differences between MVO groups as indicated (Kruskal-Wallis test with Dunn's multiple comparisons test) (n=47, by MVO group: zero: n=17, low: n=13, high: n=17). * p<0.05, ** p<0.01, ***p<0.001, ns = not significant.

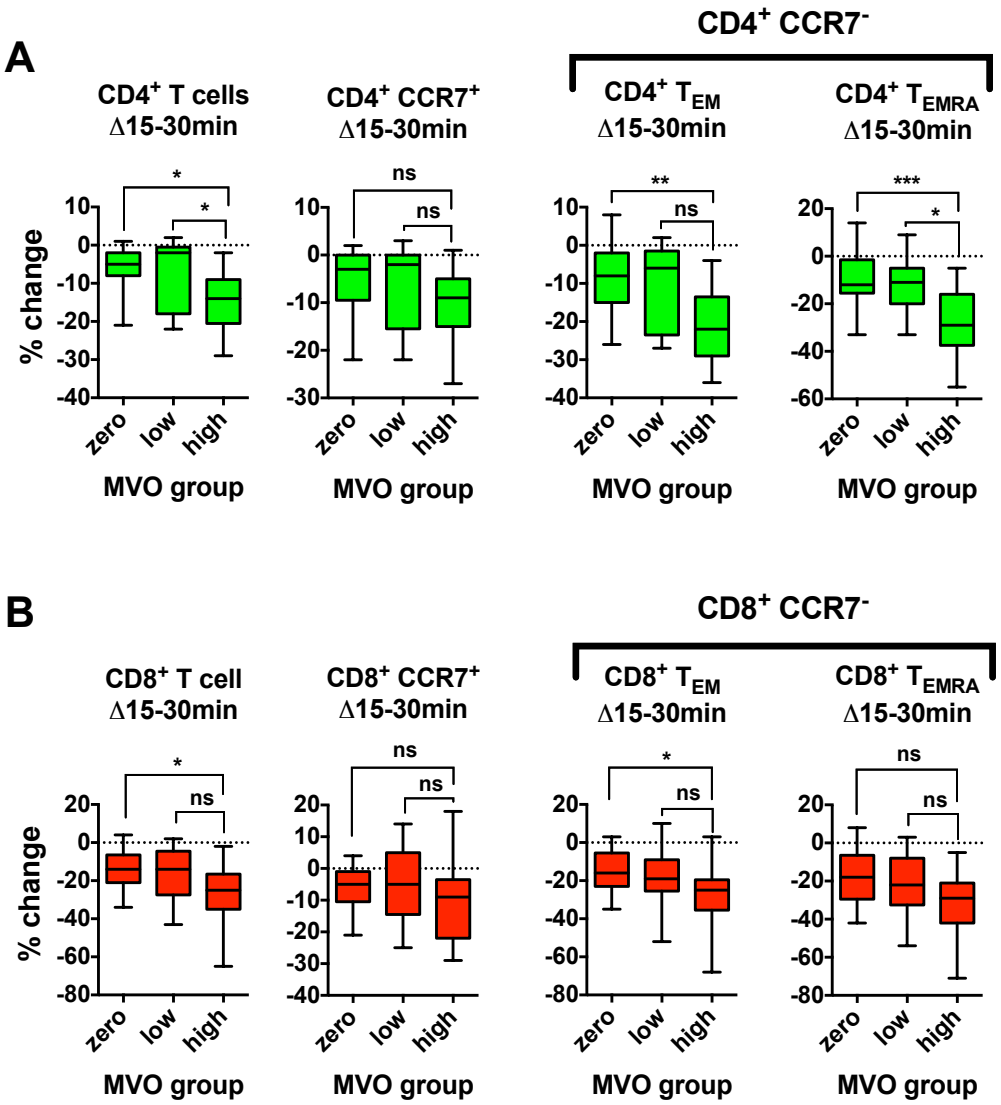

Figure 6.6: Relationship between MVO group and early post-reperfusion change (Δ15-30min) in T cell subsets in STEMI patients undergoing cardiac MRI for **A:** total $CD4^+$ T cells, $CD4^+$ $CCR7^+$ (T_N and T_{CM} combined) cells, and $CD4^+$ $CCR7^-$ effector (T_{EM} and T_{EMRA}) subsets. **B:** As above for total $CD8^+$ T cells and subsets. Box plots display median (central line), 25th and 75th (limits of box), and range (error bars). Statistics refer to differences between MVO groups as indicated (Kruskal-Wallis test with Dunn's multiple comparisons test) (n=47, by MVO group: zero: n=17, low: n=13, high: n=17), * $p<0.05$, ** $p<0.01$, ***$p<0.001$, ns = not significant.

6.2.6 Post-Reperfusion Cellular Changes are Not Significantly Associated with Infarct Size or LVEF in STEMI Patients Undergoing Cardiac MRI

Having identified the association between MVO and the early depletion of effector T cells from the circulation post-reperfusion, I next considered the relationship between cellular changes and other MRI outcomes. Firstly, patients were divided into three groups based on the infarct size, expressed as percentage of the left ventricle (small: <13.3%, medium: 13.3-23.8%, large: >23.8%, **Table 6.3**). These groups were then compared with regard to the cellular dynamics during to the total acute post-reperfusion (ΔPre-90min), early post-reperfusion (Δ15-30min), and the late post-reperfusion period (Δ90min-24hr), as had previously been done for the MVO groups. In contrast to the findings for MVO, there were no significant differences between the groups at any of these time intervals for any of the major leucocyte populations (for ΔPre-90min see **Figure 6.7**, for Δ15-30min see **Figure 6.8**, Δ90min-24hr data not shown). As such, there did not appear to be any significant relationships between leucocyte dynamics in the bloodstream in the 24 hours post-reperfusion, and the infarct size in STEMI patients treated with PPCI.

Finally, I considered whether there was any relationship between leucocyte kinetics post-PPCI and left ventricular systolic function, as measured by LVEF. Once again, this was conducted for ΔPre-90min, Δ15-30min and Δ90min-24hr. There were no significant correlations between cellular changes in any of these time intervals and LVEF for any major leucocyte population (for selected populations at ΔPre-90min and Δ15-30min see **Figure 6.9A-C** and **6.9D-F** respectively, data for Δ90min-24hr not shown). It, therefore, appears that the dynamic changes in effector T cell counts in the early post-reperfusion period have a specific relationship with the presence and extent of MVO, and not other cardiac MRI outcomes.

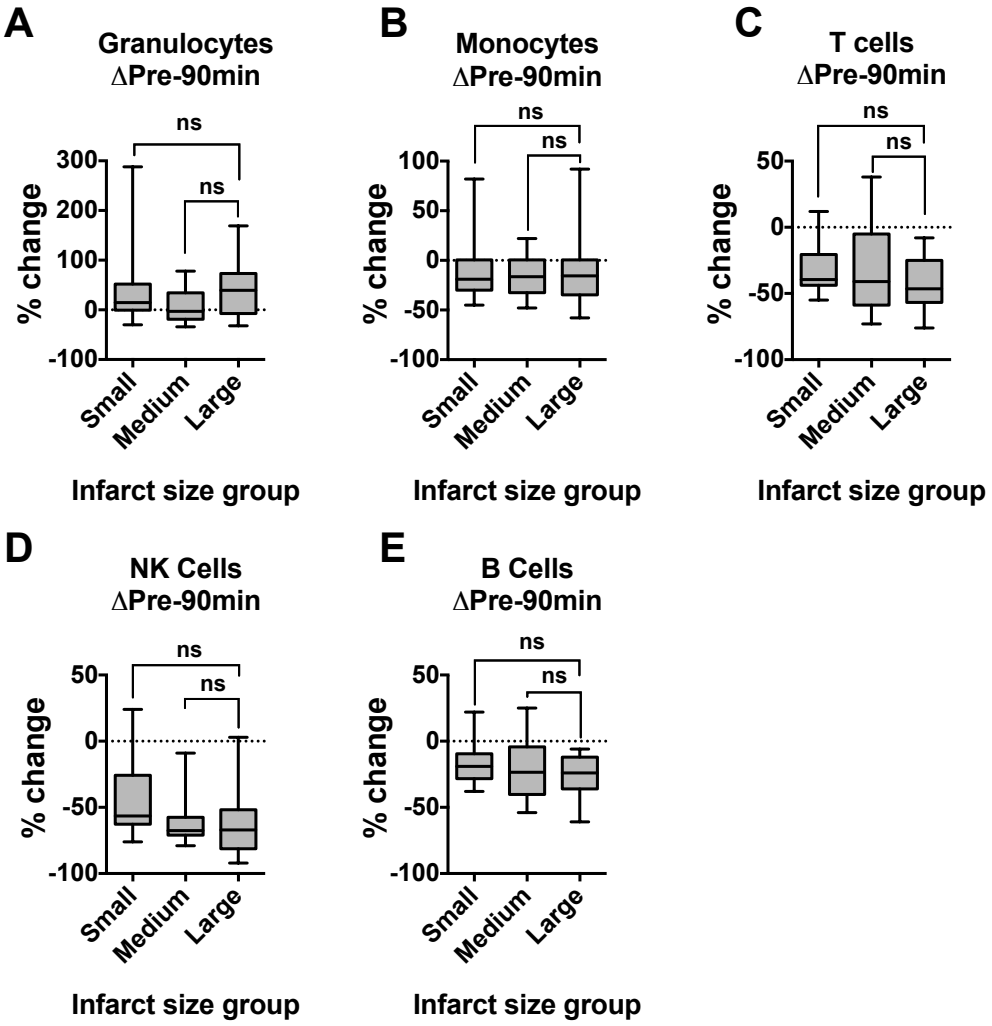

Figure 6.7: Relationship between infarct size group and total acute post-reperfusion change (Δpre-90min) in major leucocyte subsets in STEMI patients undergoing cardiac MRI for **A**: Granulocytes, **B**: Monocytes, **C**: T cells, **D**: NK cells and **E**: B cells. Box plots display median (central line), 25th and 75th (limits of box), and 5th and 95th percentiles (error bars). Statistics refer to differences between infarct size groups as indicated (Kruskal-Wallis test with Dunn's multiple comparisons test) (n=50, by infarct size group: small: n=16, medium: n=18, large: n=16). * $p<0.05$, ** $p<0.01$, ***$p<0.001$, ns = not significant.

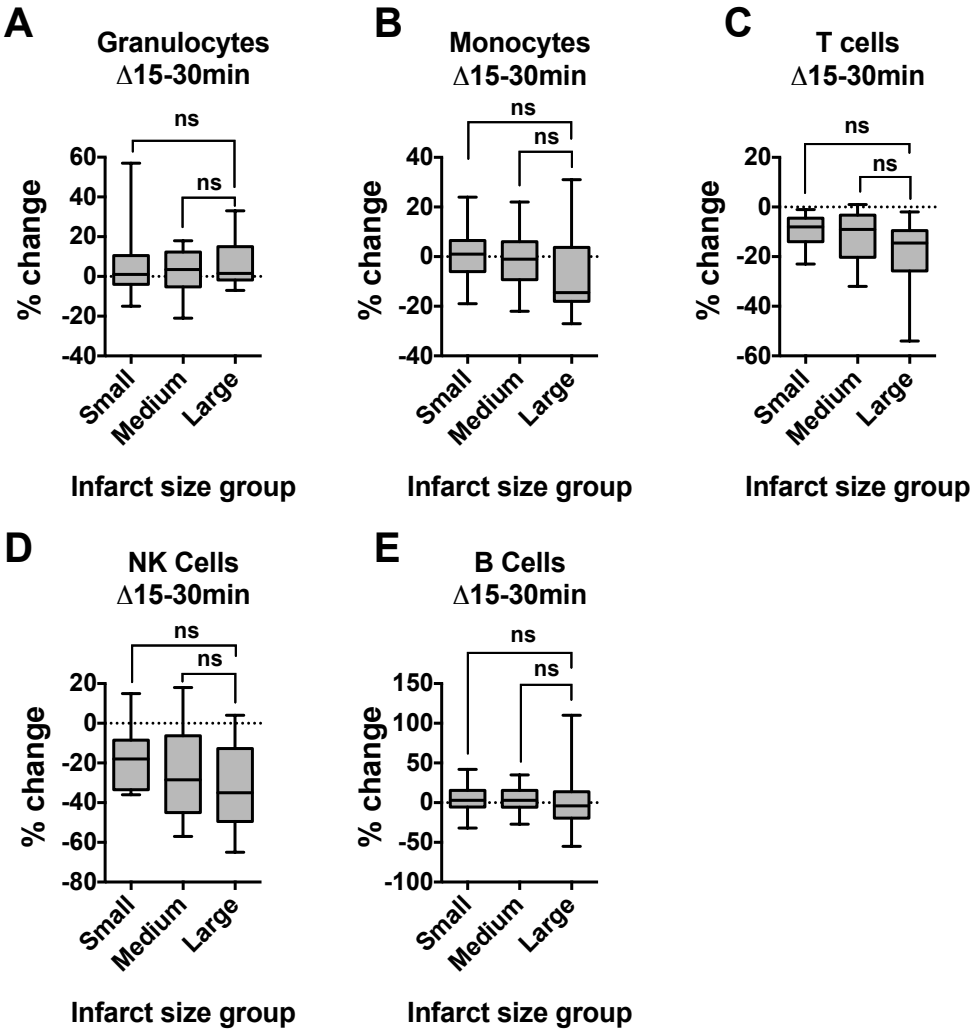

Figure 6.8: Relationship between infarct size group and early post-reperfusion change (Δ15-30min) in major leucocyte subsets in STEMI patients undergoing cardiac MRI for **A**: Granulocytes, **B**: Monocytes, **C**: T cells, **D**: NK cells and **E**: B cells. Box plots display median (central line), 25th and 75th (limits of box), and 5th and 95th percentiles (error bars). Statistics refer to differences between infarct size groups as indicated (Kruskal-Wallis test with Dunn's multiple comparisons test) (n=47, by infarct size group: small: n=13, medium: n=18, large: n=16). * $p<0.05$, ** $p<0.01$, ***$p<0.001$, ns = not significant.

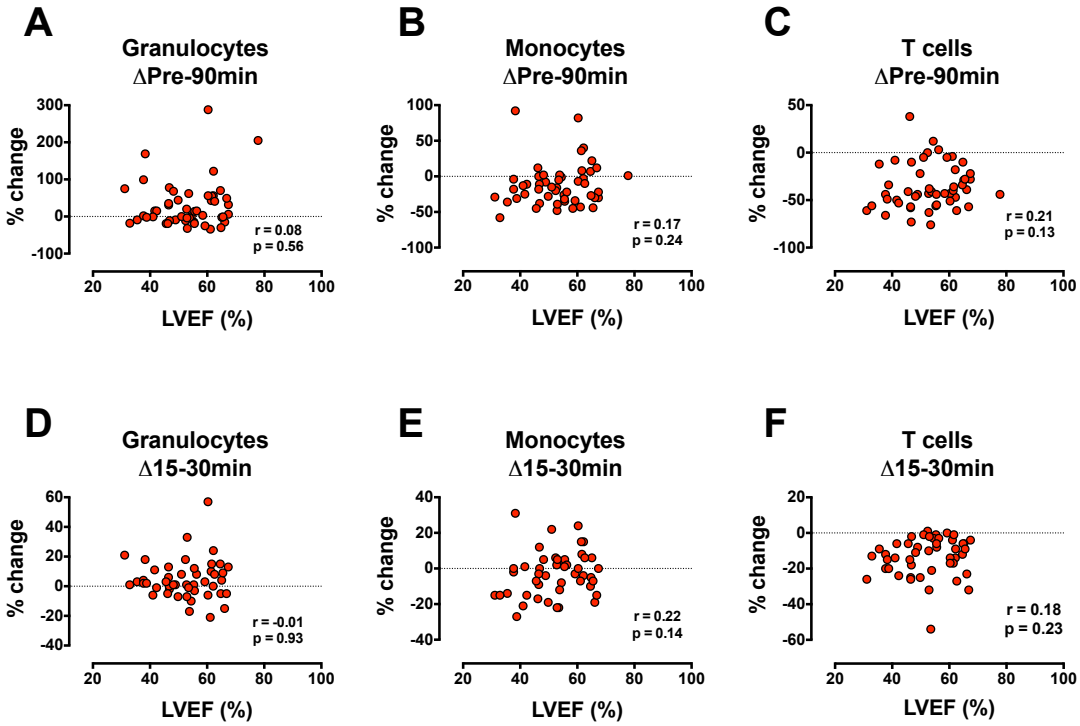

Figure 6.9: Relationship between LVEF and changes in cell counts for major leucocyte populations during total acute post-reperfusion period (Δpre-90min, n=50, **A-C**), and early post-reperfusion period (Δ15-30min, n=47, **D-F**). Data displayed for granulocytes (**A+D**), monocytes (**B+E**) and T cells (**C+F**). Statistics refer to the Spearman correlation coefficient. As shown, there were no significant correlations between the changes in cell counts and LVEF on MRI. This was also the case for all other major leucocyte subsets (B cells and NK cells, data not shown).

6.3 Discussion

The data presented in this chapter provide the first comparison of cardiac MRI outcomes in STEMI patients with a detailed analysis of post-reperfusion lymphocyte subset kinetics. The resulting associations give the first indication of a relationship between these cells and I/R injury, in the form of MVO. This is potentially a major development in cardiovascular research, given the complex and incompletely understood nature of MVO, and the current lack of any treatment. These important results have come from the utilisation of considerable resources in this study, including sophisticated flow cytometric analysis of patients' blood samples, as well as MRI imaging in the acute setting. Cardiac MRI under these circumstances can be challenging in itself, as demonstrated by the 15% failure rate in completing a scan. However, while I believe the results presented here to be a significant step forward, there are a number of limitations that must be acknowledged, most notably the correlative nature of the main findings, as I will go on to discuss in detail.

6.3.1 Reflections on MRI Outcomes and the Impact of Time-to-Scan Post-Reperfusion

Given the principal interest in myocardial I/R injury, the primary MRI outcome chosen for this study was MVO mass. The distribution of MVO among the patients undergoing MRI was highly non-linear, with a significant number of cases (n=19, 38%) developing no MVO, while 62% of cases had detectable MVO. This prevalence of MVO on LGE imaging reported here is within the range observed in previously published studies in PPCI-treated STEMI (between 25 and 69%) (de Waha et al., 2010; Eitel et al., 2014; Hombach et al., 2005; Klug et al., 2012; Niccoli et al., 2013; Wu et al., 1998b), and similar to that seen in a recent meta-analysis (56%) (van Kranenburg et al., 2014). Due to the distribution of MVO mass in the cases studied here, this parameter was best considered as a categorical variable when comparing for associations with cellular dynamics, hence the use of MVO groups. MVO itself is known to be a powerful predictor of prognosis, in terms of mortality (Bolognese et al., 2004; van Kranenburg et al., 2014) and MACE (de Waha et al., 2014; Eitel et al., 2014; Hombach et al., 2005). Regarding the

relationship with other MRI outcomes, the observed association between increasing MVO mass and infarct size, as well as reduced LVEF were unsurprising, and are in line with previously published findings (de Waha et al., 2010). Moreover, the negative correlation between MVO and myocardial salvage index in patients with interpretable STIR images was also in keeping with a recently published report of reduced salvage index in cases developing MVO (Limalanathan et al., 2013).

One potential limitation of the MRI component of this study was the lack of standardisation of the timing of the scan in relation to reperfusion. The fact that there was no correlation between scan timing and either MVO or infarct size was, however, reassuring in this regard. Nevertheless, there are published reports regarding the temporal evolution of MRI findings in this context. One study in humans found that both infarct size and MVO decreased significantly between 2 days and 1 week post-PPCI (Mather et al., 2011), while previous animal studies have shown an increase over the first 48 hours (Rochitte et al., 1998) but no change in MVO between 2 and 9 days (Wu et al., 1998a). Consequently, this remains an area of some uncertainty, and given that this study was not designed to assess the temporal development of MVO this does remain a source of potential error.

In contrast to MVO and infarct size, a positive correlation between scan timing and LVEF was observed. This is likely to reflect recovery from myocardial stunning, and possibly early infarct healing. However, LVEF was not the primary MRI outcome measure, and did not appear to be of relevance in relation to leucocyte dynamics. Consequently, this relationship is unlikely to have affected the principal findings of the study.

Finally, the issues regarding quantification of AAR and subsequent myocardial salvage index merit discussion. Difficulties were consistently noted in interpretation of STIR images in cases of non-anterior STEMI, as outlined above. As such, with the exception of the relationship with other MRI parameters, the salvage index data obtained have not been reported. The imaging methodology utilised for AAR in this study is well recognised and has been widely used in both MRI

validation studies (Francone et al., 2011; Friedrich et al., 2008; O h-Ici et al., 2012) and major clinical trials (Kim et al., 2015a; Lonborg et al., 2012; Thuny et al., 2012). In recent years, however, since the start of my own study, there has been controversy regarding the reliability and utility of this method. Artefactual enhancement in the anterior wall due to the proximity of the surface coil have previously been described (Croisille et al., 2012) and appear to have been the main cause of the issues observed in this study. However, many studies that have used this technique have not reported such issues. Consequently, it is difficult to know how widespread this finding is, and whether it relates to specific practices in image acquisition. Moreover, a recent study has reported that regions of hyperintensity on T2-weighted MRI images did not correspond to pathologically measured AAR and instead were more closely related to the area of infarction (Kim et al., 2015b). This is in direct contrast to the commonly cited animal studies supporting the use of MRI assessment of AAR (Aletras et al., 2006; García-Dorado et al., 1993). As such, this is clearly an area of considerable debate, and my own experience from this study has led me to conclude that STIR images are not ideal for this use. Alternative T2-weighted MRI protocols, resulting in bright blood images have been reported to be of superior accuracy (Payne et al., 2011), although these were not available in the present study and have also recently been questioned (Kim et al., 2015b). While the loss of salvage index as a usable outcome measure was undesirable, I do not believe this has ultimately affected the utility of the results, given the importance of MVO in this context.

6.3.2 MRI Outcomes and Cellular Dynamics: Effector T Cells are Likely to Contribute to Myocardial I/R Injury

The key finding reported in this chapter is the association between depletion of effector T cells in the early post-reperfusion period, and MVO in STEMI patients treated by PPCI. This further elucidates the work of Bodi et al. who have previously shown an association between post-PPCI lymphopaenia and MVO (Bodi et al., 2009). Moreover, two previous studies have shown an association between NLR (Akpek et al., 2012), and platelet to lymphocyte ratio (Kurtul et al., 2014) respectively, and poor myocardial perfusion following PPCI.

The pathogenesis of MVO is multifactorial, involving direct endothelial damage, leucocyte plugging of the microvasculature, platelet/fibrin embolisation and myocyte swelling (Ito, 2009). The findings reported here strongly support a potential role for effector T cells in this process.

It is, however, important to acknowledge and discuss the limitations of this part of the study. While the relationship between MVO and effector T cell dynamics is very striking, this finding is correlative in nature. As such, firm conclusions regarding causation cannot be made, and these results are primarily hypothesis generating. Nevertheless, taken in the context of previously published research in mice showing a role for IFN-γ producing $CD4^+$ T cells in myocardial I/R injury (Yang et al., 2005; Yang et al., 2006), I believe this to be the first evidence in humans of such a potential link. One way in which effector T cells could contribute to MVO is through direct trapping within the myocardial microvasculature. This hypothesis is supported by the coronary sinus data described in the previous chapter, suggesting sequestration of T cells in the myocardial vasculature early after reperfusion. Given the known functions of these cells it is conceivable that once there they may release inflammatory mediators, including IFN-γ, contributing to further leucocyte infiltration, extension of MVO, and additional myocardial damage.

At present, no specific treatment targeting myocardial I/R injury has reached routine clinical use and most interventions have proved disappointing (Hausenloy and Yellon, 2013). However, a small proof of concept study has shown potential benefit with administration of cyclosporin immediately prior to PPCI (Piot et al., 2008). While the rationale for this treatment was prevention of MPTP opening, a key event in I/R injury, it is also noteworthy that it has a profound effect on T cells, limiting their activation through the inhibition of calcineurin (Azzi et al., 2013). It is, therefore, possible that any beneficial effect in myocardial I/R injury could be mediated at least in part through this mechanism.

6.4 Conclusions

The data in this chapter show, for the first time, an association between early post-reperfusion effector T cell dynamics and myocardial I/R injury in the form of MVO. While this association does not prove a mechanistic link, it raises that possibility, particularly in the context of the existing murine studies showing a role for IFN-γ producing $CD4^+$ T cells. Should subsequent studies prove this link, T cell function in the immediate post-reperfusion phase would represent a potentially extremely important therapeutic target. As such, this opens a new and exciting avenue for further research and treatment development. However, the mechanisms behind T cell dynamics post-reperfusion remain unexplained. Consequently, preliminary investigation of this phenomenon forms the basis for the experiments described in chapter 7.

Chapter 7

Mechanisms of Post-Reperfusion T Cell Depletion

7.1 Introduction

Throughout all stages of this project, I have observed transient lymphopaenia in STEMI patients treated by PPCI. In the retrospectively analysed cohort of 1377 patients described in chapter 4, this acute lymphopaenia was shown to be predictive of poor prognosis. The cell count data in the prospectively analysed patients in chapter 5 then demonstrated that the fall in lymphocyte counts was primarily due to selective loss of T cells, as well as NK cells, from the circulation. The drop in NK cells was not specific for cases of ischaemia/reperfusion, being seen in NSTEMI as well as in STEMI. Transient T cell depletion, however, did appear to be specific for reperfused STEMI. I subsequently identified an association between the early post-reperfusion drop in CD4 effector T cell subsets and MVO, a component of myocardial I/R injury.

For the next stage of my studies, I wished to investigate the mechanism of T cell depletion post-reperfusion in STEMI. The trans-coronary gradient data in chapter 5 suggested some of these cells may be sequestered into the myocardial microvasculature, an intriguing possibility given the association with MVO. However, vast numbers of T cells were transiently depleted from the circulation, making it extremely unlikely that all, or even most of these cells could be destined for the myocardial vasculature. Moreover, given the lack of previously published studies addressing the acute activity of T cell subsets during and immediately after MI, very little is currently known about the factors controlling their kinetics. With regard to other cellular populations, it is known that chemokines are critical in leucocyte trafficking in response to ischaemia and reperfusion (Frangogiannis, 2007). Consequently, I sought to investigate the possible role of chemokines and their receptors on T cell depletion from circulating blood post-reperfusion.

7.2 Results

7.2.1 T Cell Chemokine Receptor Expression in Coronary Heart Disease

Firstly, I analysed chemokine receptor surface expression on the T cells of coronary heart disease patients. This was initially done in 5 NSTEMI patients undergoing non-emergency PCI, using a 6-colour flow cytometric assay to assess expression of 15 chemokine receptors. To do this, 4 colours were used to differentiate leucocyte subsets, including one for the chemokine receptor CCR7, with two dedicated to the other 14 chemokine receptors. The assay was repeated 7 times for each sample, using different combinations of anti-chemokine receptor antibodies on the dedicated colours, in order to assess all receptors (for full explanation of this method see section 3.3.6).

Amongst the receptors analysed, there was considerable variation in their expression on T cells from NSTEMI patients (**Figure 7.1A**). The strongest expression overall was for CXCR3, a receptor known to be important in T_H1 and $CD8^+$ T cell trafficking. There was also considerable expression of several other receptors. Of note, CCR5 and CX3CR1, both also known to be involved in T_H1 cell migration, were relatively highly expressed, as were CXCR4, CCR7 (lymph node homing receptor expressed on T_N and T_{CM} cells), and CCR4 (known role in T_H2 cell function). From the full complement of receptors studied in NSTEMI cases, I then excluded 5 receptors that appeared unlikely to contribute, given minimal expression on T cells, known alternative unrelated function and/or lack of published evidence of involvement in MI (CCR1, CCR3, CCC6, CCR9 and CXCR5). Expression of the remaining 10 receptors was then assessed acutely in T cell subsets of 5 STEMI patients undergoing PPCI. Firstly, I looked at chemokine receptor expression in $CD4^+$ and $CD8^+$ T cells separately, for both the STEMI and NSTEMI cases (**Figure 7.1B-C**). Expression of all receptors was similar between these two groups of patients. When only the effector subsets ($CCR7^-$ cells, T_{EM} and T_{EMRA} combined) were considered (**Figure 7.1D-E**), expression of CX3CR1 was significantly lower in STEMI patients, while that of CXCR4 was greater. As such, it may be that in the acute setting of STEMI prior to reperfusion CX3CR1 is downregulated, while CXCR4 is upregulated.

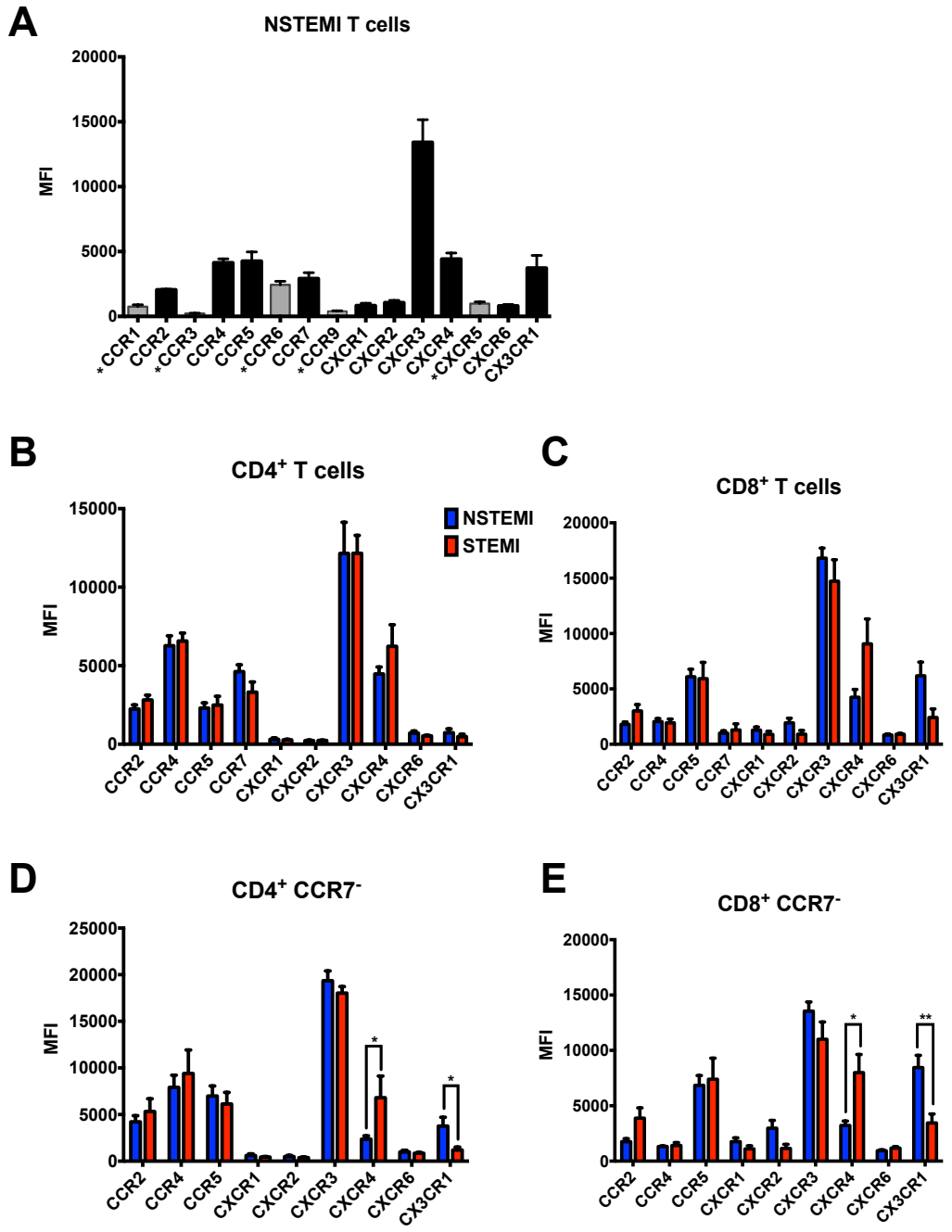

Figure 7.1: T cell chemokine receptor expression in coronary heart disease patients**. A**. Chemokine receptor expression measured by mean fluorescence intensity (MFI) in total T cells in NSTEMI patients (n=5). Receptors eliminated at this stage indicated by * and grey bars. **B+C:** Chemokine receptor expression in **B:** $CD4^+$ and **C:** $CD8^+$ T cells in NSTEMI and STEMI. **D+E:** Expression in only **D:** $CD4^+CCR7^-$ and **E:** $CD8^+CCR7^-$ T cells in NSTEMI and STEMI. Groups compared using Mann-Whitney U test (STEMI: n=5, NSTEMI: n=5). * $p<0.05$, ** $p<0.01$, ns = not significant.

7.2.2 Variation Between T Cell Subsets in Chemokine Receptor Expression in STEMI Patients and Their Relationship with Post-Reperfusion Dynamics

Next I considered the variation in surface expression of the chemokine receptors analysed between T cell subsets in STEMI patients at the pre-reperfusion time point. The chemokine receptor $CCR7^+$ was used throughout this study to classify T cell subsets, so was not included separately in this analysis. Of the other receptors studied, the majority varied significantly in their expression between the subsets assessed in this assay ($CD4^+CCR7^+$, $CD4^+CCR7^-$, $CD8^+CCR7^+$ and $CD8^+CCR7^-$ T cells). Many receptors, including CCR5, CXCR1, CXCR2, CXCR6 and CX3CR1 showed characteristically higher expression in $CCR7^-$ subsets. This may be of relevance, as these cells are known to show patterns of migration towards inflamed tissue, and also displayed greater depletion from the bloodstream post-reperfusion (see chapter 5). As such, these receptors could potentially be implicated, either individually or in combination, in post-reperfusion T cell redistribution. However, for some of these chemokine receptors, namely CXCR1, CXCR2 and CXCR6, expression was still relatively low even in the $CCR7^-$ subsets. For example, the MFI in $CD8^+CCR7^-$ cells for CXCR1 was 1110±276 units, compared to 7398±1900 for CCR5, with background fluorescence (zero expression level) of 160 units. One molecule with comparatively high expression in $CCR7^-$ T cell subsets was CX3CR1, the receptor for the chemokine fractalkine (CXCL1) (**Figure 7.2J**). A representative example of CX3CR1 expression histograms for the T cell subsets is shown in **Figure 7.3**, showing virtually no expression in $CCR7^+$ cells, but higher expression in a proportion of $CD4^+CCR7^-$ cells, and almost all $CD8^+CCR7^-$ cells, resulting in the mean fluorescence patterns seen in **Figure 7.2J**.

In order to draw potential inferences on candidate chemokine receptors in post-reperfusion T cell dynamics, I compared the pre-reperfusion expression levels, with the observed post-reperfusion (Δpre-90min) changes in T cell subset counts in the whole STEMI population (**Figure 7.4** and **Table 7.1**). In this respect one receptor, CX3CR1, stood out as showing a particularly strong relationship (r^2=0.99, p=0.006) between expression levels and the cellular drop. No other highly expressed receptor showed a significant correlation (**Figure 7.4A-E**). Although three other receptors showed a significant, albeit weaker, correlation between

their expression and the post-reperfusion drop in cell counts (**Table 7.1**), these molecules (CXCR1, CXCR2 and CXCR6) were comparatively weakly expressed. Moreover, in the cases of CXCR1 and CXCR2, these receptors are primarily involved in neutrophil trafficking, and are not considered to be major effector T cell chemokines (Bachelerie et al., 2014). Consequently, CX3CR1 appeared to be the strongest candidate for a key role in post-reperfusion T cell kinetics.

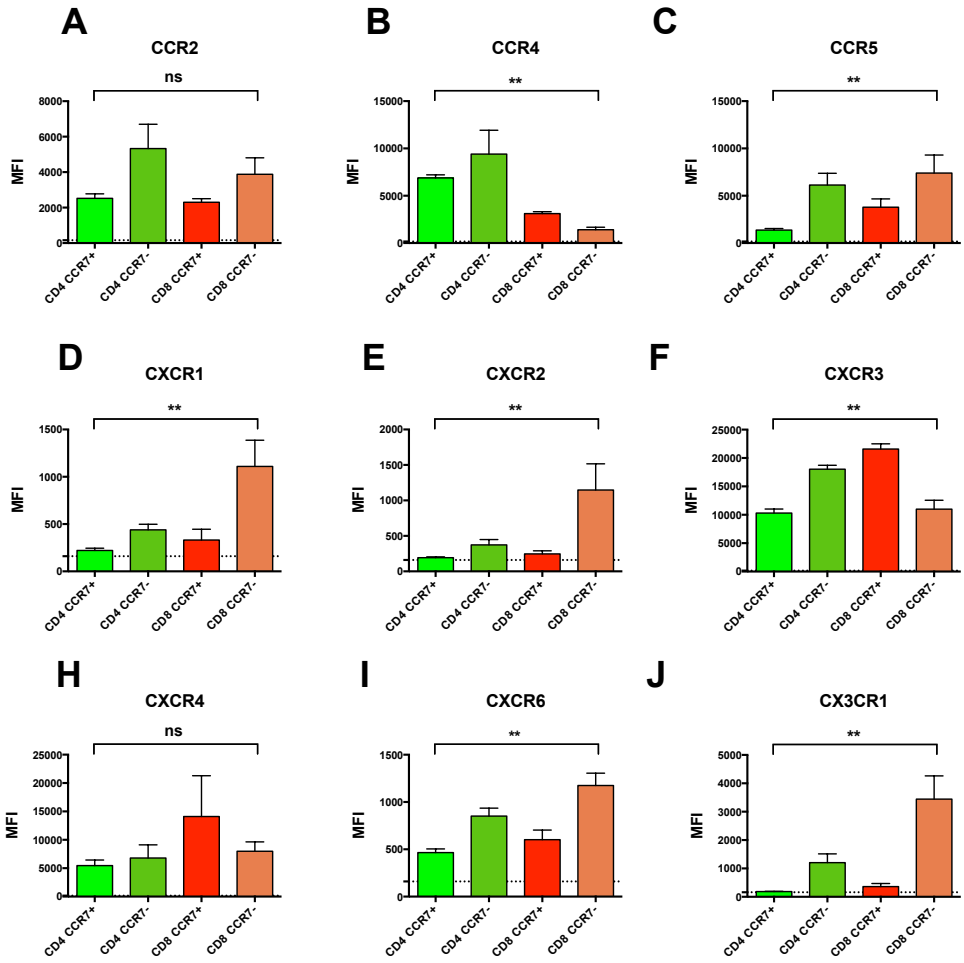

Figure 7.2: Chemokine receptor expression in T cell subsets in STEMI patients at pre-reperfusion time point. Additional dotted line and y-axis tick on each graph show approximate background fluorescence level of 160 units, indicating zero expression (derived from FMO samples). Statistics for each graph indicate the result from the overall Friedman test for the four subsets (n=5), ** $p<0.01$, ns = not significant.

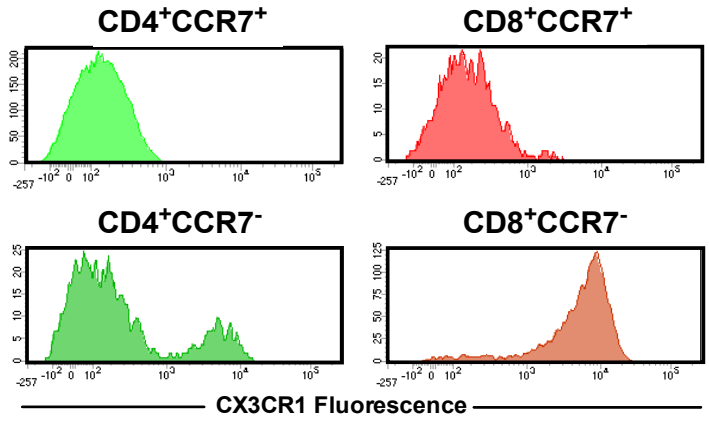

Figure 7.3: Histograms showing CX3CR1 expression in T cell subsets in STEMI patients (1 representative example of n=5).

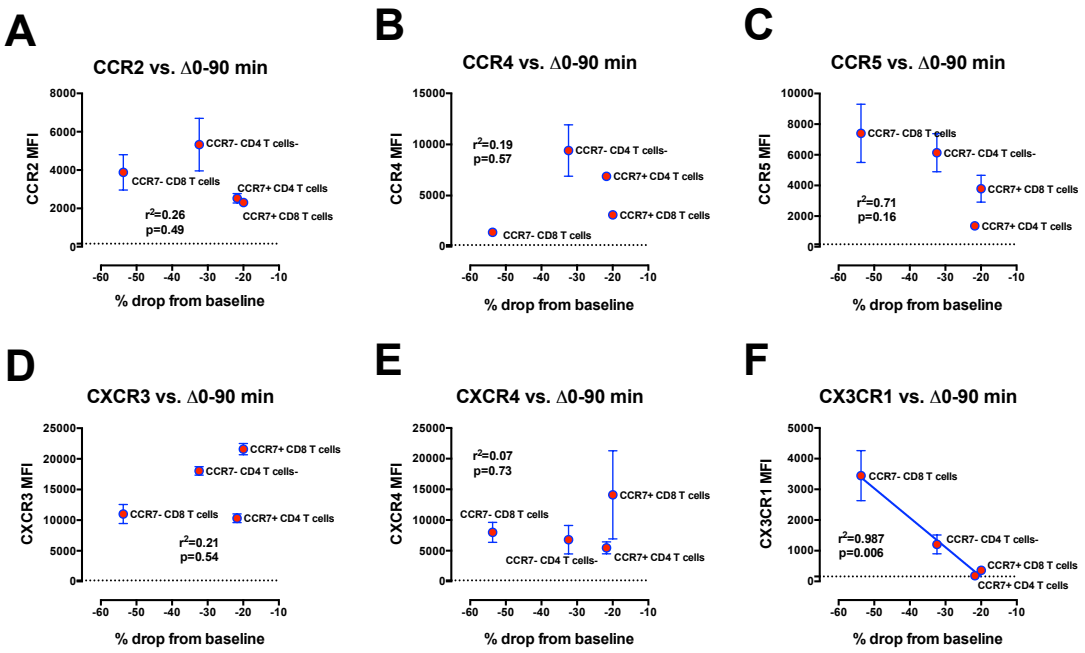

Figure 7.4: Correlations between pre-reperfusion chemokine receptor expression in T cell subsets in STEMI patients (n=5) and the observed drop in those populations post-reperfusion (pre-reperfusion to 90 minutes) in full STEMI group (n=59). Data points show mean MFI ± SEM (error bars). The chemokine receptors shown are those known to be involved in T cell trafficking in various circumstances, which also showed moderate to high levels of expression in the T cells of the STEMI patients studied. Of these, CX3CR1 (F) showed a strong correlation between subset expression and the drop post-reperfusion. Correlation as determined by linear regression and Pearson correlation coefficient.

Chemokine Receptor	Correlation (r^2) Between T Cell Subset Expression and Change in Cell Count (ΔPre-90min)	p value
CCR2	0.264	0.487
CCR4	0.187	0.568
CCR5	0.709	0.158
CXCR1	0.948	**0.026**
CXCR2	0.954	**0.023**
CXCR3	0.209	0.543
CXCR4	0.074	0.729
CXCR6	0.928	**0.037**
CX3CR1	0.987	**0.006**

Table 7.1: Correlations between T cell subset expression of chemokine receptors in STEMI patients (n=5) and the observed drop in respective subsets in the full STEMI group (pre-reperfusion to 90 minutes) (n=59). Data for all analysed chemokine receptors shown, including those with low expression and/or not known to be significantly involved in T cell trafficking. Correlation as determined by linear regression and Pearson correlation coefficient.

7.2.3 Regulation of Chemokine Receptors and Adhesion Molecules in STEMI

Having investigated the expression of chemokine receptors in T cell subsets in STEMI patients at the pre-reperfusion time point, I next considered the dynamics of these molecules during the I/R process. Firstly, gene transcription for a number of chemokine receptors and adhesion molecules was assessed in patients before reperfusion, and at the 90 minutes, 24 hours and 3-6 months time points. This was done by real-time RT-PCR analysis for expression of mRNA, and was conducted by my laboratory colleague Karim Bennaceur, using cryopreserved PBMCs that I had isolated from study patients' blood samples. As such, the resulting data (presented in **Figure 7.5** and **Table 7.2**) reflect gene transcription in all PBMCs (total lymphocytes and monocytes combined), rather than in any specific subsets. On the basis that initial transcriptional levels were likely to be affected by the acute ischaemic process, these data are presented relative to the value obtained at 3-6 months, by which time the influence of acute events would have subsided and the levels more likely to reflect genuine baseline values. Of the molecules studied, CX3CR1 once again stood out, showing the most striking regulation across the time period studied. It initially appeared to be downregulated (median relative value: 0.17 [IQR: 0.12; 0.54]), before increasing to a level similar to the post-morbid baseline by 24 hours (1.14 [0.57; 1.99], **Figure 7.5A**). The change in transcription of this molecule was highly significant, with an overall $p<0.0001$. The molecule with the next most striking regulation was CXCR4, which was initially upregulated before a decline to basal levels (**Figure 7.5C**). These findings are in keeping with the surface expression data for $CCR7^-$ T cell subsets, which had shown lower CX3CR1 and higher CXCR4 levels in STEMI compared to NSTEMI (**Figure 7.1D-E**). However, it must be remembered that the RT-PCR data do not relate to specific subsets, but to PBMCs as a whole, so will have been heavily influenced by transcription in monocytes and other lymphocyte populations. Nevertheless, the extremely marked regulation of CX3CR1 expression pre and post-reperfusion in STEMI is in keeping with a potentially important role for this receptor in leucocyte biology in this setting.

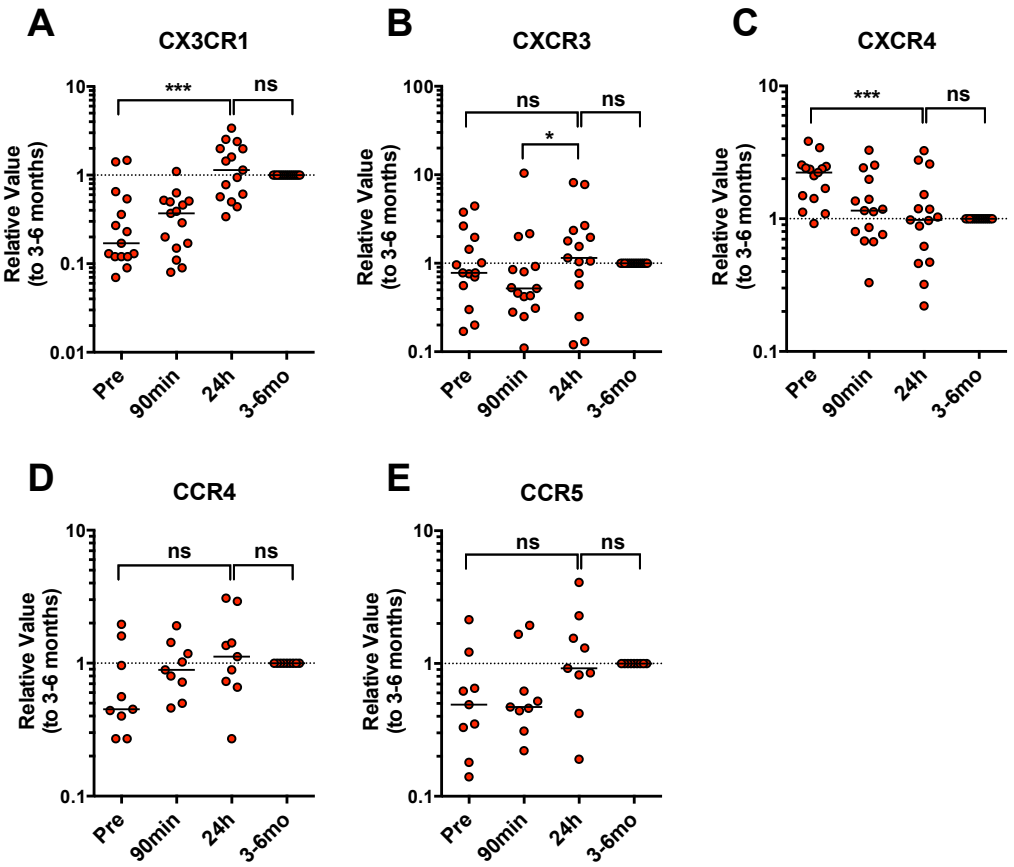

Figure 7.5: Quantitative RT-PCR data for expression of mRNA of selected chemokine receptors in PBMCs in STEMI patients. Scatter plots show all values with black line at median. Time points analysed were pre-reperfusion, 90 minutes, 24 hours and 3-6 months post-reperfusion. The relative expression of each gene in the different samples was calculated by the ΔΔCT comparative expression method and the ΔCT values calculated using the mean CT values for the housekeeping gene (18s) and the CT value for each target gene as described in section 3.5.4. Data for each time point are expressed relative to the 3-6 months level (post-morbid baseline). Statistics refer to Friedman test with Dunn's multiple comparisons test for indicated time points. (A-C: n=15, D+E: n=9). * $p<0.05$, *** $p<0.001$, ns = not significant.

Molecule	n	Pre-reperfusion	90 min	24 hr	3 months	p value
CX3CR1	15	0.17 (0.12; 0.54)	0.37 (0.15; 0.51)	1.14 (0.57; 1.99)	1.00	**<0.0001**
CXCR1	15	0.56 (0.24; 1.96)	0.66 (0.34; 0.90)	1.57 (0.83; 6.23)	1.00	0.114
CXCR3	15	0.78 (1.56; 1.96)	0.52 (0.31; 0.92)	1.15 (0.57; 2.35)	1.00	**0.028**
CXCR4	15	2.23 (1.42; 2.48)	1.15 (0.76; 1.98)	0.98 (0.47; 1.52)	1.00	**0.003**
CD11a	9	0.56 (0.43; 1.35)	0.82 (0.59; 1.10)	1.12 (0.62; 2.28)	1.00	0.200
CD11b	9	1.00 (0.61; 1.73)	1.59 (1.01; 1.96)	1.62 (0.54; 2.01)	1.00	0.324
CD62L	9	0.58 (0.39; 0.67)	1.03 (0.71; 1.45)	1.06 (0.77; 1.37)	1.00	**0.008**
CCR4	9	0.45 (0.34; 1.28)	0.89 (0.61; 1.31)	1.12 (0.70; 2.17)	1.00	0.413
CCR5	9	0.49 (0.26; 0.94)	0.47 (0.38; 1.14)	0.92 (0.62; 1.92)	1.00	0.081
CCR7	9	0.60 (0.51; 0.91)	0.88 (0.54; 1.28)	1.04 (0.75; 1.62)	1.00	0.108

Table 7.2: Quantitative RT-PCR data for expression of mRNA for all chemokine receptors and adhesion molecules analysed in PBMCs in STEMI patients. Data are expressed relative to the 3-6 months level (post-morbid baseline). Displayed as median with interquartile range, p value from overall Friedman test for each molecule.

7.2.4 Time Courses of Serum Fractalkine Concentration and Surface CX3CR1 Expression in Reperfused STEMI

Given the above findings, I wished to investigate the CX3CR1/fractalkine axis further. Firstly, the serum concentration of the ligand, fractalkine (sFKN), was quantified using an ELISA assay. This was conducted by my laboratory colleague, Evgeniya Shmeleva, using serum samples that I had isolated from study patients' blood. Fractalkine levels followed a characteristic time course, with an initial drop until 15 minutes post-reperfusion, followed by a significant rise and peak at 90 minutes, coinciding with the nadir in T cell counts (**Figure 7.6A**). Next, I studied the change in surface expression of the receptor, CX3CR1, on T cell subsets over time (**Figure 7.6B**). Surprisingly, in contrast to the gene transcription data, there was a significant decline in expression after reperfusion in the CX3CR1 expressing T cell subsets ($CCR7^-$ cells), before a recovery to near pre-reperfusion levels at 24 hours. I concluded that this apparent decrease in CX3CR1 surface expression could be due to one or more of three possibilities. There could be cell-by-cell downregulation, selective loss of CX3CR1 expressing cells, or an interaction between the ligand and the receptor leading to receptor internalisation or blockade. Given the discrepancy with the gene transcription data, I considered that a receptor-ligand interaction could be contributing. Consequently, I conducted an in-vitro competition assay to address the question of whether exposure to fractalkine alters the apparent surface expression of the CX3CR1 molecule on T cells. This involved preincubation of healthy donor blood with varying concentrations of soluble fractalkine, prior to surface staining and running the CX3CR1 quantification assay. I found that in CX3CR1 expressing cells the addition of fractalkine leads to a reduction in CX3CR1 MFI (**Figure 7.7**). This could potentially be mediated through simple blockade of the receptor by ligand binding, resulting in competition and prevention of binding to the fluorochrome-labelled antibody, or by ligand mediated internalisation of the receptor. Either way, this could explain the discrepancy between gene transcription data suggesting upregulation of CX3CR1 in PBMCs post-reperfusion, and surface expression data demonstrating reduced fluorescence in this time period.

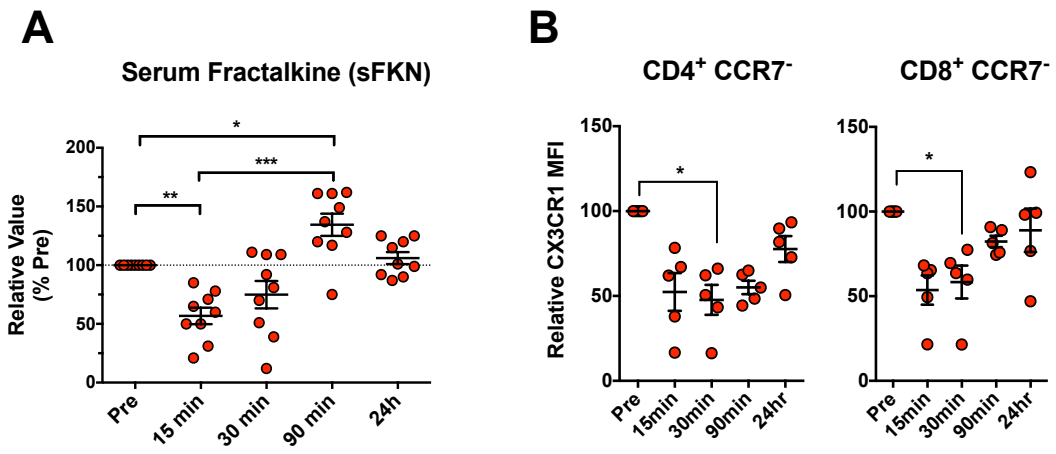

Figure 7.6: Time courses in STEMI patients for **A**: serum soluble fractalkine (sFKN) concentration and **B:** CX3CR1 expression (measured by MFI) in $CD4^+$ $CCR7^-$ and $CD8^+$ $CCR7^-$ T cell subsets. All values given are expressed relative to pre-reperfusion level, on a case-by-case basis. Time points compared using repeated measures one-way ANOVA (after meeting normality testing criteria) with Tukey's multiple comparisons test (A: n=9, B: n=5). * $p<0.05$, ** $p<0.01$, *** $p<0.001$.

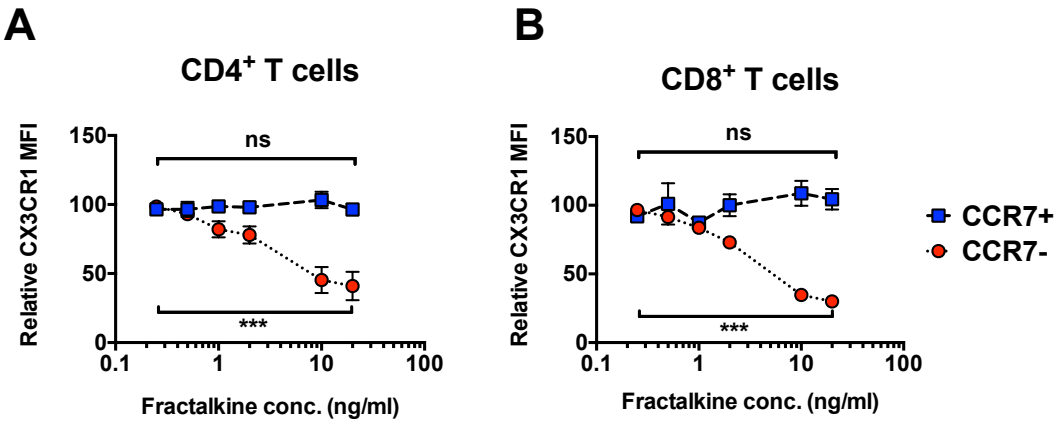

Figure 7.7: In-vitro assay showing effect of fractalkine pre-incubation on CX3CR1 fluorescence in **A:** $CD4^+$ T cell subsets and **B:** $CD8^+$ T cell subsets in healthy donors (n=3). CX3CR1 expression assay was performed after 1 hour of preincubation of blood with indicated concentration of fractalkine. Fluorescence expressed as MFI relative to baseline value (i.e. no fractalkine added). Subsets expressing CX3CR1 ($CCR7^-$) show decline in relative fluorescence with increasing doses of fractalkine, whereas subsets that express little or no CX3CR1 ($CCR7^+$) do not. Statistics refer to overall Friedman test for $CCR7^+$ (upper) and $CCR7^-$ (lower) subsets, showing variation in CX3CR1 fluorescence across fractalkine concentration as indicated. *** $p<0.001$, ns = not significant.

7.3 Discussion

7.3.1 T Cell Chemokine Receptor Expression in Myocardial Infarction

Our understanding of the role of leucocytes at all stages of coronary heart disease is currently increasing rapidly. It is now recognised that the underlying cause of ischaemic heart disease, atherosclerosis, is primarily an inflammatory disorder driven particularly by the activity of monocytes and T cells within the vessel intima (Galkina and Ley, 2009; Hansson, 2005). At later stages, inflammatory leucocytes are also critical in causing destabilisation of atherosclerotic plaques, leading to acute vascular events including MI (Bentzon et al., 2014). Moreover, the role of leucocytes during the various stages of MI, including I/R, is becoming increasingly understood. While previous attention has mostly focussed on monocytes, research into the role of lymphocytes, and T cells in particular, is now an expanding field (Hofmann and Frantz, 2015). The recruitment of T cells to the microvasculature and myocardium, as with other leucocyte populations, is controlled by chemokines and their interaction with receptors on the cell surface. The differential expression of chemokine receptors on T cells is, therefore, of importance in understanding their migration patterns under these circumstances.

In the first part of this chapter, I have performed the first comparative analysis of T cell chemokine receptor expression in human patients undergoing treatment for STEMI and NSTEMI. I demonstrated that in both of these patient groups, at the time of PCI, $CD4^+$ T cells express high levels of CXCR3 in particular, as well as CCR4 and CXCR4. The first of these receptors is typically associated with T_H1 cells, which are known to be pro-inflammatory and produce the signature cytokine IFN-γ. These cells are thought to be harmful in MI (Cheng et al., 2005) and myocardial I/R (Yang et al., 2006). CXCR3 has three known ligands, CXCL9, CXCL10 (IP-10) and CXCL11 (Bachelerie et al., 2014), of which CXCL10 is known to be upregulated in MI (Dewald et al., 2004; Frangogiannis et al., 2001). This chemokine also has a variety of CXCR3-independent effects in MI including limiting maladaptive fibrotic changes during infarct healing (Saxena et al., 2014a; van den Borne et al., 2014). However, all three CXCR3 ligands also act as chemoattractants for T_H1 cells, although the importance of this effect in MI is unknown. CCR4, on the other hand,

is more typically associated with T_H2 cells, as well as some other subsets such as T_H17 and T_{reg} cells (Bachelerie et al., 2014). These cell types are thought to have a variety of both pathogenic and beneficial subset-specific effects in MI, as described in section 1.4.7. However, the particular role of these molecules, and their chemokine ligands, in leucocyte recruitment in MI is unknown.

With regard to $CD8^+$ T cells, the highest expression of any chemokine receptors was again seen for CXCR3, followed by CCR5 and CXCR4. Of these, CCR5 could potentially be of interest, as it is a key receptor for the chemokine CCL5 (RANTES) (Bachelerie et al., 2014). This chemokine is thought to contribute to inflammatory cell migration in myocardial I/R, with blockade resulting in reduced monocyte and neutrophil infiltration and diminished infarct size in mice (Braunersreuther et al., 2010). However, once again, expression did not vary between T cells in NSTEMI or STEMI. Furthermore the role, if any, of $CD8^+$ T cells in MI and I/R remains elusive, with most studies in this area focussing on $CD4^+$ T cells. Indeed, my own data included in chapter 6 showed a very strong association between early depletion of $CD4^+$ T cells, while such striking findings were not seen for $CD8^+$ T cells.

There was no difference in expression of the chemokine receptors discussed above between the STEMI and NSTEMI patients. The only receptors that varied in this regard were CX3CR1 and CXCR4, and these differences were only seen in $CCR7^-$ subsets of $CD4^+$ and $CD8^+$ T cells (i.e. T_{EM} and T_{EMRA} cells). Expression was lower for CX3CR1 and higher for CXCR4 in $CCR7^-$ T cells from STEMI patients compared to NSTEMI. This may reflect changes induced by the greater acute ischaemic burden in STEMI group. Potential explanations for this could be alterations in gene transcription, or changes in the surface availability of the receptor through ligand-receptor interactions. For instance, if T cells from STEMI patients had been exposed to greater quantities of the ligand fractalkine, this could lead to receptor internalisation and lower availability on the cell surface. However, it is noteworthy that these findings are also in keeping with the RT-PCR data, suggesting initial downregulation of CX3CR1 and upregulation of CXCR4 at the pre-reperfusion time point, supporting the concept of transcriptional regulation. Of these receptors, CX3CR1, in particular, is known to be an important chemokine receptor in effector T cells. Its role in relation to T cell function in MI and reperfusion, however, has not

previously been investigated. The observed relationship between CX3CR1 expression and T cell depletion post-reperfusion, which I will go on to discuss further, raises the intriguing possibility of a contribution to effector T cell migration in this setting.

7.3.2 T Cell Subset CX3CR1 Expression and Serum Fractalkine Dynamics Suggest a Critical Role for this Chemokine

The receptor CX3CR1 has only one known ligand, the chemokine fractalkine (CX3CL1). This unique chemokine exists as both a membrane bound adhesion molecule, where it contributes to leucocyte binding and arrest on the vascular endothelium, and a soluble secreted form (sFKN) acting as a conventional chemoattractant (Umehara et al., 2004). It is known to contribute to multiple cardiovascular diseases and is thought to have an important role in atherogenesis and plaque destabilisation in coronary heart disease (Damas et al., 2005). Furthermore, it has previously been shown that in the context of chronic CMV infection $CD4^+$ T cells are able to induce fractalkine secretion by endothelial cells through production of IFN-γ and TNF-α, inducing further leucocyte recruitment and direct endothelial damage (Bolovan-Fritts et al., 2004; Bolovan-Fritts and Spector, 2008). The fractalkine receptor, CX3CR1, stood out among the chemokine receptors studied as showing a striking correlation between expression in T cell subsets and their depletion from the circulation following reperfusion in STEMI. Amongst T cell subsets, CX3CR1 expression was limited almost exclusively to $CCR7^-$ cells, with greater prominence on $CD8^+$ than $CD4^+$ T cells. This was the only chemokine receptor that showed both moderate to high expression on T cells, and a significant correlation between its expression and the differential drops in T cell subsets post-reperfusion. Furthermore, the gene expression data from PBMCs revealed that this receptor is highly regulated during MI and the I/R process, supporting a significant role in cellular biology during these events.

In keeping with one other study investigating fractalkine levels in STEMI (Njerve et al., 2014), I have also shown a peak in sFKN following reperfusion, coinciding with the nadir in T cell counts. Prior to this rise in sFKN, however, there was an early drop by 15 minutes after reperfusion. My subsequent in vitro competition assay

showed that pre-incubation with fractalkine resulted in a reduction in measured surface expression of CX3CR1. This supports the concept of ligand binding leading to either internalisation of the receptor or blockade, preventing binding of the fluorochrome-labelled antibody. Such an effect could be one potential explanation for the rapid decline in CX3CR1 expression observed in $CCR7^-$ T cells following reperfusion in STEMI. Moreover, it could also be a contributory factor in the lower CX3CR1 expression seen in STEMI patients compared to NSTEMI. The concept of ligand mediated internalisation of chemokine receptors is well recognised, and forms an important regulatory mechanism for chemokine mediated cellular responses (Neel et al., 2005; Marchese, 2014).

The combination of findings described in this chapter has led me to develop the following hypothesis. I propose that prior to reperfusion in STEMI, CX3CR1 expression in effector T cells may already be lower than normal secondary to receptor internalisation (and possibly downregulation) due to fractalkine release driven by the acute ischaemic insult and tissue damage. Nevertheless, although lower than in NSTEMI patients, CX3CR1 expression still remains significant in effector T cells in STEMI patients at that time point, as demonstrated by my chemokine receptor expression assay. Following reperfusion, any available fractalkine may be rapidly bound by CX3CR1 expressing leucocytes, many of which also bind membrane-bound fractalkine on inflamed vascular endothelium, resulting in their margination from the circulation and the observed drop in circulating T cell counts. Continued release of fractalkine from activated, inflamed endothelium may be augmented secondary to inflammatory cytokine production by effector T cells, leading to the peak seen at 90 minutes coinciding with the nadir in circulating T cell counts. Furthermore, given the role of fractalkine in leucocyte margination, and the contribution of leucocyte plugging to the development of MVO, it is conceivable that fractalkine mediated binding of leucocytes to vascular endothelium within the reperfused microcirculation could affect the extent of MVO. This chemokine is known to mediate effector T cell sequestration in a number of other disease processes, including atopic dermatitis (Staumont-Sallé et al., 2014), rheumatoid arthritis (Nanki et al., 2002), and multiple sclerosis (Broux et al., 2012), in each of which these cells are thought to contribute critically to disease mechanisms. Moreover, in an in vitro experimental model using leucocytes

from human CMV positive individuals, stimulated PMBCs have been shown to cause endothelial cell damage in a CX3CR1/fractalkine dependent manner (Bolovan-Fritts and Spector, 2008). Leucocyte plugging and endothelial damage are known to be major contributing causes of MVO (Ito, 2009; Schwartz and Kloner, 2012), and represent plausible mechanisms through which T cells could mediate this effect. Release of inflammatory cytokines by effector T cells may also induce further endothelial activation and infiltration of other leucocytes, including neutrophils, compounding the problem. This hypothesis is supported by previously published murine data demonstrating that T cell deficiency in Rag1 KO mice reduces myocardial neutrophil infiltration and protects against I/R injury, while reconstitution with $CD4^+$ T cells able to produce IFN-γ abolishes this protection (Yang et al., 2006). It is noteworthy, however, that in my study even T cell subsets not expressing CX3CR1 (e.g. $CCR7^+$ $CD4^+$ T cells, and B cells) displayed an approximately 20% drop in circulating counts after reperfusion, indicating that signalling through this chemokine receptor is not the sole mechanism behind lymphocyte depletion.

One question that does arise from this hypothesis, is that of why $CD4^+$ T cell kinetics show a very strong relationship with MVO, while those of $CD8^+$ T cells do not, despite the fact that $CD8^+$ T cells show greater depletion from the circulation after reperfusion, as well as greater CX3CR1 expression. I propose that this apparent paradox could be explained by the different functional impact that these cells may have once present in the reperfused myocardium/microvasculature. It is likely that effector $CD4^+$ T cell subsets would have highly pro-inflammatory effects in this setting, through production and release of cytokines such as interferon-γ. While $CD8^+$ T cells, on the other hand, can secrete pro-inflammatory cytokines, this is not generally their principal function, and they would seem less likely to play a significant role in progagation of inflammation in this setting. Thus, any impact of T cells on MVO is likely to be dependent on their function, rather than merely their presence within the reperfused zone. Consequently, it is quite possible that $CD8^+$ T cells could be sequestered into the microvasculature in similar numbers to $CD4^+$ cells, yet not have the same impact, and therefore, not show a clear relationship between cellular kinetics and MVO.

7.3.3 Limitations of Mechanistic Data and the Resulting Hypothesis

There are some important limitations in the data described in this chapter that must be acknowledged. Firstly, the numbers of patients included in the analysis of chemokine receptors was small, and as such, it is possible that genuine variations in the expression of these molecules could have been missed. Nevertheless, I was able to detect significant differences in the expression of CX3CR1 and CXCR4 in effector T cell subsets between STEMI and NSTEMI patients. One further limitation, however, is the fact that there was no healthy control group. While STEMI and NSTEMI cases were compared, it is possible that expression may be been different from normal in both of these groups, given the clinical scenario. However, the NSTEMI patients were studied at a later time point in terms of the evolution of their MI, given that blood was taken at the time of PCI procedure, which in this group was conducted on a non-emergency basis usually several days after the acute event. Consequently, it is likely that the acute effects of the infarct will have reached a more settled state by this time, allowing a valid comparison with the STEMI patients at the time of their acute presentation.

A further limitation applies to the interpretation of the RT-PCR data. Crucially, this was performed using unsorted cryopreserved PBMCs from patients' blood samples, and therefore, reflects overall gene transcription in these cells, rather than in individual leucocyte subsets. This was done due to practical constraints preventing the use of sorted T lymphocytes, rather than unsorted PBMCs. The use of sorted cells would clearly have been preferable, and resulted in data that could have been far more clearly compared with the T cell kinetics data described in chapter 5. However, to have conducted this analysis on sorted cells would have introduced further practical stages that would not have been feasible with the due to time and personnel constraints. Consequently, this data must be interpreted with caution. However, the fact that clear regulation was seen for certain molecules, notably CX3CR1, does still point to a role for these receptors during the MI and I/R process. However, the implications of these findings are uncertain, and this data alone does not allow further characterisation of what that role may be.

The key finding that led to the development of the hypothesis described above was the significant correlation between CX3CR1 expression in T cell subsets, and their depletion from the circulation post-reperfusion. This fact, combined with the clear regulation of CX3CR1 gene transcription, post-reperfusion changes in T cell surface expression, and changes in serum levels of the ligand, pointed to a key role in T cell dynamics. However, it is important to acknowledge that the findings were correlative in nature, and therefore, not proof of a mechanistic link. As in previous chapters, this fact highlights one of the limitations in conducting mechanistic research such as this in observational studies in humans. Only through blocking the mechanism in an animal model would it be possible to prove or disprove the suggested explanation of my findings. Nevertheless, research in humans does have many advantages, as outlined previously, and hypotheses generated can subsequently be robustly tested using an appropriate animal model where available.

7.4 Conclusions

As discussed in detail above, the mechanistic insights described in this chapter are primarily hypothesis generating. Nevertheless, the findings described do point to a possible role for the fractalkine/CX3CR1 chemokine axis in T cell dynamics post-reperfusion in STEMI. Should this mechanism subsequently be proven and shown to contribute to I/R injury in the form of MVO, it could represent a major new therapeutic target. Consequently, these findings open up a new avenue for further research, which may be of significant therapeutic potential in the future.

Chapter 8

Cytomegalovirus and the Cellular Immune Response Post-STEMI

8.1 Introduction

Cytomegalovirus (CMV) is an extremely common herpes virus in humans, affecting the majority of adults in developed countries (Griffiths et al., 2015). Following initial infection, it establishes latency that is never cleared, although a robust T cell mediated immune response is thought to be crucial in controlling viral reactivation and preventing overt disease (Crough and Khanna, 2009). The immune system dedicates more resources to the control of CMV than any other infection, one implication of which is a profound alteration of the composition of the T cell compartment. In particular, there is expansion of the effector memory pool (both T_{EM} and T_{EMRA}) of $CD4^+$ and $CD8^+$ T cells, with a concurrent decrease in naïve cells (Appay et al., 2002; Pourgheysari et al., 2007; van de Berg et al., 2008). There is also considerable evidence suggesting a link between chronic CMV infection and coronary heart disease. In a multivariate analysis of patients in the HOPE study, Smieja et al. reported an increased risk of cardiovascular events in CMV positive individuals (Smieja et al., 2003). Furthermore, in a large UK based cohort study, Saava et al. reported a 42% increase in mortality in CMV positive patients, exclusively due to cardiovascular deaths (Savva et al., 2013). It is thought that CMV may play a role in both the development of atherosclerosis and the destabilisation of plaques leading to MI, possibly through inducing a long-term low grade inflammatory state (Popović et al., 2012). Whether CMV infection has any impact on I/R injury sustained during MI, however, has not been studied.

In previous chapters I have established that, following reperfusion in STEMI, a dramatic response occurs involving acute transient depletion of lymphocytes from the bloodstream. This dynamic change in lymphocyte counts varies between subpopulations, with effector T cell subsets showing a particularly large fall. Moreover, it appears likely that some T cells are sequestered into the reperfused myocardial microvascular network, where they may contribute to I/R injury by influencing MVO. It is noteworthy that in chapter 6, $CD4^+$ T_{EMRA} cells showed a particularly strong relationship between their post-reperfusion dynamics and MVO. It is known that chronic CMV infection has a profound effect on the number and function of these highly differentiated T cells (van de Berg et al., 2008). In the previous chapter, I have also identified an associated between the expression of

the chemokine receptor CX3CR1 on T cell subsets, and their depletion following reperfusion. Latent CMV infection is known to result in increased numbers of highly differentiated T cells expressing CX3CR1 (van de Berg et al., 2012). Several studies have shown that such cells obtained from CMV positive patients can trigger damage to activated endothelium in vitro, and that fractalkine/CX3CR1 interactions are critical in this process (Bolovan-Fritts et al., 2007; Bolovan-Fritts and Spector, 2008; van de Berg et al., 2012). Both endothelial damage and leucocyte accumulation within the microvasculature are recognised contributory factors in MVO (Ito, 2009). Given this fact, the observed association between T cell dynamics and MVO, and the known influence of CMV infection on the T cell subsets that show the most dramatic changes post-reperfusion, I considered whether CMV serostatus may influence the cellular and MRI findings of the patients in my study. I hypothesised that transient T cell depletion following reperfusion may be more marked in CMV seropositive than seronegative patients, and may also be associated with a greater extent of MVO.

8.2 Results

8.2.1 Baseline Characteristics of CMV Positive and Negative STEMI Groups

In order to investigate the influence of latent CMV infection on the T cell response following reperfusion in STEMI, the patients were divided into two groups based on CMV serostatus (**Table 8.1**). In general, these groups were very similar in terms of their baseline characteristics, with the exception of age and sex. Unsurprisingly, given that rates of CMV positivity increase with age, the CMV positive group were on average 7.2 years older than CMV negative patients (p=0.011). There was also a lower proportion of males in the CMV positive group (63.6%) compared to the CMV negative patients (88.5%, p=0.038). There were no other statistically significant differences between the groups in terms of baseline variables, procedural characteristics, pre-admission medication (**Table 8.1**) or treatment during admission (data not shown).

	CMV Serostatus		p value
	Negative	**Positive**	
n	26	33	n/a
Age	55.3 ± 10.2	62.5 ± 10.1	**0.011**
Male sex	23 (88.5)	21 (63.6)	**0.038**
BMI	27.5 ± 4.7	26.2 ± 4.4	0.202
Diabetes mellitus	1 (3.8)	5 (15.2)	0.215
Family history of CAD	8 (30.8)	15 (45.5)	0.177
Active smoker	14 (53.8)	17 (51.5)	1.000
Hypertension	6 (23.1)	13 (39.4)	0.263
Anterior MI	14 (53.8)	14 (42.4)	0.438
Serum cholesterol (mmol/l)	5.3 ± 1.0	5.3 ± 1.1	0.630
Serum creatinine (μmol/l)	84.0 ± 19.6	77.2 ± 14.2	0.181
Peak troponin T (ng/l)	4937 ± 3627	5047 ± 3238	0.867
Procedural Characteristics			
Door-to-balloon time (minutes)	24.9 ± 12.9	28.4 ± 15.4	0.293
Onset-to-reperfusion time (minutes)	152.3 ± 80.7	174.2 ± 81.8	0.192
Pre-PCI flow (TIMI 0/1/2/3)	25/1/0/0	30/3/0/0	0.623
Post-PCI flow (TIMI 0/1/2/3)	0/0/0/26	0/0/0/33	n/a
Vascular access (radial/femoral)	25/1	31/2	1.000
Pre-admission Medication			
Statin therapy	4 (15.4)	6 (18.2)	1.000
B-blocker	1 (3.8)	1 (3.0)	1.000
Aspirin	2 (7.7)	3 (9.1)	1.000
ACE-inhibitor/ARB	2 (7.7)	4 (12.1)	0.685

Table 8.1: Baseline data for CMV negative and positive STEMI patients. Continuous variables expressed as mean ± SD and compared using Mann-Whitney U test. Categorical variables expressed as n (%) and compared using chi-square (χ^2) or Fisher's exact test as appropriate.

8.2.2 Differences in Leucocyte Subset Counts in STEMI Patients Between CMV Groups

Next I considered whether there were any differences between the counts of the major leucocyte subsets between the CMV negative and positive groups (**Figure 8.1**). At the pre-reperfusion time-point there were no significant differences between the counts of granulocytes, monocytes, NK cells, B cells or total T cells (**Figure 8.1A-E**). At 90 minutes post-reperfusion, the time point at which cell counts tended to be most dramatically altered compared to pre-reperfusion, there were still no differences in these major leucocyte populations between the CMV groups (**Figure 8.1A-E**).

When the major T cell subsets ($CD4^+$ and $CD8^+$ T cells) were considered separately, the first differences between CMV groups were revealed (**Figure 8.1F-G**). There were no differences in $CD4^+$ T cell counts, either pre-reperfusion or at 90 minutes post-reperfusion (**Figure 8.1F**). However, the $CD8^+$ T cell count on the initial sample was significantly higher in the CMV positive patients (572±66 cells/μl vs. 395±65 cells/μl, p=0.016, **Figure 8.1G**). By 90 minutes, following the post-reperfusion decline in $CD8^+$ T cell counts, the difference was no longer significant (243±25 cells/μl vs. 182±21 cells/μl, p=0.069).

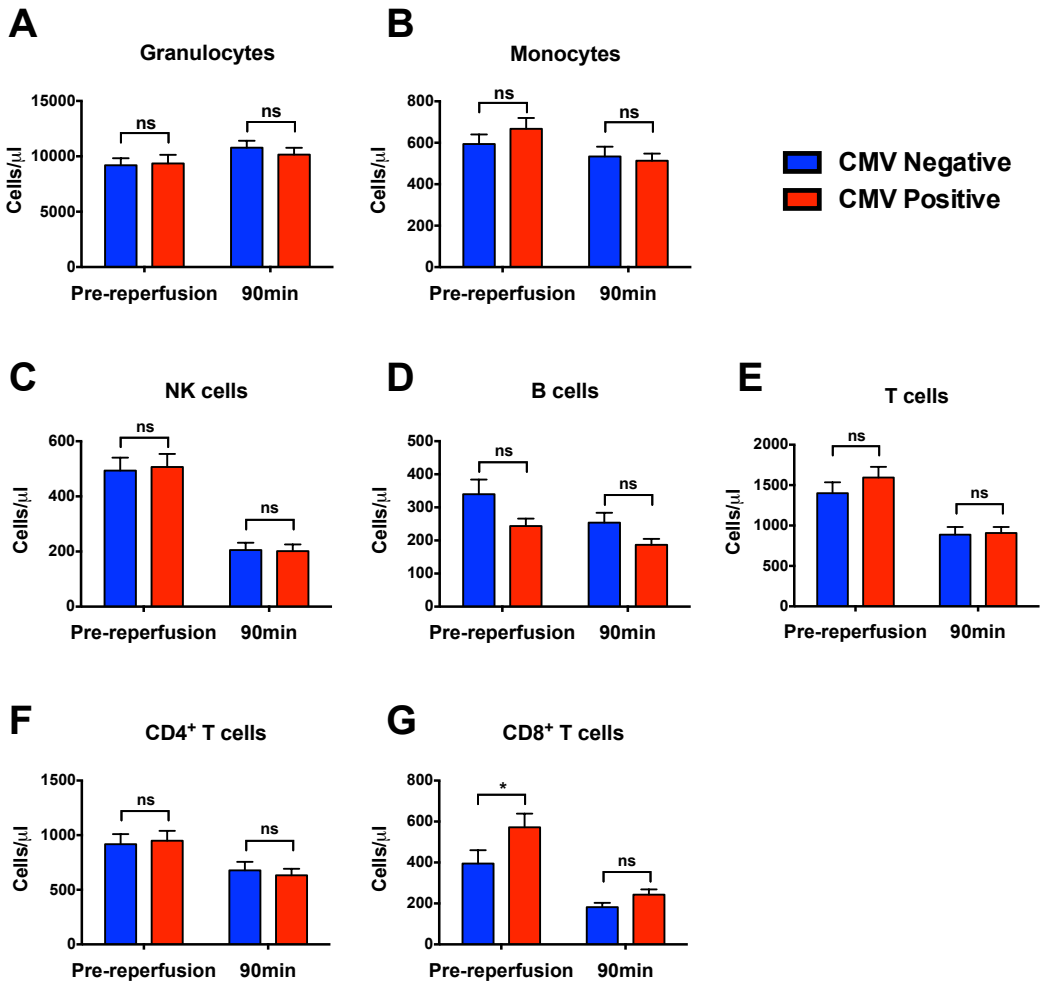

Figure 8.1: Absolute counts of leucocyte subsets in CMV negative and positive STEMI patients. Graphs show counts at pre-reperfusion and 90 minute time points for **A:** Granulocytes, **B:** Monocytes, **C:** NK cells, **D:** B cells, **E:** Total T cells, **F:** CD4+ T cells and **G:** CD8+ T cells. Groups compared using Mann-Whitney U test (total n=59, CMV-ve n=26, CMV+ve n=33). * $p<0.05$, ns = not significant.

The significant difference in baseline $CD8^+$ T cell counts between CMV groups was further reflected in the $CD4^+$ to $CD8^+$ T cell ratio (**Figure 8.2A**). The mean ratio in CMV negative patients was 3.0±0.3 compared to 2.0±0.2 in the CMV positive group (p=0.002). Although the absolute counts of $CD4^+$ and $CD8^+$ T cells did not significantly differ between the CMV groups at 90 minutes, this ratio was still significantly different at that time (4.3±0.5 vs. 3.7±0.3, for CMV positive vs. negative respectively, p=0.015, data not shown).

The most striking differences between CMV negative and positive patients, however, were in the distribution of the finer subsets within the $CD4^+$ and $CD8^+$ T cell compartments. The pre-reperfusion absolute counts and percentages for these subsets are shown in **Figure 8.2B-E**. In particular, CMV positive patients had significantly greater numbers of both $CD4^+$ and $CD8^+$ T_{EMRA} cells. On the pre-reperfusion samples, the mean $CD4^+$ T_{EMRA} count was 84±19 cells/μl in CMV positive patients, compared to 26±4 cells/μl in CMV negative patients (p=0.006), while the corresponding counts for $CD8^+$ T_{EMRA} cells were 369±46 cells/μl and 201±42 cells/μl (p<0.001). Although there were no statistically significant differences between CMV groups for the absolute counts of T_N, T_{CM} or T_{EM} cells (**Figure 8.2B-C**), the percentage composition of the $CD4^+$ and $CD8^+$ T cells compartments significantly differed for each of the subsets (**Figure 8.2D-E**). For both $CD4^+$ and $CD8^+$ T cells, CMV negative patients had proportionately more T_N and T_{CM} cells. T_{EM} cells, on the other hand, represented a greater proportion of $CD4^+$ T cells in CMV positive patients, while the opposite was true for $CD8^+$ T cells. Unsurprisingly, T_{EMRA} cells were significantly more abundant as a percentage of both $CD4^+$ and $CD8^+$ T cells in CMV positive individuals.

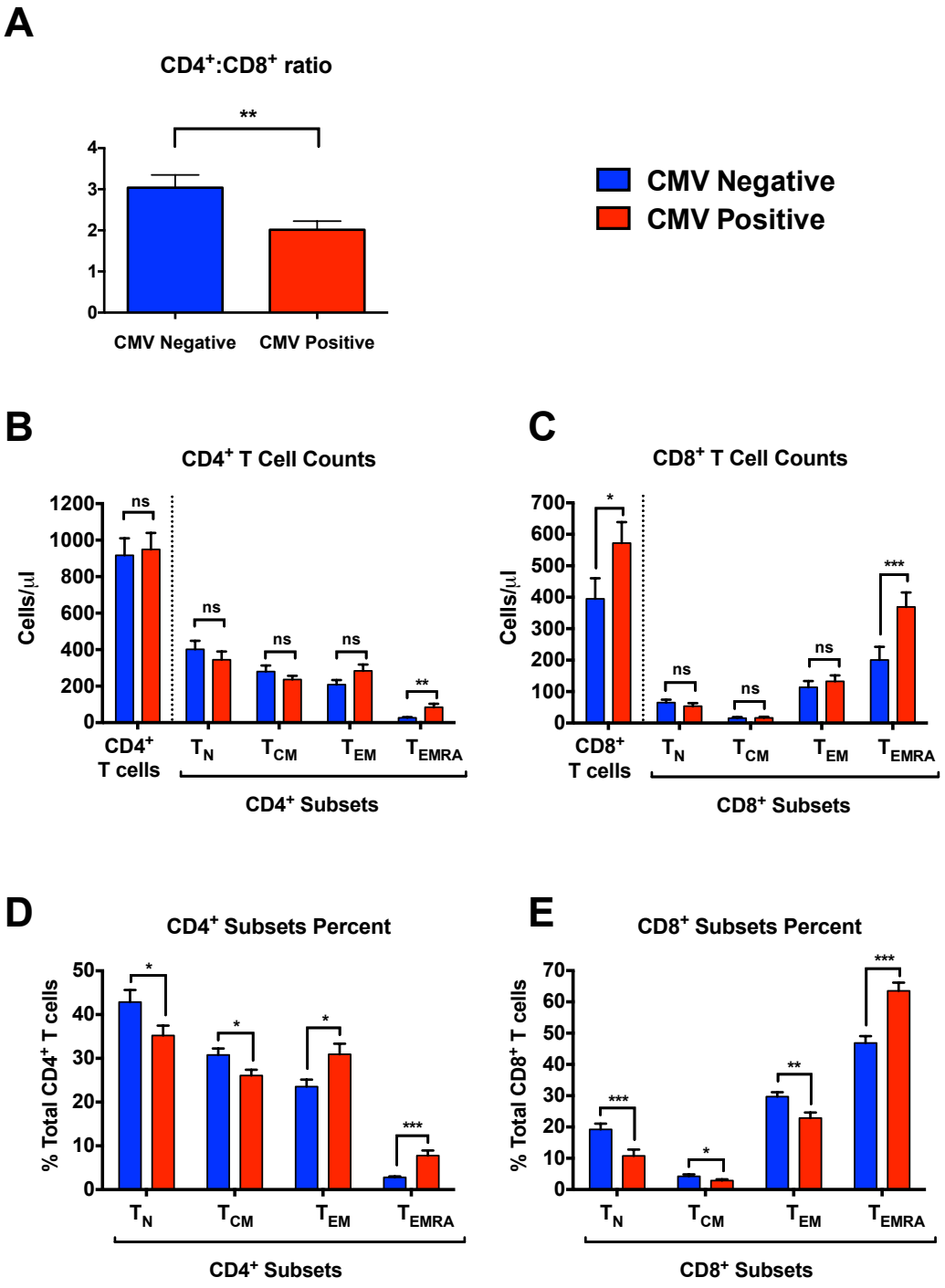

Figure 8.2: T cell subsets in CMV negative and positive STEMI patients at pre-reperfusion time point. **A:** CD4+ to CD8+ T cell ratio. **B+C:** Absolute counts of CD4+ (**B**) and CD8+ T cells (**C**). **D+E:** percentages of CD4+ (**D**) and CD8+ T cell subsets (**E**) in relation to parent population. Groups compared using Mann-Whitney U test (total n=59, CMV-ve n=26, CMV+ve n=33). * $p<0.05$, ** $p<0.01$, *** $p<0.001$ ns = not significant.

Next I considered the expression of the co-stimulatory molecule CD27 on the effector T cell subsets (T_{EM} and T_{EMRA}) in the CMV negative and positive groups (**Figure 8.3**). As previously discussed, expression of this molecule is lost on highly differentiated cells, and this lack of expression is indicative of potent effector function. In this regard, the differences between CMV negative and positive patients were very striking. The absolute counts of $CD27^-$ T_{EM} and T_{EMRA} cells were significantly higher for both $CD4^+$ (**Figure 8.3A**) and $CD8^+$ T cells (**Figure 8.3B**) in CMV positive individuals. The difference in numbers of $CD27^-$ $CD4^+$ T_{EMRA} cells was particularly dramatic, with a mean of 63±18 cells/μl in CMV positive individuals, compared to 3±2 cells/μl in the CMV negative group ($p<0.001$). Moreover, when the proportion of each effector subset expressing CD27 was considered, this was highly significantly lower ($p<0.001$) in CMV positive patients for all four subsets ($CD4^+$ T_{EM}, $CD4^+$ T_{EMRA}, $CD8^+$ T_{EM} and $CD8^+$ T_{EMRA}, **Figure 8.3C**). As such, as a component of the T cell mediated immune response, it was clear that the CMV positive patients had a far greater overall load of the highly potent $CD27^-$ effector T cell subsets than the CMV negative patients.

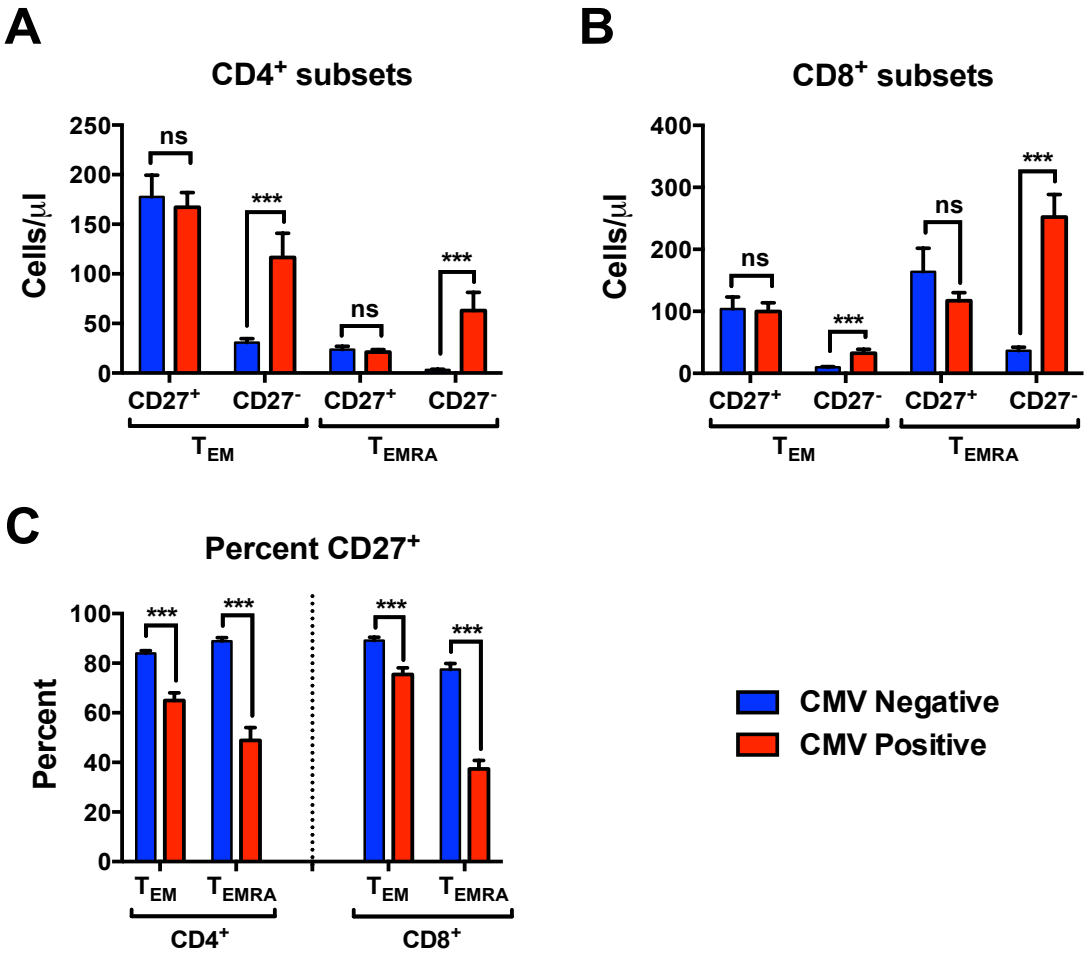

Figure 8.3: CD27 expression in effector T cell subsets (T_{EM} and T_{EMRA}) at pre-reperfusion time point. **A:** Absolute counts of CD4+ T_{EM} and T_{EMRA} subsets for CMV negative and CMV positive patients, further subdivided by CD27 expression, **B:** As above for CD8+ T_{EM} and T_{EMRA} subsets, **C:** Percent CD27 positivity for CD4+ and CD8+ T_{EM} and T_{EMRA} in CMV negative and CMV positive patients. Groups compared using Mann-Whitney U test (total n=59, CMV-ve n=26, CMV+ve n=33). *** $p<0.001$ ns = not significant.

8.2.3 Differences in the T Cell Response Post-Reperfusion in CMV Positive and Negative STEMI Patients

Having shown in chapter 6 the potential importance of the early post-reperfusion drop in T cell counts between 15 and 30 minutes, I next considered whether this response varied between CMV negative and positive patients (**Figure 8.4**). There was a significantly greater drop in total $CD4^+$ T cell counts in the CMV positive patients (median: -12.5% [IQR: -18; -5]) than CMV negative patients (-2.5% [-11.5; -1], p=0.011, **Figure 8.4A**) over this time period. Interestingly, of the next hierarchy of T cell subsets, only $CD4^+$ T_{CM} and $CD8^+$ T_N cells showed a significantly different percentage drop in this time period between CMV groups, both dropping more in CMV positive cells. However, although the proportional change in effector T cell counts did not differ between the CMV groups, it must be remembered that the CMV positive patients had higher baseline counts of the highly differentiated subsets (as described above and shown in **Figures 8.2 and 8.3**). Similar percentage changes, therefore, equate to a greater drop in total effector T cell counts, in terms of absolute numbers (**Figure 8.4C+D**). In the case of $CD4^+CCR7^-$ cells (T_{EM} and T_{EMRA} combined), for example, the median change in absolute cell count in this time period was -37.5 cells/μl (IQR: -70.5; -11) for CMV positive patients, compared to -14.5 cells/μl (-31; -3) in CMV negative patients (p=0.037, **Figure 8.4C**).

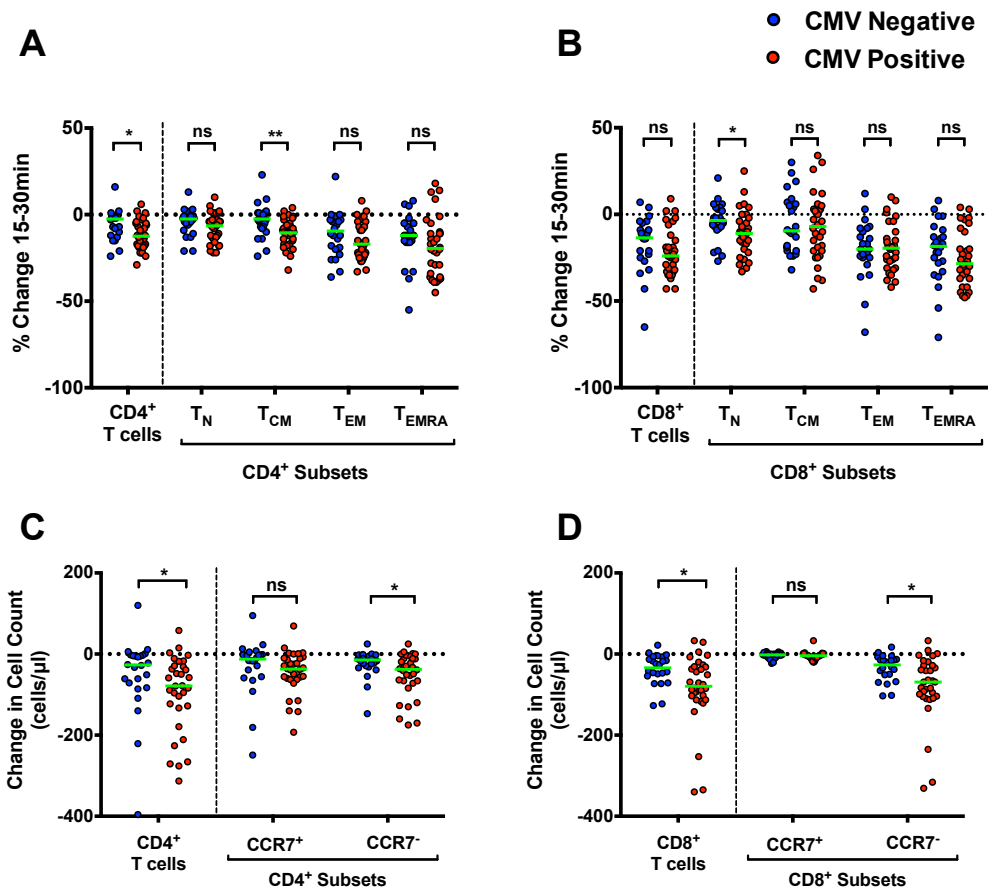

Figure 8.4: Scatter plots showing change in cell counts during early post-reperfusion time period (Δ15-30min). **A+B:** Percentage change of **A:** CD4+ T cells and subsets and **B:** CD8+ T cells and subsets. **C+D:** Absolute change in cell counts of **C:** CD4+ T cells and subsets and **B:** CD8+ T cells and subsets. **NB**: One extreme outlier point missing from **D** for a CMV negative patient with very large drop in CD8+ T cells. Statistics refer to Mann-Whitney U test for CMV positive vs. CMV negative patients for each population as indicated. (total n=56, CMV-ve n=24, CMV+ve n=32), * $p<0.05$, ** $p<0.01$, *** $p<0.001$, ns = not significant.

8.2.4 MRI Outcomes in CMV Serostatus Groups and the Relationship with Early Post-Reperfusion Effector T Cell Dynamics

Next I considered whether there were any differences in the MRI outcomes following PPCI for STEMI in the CMV positive and negative groups (**Figure 8.5**). There were no significant differences for any of the major MRI parameters. However, with the limited sample size in this study for patients undergoing cardiac MRI (CMV negative n=24, CMV positive n=26), it may well be that there was not adequate power to detect differences between these groups in terms of MRI outcomes.

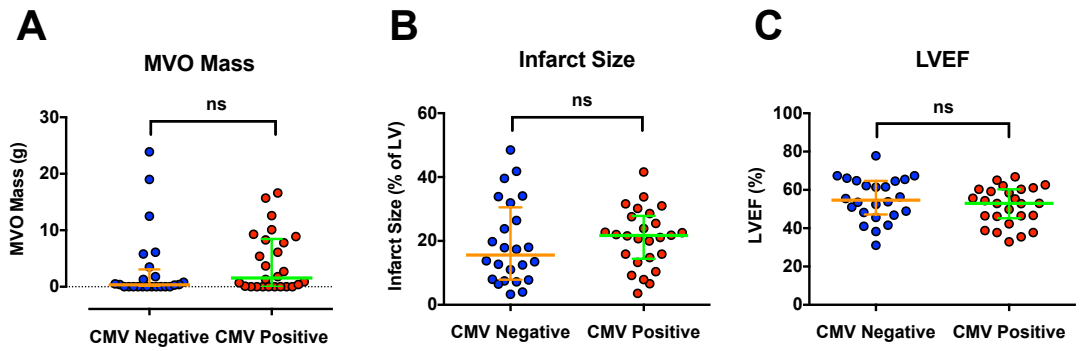

Figure 8.5: MRI outcomes in CMV negative and positive patients. Scatter plots show all data points and medians (central orange or green line) with 25th and 75th percentiles. **A**: MVO mass, **B**: Infarct size, expressed as percentage of LV, and **C**: LVEF. Groups compared using Mann-Whitney U test (total n=50, CMV-ve n=24, CMV+ve n=26), ns = not significant.

Given the association between early post-reperfusion effector T cell depletion and MVO described in chapter 6, I considered whether this applied differently between CMV negative and positive patients (**Figure 8.6**). When the CMV positive patients were considered alone, a very similar trend was seen to that of the overall population. There was a significant association between MVO group and the early drop in both total $CD4^+$ and $CD8^+$ T cells (**Figure 8.6A+B**). When the finer subpopulations were considered, there was no significant relationship with MVO group for either $CD4^+$ or $CD8^+$ $CCR7^+$ cells. In contrast, the $CCR7^-$ subsets, with the exception of $CD8^+$ T_{EMRA} cells, all showed a significant relationship with MVO, with a greater drop in the high MVO group than the zero MVO group. As with the overall STEMI patients (chapter 6, **Figure 6.6A**), this finding was most striking for the rare

$CD4^+$ T_{EMRA} cells (high MVO group: -34% [-38, -21] vs. zero MVO group: -4% [-15.5, +9.5], p<0.001, **Figure 8.6A**). In contrast, when the CMV negative patients were considered separately, there were no significant relationships between the MVO group and the early post-reperfusion change for any T cell subsets (**Figure 8.6C+D**). Consequently, it appears that the relationship between MVO and effector T cell dynamics seen in the overall STEMI group was driven by the findings in CMV positive patients.

Finally, I considered whether this difference between CMV positive and negative patients was due to the higher proportion of highly differentiated $CD27^-$ effector T cells present in the former group. To address this question I looked specifically at the drop in $CD4^+$ and $CD8^+$ $CD27^-$ effector cells ($CD4^+CCR7^-CD27^-$ and $CD8^+CCR7^-CD27^-$). When considering the early post-reperfusion change in cell counts in all STEMI patients, there was a highly significant relationship for the drop in $CD4^+CCR7^-CD27^-$ cells, with greater cellular depletion seen with increasing MVO (**Figure 8.7A**). When the CMV groups were analysed separately, this relationship remained in CMV positive but not negative patients (**Figure 8.7B**). However, when analysing percentage changes in cell counts, the fact that the absolute numbers of $CD27^-$ effector T cells are higher in CMV positive patients is not considered. Therefore, I also performed the same analysis using the absolute change in cell counts (**Figure 8.7C-D**). Once again, there was a highly significant relationship between the drop in $CD4^+CCR7^-CD27^-$ T cell count and MVO group for the overall STEMI patients, as well as the CMV positive group, but not the CMV negative patients. When using the absolute change in cell counts, there was also a significant relationship for $CD8^+CCR7^-CD27^-$ T cells in CMV positive, but not CMV negative patients (**Figure 8.7D**). The fact that most observations were consistent for both absolute and percentage changes in cell counts suggests that functional as well as numerical differences in these cells between CMV groups may be responsible for the presence of significant findings in only CMV positive patients.

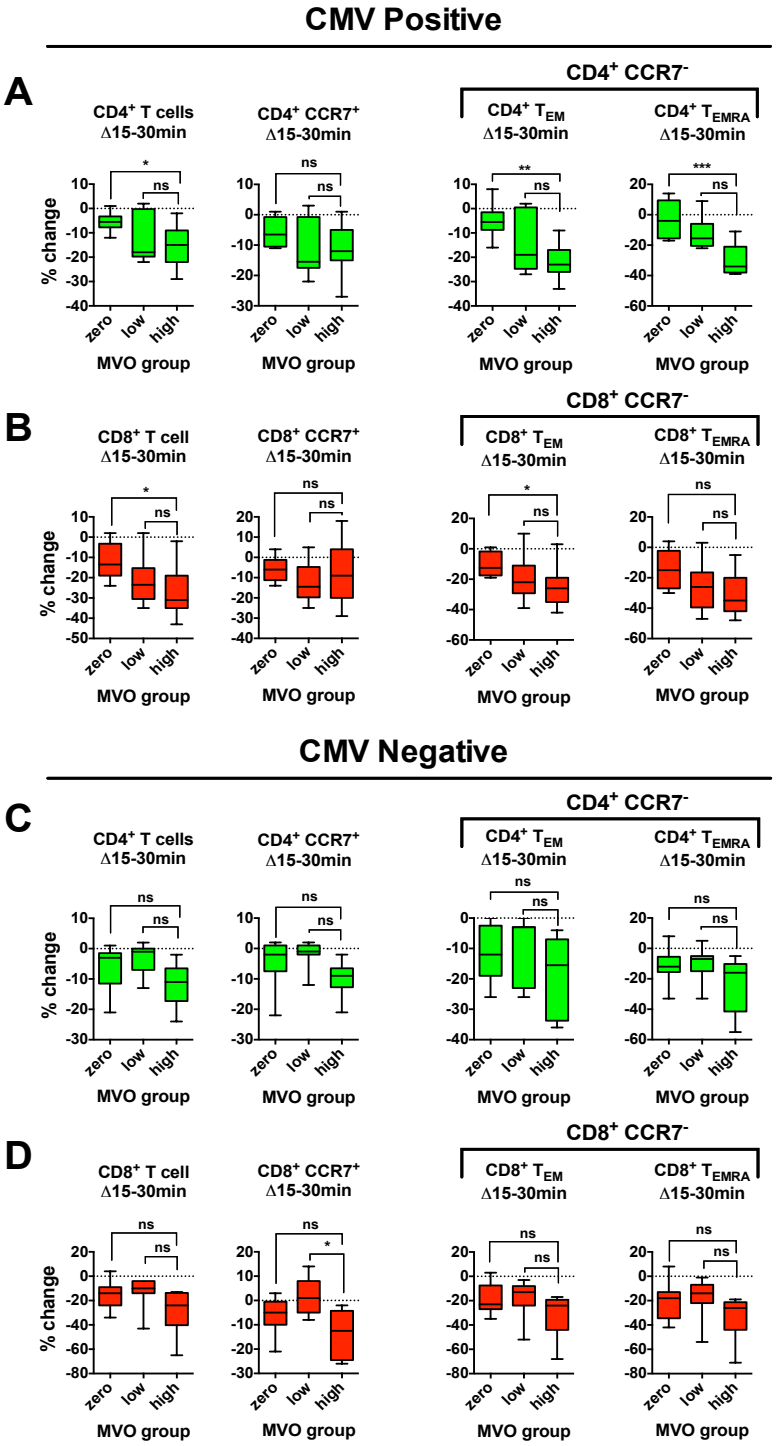

Figure 8.6: Relationship between MVO group and Δ15-30min for T cell subsets, separately for CMV positive (**A+B**) and CMV negative (**C+D**) patients. **A+C:** total CD4+ T cells, CD4+ CCR7+ (T_N and T_{CM} combined) cells, and CD4+ CCR7- effector (T_{EM} and T_{EMRA}) subsets. **B+D:** As above for total CD8+ T cells and subsets. Box plots display median (central line), 25th and 75th (limits of box), and range (error bars). Statistics refer to differences between MVO groups as indicated (Kruskal-Wallis test with Dunn's multiple comparisons test) (Total n=47, CMV positive n=25 [8 zero, 6 low, 11 high], CMV negative n=22 [9 zero, 7 low, 6 high]). * p<0.05, ** p<0.01, ***p<0.001, ns = not significant.

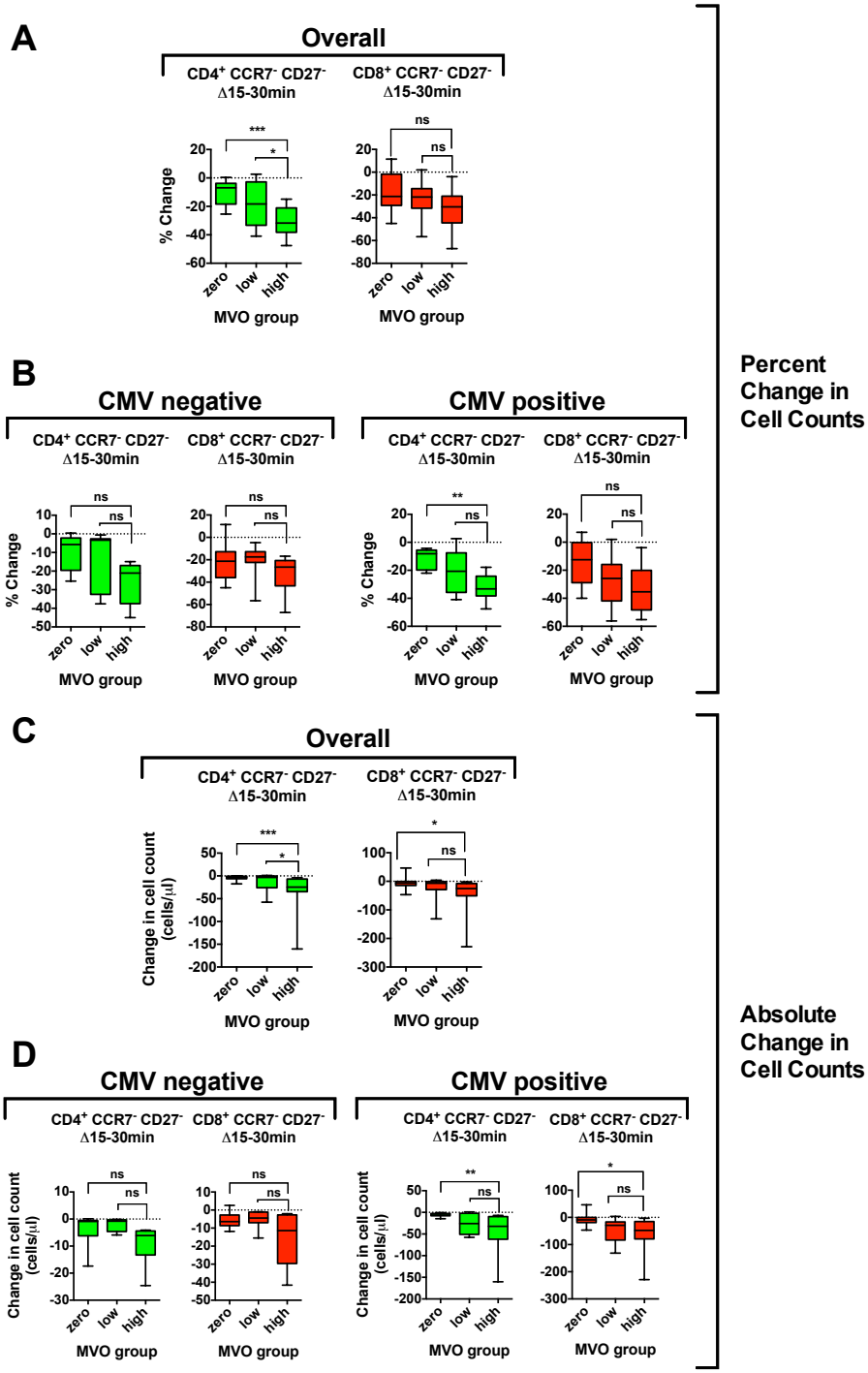

Figure 8.7: Relationship between MVO group and Δ15-30min for CCR7-CD27- T cell subsets. **A+B:** Relationship between percentage change in cell counts and MVO group in **A:** all STEMI patients, and **B:** CMV negative and positive patients separately. **C+D:** Relationship between absolute change in cell counts and MVO group in **C:** all STEMI patients, and **D:** CMV negative and positive patients separately. Box plots display median (central line), 25th and 75th (limits of box), and range (error bars). Statistics refer to differences between MVO groups as indicated (Kruskal-Wallis test with Dunn's multiple comparisons test) (Total n=47, CMV positive n=25 [8 zero, 6 low, 11 high], CMV negative n=22 [9 zero, 7 low, 6 high]). * p<0.05, ** p<0.01, ***p<0.001, ns = not significant.

8.3 Discussion

The data presented in this chapter include the first comparison of lymphocyte subsets in acute STEMI patients between CMV negative and positive patients. I have then gone on to investigate whether the dynamic changes occurring early after reperfusion differ between these groups, before further studying the relationship between early T cell depletion and MVO. In doing so, this sheds further light on this important component of myocardial I/R injury, identifying a possible effect of latent CMV infection on the contribution of T cells to myocardial damage post-reperfusion.

8.3.1 The Relevance of Latent CMV Infection in Coronary Heart Disease

While it is already known that CMV seropositivity confers increased risk of cardiovascular death in patients over the age of 65 (Savva et al., 2013), the reasons behind this are not fully understood. Given the highly immunodominant response that CMV infection induces, it seems feasible that alteration of the immune system could contribute to this observed effect on cardiovascular mortality. CMV mediated effects on the immune system could be relevant to cardiovascular disease and MI in a number of ways.

Firstly, a skewing of T cell responses towards a more inflammatory T_H1 response could increase atherogenesis, leading to higher rates of coronary artery disease. T cells are known to contribute to development of atherosclerosis, and memory $CD4^+$ T cells in particular, are found in atherosclerotic plaques, where a T_H1 phenotype is predominant (Ait-Oufella et al., 2014; Galkina and Ley, 2009; Stemme et al., 1992). One recent study has shown an association between both decreased naïve and increased memory $CD4^+$ T cells in the blood, and subclinical atherosclerosis in otherwise healthy individuals (Olson et al., 2013). Unsurprisingly, in that study, positive CMV serology was strongly associated with such a T cell phenotype. A further study demonstrated an association between a T_H1 bias in circulating $CD4^+$ T cells and subclinical atherosclerosis, also finding this T cell phenotype to be strongly associated with CMV serostatus (Tracy et al., 2013).

As such, it seems feasible that the ability of chronic latent CMV infection to skew the T cell compartment towards a more highly differentiated, pro-inflammatory phenotype may contribute to initial atherogenesis, prior to MI. Moreover, it has been proposed that CMV infection and reactivation may play a role in precipitating MI, through destabilisation of coronary atherosclerotic plaques by pro-inflammatory mechanisms (Söderberg-Nauclér, 2006). This theory, however, has been controversial with conflicting reports in the literature (Núñez et al., 2012). One recent case control study reported a higher rate of detection of CMV DNA in coronary artery atherosclerotic plaques from individuals who died from MI than in incidental plaques from a control group of those with non-cardiac mortality (Prösch et al., 2000). While this finding suggests viral replication in unstable coronary plaques, other groups have not consistently detected evidence of active CMV infection or reactivation (Borgia et al., 2001; Gredmark et al., 2007; Núñez et al., 2012). Furthermore, any active CMV replication around the time of MI could be a result of either viral reactivation prior to or precipitated by the acute infarction.

The findings described in this chapter confirm that CMV positive patients at the time of MI do indeed have proportionately fewer circulating naïve T cells, and more T_{EMRA} cells than CMV negative patients. While this is consistent with the previously published effects of CMV infection on T cells (van de Berg et al., 2008), this is the first time that these findings have been shown in an acute MI patient group. However, the design of this study does not allow for any inferences to be drawn regarding the role of CMV serostatus in the development of atherosclerosis or plaque destabilisation. Nevertheless, the observation of a T cell phenotype in CMV positive STEMI patients thought to be associated with these processes remains relevant, potentially in keeping with a role for CMV infection in driving disease.

8.3.2 The Influence of CMV Serostatus on Myocardial Infarction and Ischaemia/Reperfusion Injury

A further way in which latent CMV infection could be relevant in MI is by influencing the immune response to ischaemia and reperfusion. In this respect, the early post-reperfusion time period was of particular interest, given the

relationship with MVO described in chapter 6. Both groups (CMV negative and positive) were found to display the characteristic post-reperfusion acute depletion of circulating T cells described in chapter 5. However, because of the greater numbers of highly differentiated effector T cells in CMV positive patients, this corresponded to a greater absolute drop in the circulating counts of these cells, in spite of similar percentage drops in the two groups. Given the trans-coronary gradient data described in chapter 5, indicating loss of T cells within the myocardial circulation, it is conceivable that this could equate to greater sequestration of effector T cells within the reperfused myocardial microvasculature. However, this inference is primarily hypothesis generating, as it remains unproven in this study. To do so would require direct comparison of trans-coronary gradients between CMV negative and positive patients, something that was not possible with the low number of coronary sinus samples obtained here.

Next, I went on to compare the MRI outcomes following STEMI between CMV positive and negative patients. There were no statistically significant differences in infarct size, MVO or LVEF. Consequently, I have been unable to conclude that CMV serostatus affects these outcome measures. However, there were weaknesses in the study that must be considered in this regard. Most importantly, the relatively small sample size may not have been sufficient to provide adequate power to detect a genuine difference between the two groups. While considerable efforts were made to enrol as many patients as possible, recruitment was extremely challenging and time consuming, limiting the total number of study participants. While the final numbers recruited were certainly adequate to allow a valid analysis of cellular data (chapter 5) and overall MRI findings (chapter 6), it may be that once the STEMI patients were divided into CMV positive and negative groups the sample sizes were no longer sufficient. This will have caused particular challenges when trying to detect differences in MRI findings, given the other factors that influence these. Such additional variables, most notably the infarct territory, lead to considerable variability within the MRI outcomes.

In spite of the lack of significant differences in MRI findings between the CMV groups, I was able to assess whether the relationship observed in the overall

STEMI group between early effector T cell depletion and MVO groups differed depending on CMV status. In doing so, I found that that this association was present in the CMV positive patients, but not the CMV negative group. It therefore seems likely that this finding in the overall population was driven by the presence of CMV positive patients. While not conclusive of any causative link, the association between effector T cell depletion and MVO is the first evidence in humans linking T cells to myocardial I/R injury, supporting the findings of previous murine studies (Yang et al., 2005; Yang et al., 2006). It is worth noting that the T cell subpopulations whose dynamics were most strongly associated with MVO (e.g. $CD4^+$ T_{EMRA} cells) were found in significantly greater numbers in CMV positive patients. Furthermore, specific analysis of $CD27^-$ effector T cells outlined in this chapter, pointed to a possible role for $CD4^+CCR7^-CD27^-$ T cells (i.e. the most highly differentiated $CD4^+$ T_{EM} and T_{EMRA} cells) in CMV positive patients, and in the overall population. These cells were also vastly more numerous in CMV positive compared to CMV negative individuals.

In summary, the observed differences between CMV groups, in terms of T cell subset counts and their post-reperfusion dynamics, raise the possibility that in CMV positive patients greater numbers of highly differentiated T cells may be recruited to the myocardial microvascular network. There, they could potentially influence the extent of MVO. At this stage, however, this hypothesis remains unproven, and would need to be tested in larger studies, particularly given the lack of a clear difference in the extent of MVO seen between CMV groups.

8.4 Conclusions

The findings described in this chapter advance existing knowledge of the effects of latent CMV infection on T cell mediated immunity in cardiovascular patients. Detailed analysis of T cell subsets in STEMI patients has been performed for the first time, confirming the presence of increased highly differentiated effector subsets in CMV positive patients. The subsequent analysis of the relationship between post-reperfusion cellular dynamics and MVO has raised the intriguing possibility that latent CMV infection could affect this component of I/R injury,

though its influence on T cells. This hypothesis merits further investigation in future studies.

Chapter 9

General Discussion and Conclusions

9.1 Summary of Major Findings

9.1.1 Introduction

The results presented in this thesis significantly develop and expand current knowledge on the role of T lymphocytes in MI. Firstly, I retrospectively analysed a large cohort of STEMI patients treated by PPCI. In doing so I demonstrated for the first time the prognostic relevance of low lymphocyte counts following reperfusion therapy. I have then gone on to conduct a prospective observational study in 59 STEMI patients, in addition to 20 NSTEMI control patients, performing a detailed analysis of leucocyte subset dynamics following reperfusion, focussing particularly on T cell subpopulations. This has resulted in the most comprehensive and elaborate analysis of T cell kinetics in MI published to date. Furthermore, by conducting cardiac MRI scans in these STEMI patients, I was able to assess the relationship between these kinetics and MRI outcomes, notably MVO, an important component of myocardial I/R injury. This revealed an association between early depletion of effector T cells, in particular $CD4^+$ effector T cells, and MVO. This finding, combined with trans-coronary gradient data suggesting sequestration of T cells within the myocardial vasculature, has led to the deduction that these cells may contribute to MVO, and therefore myocardial I/R injury. Subsequent investigation of potential mechanisms behind these observations has suggested a key role for the chemokine fractalkine and its receptor CX3CR1. Moreover, chronic latent CMV infection, which has a profound influence on the T cell compartment, may contribute to these effects.

9.1.2 Lymphopaenia Post-PPCI in STEMI Predicts Increased Long-Term Mortality

In chapter 4 I described a retrospective analysis of leucocyte counts in 1377 consecutive STEMI patients treated with PPCI and discharged alive. Firstly, analysis of leucocyte temporal dynamics revealed a decline in lymphocyte counts after PPCI compared to baseline, followed by recovery. Division of the patients into four quartiles based on the minimum lymphocyte count recorded during

admission revealed significantly higher mortality rates in those with lower counts. Two Cox regression analysis models were then used to confirm that the presence of post-PPCI lymphopaenia was an independent predictor of increased mortality after correction for confounding variables. In the first of these models, the lymphocyte quartile was entered as a categorical variable, and membership of the lower two quartiles was independently associated with elevated mortality compared to the highest quartile (e.g. HR: 2.75 [95% CI: 1.16-6.55], p=0.022 for quartile 1 vs. quartile 4). In the second model, the lymphocyte, monocyte and neutrophil counts at the time of the lymphocyte nadir were entered as continuous variables. Higher lymphocyte counts independently predicted lower mortality (HR: 0.56 [0.37-0.84] per 1000 cells/μl, p=0.005), while higher monocyte counts were associated with increased mortality (HR: 2.59 [1.69-3.97], p<0.001).

These findings confirm the poor prognostic implications of lymphopaenia in STEMI treated with PPCI, complementing the existing knowledge in this field. They are consistent with the many studies that have shown the importance of neutrophil to lymphocyte ratio (Akpek et al., 2012; Arbel et al., 2014; Cho et al., 2011; Han et al., 2013; He et al., 2014; Kaya et al., 2013; Shen et al., 2010). I have added to this knowledge by specifically addressing the relevance of the minimum lymphocyte count, independent of confounding variables, therefore highlighting the importance of post-PPCI lymphopaenia. Moreover, the clinical relevance of circulating lymphocyte counts justifies the use of blood samples in the further investigation of the role of these cells in STEMI, in spite of the fact that the majority of total body lymphocytes are found outwith the bloodstream.

9.1.3 Detailed Analysis of Leucocyte Subset Kinetics in STEMI Reveals Post-Reperfusion Depletion of Effector T Cell Subsets

In the prospectively enrolled cohort of 59 STEMI patients I performed a detailed analysis of leucocyte kinetics. This differed from any previously published data in two key ways. Firstly, there had been no previous thorough investigation of T cell subset dynamics in humans in this setting. Secondly, I studied blood samples obtained at very early time points after reperfusion. Consequently, this allowed the

first analysis of temporal leucocyte subset trends in the immediate post-reperfusion period, during which I/R injury rapidly develops.

Firstly, I confirmed significant loss of lymphocytes from the circulation within the first 90 minutes following reperfusion in STEMI, prior to their recovery by 24 hours. These changes were not seen in the NSTEMI group. This was in keeping with the crude temporal trend seen in the large retrospective cohort studied in this project, as well as two previous studies to have reported such findings in STEMI patients (Bodi et al., 2009; Husser et al., 2011). There was also a small drop in monocytes over this period. Further analysis of lymphocyte subsets revealed that the overall drop was primarily driven by loss of T cells and NK cells. While NK cells were seen to drop after PCI in both STEMI and NSTEMI patients, the drop in T cells only occurred in the STEMI group, suggesting that this finding was specific for cases of acute ischaemia/reperfusion, rather than a procedurally induced phenomenon. Next, detailed analysis of T cell subsets demonstrated that $CD8^+$ T cells fell by more than $CD4^+$ T cells, and that within each of these populations a greater drop was seen with increasing levels of cellular differentiation. As such, the largest drops were seen in highly differentiated effector T cells ($CCR7^-$ cells, which consist of T_{EM} and T_{EMRA}), particularly in those lacking expression of CD27, a sign of advanced differentiation status and potent effector function.

Next, I analysed trans-coronary gradients in leucocyte subset counts to assess whether some cells may be sequestered into the myocardium or myocardial microvasculature during the post-reperfusion period. This revealed that in cases of anterior MI (in which the reperfused myocardium is drained via the coronary sinus) a significant drop was seen in the counts of $CD4^+$ and $CD8^+$ T cells when sampling was conducted within 45 minutes of reperfusion. This suggests that during the early post-reperfusion period, when T cell kinetics are at their most dramatic, some cells are taken up within the myocardial vasculature. However, given the vast numbers of T cells 'lost' from the circulation in this early period, it seems very unlikely that the majority of these cells are destined for the myocardial circulation. Nevertheless, given the strong evidence for a central role for $CD4^+$ T cells in myocardial I/R injury in mice (Yang et al., 2006), this supports the possibility that some T cells are sequestered within this zone, where they

contribute to injury. Possible mechanisms for this could include influencing MVO, through microvascular plugging and the release of inflammatory mediators, driving endothelial damage and further leucocyte infiltration.

9.1.4 Early Post-Reperfusion Effector T Cell Dynamics are Associated with Microvascular Obstruction on Cardiac MRI

In order to allow comparison of the cellular findings described above with outcome measures relating to infarct size and I/R injury, cardiac MRI scanning was conducted in the STEMI patients. Although technical limitations hindered the use of myocardial salvage index as an outcome measure, infarct size, LVEF and MVO were assessed and compared to the leucocyte subset kinetics observed. There were no significant relationships between cellular changes and either infarct size or LVEF. However, a strong association was observed between early post-reperfusion depletion of T cells from the circulation and MVO. This overall finding was driven by the effector T cell subsets, in particular $CD4^+$ T_{EM} and T_{EMRA} cells. Given that MVO is one component of I/R injury, this is the first identified link in humans between $CD4^+$ T cells and myocardial I/R injury. This key finding represents, in my opinion, the single most important and clinically relevant contribution to the literature described in this thesis, and forms the basis for my recent paper published in the Journal of Clinical Investigation (Boag et al., 2015). While this finding is essentially correlative, and does not prove a causative link, it is nevertheless in keeping with existing knowledge from mouse models of myocardial I/R injury (Yang et al., 2005; Yang et al., 2006). Moreover, in these murine studies, a comparable decrease in circulating lymphocyte numbers following reperfusion was observed (Yang et al., 2006), suggesting that similar processes to those seen here in humans may be underway.

9.1.5 Analysis of Chemokine Receptor Expression Suggests a Key Role for the Fractalkine/CX3CR1 Axis in Post-Reperfusion T Cell Kinetics

In chapter 7 I described a detailed analysis of surface chemokine receptor expression on T cell subsets in coronary heart disease patients. This was

conducted in 5 NSTEMI and 5 STEMI cases, allowing comparison between these groups. While there were no differences identified for chemokine receptor expression in the overall T cell pool, significant differences were observed when effector T cell subsets (CCR7$^-$ cells, T_{EM} and T_{EMRA} combined) were analysed separately. In particular, I found lower pre-PPCI expression of the fractalkine receptor, CX3CR1, in the STEMI group. I then assessed the differential expression of each chemokine receptor between T cell subsets in STEMI patients, identifying significant variation for the majority of receptors analysed. Of the moderate to highly expressed receptors, CCR4, CCR5, CXCR3 and CX3CR1 had expression patterns varying significantly between T cell subsets. Next, I assessed whether there were any significant correlations between these expression patterns, and the differential early post-reperfusion kinetics in T cell subsets. Once again, CX3CR1 stood out as showing a highly significant correlation, with subsets displaying higher expression (CCR7$^-$ subsets) undergoing greater depletion following reperfusion. I then went on to study the CX3CR1 ligand fractalkine. In keeping with one other study investigating fractalkine levels in this setting (Njerve et al., 2014), there was a peak in serum levels at 90 minutes after reperfusion. This rise followed an early drop that occurred by 15 minutes post-reperfusion. I subsequently demonstrated in-vitro evidence of binding between CX3CR1 on the surface of lymphocytes and recombinant soluble fractalkine, leading to a decrease in measured CX3CR1 surface expression. Finally, gene expression data showed that CX3CR1 is highly regulated in PBMCs during STEMI and I/R, with initial downregulation at presentation followed by upregulation after reperfusion.

Combined with the cellular and MRI data described above, these findings led to the hypothesis that, following reperfusion, soluble and endothelial membrane-bound fractalkine are rapidly ligated by CX3CR1 expressing leucocytes, triggering their margination from the circulation. Given the expression of CX3CR1 on effector T cells, these cells are likely to be sequestered at sites of endothelial activation, where they may induce further fractalkine production by the release of inflammatory mediators. This concept is supported by the work of Bolovan-Fritts et al., who have shown in-vitro evidence of fractalkine induction in endothelial cells by human CD4$^+$ T cells (Bolovan-Fritts et al., 2004). Furthermore, the same group have published evidence of fractalkine/CX3CR1 dependent endothelial

damage, with a key role for CD4+ T cell derived inflammatory cytokines (Bolovan-Fritts et al., 2007; Bolovan-Fritts and Spector, 2008). Moreover, fractalkine is known to contribute to pathogenic effector T cell sequestration in a number of other disease processes (Staumont-Sallé et al., 2014; Nanki et al., 2002; Broux et al., 2012). I propose that fractalkine mediated sequestration of effector T cells occurs after reperfusion within the myocardial microvasculature, and may influence the development of MVO, leading to the observed association with T cell kinetics. Given that leucocyte plugging and endothelial damage are known to contribute to the pathogenesis of MVO (Ito, 2009; Schwartz and Kloner, 2012), these are feasible mechanisms through which T cells could have this deleterious effect.

9.1.6 The Significant Association Between T Cell Kinetics and Microvascular Obstruction was Driven by Findings in CMV Seropositive Patients

Finally, in chapter 8 I investigated whether CMV serostatus had any impact on the findings in STEMI patients. In particular, I studied whether there were any differences in the composition of the T cell compartment, post-reperfusion dynamics, MRI outcomes, and the relationship between T cell kinetics and MVO. The reason for conducting this analysis was because of the known profound effects of latent CMV infection on T cell mediated immunity (van de Berg et al., 2008), as well as the association between CMV serostatus and cardiovascular disease (Savva et al., 2013; Smieja et al., 2003). Furthermore, the previously discussed findings of Bolovan-Fritts et al. regarding in-vitro fractalkine induction by CD4+ T cells and fractalkine/CX3CR1 mediated endothelial damage were specific for T cells derived from CMV seropositive individuals (Bolovan-Fritts et al., 2004; Bolovan-Fritts et al., 2007; Bolovan-Fritts and Spector, 2008).

Firstly, I demonstrated clear differences between the T cell compartments of CMV negative and positive STEMI patients. In keeping with observations outwith this clinical setting (van de Berg et al., 2008), CMV positive individuals had a lower CD4+/CD8+ ratio, fewer naïve T cells, and proportionately more highly differentiated T cells, including both CD4+ and CD8+ T_{EMRA} cells. Moreover, of the effector T cell subsets, a much higher proportion of cells in the CMV positive

patients did not express CD27, in keeping with high differentiation status and potent effector function (Hamann et al., 1997; Okada et al., 2008). On assessing early post-reperfusion T cell kinetics, I found that the percentage changes in T cell subsets were similar between CMV negative and positive patients. However, the differences in baseline levels meant that the absolute numbers of effector T cells lost from the circulation over this period were greater in CMV positive individuals. Taken in the context of the data from other chapters, this could suggest a higher burden of T cell sequestration in the myocardial microvasculature in CMV positive patients. In terms of MRI outcomes, however, there were no significant differences between the CMV groups for infarct size, MVO or LVEF, although the study may have lacked adequate power to fully determine this.

Finally, I assessed the relationship between T cell kinetics and MVO separately in the CMV groups. I found that, as in the overall population described in chapter 6, there was a significant association between early effector T cell depletion, particular in the case of $CD4^+$ T cells, and MVO in CMV positive patients. In contrast, this was not seen in the CMV negative group. As such, the findings in the overall population appear to be driven primarily by CMV positive patients. While this suggests a possible role for latent CMV infection in the contribution of T cells to myocardial I/R injury, this hypothesis would require further investigation in larger studies.

9.2 Clinical Relevance

The clinical implications of the work described in this thesis are potentially far reaching. As things stand, despite many attempts at pharmacological and procedural therapy, no treatment for myocardial I/R injury has yet shown conclusive evidence of benefit and reached routine clinical use (Hausenloy and Yellon, 2013). Given that I/R injury is thought to contribute up to 50% of final infarct size (Yellon and Hausenloy, 2007), it represents an enormously important therapeutic target, which has not yet been successfully exploited. Approximately 500 people per million of the population are admitted to hospital with STEMI in the UK each year (Widimsky et al., 2010). Although in-hospital survival has improved in such cases with the development of PPCI, the subsequent mortality and morbidity remain considerable, in part due to the development of heart failure secondary to loss of viable myocardium and adverse remodelling (Kaul et al., 2013). Consequently, treatment strategies that would be able to reduce the final infarct size after PPCI would be of great benefit. By identifying T cells as likely contributors in human myocardial I/R injury, my findings highlight a potential future treatment target, opening up new avenues for further research.

The detailed analysis of T cell subsets described in this work, as well the identification of a likely mechanistic role for fractalkine/CX3CR1 in T cell kinetics may allow the development of highly targeted therapy in the future. This is of particular importance given the complex subset specific effects of T cells in myocardial injury and healing (Hofmann and Frantz, 2015). While most existing data come from animal studies, it seems highly likely that conventional $CD4^+$ T cells have a primarily pathogenic role in the early stages after reperfusion (Yang et al., 2006), and this is supported by my own work in human patients. However, even in this early time period, there is evidence from murine studies of a protective role for some T cell subsets, particularly T_{reg} cells (Xia et al., 2015). Only by further research, in both animal models and humans, will we be able to better understand the complex cellular processes occurring during ischaemia/reperfusion, allowing development of highly targeted treatment. It is conceivable that in the future, should our findings and subsequent hypotheses be confirmed, treatment could be administered just prior to or at the point of

reperfusion, targeting specific T cell subsets, such as T_H1 $CD4^+$ T cells. One way to do this could be to block or inhibit specific chemokine receptors on the cell surface, given the variation in their expression between different subsets. For example, it is plausible that blockade of CX3CR1, which appears likely to have a role in effector T cell sequestration, could prevent trapping of these cells within the myocardial microvasculature. This could potentially cause a reduction in MVO, leading to a major beneficial impact on the clinical outcome.

In addition to subset specific T cell effects, another important issue that must be considered is the impact of timing on any potential therapeutic intervention. I have conducted the first detailed analysis of temporal trends in lymphocyte subsets, particularly in the early stages after reperfusion. The trans-coronary gradient data suggested that T cell infiltration into the myocardial vasculature is likely to occur very early, within 45 minutes of reperfusion. This is important, as it highlights the point that any intervention targeting these cells would need to be delivered early, prior to or at the time of reperfusion, in order not to miss a narrow therapeutic window. However, previously published studies in mice also suggest a protective role for T cells at later stages in myocardial healing, reducing adverse remodelling and subsequent LV dysfunction (Hofmann et al., 2012; Tang et al., 2012; Weirather et al., 2014). Consequently, it seems likely that treatment targeting T cells in STEMI would be most likely to be beneficial if it acted only within the early post-reperfusion period, while not inhibiting later beneficial effects. This knowledge may impact the choice of future drugs to test in this setting, based around their pharmacokinetic and pharmacodynamic properties.

9.3 Limitations

There are several limitations to this study that must be acknowledged and considered, many of which have been discussed in the relevant chapters throughout this thesis. The principal limitations relate to the difficulties in conducting mechanistic research in human subjects. In particular, it is very difficult to demonstrate causation in disease processes in human observational studies. As such, my findings regarding the relationship between effector T cell dynamics and MVO are correlative in nature. The same criticism can be applied to my findings of a correlation between T cell subset CX3CR1 expression and cellular depletion from the bloodstream following reperfusion. While these discoveries provide fascinating insights and represent a major advance in our understanding of the role of T cells in myocardial I/R injury, it must be recognised that they represent associations and do not prove a causative link. To do so would require blockade and reconstitution of an effect in an animal model, for instance through deletion of CX3CR1 or fractalkine in a murine myocardial I/R model. However, such strategies also have significant disadvantages, most notably the difficulty in achieving a model that suitably replicates the clinical scenario in humans, as well as the significant differences that exist between the human and murine immune systems. Consequently, the work described in this thesis has the considerable advantage of directly investigating the human immune system in the real clinical setting of STEMI treated by PPCI. This allows us to advance our understanding and develop new hypotheses, which can perhaps go on to be tested in animal models. While the involvement of the acquired immune system in myocardial injury and repair is gaining increasing interest (Hofmann and Frantz, 2015), it remains significantly under-investigated and further studies would be greatly welcomed.

There are also some further smaller limitations that apply to specific aspects of this research. The retrospective analysis of 1377 STEMI patients outlined in chapter 4 was limited by the availability of blood test results obtained for clinical purposes. Consequently, these did not occur at standardised times, and in many cases some samples were not available. For instance, the majority of patients did not have blood tests taken on day 2 post-PPCI, and therefore lacked any results for this time point. Furthermore, there was considerable variation in the timing of

samples, particularly those obtained before and after admission, which were also acquired for clinical reasons in unknown circumstances. This primarily affected the validity of the temporal trends observed in leucocyte counts in that part of the study. However, detailed analysis at well standardised time points was subsequently conducted in the prospective cohort described in chapter 5, allowing robust characterisation of leucocyte subset kinetics in STEMI.

The main limitation specifically relating to the prospective cohort analysis was the unavailability of an optimal control group. A cohort of NSTEMI patients undergoing non-emergency PCI was used for this purpose. As both the STEMI and NSTEMI groups underwent the same PCI procedure, this allowed confirmation that any observed differences were not merely procedurally induced. Given that the main difference between these groups was the presence of an acute ischaemia/reperfusion process, it therefore follows that differences in leucocyte behaviour were likely to be related to this phenomenon. However, it is important to acknowledge that the NSTEMI patients were not an ideal control group, given the previously discussed additional differences compared to the STEMI patients, both in terms of clinical circumstances and baseline variables (see section 5.3.1). Nevertheless, this was the best available option, as the theoretical ideal control group of STEMI patients not undergoing I/R would clearly not be ethically acceptable in a human population.

One final limitation that must be considered is the relatively small sample size in the prospective component of this study. Recruitment to the study was extremely challenging and very labour intensive. All STEMI patients had to be recruited at the time of arrival in hospital, day or night, and needed to be able to provide informed consent in an acute emergency environment. Furthermore, the exclusion criteria, in particular the ability to undergo cardiac MRI scanning, limited the number of suitable patients. Combined with the existence of competing studies being undertaken in the department simultaneously, these issues limited the total number of STEMI patients I was able to recruit during the study period to 60. While this was adequate to assess for associations between cellular kinetics and MRI outcomes, it became a particular weakness when patients were further divided by CMV serostatus. As such, it is unlikely that the study had adequate

power to truly determine whether CMV status had an impact on the MRI end-points assessed. Nevertheless, it remains noteworthy that the association between MVO and effector T cell kinetics seen in the total STEMI group was only significant in the CMV positive patients, and not the CMV negative group. Moreover, there were clear significant differences in the composition of the T cell compartment between the CMV groups. However, while collectively these findings do suggest a potential role for CMV status in T cell responses post-PPCI for STEMI, this would require further investigation in larger studies to confirm an effect.

9.4 Future Work

While my research has shed new light on the involvement of T lymphocytes in MI and I/R injury, further work is required in this field to fully develop the therapeutic potential. The work outlined in this project will lead on to a number of further studies by my colleagues and collaborators, into which I will continue to maintain an input following completion of my clinical research training fellowship.

Given the limitations of mechanistic research in humans, one important future development will be to continue to investigate the involvement of T cells, and the chemokine fractalkine, in a mouse model of reperfused MI. Work in this area is already under way in my supervisor's laboratory, with intriguing preliminary studies showing infiltration of CX3CR1 expressing T cells into the myocardium. Later stages of this work will include blockade of this chemokine/receptor axis, which could be conducted through deletion or inhibition of the receptor CX3CR1, or the chemokine fractalkine itself. A resultant reduction in T cell infiltration, with associated amelioration of I/R injury, would support my own findings, and be a major step towards proving a role for T cells and fractalkine in this setting. Subsequent reconstitution experiments, reinstating full I/R injury and T cell infiltration with reversal of fractalkine blockade would provide conclusive evidence of such an effect.

While studies in an animal model may allow more detailed and definitive assessment of the mechanisms of T cell kinetics and I/R injury, therapeutic trials in humans of T cell modifying drugs are already underway. As outlined previously, two small clinical trials have previously shown benefit in the use of cyclosporin prior to PPCI in STEMI to reduce I/R injury, with one showing a reduction in infarct size (Piot et al., 2008), while the another reported reduced adverse LV remodelling (Mewton et al., 2010). A large international multicentre trial (the CIRCUS trial) has recently reported its one year follow-up findings, disappointingly failing to show any clinical benefit from cyclosporin treatment prior to PPCI (as measured by a composite end-point of death, worsening heart failure during initial admission, readmission due to heart failure or adverse LV remodelling) (Cung et al., 2015). However, while cyclosporin has profound effects on T cells, limiting

their activation, this was not the rationale for its use in these studies, and consequently immunological parameters have not been considered. A further single centre clinical trial is under way at the Freeman Hospital, Newcastle upon Tyne, specifically investigating the impact of pre-PPCI cyclosporin on T cell kinetics, as well as MRI outcome measures including MVO. Moreover, amongst the other factors that will be considered in this study is CMV serostatus, helping to answer the question of the impact of latent CMV infection. This study will provide further valuable information on the effectiveness of cyclosporin in this context. However, as more mechanistic research is carried out, both in humans and in animal models, it may be possible to develop more targeted treatments, affecting only T cell subsets that are pathogenic in this context, such as T_H1 $CD4^+$ T cells.

9.5 Conclusions

The results of my research confirm the prognostic significance of lymphopaenia following PPCI for STEMI and demonstrate a characteristic pattern of lymphocyte subset depletion following reperfusion. Crucially, the data also suggest a role for effector T cells in the development of MVO and myocardial I/R injury. I have identified the chemokine fractalkine as a prime candidate to have critical function in post-reperfusion T cell kinetics. Furthermore, differences in T cell subsets between CMV negative and positive STEMI patients, combined with the relationship between cellular kinetics and MVO, suggest that latent CMV infection may influence this process. These finding could potentially have considerable clinical implications. No effective treatment is currently in use to ameliorate I/R injury in patients following PPCI. My observations identify a potential therapeutic target, opening up a new avenue for further research and future treatment development.

References

Abbas, A.K., Murphy, K.M. & Sher, A. (1996) Functional diversity of helper T lymphocytes. *Nature*, **383**, 787-793.

Abbate, A. et al. (2004) Widespread myocardial inflammation and infarct-related artery patency. *Circulation*, **110**, 46-50.

Abbate, A. et al. (2008) Sudden coronary death, fatal acute myocardial infarction and widespread coronary and myocardial inflammation. *Heart*, **94**, 737-742.

Ait-Oufella, H. et al. (2014) Adaptive (T and B cells) immunity and control by dendritic cells in atherosclerosis. *Circ Res*, **114**, 1640-1660.

Akashi, K. et al. (2000) A clonogenic common myeloid progenitor that gives rise to all myeloid lineages. *Nature*, **404**, 193-197.

Akbar, A.N. et al. (1988) Loss of CD45R and gain of UCHL1 reactivity is a feature of primed T cells. *J Immunol*, **140**, 2171-2178.

Akpek, M. et al. (2012) Relation of neutrophil/lymphocyte ratio to coronary flow to in-hospital major adverse cardiac events in patients with ST-elevated myocardial infarction undergoing primary coronary intervention. *Am J Cardiol*, **110**, 621-627.

Al-Ahmad, R.S., Mahafzah, A.M. & Al-Mousa, E.N. (2004) Immunological changes in acute myocardial infarction. *Saudi Med J*, **25**, 923-928.

Aletras, A.H. et al. (2006) Retrospective determination of the area at risk for reperfused acute myocardial infarction with T2-weighted cardiac magnetic resonance imaging: histopathological and displacement encoding with stimulated echoes (DENSE) functional validations. *Circulation*, **113**, 1865-1870.

Anderson, J.L. et al. (2011) 2011 ACCF/AHA Focused Update Incorporated Into the ACC/AHA 2007 Guidelines for the Management of Patients With Unstable Angina/Non-ST-Elevation Myocardial Infarction: a report of the American College of Cardiology Foundation/American Heart Association Task Force on Practice Guidelines. *Circulation*, **123**, e426-579.

Andreu-Ballester, J.C. et al. (2012) Values for alphabeta and gammadelta T-lymphocytes and CD4+, CD8+, and CD56+ subsets in healthy adult subjects: assessment by age and gender. *Cytometry B Clin Cytom*, **82**, 238-244.

Antonopoulos, A.S. et al. (2012) Statins as anti-inflammatory agents in atherogenesis: molecular mechanisms and lessons from the recent clinical trials. *Curr Pharm Des*, **18**, 1519-1530.

Appay, V. et al. (2002) Memory CD8+ T cells vary in differentiation phenotype in different persistent virus infections. *Nat Med*, **8**, 379-385.

Appay, V. et al. (2008) Phenotype and function of human T lymphocyte subsets: consensus and issues. *Cytometry A*, **73**, 975-983.

Arbel, Y. et al. (2014) Higher neutrophil/lymphocyte ratio is related to lower ejection fraction and higher long-term all-cause mortality in ST-elevation myocardial infarction patients. *Can J Cardiol*, **30**, 1177-1182.

Armstrong, P.W. et al. (2007) Pexelizumab for acute ST-elevation myocardial infarction in patients undergoing primary percutaneous coronary intervention: a randomized controlled trial. *JAMA*, **297**, 43-51.

Atar, D. et al. (2009) Effect of intravenous FX06 as an adjunct to primary percutaneous coronary intervention for acute ST-segment elevation myocardial infarction results of the F.I.R.E. (Efficacy of FX06 in the Prevention of Myocardial Reperfusion Injury) trial. *J Am Coll Cardiol*, **53**, 720-729.

Azzi, J.R., Sayegh, M.H. & Mallat, S.G. (2013) Calcineurin inhibitors: 40 years later, can't live without. *J Immunol*, **191**, 5785-5791.

Bachelerie, F. et al. (2014) International Union of Basic and Clinical Pharmacology. [corrected]. LXXXIX. Update on the extended family of chemokine receptors and introducing a new nomenclature for atypical chemokine receptors. *Pharmacol Rev*, **66**, 1-79.

Baggiolini, M. (2001) Chemokines in pathology and medicine. *J Intern Med*, **250**, 91-104.

Bar, F.W. et al. (2006) Results of the first clinical study of adjunctive CAldaret (MCC-135) in patients undergoing primary percutaneous coronary intervention for ST-Elevation Myocardial Infarction: the randomized multicentre CASTEMI study. *Eur Heart J*, **27**, 2516-2523.

Baran, K.W. et al. (2001) Double-blind, randomized trial of an anti-CD18 antibody in conjunction with recombinant tissue plasminogen activator for acute myocardial infarction: limitation of myocardial infarction following thrombolysis in acute myocardial infarction (LIMIT AMI) study. *Circulation*, **104**, 2778-2783.

Barron, H.V. et al. (2000) Association between white blood cell count, epicardial blood flow, myocardial perfusion, and clinical outcomes in the setting of acute myocardial infarction: a thrombolysis in myocardial infarction 10 substudy. *Circulation*, **102**, 2329-2334.

Barry, S.P. et al. (2013) Enhanced IL-17 signalling following myocardial ischaemia/reperfusion injury. *Int J Cardiol*, **163**, 326-334.

Behar, S. et al. (1994) Prognosis of early versus late ventricular fibrillation complicating acute myocardial infarction. *Int J Cardiol*, **45**, 191-198.

Bentzon, J.F. et al. (2014) Mechanisms of plaque formation and rupture. *Circ Res*, **114**, 1852-1866.

Berry, C. et al. (2010) Magnetic resonance imaging delineates the ischemic area at risk and myocardial salvage in patients with acute myocardial infarction. *Circ Cardiovasc Imaging*, **3**, 527-535.

Biglands, J.D., Radjenovic, A. & Ridgway, J.P. (2012) Cardiovascular magnetic resonance physics for clinicians: Part II. *J Cardiovasc Magn Reson*, **14**, 66.

Blackman, M.A. & Woodland, D.L. (2011) The narrowing of the CD8 T cell repertoire in old age. *Curr Opin Immunol*, **23**, 537-542.

Blancke, F. et al. (2005) Systemic inflammation and reperfusion injury in patients with acute myocardial infarction. *Mediators Inflamm*, **2005**, 385-389.

Blom, B. & Spits, H. (2006) Development of human lymphoid cells. *Annu Rev Immunol*, **24**, 287-320.

Boag, S.E. et al. (2015) T lymphocytes and fractalkine contribute to myocardial ischemia/reperfusion injury in patients. *J Clin Invest*, **125**, 3063-3076.

Bodi, V. et al. (2009) Post-reperfusion lymphopaenia and microvascular obstruction in ST-segment elevation acute myocardial infarction. *Rev Esp Cardiol*, **62**, 1109-1117.

Boehm, T. (2011) Design principles of adaptive immune systems. *Nat Rev Immunol*, **11**, 307-317.

Bolli, R. & Marbán, E. (1999) Molecular and cellular mechanisms of myocardial stunning. *Physiol Rev*, **79**, 609-634.

Bolognese, L. et al. (2004) Impact of microvascular dysfunction on left ventricular remodeling and long-term clinical outcome after primary coronary angioplasty for acute myocardial infarction. *Circulation*, **109**, 1121-1126.

Bolovan-Fritts, C.A. & Spector, S.A. (2008) Endothelial damage from cytomegalovirus-specific host immune response can be prevented by targeted disruption of fractalkine-CX3CR1 interaction. *Blood*, **111**, 175-182.

Bolovan-Fritts, C.A., Trout, R.N. & Spector, S.A. (2004) Human cytomegalovirus-specific CD4+-T-cell cytokine response induces fractalkine in endothelial cells. *J Virol*, **78**, 13173-13181.

Bolovan-Fritts, C.A., Trout, R.N. & Spector, S.A. (2007) High T-cell response to human cytomegalovirus induces chemokine-mediated endothelial cell damage. *Blood*, **110**, 1857-1863.

Bonecchi, R. et al. (1998) Differential expression of chemokine receptors and chemotactic responsiveness of type 1 T helper cells (Th1s) and Th2s. *J Exp Med*, **187**, 129-134.

Bonow, R.O. et al. (2011) *Braunwald's Heart Disease: A Textbook of Cardiovascular Medicine*. Philadelphia, Saunders/Elselvier.

Borgia, M.C. et al. (2001) Further evidence against the implication of active cytomegalovirus infection in vascular atherosclerotic diseases. *Atherosclerosis*, **157**, 457-462.

Boyle, E.M. et al. (1998) Inhibition of interleukin-8 blocks myocardial ischemia-reperfusion injury. *J Thorac Cardiovasc Surg*, **116**, 114-121.

Braunersreuther, V. et al. (2010) Chemokine CCL5/RANTES inhibition reduces myocardial reperfusion injury in atherosclerotic mice. *J Mol Cell Cardiol*, **48**, 789-798.

Braunwald, E. & Kloner, R.A. (1985) Myocardial reperfusion: a double-edged sword? *J Clin Invest*, **76**, 1713-1719.

Broux, B. et al. (2012) CX(3)CR1 drives cytotoxic CD4(+)CD28(-) T cells into the brain of multiple sclerosis patients. *J Autoimmun*, **38**, 10-19.

Bujak, M. et al. (2009) Induction of the CXC chemokine interferon-gamma-inducible protein 10 regulates the reparative response following myocardial infarction. *Circ Res*, **105**, 973-983.

Burne, M.J. et al. (2001) Identification of the CD4(+) T cell as a major pathogenic factor in ischemic acute renal failure. *J Clin Invest*, **108**, 1283-1290.

Caldwell, C.C. et al. (2005) Divergent functions of CD4+ T lymphocytes in acute liver inflammation and injury after ischemia-reperfusion. *Am J Physiol Gastrointest Liver Physiol*, **289**, G969-76.

Camm, A.J., Lüscher, T.F. & Serruys, P.W. (2009) *The ESC Textbook of Cardiovascular Medicine*. Oxford, Oxford University Press.

Cannon, C.P. et al. (2001) Association of white blood cell count with increased mortality in acute myocardial infarction and unstable angina pectoris. OPUS-TIMI 16 Investigators. *Am J Cardiol*, **87**, 636-9, A10.

Carding, S.R. & Egan, P.J. (2002) Gammadelta T cells: functional plasticity and heterogeneity. *Nat Rev Immunol*, **2**, 336-345.

Cavalera, M. & Frangogiannis, N.G. (2014) Targeting the chemokines in cardiac repair. *Curr Pharm Des*, **20**, 1971-1979.

Chan, W. et al. (2012) Effect of iron chelation on myocardial infarct size and oxidative stress in ST-elevation-myocardial infarction. *Circ Cardiovasc Interv*, **5**, 270-278.

Chandrasekar, B., Smith, J.B. & Freeman, G.L. (2001) Ischemia-reperfusion of rat myocardium activates nuclear factor-KappaB and induces neutrophil infiltration via lipopolysaccharide-induced CXC chemokine. *Circulation*, **103**, 2296-2302.

Chatelain, P. et al. (1987) Neutrophil accumulation in experimental myocardial infarcts: relation with extent of injury and effect of reperfusion. *Circulation*, **75**, 1083-1090.

Cheng, X. et al. (2005) TH1/TH2 functional imbalance after acute myocardial infarction: coronary arterial inflammation or myocardial inflammation. *J Clin Immunol*, **25**, 246-253.

Chidrawar, S. et al. (2009) Cytomegalovirus-seropositivity has a profound influence on the magnitude of major lymphoid subsets within healthy individuals. *Clin Exp Immunol*, **155**, 423-432.

Chien, Y.H., Meyer, C. & Bonneville, M. (2014) γδ T cells: first line of defense and beyond. *Annu Rev Immunol*, **32**, 121-155.

Childs, H. et al. (2011) Comparison of long and short axis quantification of left ventricular volume parameters by cardiovascular magnetic resonance, with ex-vivo validation. *J Cardiovasc Magn Reson*, **13**, 40.

Cho, K.H. et al. (2011) Value of early risk stratification using hemoglobin level and neutrophil-to-lymphocyte ratio in patients with ST-elevation myocardial infarction undergoing primary percutaneous coronary intervention. *Am J Cardiol*, **107**, 849-856.

Christia, P. et al. (2013) Systematic characterization of myocardial inflammation, repair, and remodeling in a mouse model of reperfused myocardial infarction. *J Histochem Cytochem*, **61**, 555-570.

Christia, P. & Frangogiannis, N.G. (2013) Targeting inflammatory pathways in myocardial infarction. *Eur J Clin Invest*, **43**, 986-995.

Clark-Lewis, I. et al. (1995) Structure-activity relationships of chemokines. *J Leukoc Biol*, **57**, 703-711.

Clement, L.T. (1992) Isoforms of the CD45 common leukocyte antigen family: markers for human T-cell differentiation. *J Clin Immunol*, **12**, 1-10.

Combadière, B. et al. (2003) The chemokine receptor CX3CR1 controls homing and anti-viral potencies of CD8 effector-memory T lymphocytes in HIV-infected patients. *AIDS*, **17**, 1279-1290.

Croisille, P., Kim, H.W. & Kim, R.J. (2012) Controversies in cardiovascular MR imaging: T2-weighted imaging should not be used to delineate the area at risk in ischemic myocardial injury. *Radiology*, **265**, 12-22.

Crough, T. & Khanna, R. (2009) Immunobiology of human cytomegalovirus: from bench to bedside. *Clin Microbiol Rev*, **22**, 76-98, Table of Contents.

Cung, T.T. et al. (2015) Cyclosporine before PCI in Patients with Acute Myocardial Infarction. *N Engl J Med*, **373**, 1021-1031.

Dagres, N. & Hindricks, G. (2013) Risk stratification after myocardial infarction: is left ventricular ejection fraction enough to prevent sudden cardiac death. *Eur Heart J*, **34**, 1964-1971.

Damas, J.K. et al. (2005) Expression of fractalkine (CX3CL1) and its receptor, CX3CR1, is elevated in coronary artery disease and is reduced during statin therapy. *Arterioscler Thromb Vasc Biol*, **25**, 2567-2572.

Dave, V.P. (2009) Hierarchical role of CD3 chains in thymocyte development. *Immunol Rev*, **232**, 22-33.

Day, Y.J. et al. (2006) Renal ischemia-reperfusion injury and adenosine 2A receptor-mediated tissue protection: the role of CD4+ T cells and IFN-gamma. *J Immunol*, **176**, 3108-3114.

de Haan, J.J. et al. (2013) Danger signals in the initiation of the inflammatory response after myocardial infarction. *Mediators Inflamm*, **2013**, 206039.

De Luca, G. et al. (2003) Symptom-onset-to-balloon time and mortality in patients with acute myocardial infarction treated by primary angioplasty. *J Am Coll Cardiol*, **42**, 991-997.

de Perrot, M. et al. (2003) Recipient T cells mediate reperfusion injury after lung transplantation in the rat. *J Immunol*, **171**, 4995-5002.

de Waha, S. et al. (2010) Impact of early vs. late microvascular obstruction assessed by magnetic resonance imaging on long-term outcome after ST-elevation myocardial

infarction: a comparison with traditional prognostic markers. *Eur Heart J*, **31**, 2660-2668.

de Waha, S. et al. (2014) Prognosis after ST-elevation myocardial infarction: a study on cardiac magnetic resonance imaging versus clinical routine. *Trials*, **15**, 249.

Dewald, O. et al. (2004) Of mice and dogs: species-specific differences in the inflammatory response following myocardial infarction. *Am J Pathol*, **164**, 665-677.

Dewald, O. et al. (2005) CCL2/Monocyte Chemoattractant Protein-1 regulates inflammatory responses critical to healing myocardial infarcts. *Circ Res*, **96**, 881-889.

DeWood, M.A. et al. (1980) Prevalence of total coronary occlusion during the early hours of transmural myocardial infarction. *N Engl J Med*, **303**, 897-902.

Di Lisa, F. & Bernardi, P. (2006) Mitochondria and ischemia-reperfusion injury of the heart: fixing a hole. *Cardiovasc Res*, **70**, 191-199.

Dirksen, M.T. et al. (2007) Reperfusion injury in humans: a review of clinical trials on reperfusion injury inhibitory strategies. *Cardiovasc Res*, **74**, 343-355.

Dobaczewski, M. et al. (2010) CCR5 signaling suppresses inflammation and reduces adverse remodeling of the infarcted heart, mediating recruitment of regulatory T cells. *Am J Pathol*, **176**, 2177-2187.

Doulatov, S. et al. (2012) Hematopoiesis: a human perspective. *Cell Stem Cell*, **10**, 120-136.

Dragu, R. et al. (2008) Predictive value of white blood cell subtypes for long-term outcome following myocardial infarction. *Atherosclerosis*, **196**, 405-412.

Duilio, C. et al. (2001) Neutrophils are primary source of O2 radicals during reperfusion after prolonged myocardial ischemia. *Am J Physiol Heart Circ Physiol*, **280**, H2649-57.

Durante, A. & Camici, P.G. (2015) Novel insights into an “old” phenomenon: the no reflow. *Int J Cardiol*, **187**, 273-280.

Eitel, I. et al. (2014) Comprehensive Prognosis Assessment by CMR Imaging After ST-Segment Elevation Myocardial Infarction. *J Am Coll Cardiol*, **64**, 1217-1226.

Falk, E. (2006) Pathogenesis of atherosclerosis. *J Am Coll Cardiol*, **47**, C7-12.

Falk, E. et al. (2013) Update on acute coronary syndromes: the pathologists’ view. *Eur Heart J*, **34**, 719-728.

Farber, D.L., Yudanin, N.A. & Restifo, N.P. (2014) Human memory T cells: generation, compartmentalization and homeostasis. *Nat Rev Immunol*, **14**, 24-35.

Faxon, D.P. et al. (2002) The effect of blockade of the CD11/CD18 integrin receptor on infarct size in patients with acute myocardial infarction treated with direct angioplasty: the results of the HALT-MI study. *J Am Coll Cardiol*, **40**, 1199-1204.

Ferreira, P.F. et al. (2013) Cardiovascular magnetic resonance artefacts. *J Cardiovasc Magn Reson*, **15**, 41.

Fiorina, P. et al. (2006) Role of CXC chemokine receptor 3 pathway in renal ischemic injury. *J Am Soc Nephrol*, **17**, 716-723.

Flaherty, J.T. et al. (1994) Recombinant human superoxide dismutase (h-SOD) fails to improve recovery of ventricular function in patients undergoing coronary angioplasty for acute myocardial infarction. *Circulation*, **89**, 1982-1991.
Florian, A. et al. (2011) Cardiac magnetic resonance imaging in ischemic heart disease: a clinical review. *J Med Life*, **4**, 330-345.

Fox, K.A. et al. (2006) Prediction of risk of death and myocardial infarction in the six months after presentation with acute coronary syndrome: prospective multinational observational study (GRACE). *BMJ*, **333**, 1091.

Francone, M. et al. (2011) Utility of T2-weighted short-tau inversion recovery (STIR) sequences in cardiac MRI: an overview of clinical applications in ischaemic and non-ischaemic heart disease. *Radiol Med*, **116**, 32-46.

Frangogiannis, N.G. (2007) Chemokines in ischemia and reperfusion. *Thromb Haemost*, **97**, 738-747.

Frangogiannis, N.G. (2012) Regulation of the inflammatory response in cardiac repair. *Circ Res*, **110**, 159-173.

Frangogiannis, N.G. (2014) The inflammatory response in myocardial injury, repair, and remodelling. *Nat Rev Cardiol*, **11**, 255-265.

Frangogiannis, N.G. & Entman, M.L. (2005) Chemokines in myocardial ischemia. *Trends Cardiovasc Med*, **15**, 163-169.

Frangogiannis, N.G. et al. (2001) Induction and suppression of interferon-inducible protein 10 in reperfused myocardial infarcts may regulate angiogenesis. *FASEB J*, **15**, 1428-1430.

Freixa, X. et al. (2012) Ischaemic postconditioning revisited: lack of effects on infarct size following primary percutaneous coronary intervention. *Eur Heart J*, **33**, 103-112.

Friedrich, M.G. et al. (2008) The salvaged area at risk in reperfused acute myocardial infarction as visualized by cardiovascular magnetic resonance. *J Am Coll Cardiol*, **51**, 1581-1587.

Furman, M.I. et al. (1996) Effect of elevated leukocyte count on in-hospital mortality following acute myocardial infarction. *Am J Cardiol*, **78**, 945-948.

Galkina, E. & Ley, K. (2009) Immune and inflammatory mechanisms of atherosclerosis. *Annu Rev Immunol*, **27**, 165-197.

Ganusov, V.V. & De Boer, R.J. (2007) Do most lymphocytes in humans really reside in the gut? *Trends Immunol*, **28**, 514-518.

García-Dorado, D. et al. (1993) Analysis of myocardial oedema by magnetic resonance imaging early after coronary artery occlusion with or without reperfusion. *Cardiovasc Res*, **27**, 1462-1469.

Garcia-Dorado, D. et al. (2014) Protection against myocardial ischemia-reperfusion injury in clinical practice. *Rev Esp Cardiol (Engl Ed)*, **67**, 394-404.

Geginat, J., Lanzavecchia, A. & Sallusto, F. (2003) Proliferation and differentiation potential of human CD8+ memory T-cell subsets in response to antigen or homeostatic cytokines. *Blood*, **101**, 4260-4266.

Ghaffari, S. et al. (2013) The effect of prethrombolytic cyclosporine-A injection on clinical outcome of acute anterior ST-elevation myocardial infarction. *Cardiovasc Ther*, **31**, e34-9.

Grailer, J.J., Kodera, M. & Steeber, D.A. (2009) L-selectin: role in regulating homeostasis and cutaneous inflammation. *J Dermatol Sci*, **56**, 141-147.

Granger, C.B. et al. (2003) Pexelizumab, an anti-C5 complement antibody, as adjunctive therapy to primary percutaneous coronary intervention in acute myocardial infarction: the COMplement inhibition in Myocardial infarction treated with Angioplasty (COMMA) trial. *Circulation*, **108**, 1184-1190.

Gray, D. (2006) Thrombolysis: past, present, and future. *Postgrad Med J*, **82**, 372-375.
Gredmark, S. et al. (2007) Active cytomegalovirus replication in patients with coronary disease. *Scand Cardiovasc J*, **41**, 230-234.

Griffiths, P., Baraniak, I. & Reeves, M. (2015) The pathogenesis of human cytomegalovirus. *J Pathol*, **235**, 288-297.

GISSI (Gruppo Italiano per lo Studio della Streptochinasi nell'Infarto Miocardico). (1986) Effectiveness of intravenous thrombolytic treatment in acute myocardial infarction. *Lancet*, **1**, 397-402.

Hahn, J.Y. et al. (2013) Ischemic postconditioning during primary percutaneous coronary intervention: the effects of postconditioning on myocardial reperfusion in patients with ST-segment elevation myocardial infarction (POST) randomized trial. *Circulation*, **128**, 1889-1896.

Hahn, J.Y. et al. (2015) Long-term effects of ischemic postconditioning on clinical outcomes: 1-year follow-up of the POST randomized trial. *Am Heart J*, **169**, 639-646.

Halestrap, A.P. (2009) What is the mitochondrial permeability transition pore? *J Mol Cell Cardiol*, **46**, 821-831.

Hamann, D. et al. (1997) Phenotypic and functional separation of memory and effector human CD8+ T cells. *J Exp Med*, **186**, 1407-1418.

Hamm, C.W. et al. (2011) ESC Guidelines for the management of acute coronary syndromes in patients presenting without persistent ST-segment elevation: The Task Force for the management of acute coronary syndromes (ACS) in patients presenting without persistent ST-segment elevation of the European Society of Cardiology (ESC). *Eur Heart J*, **32**, 2999-3054.

Han, Y.C. et al. (2013) Neutrophil to Lymphocyte Ratio Predicts Long-Term Clinical Outcomes in Patients with ST-Segment Elevation Myocardial Infarction Undergoing Primary Percutaneous Coronary Intervention. *Korean Circ J*, **43**, 93-99.

Hansson, G.K. (2005) Inflammation, atherosclerosis, and coronary artery disease. *N Engl J Med*, **352**, 1685-1695.

Hansson, G.K. & Libby, P. (2006) The immune response in atherosclerosis: a double-edged sword. *Nat Rev Immunol*, **6**, 508-519.

Harty, J.T., Tvinnereim, A.R. & White, D.W. (2000) CD8+ T cell effector mechanisms in resistance to infection. *Annu Rev Immunol*, **18**, 275-308.

Hausenloy, D.J., Ong, S.B. & Yellon, D.M. (2009) The mitochondrial permeability transition pore as a target for preconditioning and postconditioning. *Basic Res Cardiol*, **104**, 189-202.

Hausenloy, D.J., Tsang, A. & Yellon, D.M. (2005) The reperfusion injury salvage kinase pathway: a common target for both ischemic preconditioning and postconditioning. *Trends Cardiovasc Med*, **15**, 69-75.

Hausenloy, D.J. & Yellon, D.M. (2007) Reperfusion injury salvage kinase signalling: taking a RISK for cardioprotection. *Heart Fail Rev*, **12**, 217-234.

Hausenloy, D.J. & Yellon, D.M. (2013) Myocardial ischemia-reperfusion injury: a neglected therapeutic target. *J Clin Invest*, **123**, 92-100.

Hayward, R. et al. (1999) Recombinant soluble P-selectin glycoprotein ligand-1 protects against myocardial ischemic reperfusion injury in cats. *Cardiovasc Res*, **41**, 65-76.

He, J. et al. (2014) Neutrophil-to-lymphocyte ratio (NLR) predicts mortality and adverse-outcomes after ST-segment elevation myocardial infarction in Chinese people. *Int J Clin Exp Pathol*, **7**, 4045-4056.

Hellermann, J.P. et al. (2003) Incidence of heart failure after myocardial infarction: is it changing over time? *Am J Epidemiol*, **157**, 1101-1107.

Henson, S.M., Riddell, N.E. & Akbar, A.N. (2012) Properties of end-stage human T cells defined by CD45RA re-expression. *Curr Opin Immunol*, **24**, 476-481.

Heusch, G., Boengler, K. & Schulz, R. (2010) Inhibition of mitochondrial permeability transition pore opening: the Holy Grail of cardioprotection. *Basic Res Cardiol*, **105**, 151-154.

Hochegger, K. et al. (2007) Role of alpha/beta and gamma/delta T cells in renal ischemia-reperfusion injury. *Am J Physiol Renal Physiol*, **293**, F741-7.

Hoffmann, J. & Akira, S. (2013) Innate immunity. *Curr Opin Immunol*, **25**, 1-3.

Hoffmann, J. et al. (2012) High-throughput 13-parameter immunophenotyping identifies shifts in the circulating T-cell compartment following reperfusion in patients with acute myocardial infarction. *PLoS One*, **7**, e47155.

Hofmann, U. et al. (2012) Activation of CD4+ T lymphocytes improves wound healing and survival after experimental myocardial infarction in mice. *Circulation*, **125**, 1652-1663.

Hofmann, U. & Frantz, S. (2015) Role of lymphocytes in myocardial injury, healing, and remodeling after myocardial infarction. *Circ Res*, **116**, 354-367.

Hombach, V. et al. (2005) Sequelae of acute myocardial infarction regarding cardiac structure and function and their prognostic significance as assessed by magnetic resonance imaging. *Eur Heart J*, **26**, 549-557.

Homma, T. et al. (2013) Activation of invariant natural killer T cells by α-galactosylceramide ameliorates myocardial ischemia/reperfusion injury in mice. *J Mol Cell Cardiol*, **62**, 179-188.

Hong, Y.J. et al. (2007) Relationship between peripheral monocytosis and nonrecovery of left ventricular function in patients with left ventricular dysfunction complicated with acute myocardial infarction. *Circ J*, **71**, 1219-1224.

Huang, Y., Rabb, H. & Womer, K.L. (2007) Ischemia-reperfusion and immediate T cell responses. *Cell Immunol*, **248**, 4-11.

Hundley, W.G. et al. (2010) ACCF/ACR/AHA/NASCI/SCMR 2010 expert consensus document on cardiovascular magnetic resonance: a report of the American College of Cardiology Foundation Task Force on Expert Consensus Documents. *J Am Coll Cardiol*, **55**, 2614-2662.

Huppert, F.A. et al. (2003) Survival in a population sample is predicted by proportions of lymphocyte subsets. *Mech Ageing Dev*, **124**, 449-451.

Husser, O. et al. (2011) White blood cell subtypes after STEMI: temporal evolution, association with cardiovascular magnetic resonance--derived infarct size and impact on outcome. *Inflammation*, **34**, 73-84.

Imai, T. et al. (1997) Identification and molecular characterization of fractalkine receptor CX3CR1, which mediates both leukocyte migration and adhesion. *Cell*, **91**, 521-530.

Imanishi, T. et al. (2007) Cutting edge: TLR2 directly triggers Th1 effector functions. *J Immunol*, **178**, 6715-6719.

Ioannou, A., Dalle Lucca, J. & Tsokos, G.C. (2011) Immunopathogenesis of ischemia/reperfusion-associated tissue damage. *Clin Immunol*, **141**, 3-14.

ISIS-2 Collaborative Group. (1988) Randomised trial of intravenous streptokinase, oral aspirin, both, or neither among 17,187 cases of suspected acute myocardial infarction: ISIS-2. *Lancet*, **2**, 349-360.

Ito, H. (2009) No-reflow phenomenon in patients with acute myocardial infarction: its pathophysiology and clinical implications. *Acta Med Okayama*, **63**, 161-168.

Ito, H. et al. (1996) Clinical implications of the 'no reflow' phenomenon. A predictor of complications and left ventricular remodeling in reperfused anterior wall myocardial infarction. *Circulation*, **93**, 223-228.

Iwasaki, A. & Medzhitov, R. (2015) Control of adaptive immunity by the innate immune system. *Nat Immunol*, **16**, 343-353.

Iwakura, K. et al. (1996) Alternation in the coronary blood flow velocity pattern in patients with no reflow and reperfused acute myocardial infarction. *Circulation*, **94**, 1269-1275.

Jiang, S. & Dong, C. (2013) A complex issue on CD4(+) T-cell subsets. *Immunol Rev*, **252**, 5-11.

Jolly, S.R. et al. (1986) Reduction of myocardial infarct size by neutrophil depletion: effect of duration of occlusion. *Am Heart J*, **112**, 682-690.

Judd, R.M. et al. (1995) Physiological basis of myocardial contrast enhancement in fast magnetic resonance images of 2-day-old reperfused canine infarcts. *Circulation*, **92**, 1902-1910.

Jun, C. et al. (2014) Protective effect of CD4(+)CD25(high)CD127(low) regulatory T cells in renal ischemia-reperfusion injury. *Cell Immunol*, **289**, 106-111.

Jung, K. et al. (2013) Endoscopic time-lapse imaging of immune cells in infarcted mouse hearts. *Circ Res*, **112**, 891-899.

Jung, S. et al. (2000) Analysis of fractalkine receptor CX(3)CR1 function by targeted deletion and green fluorescent protein reporter gene insertion. *Mol Cell Biol*, **20**, 4106-4114.

Karahan, Z. et al. (2015) Effect of Hematologic Parameters on Microvascular Reperfusion in Patients With ST-Segment Elevation Myocardial Infarction Treated With Primary Percutaneous Coronary Intervention. *Angiology*,

Kaul, P. et al. (2013) Incidence of heart failure and mortality after acute coronary syndromes. *Am Heart J*, **165**, 379-85.e2.

Kaya, M.G. et al. (2013) Prognostic value of neutrophil/lymphocyte ratio in patients with ST-elevated myocardial infarction undergoing primary coronary intervention: a prospective, multicenter study. *Int J Cardiol*, **168**, 1154-1159.

Keeley, E.C., Boura, J.A. & Grines, C.L. (2003) Primary angioplasty versus intravenous thrombolytic therapy for acute myocardial infarction: a quantitative review of 23 randomised trials. *Lancet*, **361**, 13-20.

Khan, N. et al. (2002) Cytomegalovirus seropositivity drives the CD8 T cell repertoire toward greater clonality in healthy elderly individuals. *J Immunol*, **169**, 1984-1992.

Khandoga, A. et al. (2006) CD4+ T cells contribute to postischemic liver injury in mice by interacting with sinusoidal endothelium and platelets. *Hepatology*, **43**, 306-315.

Kim, E.K. et al. (2015a) Effect of ischemic postconditioning on myocardial salvage in patients undergoing primary percutaneous coronary intervention for ST-segment elevation myocardial infarction: cardiac magnetic resonance substudy of the POST randomized trial. *Int J Cardiovasc Imaging*, **31**, 629-637.

Kim, H.W. et al. (2015b) Relationship of T2-Weighted MRI Myocardial Hyperintensity and the Ischemic Area-At-Risk. *Circ Res*, **117**, 254-265.

Kinsey, G.R. et al. (2009) Regulatory T cells suppress innate immunity in kidney ischemia-reperfusion injury. *J Am Soc Nephrol*, **20**, 1744-1753.

Kirtane, A.J. et al. (2004) Association of peripheral neutrophilia with adverse angiographic outcomes in ST-elevation myocardial infarction. *Am J Cardiol*, **93**, 532-536.

Klein, L. et al. (2009) Antigen presentation in the thymus for positive selection and central tolerance induction. *Nat Rev Immunol*, **9**, 833-844.

Kloner, R.A. et al. (1998) Medical and cellular implications of stunning, hibernation, and preconditioning: an NHLBI workshop. *Circulation*, **97**, 1848-1867.

Kloner, R.A. et al. (2006) Impact of time to therapy and reperfusion modality on the efficacy of adenosine in acute myocardial infarction: the AMISTAD-2 trial. *Eur Heart J*, **27**, 2400-2405.

Kloner, R.A., Ganote, C.E. & Jennings, R.B. (1974) The “no-reflow” phenomenon after temporary coronary occlusion in the dog. *J Clin Invest*, **54**, 1496-1508.

Klug, G. et al. (2012) Prognostic value at 5 years of microvascular obstruction after acute myocardial infarction assessed by cardiovascular magnetic resonance. *J Cardiovasc Magn Reson*, **14**, 46.

Koch, S. et al. (2008) Multiparameter flow cytometric analysis of CD4 and CD8 T cell subsets in young and old people. *Immun Ageing*, **5**, 6.

Koch, U. & Radtke, F. (2011) Mechanisms of T cell development and transformation. *Annu Rev Cell Dev Biol*, **27**, 539-562.

Krug, A., Du, M.D.R. & Korb, G. (1966) Blood supply of the myocardium after temporary coronary occlusion. *Circ Res*, **19**, 57-62.

Kuboki, S. et al. (2009) Distinct contributions of CD4+ T cell subsets in hepatic ischemia/reperfusion injury. *Am J Physiol Gastrointest Liver Physiol*, **296**, G1054-9.

Kuhns, M.S. & Badgandi, H.B. (2012) Piecing together the family portrait of TCR-CD3 complexes. *Immunol Rev*, **250**, 120-143.

Kuijpers, T.W. et al. (2003) Frequencies of circulating cytolytic, CD45RA+CD27-, CD8+ T lymphocytes depend on infection with CMV. *J Immunol*, **170**, 4342-4348.

Kukielka, G.L. et al. (1995) Interleukin-8 gene induction in the myocardium after ischemia and reperfusion in vivo. *J Clin Invest*, **95**, 89-103.

Kumar, A.G. et al. (1997) Induction of monocyte chemoattractant protein-1 in the small veins of the ischemic and reperfused canine myocardium. *Circulation*, **95**, 693-700.

Kurtul, A. et al. (2014) Usefulness of the platelet-to-lymphocyte ratio in predicting angiographic reflow after primary percutaneous coronary intervention in patients with acute ST-segment elevation myocardial infarction. *Am J Cardiol*, **114**, 342-347.

Lakshminarayanan, V. et al. (2001) Reactive oxygen intermediates induce monocyte chemotactic protein-1 in vascular endothelium after brief ischemia. *Am J Pathol*, **159**, 1301-1311.

Lappas, C.M. et al. (2006) Adenosine A2A receptor activation reduces hepatic ischemia reperfusion injury by inhibiting CD1d-dependent NKT cell activation. *J Exp Med*, **203**, 2639-2648.

Le, Y. et al. (2004) Chemokines and chemokine receptors: their manifold roles in homeostasis and disease. *Cell Mol Immunol*, **1**, 95-104.

Lee, W.W. et al. (2012) PET/MRI of inflammation in myocardial infarction. *J Am Coll Cardiol*, **59**, 153-163.

Ley, K. (1996) Molecular mechanisms of leukocyte recruitment in the inflammatory process. *Cardiovasc Res*, **32**, 733-742.

Liao, Y.H. et al. (2012) Interleukin-17A contributes to myocardial ischemia/reperfusion injury by regulating cardiomyocyte apoptosis and neutrophil infiltration. *J Am Coll Cardiol*, **59**, 420-429.

Liehn, E.A. et al. (2008) Ccr1 deficiency reduces inflammatory remodelling and preserves left ventricular function after myocardial infarction. *J Cell Mol Med*, **12**, 496-506.

Liehn, E.A. et al. (2010) A new monocyte chemotactic protein-1/chemokine CC motif ligand-2 competitor limiting neointima formation and myocardial ischemia/reperfusion injury in mice. *J Am Coll Cardiol*, **56**, 1847-1857.

Liehn, E.A. et al. (2011a) Repair after myocardial infarction, between fantasy and reality: the role of chemokines. *J Am Coll Cardiol*, **58**, 2357-2362.

Liehn, E.A. et al. (2011b) Double-edged role of the CXCL12/CXCR4 axis in experimental myocardial infarction. *J Am Coll Cardiol*, **58**, 2415-2423.

Limalanathan, S. et al. (2014) Effect of ischemic postconditioning on infarct size in patients with ST-elevation myocardial infarction treated by primary PCI results of the POSTEMI (POstconditioning in ST-Elevation Myocardial Infarction) randomized trial. *J Am Heart Assoc*, **3**, e000679.

Limalanathan, S. et al. (2013) Myocardial salvage is reduced in primary PCI-treated STEMI patients with microvascular obstruction, demonstrated by early and late CMR. *PLoS One*, **8**, e71780.

Limbruno, U. et al. (2005) Distal embolization during primary angioplasty: histopathologic features and predictability. *Am Heart J*, **150**, 102-108.

Linfert, D., Chowdhry, T. & Rabb, H. (2009) Lymphocytes and ischemia-reperfusion injury. *Transplant Rev*, **23**, 1-10.

Lonborg, J. et al. (2010) Cardioprotective effects of ischemic postconditioning in patients treated with primary percutaneous coronary intervention, evaluated by magnetic resonance. *Circ Cardiovasc Interv*, **3**, 34-41.

Lonborg, J. et al. (2012) Exenatide reduces reperfusion injury in patients with ST-segment elevation myocardial infarction. *Eur Heart J*, **33**, 1491-1499.

Loukas, M. et al. (2009) Cardiac veins: a review of the literature. *Clin Anat*, **22**, 129-145.

Lusis, A.J. (2000) Atherosclerosis. *Nature*, **407**, 233-241.

Ma, X.L., Tsao, P.S. & Lefer, A.M. (1991) Antibody to CD-18 exerts endothelial and cardiac protective effects in myocardial ischemia and reperfusion. *J Clin Invest*, **88**, 1237-1243.

Male D, Brostoff J, Roth DB, Roitt IM. (2006) *Immunology. 7th Edition*. London Mosby/Elselvier.

Manning, A.S. & Hearse, D.J. (1984) Reperfusion-induced arrhythmias: mechanisms and prevention. *J Mol Cell Cardiol*, **16**, 497-518.

Marchant, D.J. et al. (2012) Inflammation in myocardial diseases. *Circ Res*, **110**, 126-144.

Marchese, A. (2014) Endocytic trafficking of chemokine receptors. *Curr Opin Cell Biol*, **27**, 72-77.

Mariani, M. et al. (2006) Significance of total and differential leucocyte count in patients with acute myocardial infarction treated with primary coronary angioplasty. *Eur Heart J*, **27**, 2511-2515.

Masopust, D. & Schenkel, J.M. (2013) The integration of T cell migration, differentiation and function. *Nat Rev Immunol*, **13**, 309-320.

Mather, A.N. et al. (2011) Timing of cardiovascular MR imaging after acute myocardial infarction: effect on estimates of infarct characteristics and prediction of late ventricular remodeling. *Radiology*, **261**, 116-126.

Matsumoto, K. et al. (2011) Regulatory T lymphocytes attenuate myocardial infarction-induced ventricular remodeling in mice. *Int Heart J*, **52**, 382-387.

Matusik, P. et al. (2012) Do we know enough about the immune pathogenesis of acute coronary syndromes to improve clinical practice? *Thromb Haemost*, **108**, 443-456.

Mehta, S.R. et al. (2005) Effect of glucose-insulin-potassium infusion on mortality in patients with acute ST-segment elevation myocardial infarction: the CREATE-ECLA randomized controlled trial. *JAMA*, **293**, 437-446.

Melnick, J.L. et al. (1983) Cytomegalovirus antigen within human arterial smooth muscle cells. *Lancet*, **2**, 644-647.

Mewton, N. et al. (2010) Effect of cyclosporine on left ventricular remodeling after reperfused myocardial infarction. *J Am Coll Cardiol*, **55**, 1200-1205.

Monassier, J.P. (2008) Reperfusion injury in acute myocardial infarction. From bench to cath lab. Part I: Basic considerations. *Arch Cardiovasc Dis*, **101**, 491-500.

Monsinjon, T., Richard, V. & Fontaine, M. (2001) Complement and its implications in cardiac ischemia/reperfusion: strategies to inhibit complement. *Fundam Clin Pharmacol*, **15**, 293-306.

Morel, O. et al. (2012) Pharmacological approaches to reperfusion therapy. *Cardiovasc Res*, **94**, 246-252.

Morimoto, H. et al. (2008) MCP-1 induces cardioprotection against ischaemia/reperfusion injury: role of reactive oxygen species. *Cardiovasc Res*, **78**, 554-562.

Morimoto, H. & Takahashi, M. (2007) Role of monocyte chemoattractant protein-1 in myocardial infarction. *Int J Biomed Sci*, **3**, 159-167.

Moschovakis, G.L. & Forster, R. (2012) Multifaceted activities of CCR7 regulate T-cell homeostasis in health and disease. *Eur J Immunol*, **42**, 1949-1955.

Mosmann, T.R., Li, L. & Sad, S. (1997) Functions of CD8 T-cell subsets secreting different cytokine patterns. *Semin Immunol*, **9**, 87-92.

Moss, P. (2010) The emerging role of cytomegalovirus in driving immune senescence: a novel therapeutic opportunity for improving health in the elderly. *Curr Opin Immunol*, **22**, 529-534.

Mosterd, A. & Hoes, A.W. (2007) Clinical epidemiology of heart failure. *Heart*, **93**, 1137-1146.

Murphy, P.M. et al. (2000) International union of pharmacology. XXII. Nomenclature for chemokine receptors. *Pharmacol Rev*, **52**, 145-176.

Murry, C.E., Jennings, R.B. & Reimer, K.A. (1986) Preconditioning with ischemia: a delay of lethal cell injury in ischemic myocardium. *Circulation*, **74**, 1124-1136.

Nahrendorf, M., Pittet, M.J. & Swirski, F.K. (2010) Monocytes: protagonists of infarct inflammation and repair after myocardial infarction. *Circulation*, **121**, 2437-2445.

Nahrendorf, M. & Swirski, F.K. (2013) Monocyte and macrophage heterogeneity in the heart. *Circ Res*, **112**, 1624-1633.

Nahrendorf, M. et al. (2007) The healing myocardium sequentially mobilizes two monocyte subsets with divergent and complementary functions. *J Exp Med*, **204**, 3037-3047.

Nallamothu, B. et al. (2007) Relationship of treatment delays and mortality in patients undergoing fibrinolysis and primary percutaneous coronary intervention. The Global Registry of Acute Coronary Events. *Heart*, **93**, 1552-1555.

Nallamothu, B.K. et al. (2015) Relation between door-to-balloon times and mortality after primary percutaneous coronary intervention over time: a retrospective study. *Lancet*, **385**, 1114-1122.

Nanki, T. et al. (2002) Migration of CX3CR1-positive T cells producing type 1 cytokines and cytotoxic molecules into the synovium of patients with rheumatoid arthritis. *Arthritis Rheum*, **46**, 2878-2883.

Nazir, S.A. et al. (2014) The REFLO-STEMI trial comparing intracoronary adenosine, sodium nitroprusside and standard therapy for the attenuation of infarct size and microvascular obstruction during primary percutaneous coronary intervention: study protocol for a randomised controlled trial. *Trials*, **15**, 371.

Ndrepepa, G. et al. (2010) Predictive factors and impact of no reflow after primary percutaneous coronary intervention in patients with acute myocardial infarction. *Circ Cardiovasc Interv*, **3**, 27-33.

Neel, N.F. et al. (2005) Chemokine receptor internalization and intracellular trafficking. *Cytokine Growth Factor Rev*, **16**, 637-658.

Newby, K.H. et al. (1998) Sustained ventricular arrhythmias in patients receiving thrombolytic therapy: incidence and outcomes. *Circulation*, **98**, 2567-2573.

Niccoli, G. et al. (2013) Open-label, randomized, placebo-controlled evaluation of intracoronary adenosine or nitroprusside after thrombus aspiration during primary percutaneous coronary intervention for the prevention of microvascular obstruction in acute myocardial infarction: the REOPEN-AMI study (Intracoronary Nitroprusside Versus Adenosine in Acute Myocardial Infarction). *JACC Cardiovasc Interv*, **6**, 580-589.

Nichols, M. et al. (2012) *European Cardiovascular Disease Statistics 2012*. European Society of Cardiology, Brussels.

Nikolich-Zugich, J. (2008) Ageing and life-long maintenance of T-cell subsets in the face of latent persistent infections. *Nat Rev Immunol*, **8**, 512-522.

Njerve, I.U. et al. (2014) Fractalkine levels are elevated early after PCI-treated ST-elevation myocardial infarction; no influence of autologous bone marrow derived stem cell injection. *Cytokine*, **69**, 131-135.

Nossuli, T.O. et al. (2001) Brief murine myocardial I/R induces chemokines in a TNF-alpha-independent manner: role of oxygen radicals. *Am J Physiol Heart Circ Physiol*, **281**, H2549-58.

Núñez, J. et al. (2012) Low rate of detection of active cytomegalovirus (CMV) infection early following acute myocardial infarction. *Atherosclerosis*, **222**, 295-297.

Nunez, J. et al. (2010) Low lymphocyte count in acute phase of ST-segment elevation myocardial infarction predicts long-term recurrent myocardial infarction. *Coron Artery Dis*, **21**, 1-7.

Núñez, J. et al. (2008) Usefulness of the neutrophil to lymphocyte ratio in predicting long-term mortality in ST segment elevation myocardial infarction. *Am J Cardiol*, **101**, 747-752.

Núñez, J. et al. (2009a) Therapeutic implications of low lymphocyte count in non-ST segment elevation acute coronary syndromes. *Eur J Intern Med*, **20**, 768-774.

Núñez, J. et al. (2009b) Relationship between low lymphocyte count and major cardiac events in patients with acute chest pain, a non-diagnostic electrocardiogram and normal troponin levels. *Atherosclerosis*, **206**, 251-257.

Nutt, S.L. et al. (2015) The generation of antibody-secreting plasma cells. *Nat Rev Immunol*, **15**, 160-171.

O h-Ici, D. et al. (2012) Cardiovascular magnetic resonance of myocardial edema using a short inversion time inversion recovery (STIR) black-blood technique: diagnostic accuracy of visual and semi-quantitative assessment. *J Cardiovasc Magn Reson*, **14**, 22.

Okada, R. et al. (2008) Phenotypic classification of human CD4+ T cell subsets and their differentiation. *Int Immunol*, **20**, 1189-1199.

Olson, N.C. et al. (2013) Decreased naive and increased memory CD4(+) T cells are associated with subclinical atherosclerosis: the multi-ethnic study of atherosclerosis. *PLoS One*, **8**, e71498.

Owen, J., Punt, J. & Stranford, S. (2013) *Kuby Immunology: 7th Edition*. New York, W. H. Freeman.

Passegue, E. et al. (2003) Normal and leukemic hematopoiesis: are leukemias a stem cell disorder or a reacquisition of stem cell characteristics? *Proc Natl Acad Sci U S A*, **100 Suppl 1**, 11842-11849.

Payne, A.R. et al. (2011) Bright-blood T2-weighted MRI has higher diagnostic accuracy than dark-blood short tau inversion recovery MRI for detection of acute myocardial infarction and for assessment of the ischemic area at risk and myocardial salvage. *Circ Cardiovasc Imaging*, **4**, 210-219.

Pedersen, F. et al. (2014) Short- and long-term cause of death in patients treated with primary PCI for STEMI. *J Am Coll Cardiol*, **64**, 2101-2108.

Pellizzon, G.G. et al. (2003) Relation of admission white blood cell count to long-term outcomes after primary coronary angioplasty for acute myocardial infarction (The Stent PAMI Trial). *Am J Cardiol*, **91**, 729-731.

Pennell, D.J. et al. (2004) Clinical indications for cardiovascular magnetic resonance (CMR): Consensus Panel report. *Eur Heart J*, **25**, 1940-1965.

Pepper, M. & Jenkins, M.K. (2011) Origins of CD4(+) effector and central memory T cells. *Nat Immunol*, **12**, 467-471.

Perazzolo Marra, M., Lima, J.A. & Iliceto, S. (2011) MRI in acute myocardial infarction. *Eur Heart J*, **32**, 284-293.

Pieper, K., Grimbacher, B. & Eibel, H. (2013) B-cell biology and development. *J Allergy Clin Immunol*, **131**, 959-971.

Piot, C. et al. (2008) Effect of cyclosporine on reperfusion injury in acute myocardial infarction. *N Engl J Med*, **359**, 473-481.

Piper, H.M. & Garcia-Dorado, D. (2012) Reducing the impact of myocardial ischaemia/reperfusion injury. *Cardiovasc Res*, **94**, 165-167.

Pizzetti, G. et al. (2001) Beneficial effects of diltiazem during myocardial reperfusion: a randomized trial in acute myocardial infarction. *Ital Heart J*, **2**, 757-765.

Popović, M. et al. (2012) Human cytomegalovirus infection and atherothrombosis. *J Thromb Thrombolysis*, **33**, 160-172.

Pourgheysari, B. et al. (2007) The cytomegalovirus-specific CD4+ T-cell response expands with age and markedly alters the CD4+ T-cell repertoire. *J Virol*, **81**, 7759-7765.

Prinz, I., Silva-Santos, B. & Pennington, D.J. (2013) Functional development of γδ T cells. *Eur J Immunol*, **43**, 1988-1994.

Prösch, S. et al. (2000) A novel link between stress and human cytomegalovirus (HCMV) infection: sympathetic hyperactivity stimulates HCMV activation. *Virology*, **272**, 357-365.

Rabb, H. et al. (2000) Pathophysiological role of T lymphocytes in renal ischemia-reperfusion injury in mice. *Am J Physiol Renal Physiol*, **279**, F525-31.

Raedschelders, K., Ansley, D.M. & Chen, D.D. (2012) The cellular and molecular origin of reactive oxygen species generation during myocardial ischemia and reperfusion. *Pharmacol Ther*, **133**, 230-255.

Rao, J., Lu, L. & Zhai, Y. (2014) T cells in organ ischemia reperfusion injury. *Curr Opin Organ Transplant*, **19**, 115-120.

Reffelmann, T. & Kloner, R.A. (2002) Microvascular reperfusion injury: rapid expansion of anatomic no reflow during reperfusion in the rabbit. *Am J Physiol Heart Circ Physiol*, **283**, H1099-107.

Reffelmann, T. & Kloner, R.A. (2006) The no-reflow phenomenon: A basic mechanism of myocardial ischemia and reperfusion. *Basic Res Cardiol*, **101**, 359-372.

Reimer, K.A. & Jennings, R.B. (1979) The "wavefront phenomenon" of myocardial ischemic cell death. II. Transmural progression of necrosis within the framework of ischemic bed size (myocardium at risk) and collateral flow. *Lab Invest*, **40**, 633-644.

Reynolds, H.R. & Hochman, J.S. (2008) Cardiogenic shock: current concepts and improving outcomes. *Circulation*, **117**, 686-697.

Ridgway, J.P. (2010) Cardiovascular magnetic resonance physics for clinicians: part I. *J Cardiovasc Magn Reson*, **12**, 71.

Rochitte, C.E. et al. (1998) Magnitude and time course of microvascular obstruction and tissue injury after acute myocardial infarction. *Circulation*, **98**, 1006-1014.

Roberts, D.L., Nakazawa, H.K. & Klocke, F.J. (1976) Origin of great cardiac vein and coronary sinus drainage within the left ventricle. *Am J Physiol*, **230**, 486-492.

Rodgers, C.T. & Robson, M.D. (2011) Cardiovascular magnetic resonance: physics and terminology. *Prog Cardiovasc Dis*, **54**, 181-190.

Ross, A.M. et al. (2005) A randomized, double-blinded, placebo-controlled multicenter trial of adenosine as an adjunct to reperfusion in the treatment of acute myocardial infarction (AMISTAD-II). *J Am Coll Cardiol*, **45**, 1775-1780.

Ruparelia, N. et al. (2013) Myocardial infarction causes inflammation and leukocyte recruitment at remote sites in the myocardium and in the renal glomerulus. *Inflamm Res*, **62**, 515-525.

Saeed, M., Hetts, S. & Wilson, M. (2010) Reperfusion injury components and manifestations determined by cardiovascular MR and MDCT imaging. *World J Radiol*, **2**, 1-14.

Sakakura, K. et al. (2013) Pathophysiology of atherosclerosis plaque progression. *Heart Lung Circ*, **22**, 399-411.

Sallusto, F., Geginat, J. & Lanzavecchia, A. (2004) Central memory and effector memory T cell subsets: function, generation, and maintenance. *Annu Rev Immunol*, **22**, 745-763.

Sallusto, F. et al. (1999) Two subsets of memory T lymphocytes with distinct homing potentials and effector functions. *Nature*, **401**, 708-712.

Sanada, S., Komuro, I. & Kitakaze, M. (2011) Pathophysiology of myocardial reperfusion injury: preconditioning, postconditioning, and translational aspects of protective measures. *Am J Physiol Heart Circ Physiol*, **301**, H1723-41.

Sathaliyawala, T. et al. (2013) Distribution and compartmentalization of human circulating and tissue-resident memory T cell subsets. *Immunity*, **38**, 187-197.

Savransky, V. et al. (2006) Role of the T-cell receptor in kidney ischemia-reperfusion injury. *Kidney Int*, **69**, 233-238.

Savva, G.M. et al. (2013) Cytomegalovirus infection is associated with increased mortality in the older population. *Aging Cell*, **12**, 381-387.

Saxena, A. et al. (2014a) CXCR3-independent actions of the CXC chemokine CXCL10 in the infarcted myocardium and in isolated cardiac fibroblasts are mediated through proteoglycans. *Cardiovasc Res*, **103**, 217-227.

Saxena, A. et al. (2014b) Regulatory T cells are recruited in the infarcted mouse myocardium and may modulate fibroblast phenotype and function. *Am J Physiol Heart Circ Physiol*, **307**, H1233-42.

Schafer, C. et al. (2001) Role of the reverse mode of the Na+/Ca2+ exchanger in reoxygenation-induced cardiomyocyte injury. *Cardiovasc Res*, **51**, 241-250.

Schenk, S. et al. (2007) Monocyte chemotactic protein-3 is a myocardial mesenchymal stem cell homing factor. *Stem Cells*, **25**, 245-251.

Schmidt-Lucke, C. et al. (2007) Specific recruitment of CD4+CD25++ regulatory T cells into the allograft in heart transplant recipients. *Am J Physiol Heart Circ Physiol*, **292**, H2425-31.

Schmitt, J. et al. (2009) Atrial fibrillation in acute myocardial infarction: a systematic review of the incidence, clinical features and prognostic implications. *Eur Heart J*, **30**, 1038-1045.

Schwartz, B.G. & Kloner, R.A. (2012) Coronary no reflow. *J Mol Cell Cardiol*, **52**, 873-882.

Sharma, V., Bell, R.M. & Yellon, D.M. (2012) Targeting reperfusion injury in acute myocardial infarction: a review of reperfusion injury pharmacotherapy. *Expert Opin Pharmacother*, **13**, 1153-1175.

Sheiban, I. et al. (1997) Recovery of left ventricular function following early reperfusion in acute myocardial infarction: a potential role for the calcium antagonist nisoldipine. *Cardiovasc Drugs Ther*, **11**, 5-16.

Shen, X. et al. (2009) CD4 T cells promote tissue inflammation via CD40 signaling without de novo activation in a murine model of liver ischemia/reperfusion injury. *Hepatology*, **50**, 1537-1546.

Shen, X.H. et al. (2010) Association of neutrophil/lymphocyte ratio with long-term mortality after ST elevation myocardial infarction treated with primary percutaneous coronary intervention. *Chin Med J (Engl)*, **123**, 3438-3443.

Shimamura, K. et al. (2005) Association of NKT cells and granulocytes with liver injury after reperfusion of the portal vein. *Cell Immunol*, **234**, 31-38.

Shinde, A.V. & Frangogiannis, N.G. (2014) Fibroblasts in myocardial infarction: a role in inflammation and repair. *J Mol Cell Cardiol*, **70**, 74-82.

Smieja, M. et al. (2003) Multiple infections and subsequent cardiovascular events in the Heart Outcomes Prevention Evaluation (HOPE) Study. *Circulation*, **107**, 251-257.

Smith-Garvin, J.E., Koretzky, G.A. & Jordan, M.S. (2009) T cell activation. *Annu Rev Immunol*, **27**, 591-619.

Sobirin, M.A. et al. (2012) Activation of natural killer T cells ameliorates postinfarct cardiac remodeling and failure in mice. *Circ Res*, **111**, 1037-1047.

Söderberg-Nauclér, C. (2006) Does cytomegalovirus play a causative role in the development of various inflammatory diseases and cancer. *J Intern Med*, **259**, 219-246.

Solana, R. et al. (2012) CMV and Immunosenescence: from basics to clinics. *Immun Ageing*, **9**, 23.

Spencer, J.H., Anderson, S.E. & Iaizzo, P.A. (2013) Human coronary venous anatomy: implications for interventions. *J Cardiovasc Transl Res*, **6**, 208-217.

Spits, H. (2002) Development of alphabeta T cells in the human thymus. *Nat Rev Immunol*, **2**, 760-772.

Spyridopoulos, I. et al. (2009) Accelerated telomere shortening in leukocyte subpopulations of patients with coronary heart disease: role of cytomegalovirus seropositivity. *Circulation*, **120**, 1364-1372.

Staat, P. et al. (2005) Postconditioning the human heart. *Circulation*, **112**, 2143-2148.

Stassen, F.R., Vainas, T. & Bruggeman, C.A. (2008) Infection and atherosclerosis. An alternative view on an outdated hypothesis. *Pharmacol Rep*, **60**, 85-92.

Staumont-Sallé, D. et al. (2014) CX_3CL1 (fractalkine) and its receptor CX_3CR1 regulate atopic dermatitis by controlling effector T cell retention in inflamed skin. *J Exp Med*, **211**, 1185-1196.

Steg, P.G. et al. (2012) ESC Guidelines for the management of acute myocardial infarction in patients presenting with ST-segment elevation. *Eur Heart J*, **33**, 2569-2619.

Stemme, S., Holm, J. & Hansson, G.K. (1992) T lymphocytes in human atherosclerotic plaques are memory cells expressing CD45RO and the integrin VLA-1. *Arterioscler Thromb*, **12**, 206-211.

Strindhall, J. et al. (2007) No Immune Risk Profile among individuals who reach 100 years of age: findings from the Swedish NONA immune longitudinal study. *Exp Gerontol*, **42**, 753-761.

Strindhall, J. et al. (2013) The inverted CD4/CD8 ratio and associated parameters in 66-year-old individuals: the Swedish HEXA immune study. *Age (Dordr)*, **35**, 985-991.

Sun, Y. (2009) Myocardial repair/remodelling following infarction: roles of local factors. *Cardiovasc Res*, **81**, 482-490.

Swirski, F.K. & Nahrendorf, M. (2013) Leukocyte behavior in atherosclerosis, myocardial infarction, and heart failure. *Science*, **339**, 161-166.

Syrjälä, H., Surcel, H.M. & Ilonen, J. (1991) Low CD4/CD8 T lymphocyte ratio in acute myocardial infarction. *Clin Exp Immunol*, **83**, 326-328.

Takata, H. & Takiguchi, M. (2006) Three memory subsets of human CD8+ T cells differently expressing three cytolytic effector molecules. *J Immunol*, **177**, 4330-4340.

Tang, T.T. et al. (2012) Regulatory T cells ameliorate cardiac remodeling after myocardial infarction. *Basic Res Cardiol*, **107**, 232.

Tarantini, G. et al. (2012) Postconditioning during coronary angioplasty in acute myocardial infarction: the POST-AMI trial. *Int J Cardiol*, **162**, 33-38.

Tarzami, S.T. et al. (2002) Chemokine expression in myocardial ischemia: MIP-2 dependent MCP-1 expression protects cardiomyocytes from cell death. *J Mol Cell Cardiol*, **34**, 209-221.

EMIP-FR Group. (2000) Effect of 48-h intravenous trimetazidine on short- and long-term outcomes of patients with acute myocardial infarction, with and without thrombolytic therapy; A double-blind, placebo-controlled, randomized trial. The EMIP-FR Group. European Myocardial Infarction Project--Free Radicals. *Eur Heart J*, **21**, 1537-1546.

Theroux, P. et al. (1998) Intravenous diltiazem in acute myocardial infarction. Diltiazem as adjunctive therapy to activase (DATA) trial. *J Am Coll Cardiol*, **32**, 620-628.

Thome, J.J. et al. (2014) Spatial map of human T cell compartmentalization and maintenance over decades of life. *Cell*, **159**, 814-828.

Thuny, F. et al. (2012) Post-conditioning reduces infarct size and edema in patients with ST-segment elevation myocardial infarction. *J Am Coll Cardiol*, **59**, 2175-2181.

Thygesen, K. et al. (2012) Third universal definition of myocardial infarction. *Eur Heart J*, **33**, 2551-2567.

Tracy, R.P. et al. (2013) T-helper type 1 bias in healthy people is associated with cytomegalovirus serology and atherosclerosis: the Multi-Ethnic Study of Atherosclerosis. *J Am Heart Assoc*, **2**, e000117.

Trepel, F. (1974) Number and distribution of lymphocytes in man. A critical analysis. *Klin Wochenschr*, **52**, 511-515.

Tsujioka, H. et al. (2009) Impact of heterogeneity of human peripheral blood monocyte subsets on myocardial salvage in patients with primary acute myocardial infarction. *J Am Coll Cardiol*, **54**, 130-138.

Tsujioka, H. et al. (2010) Post-reperfusion enhancement of CD14(+)CD16(-) monocytes and microvascular obstruction in ST-segment elevation acute myocardial infarction. *Circ J*, **74**, 1175-1182.

Turkmen, S. et al. (2013) The relationship between neutrophil/lymphocyte ratio and the TIMI flow grade in patients with STEMI undergoing primary PCI. *Eur Rev Med Pharmacol Sci*, **17**, 2185-2189.

Umehara, H. et al. (2004) Fractalkine in vascular biology: from basic research to clinical disease. *Arterioscler Thromb Vasc Biol*, **24**, 34-40.

Unutmaz, D., Pileri, P. & Abrignani, S. (1994) Antigen-independent activation of naive and memory resting T cells by a cytokine combination. *J Exp Med*, **180**, 1159-1164.

van de Berg, P.J. et al. (2008) A fingerprint left by cytomegalovirus infection in the human T cell compartment. *J Clin Virol*, **41**, 213-217.

van de Berg, P.J. et al. (2012) Cytomegalovirus-induced effector T cells cause endothelial cell damage. *Clin Vaccine Immunol*, **19**, 772-779.

van den Borne, P. et al. (2014) The multifaceted functions of CXCL10 in cardiovascular disease. *Biomed Res Int*, **2014**, 893106.

van der Laan, A.M. et al. (2012a) A proinflammatory monocyte response is associated with myocardial injury and impaired functional outcome in patients with ST-segment elevation myocardial infarction: monocytes and myocardial infarction. *Am Heart J*, **163**, 57-65.e2.

van der Laan, A.M., Nahrendorf, M. & Piek, J.J. (2012b) Healing and adverse remodelling after acute myocardial infarction: role of the cellular immune response. *Heart*, **98**, 1384-1390.

van der Laan, A.M. et al. (2014) Monocyte subset accumulation in the human heart following acute myocardial infarction and the role of the spleen as monocyte reservoir. *Eur Heart J*, **35**, 376-385.

van Kranenburg, M. et al. (2014) Prognostic value of microvascular obstruction and infarct size, as measured by CMR in STEMI patients. *JACC Cardiovasc Imaging*, **7**, 930-939.

Vermes, E. et al. (2013) Auto-threshold quantification of late gadolinium enhancement in patients with acute heart disease. *J Magn Reson Imaging*, **37**, 382-390.

Vinten-Johansen, J. (2004) Involvement of neutrophils in the pathogenesis of lethal myocardial reperfusion injury. *Cardiovasc Res*, **61**, 481-497.

Virmani, R. et al. (2006) Pathology of the vulnerable plaque. *J Am Coll Cardiol*, **47**, C13-8.

Vivier, E. et al. (2008) Functions of natural killer cells. *Nat Immunol*, **9**, 503-510.
Weber, C. & Noels, H. (2011) Atherosclerosis: current pathogenesis and therapeutic options. *Nat Med*, **17**, 1410-1422.

Weirather, J. et al. (2014) Foxp3+ CD4+ T cells improve healing after myocardial infarction by modulating monocyte/macrophage differentiation. *Circ Res*, **115**, 55-67.

Widimsky, P. et al. (2010) Reperfusion therapy for ST elevation acute myocardial infarction in Europe: description of the current situation in 30 countries. *Eur Heart J*, **31**, 943-957.

Wikby, A. et al. (2002) Expansions of peripheral blood CD8 T-lymphocyte subpopulations and an association with cytomegalovirus seropositivity in the elderly: the Swedish NONA immune study. *Exp Gerontol*, **37**, 445-453.

Wikby, A. et al. (2008) The immune risk profile is associated with age and gender: findings from three Swedish population studies of individuals 20-100 years of age. *Biogerontology*, **9**, 299-308.

Wikby, A. et al. (1998) Changes in CD8 and CD4 lymphocyte subsets, T cell proliferation responses and non-survival in the very old: the Swedish longitudinal OCTO-immune study. *Mech Ageing Dev*, **102**, 187-198.

Wong, P. & Pamer, E.G. (2003) CD8 T cell responses to infectious pathogens. *Annu Rev Immunol*, **21**, 29-70.

Wu, K.C. (2009) Fighting the "fire" of myocardial reperfusion injury: how to define success? *J Am Coll Cardiol*, **53**, 730-731.

Wu, K.C. (2012) CMR of microvascular obstruction and hemorrhage in myocardial infarction. *J Cardiovasc Magn Reson*, **14**, 68.

Wu, K.C. et al. (1998a) Quantification and time course of microvascular obstruction by contrast-enhanced echocardiography and magnetic resonance imaging following acute myocardial infarction and reperfusion. *J Am Coll Cardiol*, **32**, 1756-1764.

Wu, K.C. et al. (1998b) Prognostic significance of microvascular obstruction by magnetic resonance imaging in patients with acute myocardial infarction. *Circulation*, **97**, 765-772.

Xia, N. et al. (2015) Activated regulatory T-cells attenuate myocardial ischaemia/reperfusion injury through a CD39-dependent mechanism. *Clin Sci (Lond)*, **128**, 679-693.

Yamamoto, J. et al. (2000) Differential expression of the chemokine receptors by the Th1- and Th2-type effector populations within circulating CD4+ T cells. *J Leukoc Biol*, **68**, 568-574.

Yan, X. et al. (2013) Temporal dynamics of cardiac immune cell accumulation following acute myocardial infarction. *J Mol Cell Cardiol*, **62**, 24-35.

Yan, X. et al. (2012) Deleterious effect of the IL-23/IL-17A axis and γδT cells on left ventricular remodeling after myocardial infarction. *J Am Heart Assoc*, **1**, e004408.

Yang, Z. et al. (2005) Infarct-sparing effect of A2A-adenosine receptor activation is due primarily to its action on lymphocytes. *Circulation*, **111**, 2190-2197.

Yang, Z. et al. (2006) Myocardial infarct-sparing effect of adenosine A2A receptor activation is due to its action on CD4+ T lymphocytes. *Circulation*, **114**, 2056-2064.

Yang, Z. et al. (2009) CD4+ T lymphocytes mediate acute pulmonary ischemia-reperfusion injury. *J Thorac Cardiovasc Surg*, **137**, 695-702.

Yellon, D.M. & Hausenloy, D.J. (2007) Myocardial reperfusion injury. *N Engl J Med*, **357**, 1121-1135.

Yilmaz, G. et al. (2006) Role of T lymphocytes and interferon-gamma in ischemic stroke. *Circulation*, **113**, 2105-2112.

Yokota, N. et al. (2002) Protective effect of T cell depletion in murine renal ischemia-reperfusion injury. *Transplantation*, **74**, 759-763.

Zhai, Y. et al. (2008) Type I, but not type II, interferon is critical in liver injury induced after ischemia and reperfusion. *Hepatology*, **47**, 199-206.

Zhang, L. et al. (2005) High-dose glucose-insulin-potassium treatment reduces myocardial apoptosis in patients with acute myocardial infarction. *Eur J Clin Invest*, **35**, 164-170.

Zhao, Z.Q. et al. (2003) Inhibition of myocardial injury by ischemic postconditioning during reperfusion: comparison with ischemic preconditioning. *Am J Physiol Heart Circ Physiol*, **285**, H579-88.

Zinkernagel, R.M. et al. (1996) On immunological memory. *Annu Rev Immunol*, **14**, 333-367.

Zouggari, Y. et al. (2013) B lymphocytes trigger monocyte mobilization and impair heart function after acute myocardial infarction. *Nat Med*, **19**, 1273-1280.

Zuidema, M.Y. & Zhang, C. (2010) Ischemia/reperfusion injury: The role of immune cells. *World J Cardiol*, **2**, 325-332.

Zwacka, R.M. et al. (1997) CD4(+) T-lymphocytes mediate ischemia/reperfusion-induced inflammatory responses in mouse liver. *J Clin Invest*, **100**, 279-289.

Zweier, J.L., Flaherty, J.T. & Weisfeldt, M.L. (1987) Direct measurement of free radical generation following reperfusion of ischemic myocardium. *Proc Natl Acad Sci U S A*, **84**, 1404-1407.